

Towards elucidating the structural and cellular determinants of α -synuclein seeding and toxicity

Présentée le 26 août 2022

Faculté des sciences de la vie
Laboratoire de neurobiologie moléculaire et neuroprotéomique
Programme doctoral en neurosciences

pour l'obtention du grade de Docteur ès Sciences

par

Somanath JAGANNATH

Acceptée sur proposition du jury

Prof. B. D. McCabe, président du jury
Prof. H. Lashuel, directeur de thèse
Prof. R. Wade-Martins, rapporteur
Prof. S. K. Maji, rapporteur
Dr B. Schneider, rapporteur

Acknowledgments

First and foremost, my utmost gratitude goes to my supervisor Professor **Hilal A. Lashuel**, for his constant encouragement, motivation, and critical insights during our lab meetings and discussions, which made me think analytically to understand the concepts. I am thankful for giving me an opportunity to start my Ph.D. in his lab even though I had no experience in any molecular or biochemical experimental skills. I remember a quote from Professor, which is something along the lines: “if you have a goal to discover something new in the forest and if you follow the same footsteps as others, then you will not find anything new” – this makes me always think about, am I doing the right thing? And how one can do excellent science and research, exploring new ideas and being willing to take calculated risks in science to do something new. I am very fortunate to have all the conversations with Professor that shaped me, how I think and how I do and continue doing science in the future.

I would also like to thank the jury members Prof. **Brian McCabe**, Prof. **Richard Wade-Martins**, Prof. **Samir K Maji**, and Dr. **Bernard Schneider** for agreeing to be the members of my Ph.D. thesis committee and for providing their valuable knowledge and time to evaluate my Ph.D. thesis.

My special thanks go to **Dr. Gioele La Manno** for providing valuable feedback to improve chapter 4 of this thesis. It was a great pleasure having discussions on the experimental findings. And also, I am also very thankful to **Marion** for helping me with the coding, analyzing the snRNA-seq data, generation of figures and for discussion together with **Nicholas** on the snRNA-seq findings (BICC platform).

My special gratitude goes to **Senthil**, who trained me in almost every *in vitro* experimental technique in the first two chapters of my thesis. I really enjoyed the scientific discussion we had during the preparation of manuscripts, and also, I very much enjoyed playing carrom with him. I am very thankful to all the lab members for teaching me several techniques and providing me with their valuable time and guidance whenever I needed them. My sincere thanks to **Johannes** for guiding me during all experiments and helping me broaden my scientific knowledge when I started my Ph.D. in the Lashuel lab. I would also like to Thank Johannes for German translation of the abstract of my thesis. I am thankful to **Elena** for teaching me primary neuronal dissections and **Anne-Laure** for teaching me biochemical assays and valuable discussions and feedback on my findings. **JC, Johannes** and **Salvatore** for giving a glimpse of performing stereotaxic injections. I would also like to thank Salvatore for guiding me and helping me with *in vivo* stereotaxic injections, brain sectioning, and immunohistochemistry – I really enjoyed working with you **Salvatore**! I am thankful to **Pedro** for working together to identify if oligomers exist in the neuronal

seeding model and for our countless jokes. It was a pleasure working with Pedro. I am also very thankful for **Dora** joining the oligomer project to assess the toxicity of oligomers. Finally, I highly appreciate the help and suggestions from **Sonia** for teaching me how to prepare aSyn fibrils, and **Kamil** for teaching me expression and purification of aSyn monomers and oligomers.

I want to thank also, **Davide** (CIME platform) for teaching me how to take nice TEM images, **Jessica** (histology platform) for teaching me how to use microtomes and cryotome, Jose and Thierry (BIOP platform) for teaching me confocal and live cell imaging microscopes. I am also thankful to Driss, Lorene, Yllza, and Jonathan for always making time to timely ordering reagents and teaching me the right way to do things in the lab.

I am also very thankful for all past and present members of the Lashuel lab for the fruitful discussions and for creating a very healthy and constructive environment for the scientific and peaceful growth: **Ramanath, Senthil, Pedro, Anne-Laure, Yllza, Dora, Salvatore, Sonia, Iman, Raja, Nathan, Ahmed, Enzo, Gopi, Firat, Galina, Till**. My special thanks to Marie for all the administrative support and for planning everything and making our life go smooth.

Finally, I am immensely thankful to my pappu, mammi and siblings for their continuous support, care, and encouragement; without them, it would not have been possible to do my Ph.D. And also, I would like to thank Sneha, my life partner, for always being on my side and for being a perfect life partner, full of optimism, support, understanding, caring and bringing colors of joy to my life.

Abstract

Although it has been nearly two and half decades since the discovery of alpha-synuclein (aSyn) as the major component of Lewy bodies (LBs), our understanding of the involvement of different aSyn species, their seeding, spreading and toxicity in Parkinson's disease (PD) is limited. One of the major causes underlying this knowledge gap is the unavailability of adequate tools, techniques, and model systems to capture, monitor, and evaluate the role of different aSyn species in the disease process. In addition, our understanding of cell-type specific contributions to disease pathogenesis is limited. In this thesis, we systematically address the current knowledge gaps and elucidate the structural and cellular determinants of aSyn seeding and toxicity using cellular and animal model systems of PD.

In the first chapter of this thesis, we describe an antibody characterization and validation pipeline that allows a systematic investigation of the specificity of aSyn antibodies using well-defined and well-characterized preparations of various aSyn species, including monomers, fibrils, and different oligomer preparations that are characterized by distinct morphological, chemical and secondary structure properties. This pipeline was used to characterize 18 aSyn antibodies, 16 of which have been reported as conformation- or oligomer-specific antibodies, using an array of techniques, including immunoblot analysis (slot blot and Western blot), a digital ELISA assay using single molecule array technology and surface plasmon resonance. Our results show that i) none of the antibodies tested are specific for one particular type of aSyn species, including monomers, oligomers or fibrils; ii) all antibodies that were reported to be oligomer-specific also recognized fibrillar aSyn; and iii) a few antibodies (e.g., the antibody clone 26F1, 5G4) showed high specificity for oligomers and fibrils but did not bind to monomers. These findings suggest that most aSyn aggregate-specific antibodies cannot be used to differentiate between oligomers and fibrils, thus highlighting the importance of exercising caution when interpreting results obtained using these antibodies. Our results underscore the critical importance of the characterization and validation of antibodies before their use in mechanistic studies and as diagnostic and therapeutic agents.

In the second chapter of this thesis, we systematically addressed the current knowledge gaps on the role of aSyn oligomers in the initiation, seeding and pathology spreading and toxicity. Towards this goal, we used different biophysical approaches to investigate aSyn seeding *in vitro* and in neurons and animal models of aSyn seeding and pathology spreading. First, we determined whether oligomers are formed in the pre-formed fibril (PFF)-based neuronal seeding model. Using size exclusion chromatography (SEC) fractionation of the soluble fraction isolated from PFF-treated neurons and Western blot analysis of

extracellular media, we observed that oligomeric forms do not form in the PFF-based neuronal seeding model. Next, we investigated whether different types of oligomers exhibit seeding and toxicity properties in the primary neuronal model of PD. We report that different types of oligomers do not seed pathology *in vitro*, primary hippocampal neurons and *in vivo*, and their presence slows rather than accelerates α Syn fibrillization. Our studies reveal that fibrils and oligomer growth occurs through monomer addition, and fibrils compete more efficiently for monomer addition. Also, monomer depletion might favor oligomer dissociation or monomers, which could be cleared or re-enter the aggregation pathway through addition to fibrils. Altogether, our work points to fibrils as the most seeding competent species and suggests that they are the critical mediators of pathology spreading in PD and other synucleinopathies. Our study also points that different types of oligomers induce toxicity irrespective of their morphological, structural and chemical properties – suggesting that oligomers if present potentially cause deleterious effects on the survival of cells.

In the third chapter of this thesis, we used transcriptomics to investigate transcriptional changes in different cell types in the amygdala brain region, which is highly susceptible to developing pS129 positive aggregates in the brains of patients with PD. We performed snRNA sequencing on the amygdala isolated from PBS and PFF injected mouse brains and report findings from 6980 single-nuclei transcriptomics profiles of different cell types from the Amygdala and explored transcriptional changes and associated pathways. We identified that most of the top 100 differentially expressed genes (DEGs) are of neuronal rather than non-neuronal cell types. Furthermore, we observed that inhibitory and excitatory neurons upregulate, and non-neuronal cells downregulate several genes in these DEGs. Significantly upregulated genes in neurons are mainly involved in neuronal electrical activity. On the other hand, downregulated genes in non-neuronal cell types are involved in multiple functions from the receptor, ion and protein binding to GTPase regulatory activities and protein degradation processes. In addition, we report that the gene expression profile of a handful of PD risk genes such as *Sncap*, *Park7*, *Maob*, *Hspa8*, *Scl2a3* and *Hsf3* and some pathways that have been associated with PD are differentially altered in specific cell types. Our study highlights the involvement of unique gene expression changes and their associated pathways in different cell types in driving the disease process at an early stage in a PFF-based mouse model of PD. Understanding these cell-type dependent unique gene expression changes might pave the way for disease-modifying therapies for PD and related synucleinopathies.

Keywords: Parkinson's disease, alpha-synuclein, oligomer, antibody, conformation-specific, seeding, spreading, oligomer toxicity, Amygdala, cell-type specificity, PD risk genes

Zusammenfassung

Bereits vor nun beinahe zweieinhalb Dekaden wurde das Protein alpha-synuclein (aSyn) als Hauptkomponente der Lewy-Pathologie identifiziert. Dennoch ist unser Verständnis der Rolle verschiedener aSyn-Formen in der Entstehung, Ausbreitung und Toxizität der Pathologie in der Parkinson-Krankheit (PD) begrenzt. Grund dafür ist hauptsächlich ein Mangel an Instrumenten, Methoden und Modellen, die geeignet sind, verschiedene Formen der aSyn-Pathologie im Krankheitsprozess zu erfassen, beobachten und evaluieren. Zusätzlich verstehen wir bis heute Zelltyp-spezifische Auswirkungen auf die Pathogenese nur schlecht. In dieser Dissertation beleuchten wir systematisch die derzeitigen Wissenslücken bezüglich struktureller und zellulärer Einflussfaktoren auf die Entstehung und Auswirkungen von aSyn Pathologien in PD Zell- und Tiermodellen.

Das erste Kapitel dieser Dissertation widmet sich der Entwicklung einer systematischen Charakterisierungs- und Validierungs-Pipeline von aSyn Antikörper-Spezifitäten, basierend auf wohldefinierten Präparaten verschiedener aSyn-Formen; Monomere, Fibrille und unterschiedliche Oligomer-Typen. Alle diese Präparate wurden gründlich auf ihre morphologisch-strukturellen und chemischen Eigenschaften geprüft. Mittels unserer Pipeline wurden 18 aSyn Antikörper untersucht, darunter 16, von denen angenommen wurde, sie wären Konformations- oder Oligomer-spezifisch. Wir verwendeten eine Reihe von Techniken, darunter Immunoblots (Slot und Western Blots), digitale ELISAs (enzyme-linked immunosorbent assay, mit single molecule array Technologie) und Oberflächenplasmonenresonanz und zeigen, dass (i) keine der getesteten Antikörper spezifisch für bestimmte aSyn-Formen (Monomere, Fibrille, Oligomere) sind; (ii) alle angeblich Oligomer-spezifischen Antikörper auch Fibrille erkennen; und (iii) nur wenige Antikörper (z.B. Klon 26F1, 5G4) spezifisch für Oligomere und Fibrillen sind, also Monomere weniger gut binden. Diese Resultate zeigen, dass viele Aggregat-spezifische Antikörper nicht zur Differenzierung von Oligomeren und Fibrillen verwendet werden können. Vorsicht bei der Interpretation von mit diesen Antikörpern gewonnenen Daten ist daher geboten. Die entsprechende Charakterisierung und Validierung von aSyn Antikörpern, die für mechanistische Studien, oder gar zum diagnostischen oder therapeutischen Gebrauch eingesetzt werden sollen, ist daher unbedingt erforderlich.

Das zweite Kapitel befasst sich mit der Aufklärung der bisher unzureichend verstandenen Rolle von aSyn Oligomeren in der Auslösung, Entstehung, Ausbreitung und Toxizität von aSyn Pathologie. Dazu nutzten wir verschiedene bio-physische Methoden, um exogene aSyn Pathologie-Induzierung *in vitro*, in primären Neuronen und im Tiermodell zu beleuchten. Zuerst erkundeten wir, ob exogene aSyn Fibrille in Neuronen

zur Entstehung von Oligomeren führen. Fraktionierung durch Grössenausschluss Chromatographie und anschliessende Western Blot Analyse der löslichen Fraktion Fibrill-behandelter Neurone und des extrazellulären Mediums zeigte, dass sich keine Oligomere geformt hatten. In einem weiteren Schritt untersuchten wir, ob direkte Verabreichung von aSyn Oligomeren die Entstehung von aSyn Pathologie oder Toxizität zur Folge hat. Sowohl *in vitro* als auch in hippocampalen primären Neuronen induzierten aSyn Oligomere keine aSyn Pathologie. Sie schienen die Fibrillisierung von aSyn sogar eher zu bremsen statt zu beschleunigen. Wir zeigen des Weiteren, dass das Wachstum von aSyn Oligomeren und Fibrillen auf Hinzufügung von Monomeren beruht, und dass dieser Prozess für Fibrille effizienter ist. Ausserdem scheint die Verringerung der Monomer-Verfügbarkeit eine Monomer-Dissoziation von Oligomeren zu bewirken. Diese dissoziierten Monomere können dann abgebaut werden oder sie werden bereits existierenden Fibrillen zugefügt. Unsere Ergebnisse bestätigen aSyn Fibrille als Hauptmotoren der aSyn Pathologie-Entstehung. Sie sind daher wahrscheinlich auch die wesentlichen aSyn Formen in der Ausbreitung der aSyn Pathologie in PD und anderen Synucleinopathien.

Im dritten Kapitel wenden wir uns der Genexpressions-Regulation in Folge von aSyn Pathologie zu. Wir verwendeten Transcriptomics, um eine der am stärksten von aSyn Pathologie betroffenen Gehirnregionen in unserem Mausmodell (in dem mit exogenen aSyn Fibrillen aSyn-Pathologie ausgelöst wird) zu charakterisieren; die Amygdala. snRNA Sequenzierung von 6980 Transkriptom-Profilen einzelner Zellkerne der Amygdala gestattete uns die Identifizierung der 100 Gene, die am stärksten von der aSyn Pathologie betroffen sind («differentially expressed genes», DEGs). Die meisten der DEGs waren von neuronalem Ursprung, weniger DEGs wurden in anderen Zelltypen festgestellt. Während die meisten neuronalen DEGs auf-reguliert und in neuronale elektrische Aktivität involviert waren, wurde der Grossteil nicht-neuronaler DEGs weniger exprimiert und deren Funktionen waren breiter gestreut; sie reichten von Rezeptoren, Ionen und Protein-Bindung zu GTPase Regulierung und Protein-Abbau. Des Weiteren war eine Handvoll PD-assoziiierter Risiko-Gene differenziell in spezifischen Zelltypen von der aSyn Pathologie betroffen: z.B. Sncaip, Park7, Maob, Hspa8, Scl2a3 and Hsf3. Unsere Ergebnisse legen nahe, dass in unserem Mausmodell Zelltyp-spezifische und individuelle Muster in der Genregulation in den frühen pathologischen Prozess involviert sind. Ein besseres Verständnis für die komplexe, Zelltyp-spezifische Transkriptions-Regulierung in PD könnte die Entwicklung von dringend benötigten Behandlungsformen ermöglichen, die den Krankheitsverlauf von PD oder verwandten Synucleinopathien bremsen.

Schlüsselwörter: Parkinson-Krankheit, alpha-Synuclein, Oligomer, Anti-Körper, Konformations-Spezifität, Pathologie-Entstehung, Pathologie-Ausbreitung, Oligomer Toxizität, Amygdala, Zelltyp Spezifität

Contents

Acknowledgments	i
Abstract (English)	iii
Zusammenfassung (Deutsch).....	v
Contents	vii
List of figures	ix
List of tables	xi
Abbreviations	xii
CHAPTER 1: Introduction	
1.1 A brief history of a-synuclein.....	1
1.2 aSyn structure and function in health	2
1.3 aSyn in disease	14
1.4 aSyn misfolding and aggregation.....	22
1.5 Oligomer seeding and spreading.....	29
1.6 Cell-type dependent contributions to PD.....	32
1.7 Thesis Objectives.....	36
CHAPTER 2 How specific are the conformation-specific alpha-synuclein antibodies?	
2.1 Introduction	38
2.2 Results	44
2.3 Discussion	65
2.4 Materials and methods	69
2.5 Contributions of the authors	76

CHAPTER 3: α -synuclein fibrils are the key mediators of seeding and pathology spreading in the PFF-based seeding model

3.1 Introduction	77
3.2 Results	81
3.3 Discussion	93
3.4 Materials and methods	99
3.5 Contributions of the authors	104

CHAPTER 4: Gene expression changes in the Amygdala of a PFF-based mouse model of Parkinson's disease reveal cell-type-specific dysregulation of PD risk genes and pathways

4.1 Introduction	105
4.2 Results	107
4.3 Discussion	121
4.4 Materials and methods	123
4.5 Contributions of the authors	126

CHAPTER 5: Conclusion

5.1 Achieved results, limitations and future development.....	127
References	131
Curriculum vitae	177

List of Figures

Chapter 1

Figure 1.1: Major physiological functions of aSyn	3
Figure 1.2: A schematic illustration of aSyn domains, their functions and different conformations of aSyn in solutions and bound to lipid vesicles.....	5
Figure 1.3: A Schematic illustration of aSyn PTMs identified in LBs	7
Figure 1.4: The majority of PTM sites identified in human LBs are conserved in aSyn sequences from different species	8
Figure 1.5: Histological properties of LBs and LNs	15
Figure 1.6: Schematic depiction of cellular and animal systems and strategies used to induce aSyn aggregation and mimic PD pathology	18
Figure 1.7: <i>In vitro</i> alpha-synuclein (aSyn) aggregation process	23
Figure 1.8: Different methods to detect oligomers in the human brain tissues	26
Figure 1.9: Schematics illustrating various stages of neurodegeneration in PD patient brains.....	32

Chapter 2

Figure 2.1: A schematic illustration of antibody validation strategy	41
Figure 2.2.: Preparation and characterization of aSyn monomers, oligomers, and fibrils.....	45
Figure 2.3: Immunoblots to assess equal protein loading on the nitrocellulose membranes	48
Figure 2.4: <i>In vitro</i> binding analysis of antibodies against aSyn monomers, oligomers and fibrils using slot blots and Western blots	50
Figure 2.5: ELISA Simoa assay of antibodies against monomers, oligomers and fibrils	53
Figure 2.6: Preparation of dopamine- and HNE-induced oligomers and analysis of their stability	56
Figure 2.7: Mass spectrometry analysis of aSyn samples	57
Figure 2.8: Slot blot analysis of antibodies against aSyn monomers, DO and HO oligomers	58
Figure 2.9: Immunoreactivity of different concentrations of antibodies to aSyn species	59
Figure 2.10: SPR-based kinetic analysis of different immobilized monoclonal antibodies A17183A, MJFR-14, and SYN211	62
Figure 2.11: SPR-based kinetic analysis of different immobilized monoclonal antibodies SynO4, 26F1, 9029 and 12C6.....	64

Chapter 3

Figure 3.1: A schematic illustration of our workflow to investigate the role of aSyn oligomers in the aggregation process	80
Figure 3.2: Probing the presence of oligomers in the PFF-based neuronal seeding model in primary hippocampal neurons	82
Figure 3.3: Oligomeric aSyn with oligomer spike-in of soluble fractions of neurons treated with PFFs	83
Figure 3.4: Preparation and characterization of morphologically and structurally different human aSyn oligomers	84
Figure 3.5: Fibrils are the major seeds to induce the formation of pS129 positive aggregates in the primary hippocampal neurons	86
Figure 3.6: Fibrils act as seeds majorly to induce the formation of pS129 positive aggregates in the primary hippocampal neurons at different concentrations and different time points tested	87
Figure 3.7: Oligomers do not induce pS129 aggregate formation <i>in vivo</i>	88
Figure 3.8: ThT aggregation kinetics in the presence of human aSyn UO, DO, HO alone or in combination with fibrils	90
Figure 3.9: TEM images of different conditions with or without fibril seeds after the filtration protocol total and oligomeric fractions	90
Figure 3.10: Oligomers and fibrils reduce cellular viability metabolic activity	91
Figure 3.11: Schematic representation and model of various events that are related to the aggregation process in the presence of different seeds	95

Chapter 4

Figure 4.1: Workflow and QC of snRNA-seq from PBS and PFF amygdala brain regions	107
Figure 4.2: Dimensionality reduction, clustering and cell-type annotation	108
Figure 4.3: DEGs in different cell types in PBS and PFF amygdala samples	112
Figure 4.4: Gene Ontology enrichment analysis of molecular function terms	114
Figure 4.5: Gene Ontology enrichment analysis of cellular component terms	115
Figure 4.6: UpSet plot of PD risk genes in different cell types of Amygdala	116
Figure 4.7: Normalized mean expression level of PD risk genes in different cell types	117
Figure 4.8: Gene Ontology enrichment analysis of KEGG pathway terms	119
Figure 4.9: PD Pathway related KEGG pathway affected	120

List of Tables

Chapter 1

Table 1.1: Components of LBs based on immunohistochemical studies	17
Table 1.2: Summary of studies modeling aSyn aggregation in cellular model systems of PD	20
Table 1.3: Summary of studies modelling aSyn aggregation in animal model systems of PD	21
Table 1.4: Factors affecting aSyn aggregation	23
Table 1.5: Proposed properties of oligomers and their effect on molecular events and cellular systems.	29
Table 1.6: aSyn oligomer spreading <i>in vivo</i> model systems	31
Table 1.7: single-cell transcriptomics studies <i>in vivo</i> PD model systems	35

Chapter 2

Table 2.1: List and details of antibodies used in this study	43
Table 2.2: Immunoreactivity and binding specificity of antibodies against native structures of aSyn species by different techniques	51
Table 2.3: Immunoreactivity of antibodies against SDS and heat treated aSyn samples by Western blot analysis	52
Table 2.4: Morphologies and structural properties of oligomers used in this study	55
Table 2.5: Kinetic parameters of the antibodies binding to aSyn monomers or oligomers	63
Table 2.6: Materials and Reagents	73

Abbreviations

AD	Alzheimer's disease
a.a.	Amino acid
AAA	Amino acid analysis
AM	Amygdala
APEX	Ascorbate peroxidase
K _a	Association rate constant
aSyn	α -synuclein
AFM	Atomic force microscopy
AEB	Average Enzymes per Bead
BCA	Bicinchoninic acid assay
K _D	Binding affinity
B-LB	Brainstem LBs
Cacnb2	Calcium Voltage-Gated Channel Auxiliary Subunit Beta 2
CC	Cellular component
CNS	Central nervous system
CSF	Cerebrospinal fluid
CD	Circular dichroism
CI	Clastrum
C-LB	Cortical LBs
cAMP	Cyclic adenosine monophosphate
DLB	Dementia with Lewy bodies
DEG	Differentially expressed genes
K _d	Dissociation rate constant
DHA	Docosahexanoic acid
DO	Dopamine-induced oligomers
DA	Dopaminergic
DMV	Dorsal motor nucleus of the vagus
DSB	Double-strand break

EM	Electron microscopy
ER	Endoplasmic reticulum
ENS	Enteric nervous system
ELISA	Enzyme-linked immunosorbent assay
F	Fibrils
GABA	Gamma aminobutyric acid
GO	Gene Ontology
H&E	Hematoxylin and Eosin
HMW	High molecular weight
HCA	High-content wide-field imaging analysis
HO	HNE-induced oligomers
HNE	Hydroxynonenal
HCN	Hyperpolarization-activated cyclic nucleotide-gated
HDX-MS	Hydrogen-deuterium exchange MS
ICC	Immunocytochemistry
IHC	Immunohistochemistry
IL	Intralaminar nuclei of the thalamus
LCM	Laser capture microdissection
LSM	Laser-scanning microscope
LH	Lateral hypothalamus
LB	Lewy bodies
LN	Lewy neurites
LC-MS	Liquid chromatography-mass spectrometry
LC	Locus coeruleus
LTP	Long-term potentiation
MS	Mass spectrometry
MRN	Median raphe nucleus
mPTP	Mitochondrial permeability transition pore
MF	Molecular function

M	Monomers
MSA	Multiple system atrophy
MVB	Multivesicular bodies
NHS	N-hydroxy succinimide
N	Nitration
NMDA	N-methyl-D-aspartate
NAC	Non-amyloid component
ND	Not described
NMR	Nuclear magnetic resonance
OPC	Oligodendrocyte progenitor cells
O	Oligomer
PB	Pale body-type
PD	Parkinson's disease
PV	Parvalbumin
PPN	Pedunculopontine nucleus
P	Pellet
PMSF	Phenyl methane sulfonyl fluoride
pS129	Phosphorylation at S129
pS87	Phosphorylation at S87
PLK2	Polo-like kinase
PTM	Post-translational modifications
PFF	Preformed fibrils
PERK	Protein kinase RNA-like endoplasmic reticulum kinase
PK-PET	Proteinase K-paraffin-embedded tissue
PLA	Proximity ligation assay
ROS	Reactive oxygen species
SDS-PAGE	Sodium dodecyl sulfate–polyacrylamide gel electrophoresis
SIMOA	Single molecule array
SEC	Size-exclusion chromatography

SDS	Sodium dodecyl sulfate
SNARE	Soluble N-ethylmaleimide–sensitive factor attachment protein receptor
snRNA-seq	Single-nuclei RNA sequencing
SATB	Special AT-rich sequence-binding protein
SN	Substantia nigra
SNc	Substantia nigra pars compacta
SPR	Surface plasmon resonance
ThT	Thioflavin T
T	Total
TEM	Transmission electron microscopy
Ub	Ubiquitin
UPS	Ubiquitin-proteasome system
UMAP	Uniform Manifold Approximation and Projection
UO	Unmodified oligomers
VTA	Ventral tegmental area
XBP-1	X-box binding protein 1

Chapter 1. INTRODUCTION

1.1 A brief history of a-synuclein

In 1988, Maroteaux and colleagues first described the presence of 143 amino-acid neuron-specific protein while characterizing cholinergic synaptic proteins isolated from Pacific electric ray (*Torpedo californica*)¹. They called this neuron-specific protein “synuclein” based on its localization to presynaptic nerve terminals (syn) and nuclear envelope (nuclein). In 1994, the Goedert lab identified and demonstrated the abundant presence of 140- and 134-amino acid (a.a.) proteins in the human brain which they called “a-synuclein” (aSyn) and “b-synuclein” respectively² and highly homologous to the protein identified by Maroteaux and colleagues¹. Subsequently, another member “g-synuclein” was identified³. In 1997, two major breakthroughs were made – 1) identification of the A53T mutation in the SNCA gene (that encodes aSyn) in Italian pedigree and independent Greek families as the first genetic basis of the Parkinson’s disease (PD)⁴; 2) the detection of the aSyn protein (using antibodies raised against synthetic peptide containing 116-131 residues of human aSyn) in Lewy bodies (LB) and Lewy neurites (LN) in the postmortem brains of patients with idiopathic PD and dementia with Lewy bodies (DLB)⁵. These two studies set the basis for aSyn research as a spotlight to study PD and related neurodegenerative diseases.

In 1998, Spillantini and colleagues isolated aSyn-immunolabeled filamentous structures from sarkosyl insoluble fractions of post-mortem PD and DLB brains^{6,7}. In parallel, *in vitro* studies demonstrated that under specific conditions aSyn monomer aggregates to form filamentous structures and identified the formation of transient soluble oligomeric that populate on the pathway to aSyn fibril formation^{8,9}. Subsequent *in vitro*, cellular and animal model systems of PD showed that aggregated aSyn species are toxic when added to different cell types and form upon overexpression of aSyn in cells a different animal models¹⁰⁻¹². These studies suggested that aSyn aggregation into oligomeric and fibrillar species could be a major event in PD pathogenesis. Over last decade, increasing evidence show that aSyn is secreted by neurons and other cells and that secreted aSyn^{13,14} or extracellular addition of aSyn fibrils can recruit endogenous aSyn to trigger the formation of aSyn inclusions, cause toxicity and lead to synaptic dysfunction¹⁵⁻¹⁷. However, the exact nature of the pathogenic species or processes that regulate aSyn secretion, seeding, and pathology spreading in the brain a subject of active investigation and debates.

On the other hand, several studies have attempted to elucidated the physiological role of aSyn in the brain and aSyn has been associated with several functions, including synaptic transmission, several organellar

functions, and gene expression regulation^{18,19}. These findings suggest that several functions could be disrupted upon aSyn loss-of-function, which could in turn debilitate the disease process. However, whether the loss of soluble aSyn protein, due to its aggregation, and/or dysregulation of its physiological functions contribute to the pathogenesis of PD remains unclear. This is in large part due to the lack of functional assays and animal models where loss of aSyn function gives rise to PD-like functional deficits and clinical phenotypes. Therefore, understanding the physiological and pathophysiological roles of different forms of aSyn could have therapeutic potential to halt or slow PD progression.

1.2 aSyn structure and function in health

Although aSyn does not seem to have an essential function that is lost by its absence in rodents, several functions of aSyn have been proposed, including its roles in membrane biogenesis, lipid transport, molecular chaperone activity, SNARE-complex assembly²⁰, exocytosis²¹, endocytosis and vesicle recycling²¹⁻²³, dopamine release²⁴, dopamine synthesis and transport²⁵, ER-Golgi vesicle trafficking (functions reviewed in^{26,19}), ferrireductase activity^{27,28}, gastrointestinal immunity²⁹, activation of microglia and T-cell proliferation^{30,31}, and gene expression regulation (reviewed in³²) (Figure 1.1). This functional diversity is consistent with the presence of aSyn in the synaptic terminals and several neuronal compartments, including the nucleus^{1,33}, the Golgi apparatus^{34,35}, the endolysosomal system³⁶, the mitochondria³⁷⁻³⁹, and in the endoplasmic reticulum^{38,40,41}. Furthermore, the fact that aSyn is an intrinsically disordered protein means that it has a large conformational landscape that gives it the flexibility to transition between different folded states and/or interact with diverse sets of proteins of protein complexes. However, the nature of the molecular and environmental switches that regulate aSyn transition from one conformational state to another or from one cellular compartment to another remains unknown. In this section, we will review our current understanding of some of the well-studied aSyn functions with an emphasis on the potential role of PTMs as sequence and structural regulatory elements involved in modulating its physiological functions.

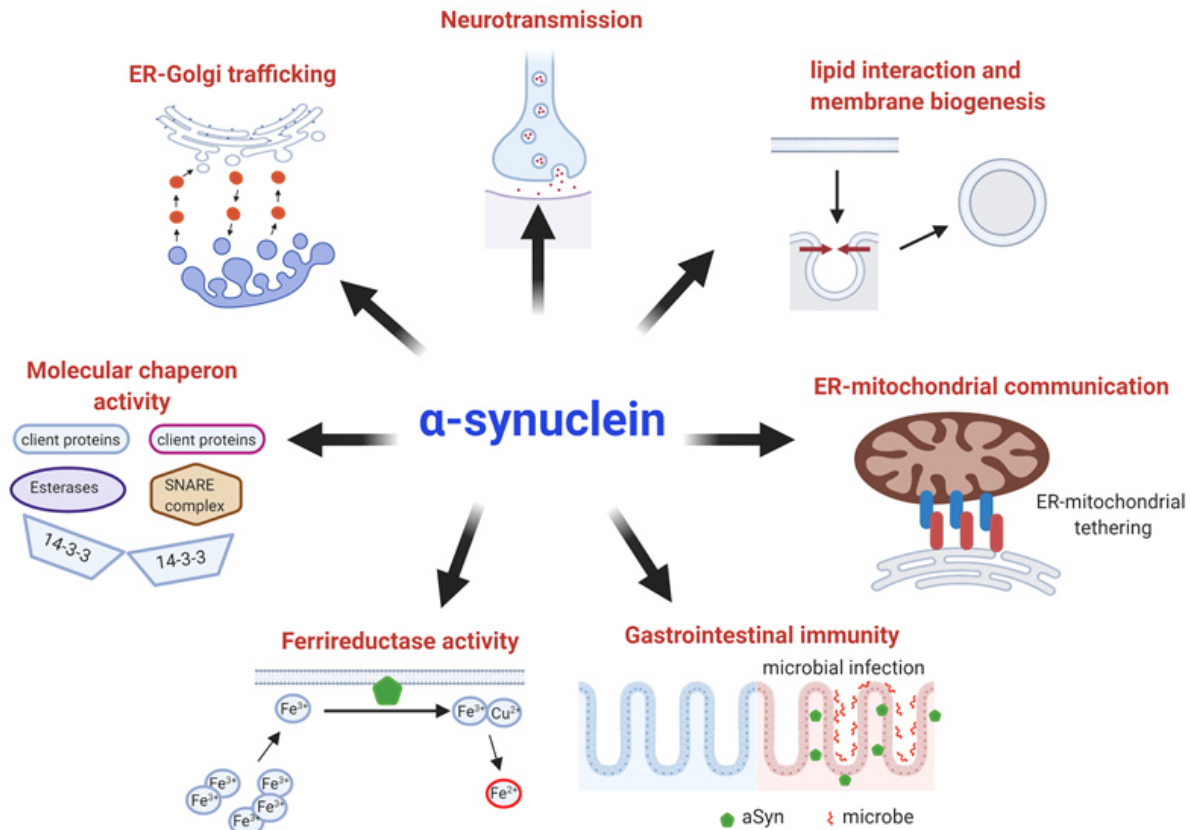


Figure 1.1: Major physiological functions of aSyn. aSyn is known to regulate a number of physiological functions, including neurotransmission, lipid interaction and membrane biogenesis, ER-mitochondrial communication, ER-Golgi trafficking, molecular chaperon activity, gastrointestinal immunity, and ferrireductase activity.

1.2.1 aSyn structure, domains and their role

To understand the potential impact of PTMs on the normal functions of aSyn, it is essential to first review what we know about the native state of aSyn, its sequence properties, including the role of the various domains in regulating its functions (Figure 1.2). Since its discovery, aSyn has been described as an intrinsically disordered protein, i.e., it exists as an ensemble of conformations and does not adopt a stable secondary structure on its own^{42,43}. Although this notion was recently challenged by a handful of groups arguing that the physiological state of aSyn is a helically folded tetramer⁴⁴⁻⁵⁰, we^{51,52} and others⁵³⁻⁵⁸ have failed to reproduce these findings and could only detect native aSyn in an unfolded monomeric state as it has been established for the past two and half decades⁴². The evidence for tetramer in most studies relies on size exclusion chromatography which shows that aSyn elutes as a 58-67 KDa protein based on globular protein standards, despite previous studies establishing that the unfolded monomeric aSyn preparations

also exhibit an apparent MW of 55-60 KDa by SEC⁵². Although *in vitro* or in-cell cross-linking experiments have also been used to provide evidence for the presence of aSyn tetramers, it is important to emphasize that the results from these experiments always show the appearance of multiple bands corresponding to dimer, tetramer, octamer as well as high molecular weight species. Under no conditions aSyn was found to cross-link as a single tetrameric species, and no other group has successfully isolated this tetrameric form of the protein from mammalian cells or other cell types. Finally, several groups have also performed in-cell NMR studies and demonstrated that aSyn in its native cellular environment exists predominantly as a monomer^{53,54,56}. These findings are consistent with recent reports by the Selkoe group showing that aSyn isolated from human brains exists mainly as a monomer, consistent with our previous findings⁵², although the authors argue that aSyn oligomers in the brain are less stable⁵⁹. Taken together, the existing data are in support of the monomer hypothesis but do not rule out the possibility that aSyn could exist in dynamic equilibrium between monomers and oligomers upon interaction with ligands, membranes, or other proteins. Further studies are needed to elucidate the molecular factors that regulate this equilibrium and to isolate and characterize such oligomers and assess their biophysical and biological properties.

At the sequence level, the N-terminal amphipathic region (a.a. 1-60) of aSyn is positively charged and has been implicated in regulating many aspects of its binding to membranes and synaptic vesicles (Figure 1.2A). This region is characterized by the presence of several imperfect 'KTKEGV' hexameric motif, which influences the propensity of the first ~80-90 amino acid residues to undergo structural changes to α -helical conformations upon binding to membranes and lipids⁶⁰⁻⁶⁵. The size and curvature of the membranes determine whether aSyn forms a single or a broken helix on membranes (Figure 1.2C). For example, highly curved small micelles favor the formation of a broken helix conformation⁶⁴⁻⁶⁷, larger and less-curved membrane surfaces induce a single extended helix that comprises the 90 residues of the protein^{68,69}. Recently, it has been demonstrated that this N-terminal region contains two sequence motifs called P1 (residues 36-42), P2 (residues 45-57) that are critical not only for controlling NAC-region mediated aSyn aggregation but also aSyn mediated membrane fusion⁷⁰.

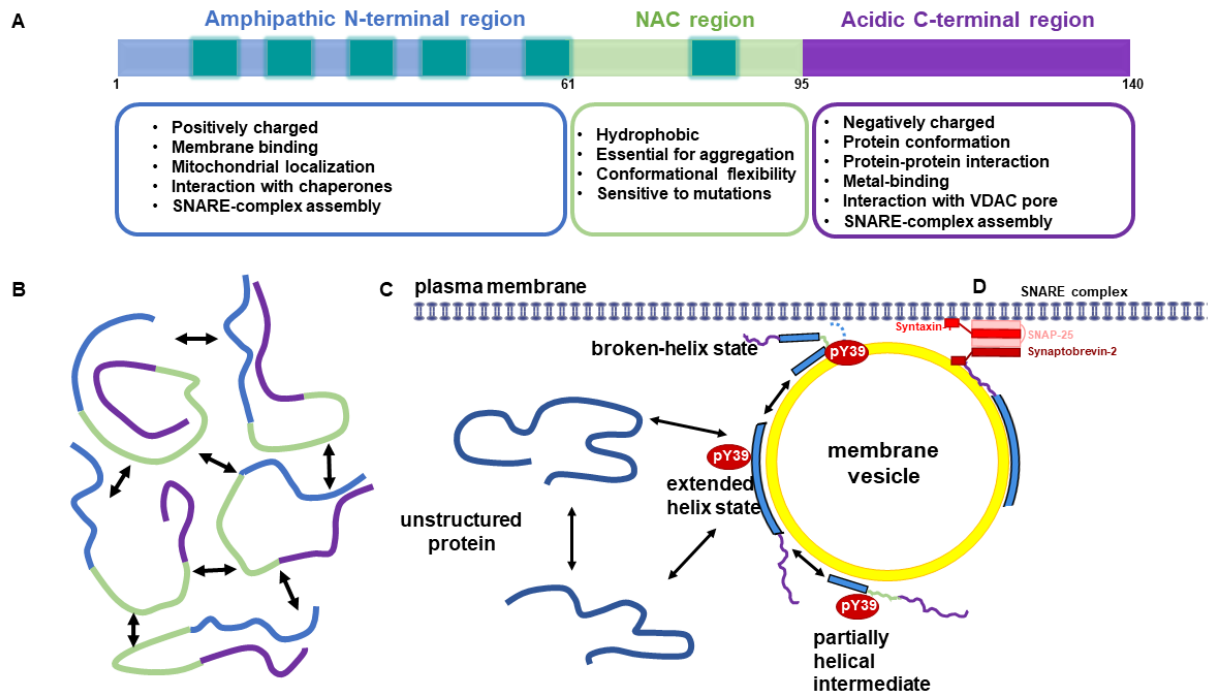


Figure 1.2: A schematic illustration of aSyn domains, their functions and different conformations of aSyn in solutions and bound to lipid vesicles. (A) Different aSyn domains and their functional involvement. Small boxes in the N-terminus and NAC region indicate conserved KTEGV hexameric motifs. (B) Monomeric aSyn with an ensemble of conformations in solution. Arrows indicate intramolecular interactions between different domains (reproduced from⁷¹). (C) aSyn in solution is unstructured, but its interaction with membranes leads to extended-helix, partially helical intermediates and broken-helix state structures. These different functions are modulated by PTMs, such as phosphorylation at Y39. aSyn is also involved in SNARE-complex assembly and synaptic vesicle docking (this figure was modified from⁷²).

Within the first 100 amino acids also lies the hydrophobic non-amyloid component (NAC) region (a.a. 61-95), which is essential for aSyn aggregation and plays a key role in the initiation of aSyn aggregation. Under conditions that favor aSyn oligomerization and fibrils formation, the aggregation-prone NAC region undergoes conformation changes from random coil to the β -sheet structure^{73,74} and constitutes the core of the fibrils. The NAC region is also involved in regulating aSyn binding to membranes. Recent studies by Fusco et al. show that N-terminus (a.a. residues 1-25) and NAC region (a.a. residues 65-97) act as dual membrane anchors to facilitate simultaneous binding aSyn to two different vesicles and thus could play a role in vesicle clustering⁷⁵. Conditions that promote the release of the NAC region from membranes also promote aSyn association and aggregation on membranes.

The acidic C-terminal region (a.a. 96-140, (enriched in glutamate, aspartate, and proline residues) adopts predominantly dynamic and disordered conformation in the monomeric, membrane-bound as well as in aggregated states (oligomers, fibrils) of aSyn⁷⁶⁻⁸⁰. This region has been shown to regulate aSyn interactions

with multiple proteins including Tau⁸¹, histones⁸²⁻⁸⁶, chaperones^{87,88}, cytoskeleton proteins (analyzed and compared in⁸⁹). Several studies have proposed that these interactions regulate different aspects of aSyn normal functions. For example, aSyn was shown to interact with Tau via its C-terminal domain and regulate the stability of axonal microtubules through stimulating protein kinase-A mediated phosphorylation of serine 262 and 356 residues⁹⁰⁻⁹³. In addition, despite its disordered conformation and distal location from the N-terminus, the C-terminus has been proposed to play a role in regulating aSyn membrane binding^{9,61-65,94-96} and to sterically stabilize and functionalize membrane surfaces⁹⁷; as well as thermo solubility and stability under stress conditions such as heat, pH, metal-induced aggregation⁹⁸. A recent study by Lautenschlaeger et al. suggested that calcium binding to the C-terminus enhances lipid- and synaptic vesicle binding capacity and modulates synaptic vesicle clustering⁹⁹. Interestingly, the C-terminal domain is also responsible for regulating aSyn interactions with polyamines^{100,101}, dopamine^{102,103}, and metal ions including Calcium (II)^{104,105}, Copper (II)¹⁰⁶⁻¹¹¹, Zinc (II)¹¹², and Iron (III)^{113,114,115}. These interactions can modulate intramolecular interactions and alter aSyn misfolding and aggregation. The diversity of aSyn protein-protein, protein-ligand and protein-metal interactions highlight the importance of unstructured acidic domain in regulating the structural and functional properties of aSyn.

NMR, hydrogen-deuterium exchange MS (HDX-MS) studies have shown that aSyn fluctuates between extended and collapsed conformations that are stabilized by intramolecular interactions between different segments of the protein¹¹⁶⁻¹²⁰. For example, i) NMR studies have consistently revealed transient intramolecular interactions between N-terminus (positively charged) and C-terminus (negatively charged) as well as, the C-terminus and NAC region of the protein⁷¹ (Figure 1.2B). It has been proposed that these intramolecular interactions contribute to i) maintaining the native and soluble state of aSyn by shielding the hydrophobic and aggregation-prone NAC region and preventing its self-association^{77,117,121}; ii) stabilizing local conformations in specific domains¹²² and iii) stabilizing the native conformations of the proteins. Therefore, mutations¹²³, molecular interactions (e.g., calcium-binding or membrane binding), or post-translational modifications (e.g., phosphorylation⁷¹, methionine oxidation¹²² or C-/N-terminal truncation^{124,125}) that occur in these regions could either stabilize or destabilize the native conformation of the protein and thus influence both its functions and propensity to aggregate⁷¹.

1.2.2 Influence of PTMs on aSyn structure and function

Given the role of the N- and C-terminal domains in regulating many aspects of the native conformation of aSyn and its molecular interactions; subcellular localization, and binding to membranes, it is not surprising

that the great majority of aSyn PTMs not only occur, but also cluster in these regions (Figure 1.3). Interestingly, most of the residues shown to undergo post-translational modification or represent putative PTM sites, including the majority of lysine, serine, threonine, tyrosine residues are highly conserved across species (Figure 1.4), suggesting that PTMs may play crucial roles in the regulation of aSyn function in health and disease.

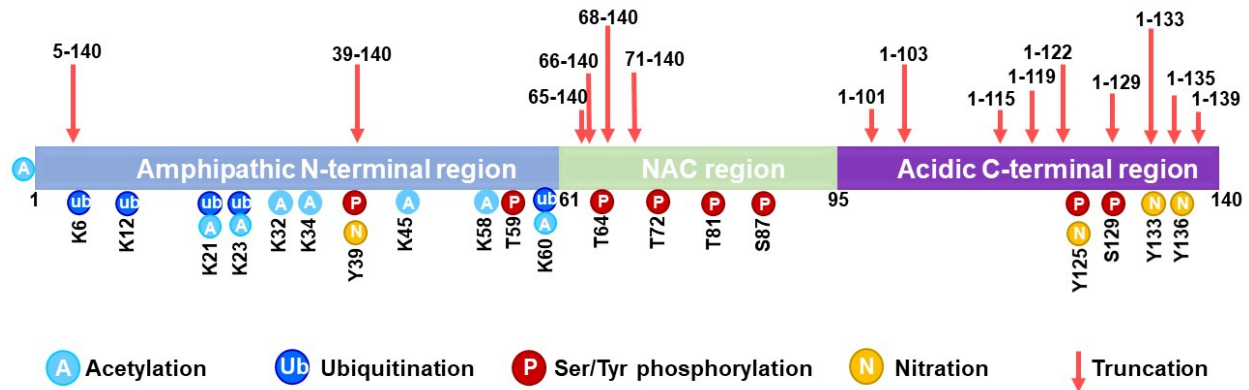


Figure 1.3: A Schematic illustration of aSyn PTMs identified in LBs. aSyn PTMs include phosphorylation, nitration, ubiquitination, truncation, and N-terminal acetylation.

One of the most-studied functions of aSyn is its propensity to bind to membranes and lipid vesicles. Several PTMs have been shown to regulate the structure and the dynamics of aSyn interactions with lipids and membranes and regulate its membrane-binding dependent functions. N-terminal acetylation, one of the most common aSyn PTMs, was shown to increase the transient helical propensity of the N-terminal domain of the protein^{126,127} and its affinity of aSyn towards lipid vesicles^{128,129}.

Tyrosine 39 is one of the residues that is subjected to both phosphorylation and nitration and occupies an important position in the broken helix conformation of aSyn as it sits in the turn between the two helices. Although phosphorylation at Y39 does not seem to alter the ensemble of conformations of monomeric aSyn in aqueous solutions, it significantly influences the structure of the membrane-bound aSyn and potentially its interaction with other proteins and vesicles. In contrast, site-specific nitration at Y39 reduces aSyn binding to synthetic vesicles¹³⁰. In the presence of lipid vesicles, phosphorylation at Y39 facilitates the interconversion of aSyn from the vesicle-bound extended helix to the broken helix state (Figure 1.2C). The broken helix state is comprised of two anti-parallel helices connected by a nonhelical linker. Phosphorylation at Y39 reduces the affinity of one of the helices, which, upon release from the membrane, makes this domain available for binding to other proteins or synaptic vesicles¹³¹. It has been proposed that phosphorylation at Y39 may serve as a molecular switch that regulates aSyn role in vesicle fusion. The recent development of antibodies that specifically recognize phosphorylated and nitrated

aSyn at Y39¹³² (Biolegend (clone A15119B); nitro Y39 (clone nSyn14)) and sensitive assays for quantifying pY39 in biological fluids should facilitate future studies aimed at understanding the role of p/nY39 in regulating aSyn properties health and disease^{133,134}.

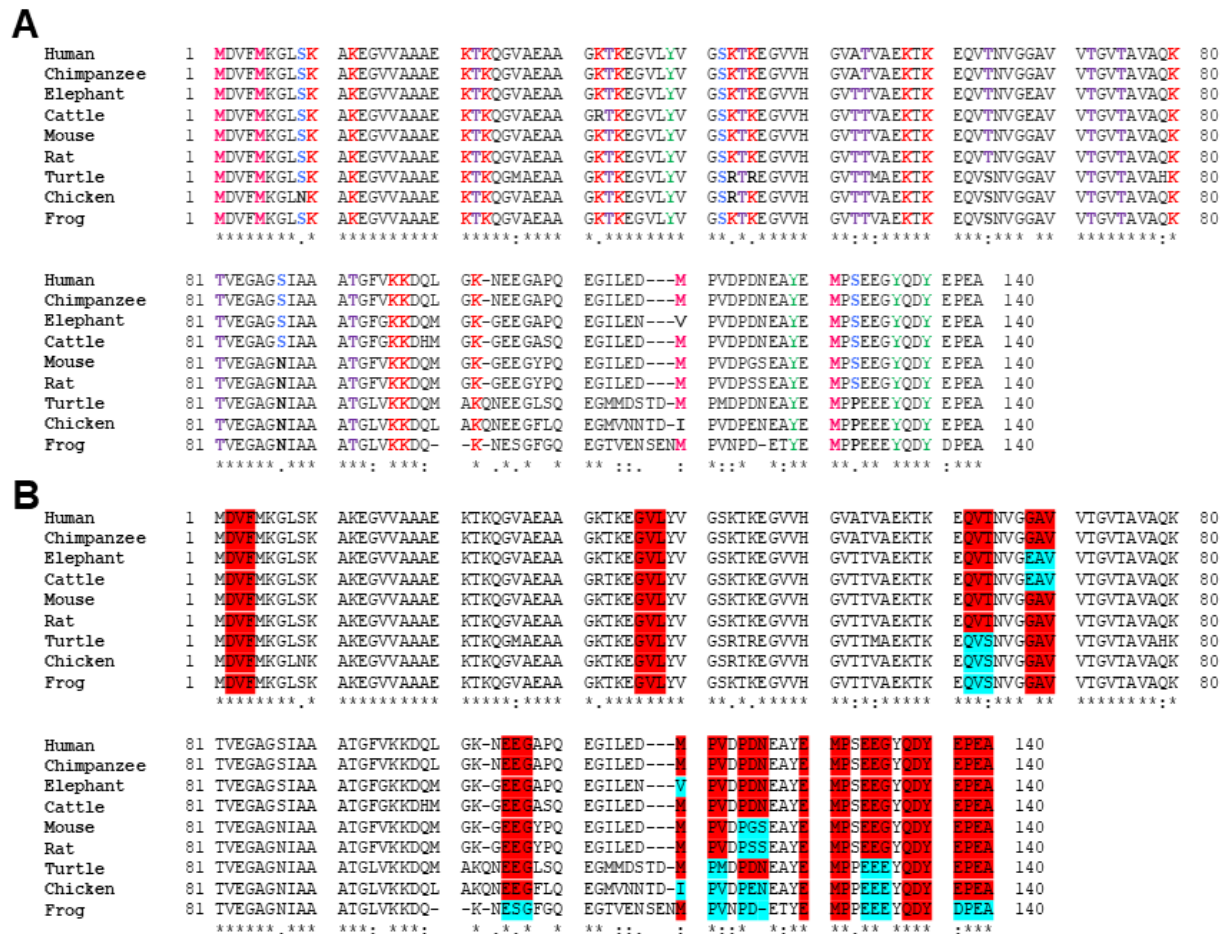


Figure 1.4: The majority of PTM sites identified in human LBs are conserved in aSyn sequences from different species. Multiple sequence alignment of aSyn from different animals generated by MUSCLE (version 3.8) (A) depicting the homology in aSyn sequence and conserved PTM sites such as phosphorylation, nitration, ubiquitination (A), and conserved a.a. residues near the cleavage sites (B) across different species. Residues marked with the same color (and in bold) indicate identical amino acid residues, and black and bold indicate non-identical amino acids. Color code for amino acid residues: Methionine: Pink; Lysine: Red; Serine: Blue; Tyrosine: Green; Threonine: Purple. An * (Asterisk) indicates fully conserved residues, a : (colon) indicates conservation between groups of strongly similar properties, a . (dot) indicates conservation between groups of weakly similar properties.

Within the NAC region, only phosphorylation at S87 (pS87) has been detected in LBs. This may reflect the fact that many of the PTMs identified in LBs and aggregated forms of aSyn may occur post aSyn aggregation⁸⁹. The NAC region is usually found within the core of aSyn oligomers and fibrils and would

thus be largely inaccessible for modification by enzymes¹³⁵. Most of the NAC region residues are involved in forming the core of the different strains of recombinant aSyn fibrils and aSyn fibrils isolated from MSA brains¹³⁶. Phosphorylation at S87 increases the conformational flexibility of aSyn and also reduces the α -helical propensity of vesicle-bound aSyn^{135,137}. It is noteworthy that phosphorylation within the N-terminal (Y39 and S87) domains stabilizes the monomeric protein and inhibit its aggregation, which suggest that they could be involved in regulating its normal functions.

Several PTMs that occur outside the membrane-binding region have also been shown to influence aSyn membrane interactions. For instance, we previously showed that site-specific nitration at Y125 results in reduced aSyn affinity towards synthetic vesicles¹³⁰. On the other hand, phosphorylation at S129 increases the conformational flexibility of aSyn, alters the intramolecular interactions N- to C-terminal interactions, and reduces solvent exposure of the N-terminus⁷¹. Studies on the effect of phosphorylation at S129 on membrane binding have yielded conflicting results ranging from no effects to significant reduction on aSyn membrane interactions^{51,94,137}. For example, a few reports have suggested little or no effect of S129 phosphorylation on aSyn-membrane-interactions using synthetic micelles/vesicles under *in vitro* conditions^{51,137}. In contrast, studies using GRK-mediated phosphorylation of aSyn S129 suggest decreased affinity of aSyn to phospholipids^{138,139}. In addition, yeast¹⁴⁰, and worm¹⁴¹ studies suggest an inhibitory effect of phosphorylation at S129 using phosphomimetic proteins, on aSyn membrane binding. This is largely due to the different approaches used to investigate phosphorylation at S129, which range from using phosphomimetics, non-specific *in vitro* phosphorylation with kinases, to semisynthetic or enzymatic site-specific phosphorylation of aSyn.

Interestingly, both the N- and C-terminus regions of aSyn are involved in the assembly of soluble N-ethylmaleimide-sensitive factor attachment protein receptor (SNARE)-complex²⁰ and SNARE-mediated vesicle docking^{142,143}. The involvement of aSyn in the assembly of this complex highlights an important role of aSyn in regulating neurotransmitter release of synaptic vesicles during increased synaptic activity. Recent reports^{142,144} suggest that, the N-terminal amphipathic and hydrophobic regions (a.a. 1-100) bind to the plasma membrane. Meanwhile, the hydrophilic C-terminal region (a.a. 101-140) interacts with the N-terminal domain of VMAP2 (a vesicle protein involved in mediating fusion of vesicles with the plasma membrane). The ability of aSyn to crossbridge vesicles and plasma membranes facilitates SNARE-dependant vesicle docking and subsequent SNARE complex assembly (Figure 1.2C)^{20,142,144}. In addition, Somayaji and colleagues recently demonstrated the intriguing presynaptic plasticity role of aSyn, wherein aSyn facilitates dopamine (neurotransmitter) release during short bursts of neuronal activity (that lasts a

few seconds) and impedes its release during the interval (that lasts a few minutes) between bursts in monoaminergic neurons²⁴. Therefore, neurotransmitter release and SNARE complex assembly are processes that are dependent on aSyn. The critical role of the C-terminus in SNARE complex assembly is further highlighted by the fact that C-terminal truncated (1-95) aSyn failed to promote SNARE-complex assembly²⁰. Since C-terminus harbors several PTM sites, these could likely act as molecular switches during the rapid SNARE-complex assembly and disassembly during increased synaptic activity or neurotransmission. Future studies are required to decipher the role of PTMs on SNARE-complex assembly and how they can regulate the sequence of events associated with this non-classical aSyn function during neurotransmission.

Although several truncated fragments have been detected in the brains of control or healthy individuals¹⁴⁵⁻¹⁴⁸ (Figure 1.3), it is unclear whether these irreversible modifications regulate aSyn normal functions or are generated to create new functional forms of the protein. It is most likely that truncations in the N-terminus or NAC domains involving the first ~100 residues of aSyn could affect the helical structure formation and its binding to membranes, thereby influencing synaptic vesicle homeostasis and exocytosis. The observation that, C-terminal truncations enhance aSyn aggregations^{6,89,124,149,150} argues against a potential functional role for these species unless they are stabilized by interaction or complex formation with other proteins or are formed in the context of a stable native form of aSyn, for example, membrane-bound aSyn species. Interestingly, Sulzer and colleagues reported that T-cells recognize specific aSyn peptides (that include a.a. 31-46 and a.a. 116-140, which harbor pY39 and pS129, respectively) generated by abnormal processing could result in helper and cytotoxic T-cell immune responses³¹. These peptides occur within the region that harbor PTMs and are part of protein fragments that are produced by cleavages that are known to occur under both physiological and pathogenic conditions.

1.2.3 The interplay between aSyn subcellular localization and PTMs

In 1988, Maroteux et al. reported the presence of a neuron-specific protein localized to the nucleus and presynaptic terminals, that they named Synuclein¹. Since then, several studies have sought to decipher the potential role of aSyn in the nucleus. Inside the nucleus, aSyn has been reported to i) interact with histone deacetylases and cause neurotoxicity when transfected with aSyn (tagged with nuclear localization signal) in SH-SY5Y neuroblastoma cells⁸⁴; ii) enhance binding to Rab8a (a Rab GTPase), which modulates post-Golgi vesicle trafficking and reduces cellular toxicity¹⁵¹ in a fruit fly model of PD

overexpressing human aSyn; and iii) bind to DNA double-strand break (DSB) and is involved in DNA repair mechanisms by facilitating catalysis of DNA end-joining by T4¹⁵².

Several observations in cell-based¹⁵³⁻¹⁵⁶ and animal model systems^{82,157-160} have suggested preferential accumulation of pS129 aSyn in the nucleus. Using a photoactivation-based approach, Goncalves and Outerio investigated aSyn intracellular dynamics in cell cultures and reported that, phosphorylation at S129 plays a role in shuttling aSyn between the cytosol and nuclear compartment¹⁶¹. The PD-linked familial mutations G51D¹⁶² and E46K¹⁶³ exhibit a more pronounced increase in pS129 aSyn level in the nucleus than the wild-type protein or other PD-linked variants. Despite the detection of pS129 by immunohistochemical and fluorescence microscopy approaches by a different group³³, biochemical evidence for nuclear pS129 aSyn remains limited, i.e. only aSyn but not pS129 was detectable in nuclear fraction by Western blotting or other biochemical methods. Previously, our lab provided evidence that pS129 can be detected in nuclear fractions by dot blots, but not by WB and suggested that this could be explained because the pS129 nuclear signal arises from the presence of a C-terminal phosphorylated peptide rather than the full-length protein¹⁶³. This could explain why the detection of pS129 by the standard SDS electrophoresis techniques is difficult. Another important consideration is the non-specific cross-reactivity of certain pS129 antibodies to some nuclear proteins that might share a partial homology epitope of pS129 antibodies^{163,164}.

Recently, new reports are emerging that focus on the role of PTM modifications on the localization and cellular functions of aSyn. For example, a study by Burman et al⁸⁸ demonstrated that phosphorylation at Y39 impairs the interaction of aSyn with chaperones HSC70 and HSP90 β , disrupts aSyn transient membrane binding, and results in re-localization of aSyn to mitochondria. In addition, phosphorylation at S129 has been reported to modulate gene expression and overall cellular homeostasis¹⁶⁵. In addition, few groups have reported the involvement of different aSyn domains where PTMs are known to occur in regulating the subcellular localization of aSyn. For instance, the first 32 a.a. residues of the N-terminus of aSyn are necessary for mitochondrial localization¹⁶⁶. Ma et al. demonstrated that N-terminus (a.a. residues 1-60) and C-terminus (a.a. residues 103-140) are required for the nuclear transport of aSyn¹⁶⁷. These, along with other reports (reviewed in ¹⁶⁸), establish the localization and interaction of aSyn with various organelles. These studies suggest that PTMs occurring in the N- and C-termini could have a broader impact on the aSyn localization and its associated functions. However, the majority of these findings were obtained from aSyn overexpression model systems (transfected mammalian cells, neurons, transgenic

animals or AAV mediated overexpression). Therefore, further studies are essential to establish whether these potential interactions and functional roles are also relevant under physiological conditions.

1.2.4 The role of PTMs in regulating aSyn clearance

Several lines of evidence suggest PTMs play an important role in regulating aSyn degradation mediated by both the proteasomal and the lysosomal systems¹⁶⁹. Chau and colleagues provided the first line of evidence on cross-talk between phosphorylation at S129 and aSyn degradation. They demonstrate that inhibition of the ubiquitin-proteasome system causes increased pS129 levels in human neuroblastoma cells¹⁷⁰. In a follow-up study, it was demonstrated that inhibition of autophagy-lysosomal degradation pathways causes the accumulation of pS129 levels in human neuroblastoma cells and rat cortical primary neurons¹⁷¹. The discovery of several enzymes that regulate aSyn phosphorylation at Y39 by c-Abl¹³³, at S129 by: PLK2^{155,172,173}, CK1 and CK2^{138,174-177}, GRKs^{138,177,178}, and LRRK2¹⁷⁹ paved the way for cellular and *in vivo* studies to investigate further the role of phosphorylation in regulating aSyn cellular properties and clearance. The polo-like kinase PLK2, which phosphorylates aSyn specifically at S129, forms a complex with aSyn and facilitates its degradation by autophagy-lysosomal pathways¹⁷³. This finding has been replicated in a yeast model of PD wherein substitution of Serine 129 by Alanine compromised clearance of aSyn via autophagy-mediated degradation pathways¹⁸⁰. Recently, Jensen and colleagues proposed an alternative mechanism for the regulation of aSyn levels by PLK2 by wherein PLK2 regulates aSyn levels through modulation of aSyn mRNA production¹⁸¹. In addition, LRRK2 is also known to phosphorylate aSyn at S129¹⁷⁹ and mutations such as G2019S in LRRK2 have been shown to increase aSyn clearance by enhancing autolysosome formation¹⁸².

Though phosphorylation at S129 was shown to enhance aSyn clearance, c-Abl mediated phosphorylation at Y39 (and also to a lesser extent at Y125) prevents its degradation via the autophagic and proteasomal pathways^{133,183}. Conversely, the pharmacological inhibition of c-Abl kinase activity induces aSyn protein degradation via both autophagy and proteasome pathways¹³³. These studies suggest that kinases that phosphorylate at Y39 and S129 play important roles in regulating aSyn levels and life cycle in response to different stressors or neuronal activity.

The UPS systems have been implicated in the degradation of aSyn^{157,169,184-186}. For example, pharmacological inhibition of UPS systems results in the accumulation of aSyn positive aggregates in the cellular and animal model systems of PD, which could be due to the failure of the proteasomal degradation pathways. Several ubiquitin ligases that ubiquitinate aSyn at multiple site have been identified, e.g.,

Nedd4 ligases^{186,187}, reticulocyte-derived ubiquitin ligase¹⁸⁸, a cullin-RING ubiquitin ligase¹⁸⁹. Ubiquitination of aSyn by these ligases has been shown to modulate aSyn degradation. For instance, Nedd4 overexpression results in the degradation of endogenous aSyn by the endosomal-lysosomal pathways¹⁸⁶ while the cullin-RING ubiquitin ligase ubiquitinates the internalized aSyn fibrils and promotes their degradation by the proteasomal and lysosomal pathways¹⁸⁹. Recently, Lashuel, Brik and Pratt labs developed methods that enable the generation of site-specifically ubiquitinated aSyn proteins *in vitro*¹⁹⁰⁻¹⁹². These advances have enabled systematic studies to determine ubiquitination could serve as a signal for degradation of aSyn. Towards this goal, Haj et al used semisynthetic protein strategies to generate mono-, di- and tetra-ubiquitinated aSyn and demonstrated that polyubiquitination is a signal for the degradation by the proteasome system. However, to the best of our knowledge there are no reports that investigated the influence of site-specific ubiquitination at K12, 21, 23 (lysine residues that are shown to be ubiquitinated in LBs) on physiological aSyn function. Future studies are required to address these.

1.2.5 aSyn PTM-dependent Interactome- a Window to understanding aSyn functions

One way to gain insights into proteins' normal function is by elucidating their native interactions with other proteins, membranes, and various organelles. Consequently, interactome studies allow mapping the biological processes and pathways wherein aSyn could act in the different cellular environments and cell types. Given that PTMs cluster in the regions implicated in regulating aSyn interactome and membrane binding, it is likely that they play important roles in regulating its interactome.

Previous studies have attempted to map the interactome of aSyn using a combination of techniques and identified several proteins that interact with aSyn, including synaptic proteins, mitochondrial proteins, endoplasmic reticulum proteins, cytoplasmic proteins, nuclear proteins, proteins associated with chaperones, cytoskeletons, protein synthesis and ribosomal proteins^{193,194}. Interestingly, Chung et al., recently combined an ascorbate peroxidase (APEX) tag-based strategy with mass spectrometry to identify proteins that interact with aSyn. This method allowed them to perform labeling in live neurons and facilitated the preservation of all membranes and aSyn-protein interactions (including transient interactions). They reported a total of 225 aSyn protein interactors, including synaptic proteins, proteins involved in endocytosis, vesicle trafficking and protein transport, the retromer complex, cytoskeleton proteins, serine/threonine-specific phosphatases, and mRNA binding proteins¹⁹⁵. Only one study has attempted to assess the effect of PTMs on modulating aSyn interactome using co-immunoprecipitation in conjunction with the mass spectrometry-based approach. McFarland and colleagues investigated the role of phosphorylation at either Y125 or S129 separately, using peptides comprising residues 101-140 on the

aSyn interactome¹⁹⁶. They showed that phosphorylated peptides (comprising either Y125 or S129) interact preferentially with some of the cytoskeleton proteins, vesicular trafficking proteins, and enzymes involved in serine phosphorylation. In contrast, the non-phosphorylated peptide preferentially interacts with mitochondrial electron transport chain complexes¹⁹⁶. This study highlights the strong impact of PTMs such as phosphorylation at S129 and Y125 or C-terminal truncations on modifying the aSyn interactome and its cellular properties. However, future studies are needed to validate these findings and reassess the effect of each PTM or multiple PTMs in the context of the full-length protein. As it is evident from these interactome studies, aSyn seems to be involved in a diverse set of functions ranging from inducing membrane curvature to the regulation of organellar function to the maintenance of synaptic vesicles at the presynaptic terminals. These different functions are modulated by different domains of aSyn. Therefore, PTMs occurring in different domains could act as molecular switches for regulating its interactome with other proteins, membranes of organelles and, therefore its functions in different subcellular compartments or cell types. Additional studies are required to delineate the sequence- and PTM-dependent interactome of endogenous aSyn and its role in regulating aSyn function in health and disease.

1.3 aSyn in disease

1.3.1 Parkinson's disease: clinical symptoms and pathological hallmarks

Parkinson's disease (PD) is a chronic and progressive neurodegenerative disease affecting 2-3% of the population over 65 years of age – PD is mainly sporadic, with only about 5-10% familial cases¹⁹⁷. PD is clinically diagnosed based on primary motor symptoms such as rigidity, resting tremor and bradykinesia and secondary motor symptoms such as gait and handwriting impairment, speech and precision grip difficulties¹⁹⁸. In addition, PD patients suffer from non-motor symptoms such as depression, apathy, anxiety, anhedonia, sleep disorders, restless legs, REM behavior disorder, insomnia, dribbling of saliva, nausea, constipation, pain and olfactory deficits¹⁹⁹, much of which usually precedes the motor symptoms.

The major pathological hallmarks of PD include loss of neuromelanin containing SNc dopaminergic (DA) neurons, accumulation of LBs and aSyn aggregates in the cytoplasm of neurons and glial cells (e.g., astrocytes)^{200,201}, astrogliosis and microgliosis²⁰². In PD brains, LBs are not only observed in early affected SN DA neurons but also in various other neurons in brain regions such as amygdala (AM), pedunculopontine nucleus (PPN), claustrum (Cl), locus coeruleus (LC), dorsal motor nucleus of the vagus

(DMV), median raphe nucleus (MRN), lateral hypothalamus (LH), ventral tegmental area (VTA)^{203,204} as well as in astrocytes²⁰¹ and oligodendrocytes²⁰⁵.

1.3.2 Lewy bodies

Initial analysis of LBs relied on conventional histological staining techniques such as Hematoxylin and Eosin (H&E), which showed brainstem LBs as dense spherical structures with the eosinophilic core, and a small pale halo. Cortical LBs lacked halo-like structure²⁰⁶. Ultrastructural studies showed that LBs are comprised of filamentous fibrillar proteins⁵. The discovery of mutations in the gene that code for the presynaptic protein aSyn in families with early-onset PD led to the identification of aSyn as the primary constituents of the fibrillary aggregates in LBs and glial inclusions^{4,5}. Subsequently, *in vitro* studies confirmed that recombinant aSyn could abnormally aggregate and form β -sheet rich fibrils that similar to those isolated post-mortems from PD brains. Although the complete inventory of the proteins within LBs remains lacking, several studies have shown that LBs contain a considerable fraction of post-translationally modified forms of aSyn. Further studies revealed that LBs contain a considerable fraction of post-translationally modified (e.g., phosphorylated at serine 129 (S129)^{207,208}, S87²⁰⁹, Y125²¹⁰, ubiquitinated²¹¹, truncated¹⁴⁵, and p62-positive aSyn²¹² (Figure 1.5).

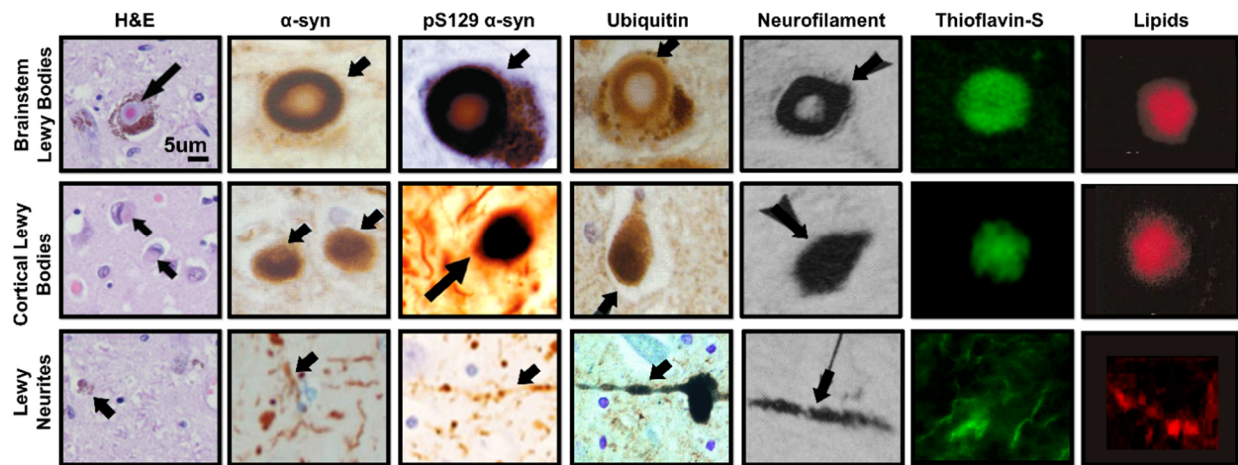


Figure 1.5. Histological properties of LBs and LNs. Morphology of brainstem Lewy bodies (LBs), cortical LBs and Lewy neurites (LNs) from histological sections of brains from individuals with Parkinson disease stained with hematoxylin and eosin (H&E)²⁰⁶, antibodies for aSyn^{206,149}, phosphorylated aSyn at S129 (pS129)^{207,213}, ubiquitin^{7,149} and neurofilament²¹⁴⁻²¹⁸, thioflavin S²¹⁹⁻²²¹ and Nile red (for lipid staining)^{222,223}. LB and LN structures are denoted by arrows (adapted from ²²⁴).

Morphologically distinct aSyn positive inclusions ranging from punctate aSyn with or without aggregation center, pale body-type (PB) with small and moderately granular aggregates, PBs with spherical bodies at their peripheries (PB/LB-type), and classical LB types with a central core and surrounding halo-like structures in the cell bodies have been described^{149,225}. Also, globular, fusiform morphology with granular texture outside the cell bodies and filamentous types in neurites were identified in nigral neurons of patients with PD²²⁶.

The morphological features of LBs is distinct in different brain regions as well as in different synucleinopathies. Several studies have attempted to explain this using chronological staging of disease development. This has been achieved primarily through immunohistochemical analysis of postmortem tissues of PD patients who died at different stages of the disease. Five stages have been proposed for brainstem LBs²²⁷ and six stages for the formation and maturation of cortical LBs²²⁸. Whether the morphological polymorphisms of LBs reflect different stages of pathology formation, different types of aggregates or aSyn pathology of varying composition remain unknown. Moreover, our knowledge regarding the contribution of molecular, cellular, and functional properties of particular cell types to develop distinct LBs remains incomplete. Based on elaborated immunohistological analyses of PD brains exhibiting LB pathology, Braak and colleagues proposed a staging hypothesis to describe PD progression which suggests that LB pathology begins either in olfactory and/or enteric neurons and subsequently spreads to other vulnerable brain regions in a retrograde or anterograde manner in sporadic PD^{203,229,230}. The Braak staging hypothesis on spreading of aSyn pathology from enteric nervous system (ENS) to central nervous system (CNS) involves spread via the vagal nerve and the DMV in the medulla oblongata, and thereafter from lower brainstem regions to the SN, eventually spreading to cortical regions^{203,231}.

1.3.3 Composition of LBs

To date, more than 100 additional proteins have been detected within LBs by immunohistochemical analysis. Initial studies identified proteins that were found in other pathological inclusions associated with other diseases, as well as cytoskeletal proteins (e.g., neurofilaments, tubulin, paired helical filaments^{225,232-239}). Later studies revealed proteins involved in various cellular processes, including proteasomal and lysosomal degradation, phosphorylation, mitochondrial function, cell cycle regulation and others (summarized in Table 1.1). As this approach has limited throughput for investigating biological pathways involved in or impacted by LB formation and maturation during disease pathogenesis, a few studies opted to perform mass spectrometry analyses to obtain the complete, unbiased proteomic profiles of LB inclusions in the brains of PD patients.

Table 1.1: Components of LBs based on immunohistochemical studies (modified from²⁴⁰). Abbreviations: B-LB: brainstem LBs; C-LB: cortical LBs; +: present; +/-: partially or weakly present; -: not-present; ND: not described; IHC: Immunohistochemistry (adapted from²²⁴)

Components	By IHC		References	Components	By IHC		References
	B- LB	C-LB			B- LB	C-LB	
α-synuclein	+	+	5, 149,207	heme oxygenase-1	+	+	241 242
Neurofilament	+	+	218,243	αB-crystallin	-	+/-	244 245
Agrin	+	ND	246	Superoxide dismutase 1	+	ND	247
14-3-3 protein	+	+	248 249	Superoxide dismutase 2	+/-	ND	247
Microtubule-associated protein (MAP) 1B	+	+	250,251	Calcium2+/ calmodulin-dependent protein kinase II	+	+	252
Synphilin-1	+	+	253 254,255	Casein kinase II	+	ND	256
Tau	+/-	+/-	257 258	Cyclin-dependent kinase 5	+	+	259 260
FKBP12	+	ND	261	Extracellular signal-regulated kinases	+	-	262
Dorfin	+	+	263 263	G-protein coupled receptor kinase 5	+	-	178
Glycogen synthase kinase-3β	+	-	264	Glycogen synthase kinase-3β	+	-	264
NUB1	+	+	265 266	Leucine-rich repeat kinase 2 (LRRK2)	+	+	267-269
Prolyl-isomerase Pin 1	+	ND	270	PINK-1	+/-	-	271
Parkin	+	+	272, 273	C-Abl	+	ND	274
SIAH-1	+	ND	275	Ikbα	+	+	276
Ubiquitin	+	+	277 278	Nfkb	+	+	279 280
Ubiquitin activating enzyme (E1)	+	+	281	P35	+	+	282
Ubiquitin-conjugating enzyme (E2) (UbcH7)	+	ND	272	Phospholipase C-δ	-	+/-	283
Dorfin	+	+	263 263	Phospholipase A2, Group VI (PLA2G6)	+	-	284
Parkin	+	+	272, 273	Tissue transglutaminase	+	ND	285
SIAH-1	+	ND	275	Map 1	+	-	286,287
TRAF 6	+	ND	288	MAP 1B	+	+	250 251
TRIM 9	+	+	289	MAP2	+	+/-	286 290 287,291
ATPase of the 26 S proteasome	ND	+/-	292	Tau	+/-	+/-	257 258
Proteasome	+	+	293 294	Neurofilament	+	+	218 243
Proteasome activators (PA700, PA28)	+	+	281	Sept4/H5	+	+	295
β-TrCP	+	+	280	Tubulin	+	ND	286
Cullin-1	+	+	280	Tubulin polymerization promoting protein/p25	+	+	296 297
HDAC4	+	+	298	MARK 1 and 2	+	+	
Multicatalytic proteinase	+/-	+	276 299	Cox IV	+/-	+	300
NEDD8	+	+	301 302	Cytochrome C	+	-	303
NUB1	+	+	265,266	Omi/htra2	+	ND	304 305
p38	+	ND	306	Pink-1	+/-	-	271
p62/sequestosome 1	+	ND	226	Pdha1	+	-	284
ROC1	+	+	280	Cyclin B	+	ND	307
Ubiquitin C-terminal hydrolase	ND	+	244	Retinoblastoma protein	+	-	308
LC3	+	+	309 310 311	Amyloid precursor protein	+	+/-	312
GABARAP/GABARAPL1	+	+	311	Calbindin	+	ND	313
GATE-16	+	+	311	Choline acetyltransferase	+/-	-	314
Glucocerebrosidase	+	+	315	Chromogranin A	+	+	279,316
NBR1	+	+	317	Synaptophysin	+/-	+/-	290,316
γ-tubulin	+	ND	286	Synaptotagmin	+	ND	318
HDAC6	+	+	319 320	Tyrosine hydroxylase (TH)	+	ND	321 314 322
Pericentrin	+	+	281	Vesicular monoamine transporter 2	+	-	323
C terminus of Hsp70-Interacting protein	+	ND	324	Complement proteins (c3d, c4d, C7, and C9))	+/-	+/-	279,325,326
Clusterin/apolipoprotein J	+/-	+	327	Immunoglobulin (igg)	+	ND	328
Dnajb6	+	+	329	Lipids	+	+	330 331
Heat-shock proteins (Hsp 27, 40, 60, 70, 90, 110)	+	+	332,333	Ykl-40	ND	+	334
Torsin A	+	+	333,335,336	Charged Multivesicular Body Protein 2B (CHMP2B)	+	+/-	337 338
Interferon-induced protein (MxA)	+/-	ND	339	Vps4	+	+	340
Proteins involved in glycoxidation (advanced glycation endproducts)	+	+	241 341	Synapsin III	+	ND	342
Caspase-cleaved TDP-43	+	+	343	Tmem230	+	+	344
DJ-1	+/-	-	345,346	Non-selenium glutathione peroxidase	+	+	347
FOXO3a	+	+	348				

Proteomic analysis of LB inclusions isolated using laser capture microdissection (LCM) from cortical neurons of patients with cortical LB disease with dementia identified a total of 296 proteins that were suggested as components of cortical LBs³⁴⁹. Interestingly, these proteins are involved in a wide array of cellular processes, such as the ubiquitin-proteasome system (UPS) (UCH-L1, ubiquitin-activating enzyme E1), folding and intracellular trafficking (heat shock cognate 71 kDa or HSC 70, 14-3-3 protein), oxidative stress (carbonyl reductase, glutathione S-transferase M3), synaptic transmission and vesicular transport (synaptotagmin-1, clathrin coat assembly protein, connexin-43), and signal transduction and apoptosis (calcium/calmodulin protein kinase, excitatory amino acid transporter and ras-GTPase-activating protein binding protein)³⁴⁹. However, this study did not report the relative abundance of these proteins in patients due to the lack of a control group. It is noteworthy that in contrast to mass spectrometry analyses of isolated LBs, several studies have performed proteomic analysis of LB-containing brain tissues such as the substantia nigra³⁵⁰⁻³⁵³, locus coeruleus³⁵⁴, and frontal cortex³⁵⁵ from PD patients. Although these studies are useful in identifying proteins that are potentially enriched in PD patients' brains, it is not possible to determine the composition of LBs from such studies, as the number of LBs is usually small in brain sections, as evidenced by the number of LBs used to grade PD. The results of these studies are summarized in detail in these excellent reviews^{356,357}.

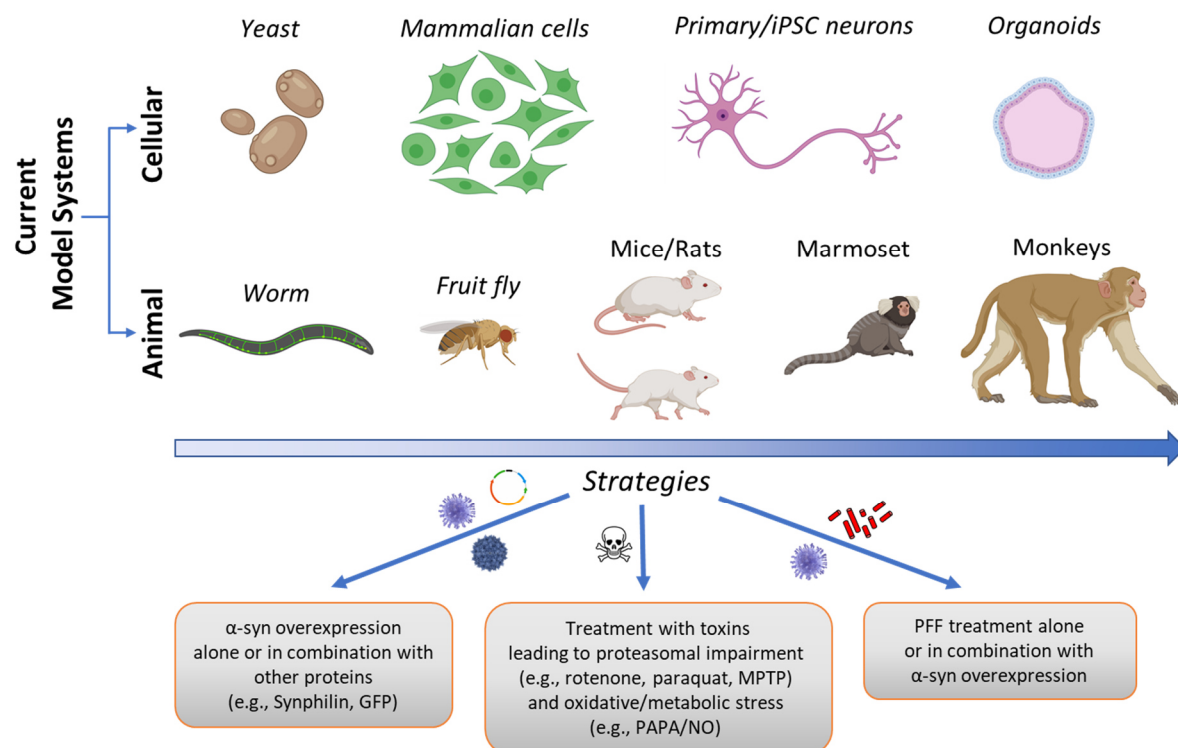


Figure 1.6: Schematic depiction of cellular and animal systems and strategies used to induce α syn aggregation and mimic PD pathology.

1.3.4 Model systems to study PD

In order to understand cellular and molecular mechanisms governing the development of LBs, their spreading and their effect on cells, many groups have employed model systems ranging from yeast, worms, fruit fly, rodents to monkeys (Figure 6). They employed strategies such as aSyn overexpression, exposure to toxins that lead to proteasomal impairment (for e.g., lactacystin, epoxomicin), mitochondrial dysfunction (for e.g., rotenone, paraquat, MPTP toxins), oxidative stress (for e.g., NO), and exposure to pre-formed fibrils (PFFs) alone or in combination with aSyn overexpression.

Initial studies employing proteasomal impairment in PC12 cells and primary neurons led to the formation of ubiquitinated inclusions, some of these showed aSyn and ThS positive^{185,358}. Similarly, oxidative/nitrative stress in neuroblastoma cell lines caused accumulation of over-expressed aSyn into insoluble aggregates³⁵⁹⁻³⁶³ that were positive for ThS and ubiquitin. Similar to the studies on proteasomal inhibition and oxidative stress, several groups have employed pharmacological agents to induce mitochondrial dysfunction. Acute and chronic MPTP administration lead to neuronal cell death³⁶⁴, only a few of these models with the chronic treatment developed neuronal inclusions^{365,366}. However, these results are not reproduced in other studies^{367,368}, and the inclusions formed in these studies were made of concentric membranes with disorganized aSyn fibrils³⁶⁵, or granular and filamentous accumulations of proteins and lipofuscin granules^{369,370}. Unfortunately, none of these models were successful in reproducing the formation of authentic LBs.

These models express higher aSyn levels compared to its physiological level and this increased levels could create a new pool of nonphysiological forms of aSyn and unintended functions of aSyn. In order to overcome these limitations, Virginia Lee and colleagues developed the neuronal seeding-based cellular and rodent models of aSyn aggregation and fibril¹⁵, which does not require overexpression of aSyn. These models are based on exposure of primary neurons to aSyn PFFs or their intracerebral injections where in the PFFs act as seeds to recruit endogenous aSyn, that later develop into LB-like inclusions. PFFs based model consistently induced the formation of aSyn aggregates that exhibit many features of authentic LBs such as hyperphosphorylation at pS129, ubiquitination, ThS reactivity and fibrillar ultrastructure in untransfected primary neurons^{15,371}. Similarly, injection of PFFs into mice brain induced formation of pS129 positive aggregates in several brain regions and resulted in 35% reduction in SN dopamine neurons at 180 days post-injection and behavioral deficits reflecting pathology and symptoms in PD patients³⁷². Different cellular and animal model systems and to what extent they reproduce key features of LBs are summarized in heatmaps (Table 1.2 and Table 1.3, adapted from ²²⁴)

Table 1.2. Summary of studies modeling aSyn aggregation in cellular model systems of PD²²⁴

Cellular Models of PD												
	Study by	Level of Characterization										
		A	B	C	D	E	F	G	H	I	J	K
1	Tabrizi et al., 2000 ¹⁷³											
	Stefanis et al., 2001 ¹⁷⁴											
	Tofaris et al., 2001 ¹⁷⁶											
	Matsuzaki et al., 2004 ¹⁷⁷											
	Pandey et al., 2006 ¹⁷⁸											
	Vekrellis et al., 2009 ¹⁷⁹											
	Welander et al., 2011 ¹⁸⁰											
	Burre et al., 2015 ¹⁸¹											
	Fares et al., 2016 ¹⁸²											
	Melnikova et al., 2020 ¹⁸⁴											
2	Engelender et al., 1999 ¹⁸⁵											
	O'Farrell et al., 2001 ¹⁸⁷											
	Tanaka et al., 2003											
	Lee et al., 2004 ¹⁸⁹											
	Smith et al., 2005 ¹⁹²											
	Buttner et al., 2010 ¹⁹³											
	Xie et al., 2010 ¹⁹⁴											
	Klucken et al., 2012 ¹⁹⁶											
	McLean et al., 2001 ¹⁷⁵											
	Outeiro and Lindquist, 2003 ¹⁹⁹											
3	Gitler et al., 2008 ⁴⁰¹											
	Opazo et al., 2008 ⁴⁰³											
	Soper et al., 2011 ⁴⁰⁵											
	Pranke et al., 2011 ⁴⁰⁷											
	Hansen et al., 2011 ⁴⁰⁹											
	Lazaro et al., 2016 ⁴¹⁰											
	Raiss et al., 2016 ⁴¹²											
	Dettmer et al., 2017 ⁴¹⁴											
	Xiao et al., 2018 ⁴¹⁵											
	Imberdis et al., 2019 ⁴¹⁷											
4	Lopes da Fonseca et al., 2016 ⁴²¹											
	Wang et al., 2019 ⁴²³											
5	Roberti et al., 2007 ⁴²⁵											
	Roberts et al., 2015 ⁴²⁷											
6	Devine et al., 2010 ⁴²⁸											
	Byers et al., 2011 ⁴²⁹											
	Soldner et al., 2011 ⁴³⁰											
	Chung et al., 2013 ⁴³¹											
	Ryan et al., 2013 ⁴³²											
	Flieri et al., 2014 ⁴³³											
	Oliveira et al., 2015 ⁴³⁴											
	Dettmer et al., 2015 ⁴³⁵											
	Lin et al., 2016 ⁴³⁶											
	Kouroupi et al., 2017 ⁴³⁷											
	Zambon et al., 2019 ⁴³⁸											

Cellular Models of PD												
	Study by	Level of Characterization										
		A	B	C	D	E	F	G	H	I	J	K
7	Ostrovova-Golts et al., 2000 ¹⁸⁰											
	McLean et al., 2001 ¹⁷⁵											
	Paxinou et al., 2001 ¹⁸³											
	Rideout et al., 2001 ¹⁸⁵											
	Tofaris et al., 2001 ¹⁷⁶											
	McNaught et al., 2002 ²⁸¹											
	Sherer et al., 2002 ²⁵⁹											
	Rideout et al., 2004 ¹⁸⁸											
	Trimmer et al., 2004 ⁴⁸³											
	Lee et al., 2002 ¹⁸²											
8	Danzer et al., 2007 ¹⁸⁶											
	Luk et al., 2009 ¹⁷¹											
	Desplats et al., 2009 ¹⁸⁸											
	Nonaka et al., 2010 ¹⁹⁰											
	Waxman and Giasson, 2011 ¹⁹²											
	Volpicelli-Daley et al., 2011 ¹¹⁵											
	Dryanovski et al., 2013 ¹⁹⁵											
	Volpicelli-Daley et al., 2014 ¹⁹⁷											
	Tran et al., 2015 ¹⁹⁸											
	Domert et al., 2016 ⁴⁰⁰											
	Mao et al., 2016 ⁴⁰²											
	Tapias et al., 2017 ⁴⁰⁴											
	Henderson et al., 2017 ⁴⁰⁶											
	Froula et al., 2018 ⁴⁰⁸											
	Mahul-Mellier et al., 2018 ³⁹											
	Grassi et al., 2018 ⁴¹¹											
	Wang et al., 2019 ⁴¹³											
	Wu et al., 2019 ¹⁷											
	Wu et al., 2019 ¹¹⁶											
	Grassi et al., 2019 ⁴¹⁸											
	Shrivastava et al., 2020 ⁴²⁰											
	Lautenschläger et al., 2020 ⁴²²											
	Morgan et al., 2020 ⁴²⁴											
	Courte et al., 2020 ⁴²⁶											
	Mahul-Mellier et al., 2020 ¹⁵											

Study Strategies

- 1 Overexpression of WT or Mutant α-syn
- 2 Overexpression of α-syn in Combination with Synphilin-1
- 3 Overexpression of α-syn Fused to Fluorescent Proteins
- 4 Overexpression of α-syn with Other Proteins
- 5 Overexpression of α-syn Tagged with Short Peptides
- 6 iPSC based models
- 7 Toxin Based Cellular Models
- 8 Cellular Models of LB Propagation

Level of characterization

- A Appearance of Inclusion-like Structures
- B pS129
- C Ubiquitin
- D p62
- E ThS/ ThT/ Amytracker/ other amyloid dyes
- F Proteinase K Resistant
- G Insoluble by Sedimentation/Fractionation
- H Presence of HMW bands
- I Aggregates by Ultrastructural Characterization
- J Seeding Activity
- K Presence of Lipids or Membranous organelles

	Positive
	Negative
	Not described
	Mixed Results/ Not Clear

Note:

"Δ" symbol indicates presence of fibrillar α-syn in inclusions identified by ultrastructural characterization (electron microscopy).

HMW bands are defined as size of α-syn protein band > 30 kDa by Western blots

Table 1.3. Summary of studies modelling aSyn aggregation in animal model systems of PD²²⁴

		Animal Models of PD										
	Study by	Level of Characterization										
		A	B	C	D	E	F	G	H	I	J	K
1	Feany and Bender et al., 2000 ⁴¹³									Δ		
	Auluck et al., 2002 ²³²											
	Takahashi et al., 2003 ⁴⁴²											
	Chen and Feany, 2005 ⁴⁴³									ω		
	Ordonez et al., 2018 ⁴⁴⁴											
2	Lakso et al., 2003 ⁴⁴⁵											
	Kuwahara et al., 2006 ⁴⁴⁶											
	Van Ham et al., 2008 ⁴⁴⁸											
	Maslah et al., 2000 ⁴⁴⁷											
	Van der Putten et al., 2000 ⁴⁴⁹											
3	Matsuoka et al., 2001 ⁴⁵³											
	Kahle et al., 2001 ⁴⁵⁵											
	Rieker et al., 2011 ⁴⁵⁷									Δ		
	Giasson et al., 2002 ⁴⁵⁹									Δ		
	Klein et al., 2002 ⁴⁶¹											
	Kirik et al., 2002 ⁴⁶³											
	Lee et al., 2002 ⁴⁶⁵											
	Lo Bianco et al., 2002 ⁴⁶⁷											
	Richfield et al., 2002 ⁴⁶⁹											
	Rockenstein et al., 2002 ⁴⁷¹											
	Neumann et al., 2002 ⁴⁷³									Δ		
	Gomez-Isla et al., 2003 ⁴⁷⁵											
	Kirik et al., 2003 ⁴⁷⁷											
	Lauwers et al., 2003 ⁴⁷⁹											
	Thiruchelvam et al., 2004 ⁴⁸¹											
	Yamada et al., 2004 ⁴⁸³											
	Chandra et al., 2005 ⁴⁸⁵											
	Eslamboli et al., 2007 ⁴⁸⁷											
	Wakamatsu et al., 2007 ⁴⁸⁸											
	St Martin et al., 2007 ⁴⁹⁰											
	Nuber et al., 2008 ⁴⁹²											
	Wakamatsu et al., 2008 ⁴⁹⁴											
	Azeredo de Silveira et al., 2009 ⁴⁹⁶											
	Daher et al., 2009 ⁴⁹⁸											
	Cao et al., 2010 ⁵⁰⁰											
	Emmer et al., 2011 ⁵⁰²											
	Decressac et al., 2012 ⁵⁰⁴											
	Lundblad et al., 2012 ⁵⁰⁶											
	Cannon et al., 2013 ⁵⁰⁸											
	Nuber et al., 2013 ⁵⁰⁸											
	Oliveras-Salva et al., 2013 ⁵¹⁰											
	Rothman et al., 2013 ⁵¹²											
	Sastry et al., 2015 ⁵¹³											
	Thakur et al., 2017 ⁵¹⁵											
	Węgrzynowicz et al., 2019 ⁵¹⁷											
4	Meredith et al., 2002 ⁴⁶⁹											
	Fornai et al., 2005 ⁴⁶⁵									Δ		
	Shimoi et al., 2005 ⁴⁶⁷											
	Alvarez-Fischer et al., 2008 ⁴⁶⁶											
	McCormack et al., 2008 ⁴⁶³											
	Meredith et al., 2008 ⁴⁶⁹											
	Gibrat et al., 2009 ⁴⁶⁶											
	Halliday et al., 2009 ⁴⁶⁷											
	Betarbet et al., 2000 ⁴⁶⁹											
	Sherer et al., 2003 ⁴⁶³											
	McNaught et al., 2004 ⁴⁶³											
	Bedford et al., 2008 ⁴⁶⁰											
	Musgrove et al., 2019 ⁴⁶⁴											

		Animal Models of PD										
	Study by	Level of Characterization										
		A	B	C	D	E	F	G	H	I	J	K
5	Bethlem and Jager, 1960 ⁴⁴⁰											
	Hansen et al., 2011 ⁴⁴⁹											
	Mougenot et al., 2012 ⁴⁴²											
	Luk et al., 2012 ⁴⁷²											
	Luk et al., 2012 ⁴⁷²											
	Guo et al., 2013 ⁴⁴⁴											
	Watts et al., 2013 ⁴⁴⁷											
	Sacino et al., 2013 ⁴⁴⁹											
	Masuda-Suzukake et al., 2013 ⁴⁵⁰											
	Sacino et al., 2014 ⁴⁵²											
	Masuda-Suzukake et al., 2014 ⁴⁵⁴											
	Recasens et al., 2014 ⁴⁵⁶											
	Sacino et al., 2014 ⁴⁵⁸											
	Paumier et al., 2015 ⁴⁶⁰											
	Osterberg et al., 2015 ⁴⁶²											
	Peelaerts et al., 2015 ⁴⁶⁴											
	Schweighauser et al., 2015 ⁴⁶⁶											
	Luk et al., 2016 ⁴⁶⁸											
	Rey et al., 2016 ⁴⁷⁰											
	Breid et al., 2016 ⁴⁷²											
	Kim et al., 2016 ⁴⁷⁴											
	Tarutani et al., 2016 ⁴⁷⁶											
	Karampetsou et al., 2017 ⁴⁷⁸											
	Abdelmotilib et al., 2017 ⁴⁸⁰											
	Blumenstock et al., 2017 ⁴⁸²											
	Rutherford et al., 2017 ⁴⁸⁴											
	Sorrentino et al., 2017 ⁴⁸⁶											
	Harms et al., 2017 ⁴⁸⁸											
	Shimozawa et al., 2017 ⁴⁹⁰											
	Nouraei et al., 2018 ⁴⁹²											
	Luna et al., 2018 ⁴⁹⁴											
	Okuzumi et al., 2018 ⁴⁹⁶											
	Rey et al., 2018 ⁴⁹⁸											
	Duffy et al., 2018 ⁴⁹⁹											
	Sorrentino et al., 2018 ⁵⁰¹											
	Milanese et al., 2018 ⁵⁰³											
	Terada et al., 2018 ⁵⁰⁵											
	Ayers et al., 2018 ⁵⁰⁷											
	Durante et al., 2019 ⁵⁰⁹											
	Chu et al., 2019 ⁵¹¹											
	Espa et al., 2019 ⁵¹³											
	Earls et al., 2019 ⁵¹⁵											
	Hayakawa et al., 2019 ⁵¹⁷											
	Zhang et al., 2019 ⁵¹⁹											
	Burtscher et al., 2019 ⁵²¹											
	Stoyka et al., 2020 ⁵²³											
	Kuo et al., 2010 ⁴⁷⁰											
6	Pan-Montojo et al., 2010 ⁵²⁵											
	Holmgvist et al., 2014 ⁵²⁷											
	Uemura et al., 2018 ⁵²⁹											
	Manfredsson et al., 2018 ⁵³¹											
	Kim et al., 2019 ⁵³³											
	Berge et al., 2019 ⁵³⁵											
	Ahn et al., 2019 ⁵³⁷											
	Challis et al., 2020 ⁵³⁹											

Study Strategies

- 1 α-syn Overexpression in Flies
- 2 α-syn Overexpression in Worms
- 3 α-syn Overexpression in Rodents/Primates
- 4 Toxin Based Animal Models
- 5 Animal Models of LB Propagation
- 6 Animal Models - Gut to Brain Axis

Level of characterization

- A Appearance of inclusion-like structures
- B pS129
- C Ubiquitin
- D p62
- E ThS/ ThT/ Amytracker/ other amyloid dyes
- F Proteinase K resistant
- G Insoluble by Sedimentation/Fractionation
- H Presence of HMW α-syn bands by WB
- I Aggregates by Ultrastructural characterization
- J Seeding activity
- K Presence of Lipids or Membranous organelles

Positive
Negative
Not described
Mixed Results/ Not Clear

Note:

“Δ” symbol indicates presence of fibrillar α-syn in inclusions identified by ultrastructural characterization (electron microscopy).

“ω” symbol indicates fibrillar α-syn identified in brain sample extractions.

HMW bands are defined as size of α-syn protein band > 30 kDa by Western blots

1.4 aSyn misfolding and aggregation

Much of what we know about the mechanisms of aSyn aggregation (Figure 1.7) was obtained from *in vitro* studies due to lack of methods and specific probe live-monitoring of aSyn misfolding and aggregation in cells and living organisms. Accumulating evidence from many studies of aSyn aggregation and fibril formation *in vitro* has shown that the process of aSyn aggregation and the nature of its aggregates are highly dependent on changes in solution conditions (such as protein concentrations, pH, salt) and interactions with metals, small molecules, mutations, and PTMs (Table 1.4). These observations suggest that subtle changes in the cellular environments or the biochemical properties of organelles (such as lysosomes) could cause a significant alteration in the kinetics and course of aSyn aggregation and pathology formation and cellular responses to these processes. *In vitro*, The process of aSyn aggregation is a nucleation dependent polymerization reaction that has a sigmoidal growth profile with three phases: lag phase, exponential and stationary phase⁵³⁵. In the lag phase, monomers accumulate to form aggregation nuclei, which is a rate limiting step in the aggregation process. These nuclei are the smallest aggregates in the fibrillation process and are stable enough to energetically more favorable to induce nucleus growth by monomer addition⁵³⁵. The initial slow nucleation phase is characterized by the formation of ordered oligomers composed of many aSyn monomers including ring-like structures⁵³⁶. During this slow phase, long-range interactions between N- and C-terminals are disrupted allowing exposure of the non-amyloid component (NAC) region that initiates aggregation⁵³⁷. In this phase, oligomers of varying sizes, morphologies, and structural features, which are either on-pathway oligomers (which continue to form fibrils) or off pathway oligomers (that do not continue to form fibrils), are formed. During the elongation phase, growth continues via primary nucleation followed by the fragmentation and secondary nucleation steps, which contribute to exponential growth phase and result in increased growth in the number of fibrils. These processes prompt oligomers to recruit aSyn monomers to grow into β -sheet rich proto-filaments, which then intertwine to form proto-fibrils and ultimately mature fibrils. In the last step, the stationary phase (plateau) is reached due to depletion of monomers.

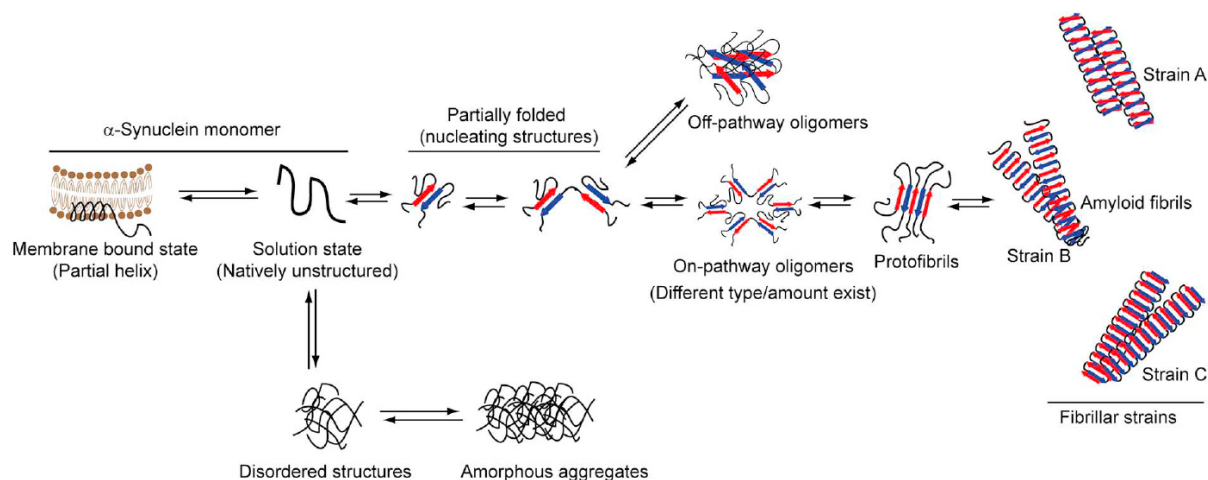


Figure 1.7: *In vitro* alpha-synuclein (aSyn) aggregation process. Different stages and intermediates underlying the formation of mature fibrils from aSyn monomers¹¹

Table 1.4. Factors affecting aSyn aggregation.

The different elements shown to influence the rate of alpha synuclein aSyn fibrillization (as elaborated in the text) are listed, with “↑” and “↓” denoting aggregation promoting and inhibiting effects, respectively. “↑/↓” refers to an inconsistent effect.

	Factor	Effect on Aggregation
Cellular microenvironment	pH	↑
	Pesticides	↑
	Metals	↑
	Lipids	↑/↓
aSyn genetic mutations	Gene duplication/triplication	↑
	Expression-increasing SNPs	↑
	Mutants: E46K, H50Q, A53T, E83Q	↑
	Mutants: A30P, G51D, A53E	↓
aSyn “LB” post translational modifications	N-terminal acetylation	No effect
	Acetylation at K6, K10, K12	↓
	Phosphorylation at Y125	No effect
	Phosphorylation at: Y39, S87	↓
	Phosphorylation at: S129	↑/↓
	O-GlcNacylation at T72, T75, T81, S87	↓
	Ubiquitination: Mono at K6, tetra at K12	↓
	Nitration at Y39, Y125, Y133, Y136	↓
	Truncations at c-terminal	↑
	Glycation at K6, K10, K12, K21, K23, K32, K34 and K43 and K45	↑

1.4.1 Evidences for and against the presence of oligomers in the brain

Several studies have been carried out to probe for the presence of oligomers in the brain and their involvement in the pathogenesis of PD. Some of the most commonly used methods to study oligomers are Immunohistochemistry, Western blotting, enzyme-linked immunosorbent assay (ELISA), immunogold labeling, proximity-ligation assay, and proteinase K-paraffin-embedded tissue (PK-PET) blot (Figure 1.8). To identify the presence of oligomers, Sharon and colleagues probed the cytosols of normal and transgenic mouse brains expressing human aSyn and the postmortem brains of patients with PD and DLB using an LB509 antibody in Western blots. They demonstrated the presence of soluble lipid-dependent aSyn oligomers and promotion of aSyn oligomerization by polyunsaturated fatty acids⁵³⁸. In support of this process, oligomers were also detected in another study using Syn33 conformational specific antibody⁵³⁹. In addition, several studies have suggested the presence of higher levels of oligomers in biological fluids, such as blood plasma and cerebrospinal fluid (CSF) in patients compared to controls^{540,541,542-544}. Interestingly, using an ELISA assay for total oligomers aSyn (Syn211) or S129-phosphorylated oligomeric-aSyn, Foulds and colleagues reported no differences in the total CSF oligomer-aSyn, CSF aSyn, or CSF pS129-aSyn in multiple system atrophy (MSA) patients compared to controls⁵⁴⁵. Many of these studies are antibody-based; thus, much of the knowledge and many of the hypotheses in the field today are based on conclusions drawn from studies relying on antibodies. However, many disadvantages associated with the antibody approach to detecting oligomers are present: (1) the use of sequence-specific antibodies that do not distinguish between oligomers and fibrils or different structural types of oligomers; (2) those that claim to be oligomer-specific are generated with the *in vitro*-prepared oligomers as immunogens. Therefore, various aSyn species detected by these so-called oligomer-specific antibodies might not capture oligomers in the actual brain pathology; and 3) some antibodies, such as A11 antibodies, are not specific for one form of amyloid and recognize a broad spectrum, for example, A11 antibody detects oligomers of a-beta, prion protein and lysozyme^{546,547}.

To overcome some of the limitations of antibody detection of monomers in the tissue samples, a PK-PET blot was developed wherein prior PK digestion allows detection of aggregates that are PK-resistant⁵⁴⁸. This method was used to detect small aSyn aggregates in synapses in the frontal and cingulate cortex of DLB patients and in the SNc of PD patients^{549,550}. However, this method fails to detect oligomers that are PK-sensitive and also this method does not distinguish between monomers and oligomers and thereby detecting mostly fibrils which show significant PK resistance.

Subsequently, the proximity ligation assay (PLA) method was developed by Alegre-Abarrategui's group⁴²⁷. In this assay, the antibody, Syn211, was conjugated to short oligonucleotides. When two antibodies are in close proximity, the oligos become ligated and act as primers for DNA polymerase to generate amplified fluorescent signals. Using this method Robert and colleagues described the presence of lightly compacted aSyn aggregates in medullary intermediary reticular zone, pyramidal cortical neurons, and reticular formation as compared to age-matched control subjects⁴²⁷. In a separate study by Sekiya and colleagues demonstrated widespread distribution and abundant accumulation of oligomer aSyn using PLA assay⁵⁵¹. This method presents an up to two-fold higher signal for oligomers compared to fibrils, and the pathology detected by this method does not rule out presence of fibrillar aSyn aggregates in the detected sample. To address this issue, new methods and techniques that allow to differentiate between many conformations of aSyn oligomers are necessary, which would allow studying their properties and relative contribution to the disease processes. This process could be performed by generating antibodies using patient-derived oligomers and using these antibodies to identify pathological aSyn oligomer diversity and their relation to disease onset and progress. Also, PET tracers that specifically detect oligomers in the brain are also required for the identification of oligomers and their role in the pathogenesis of PD. Therefore, with the development of new methods and techniques it would be possible to gain insight into early stages of aSyn aggregation, which could then be targeted for halting or slowing the disease process. Furthermore, a better and more systematic characterization of existing conformational antibodies is essential to ensure the accuracy of conclusions drawn using assays based on such antibodies.

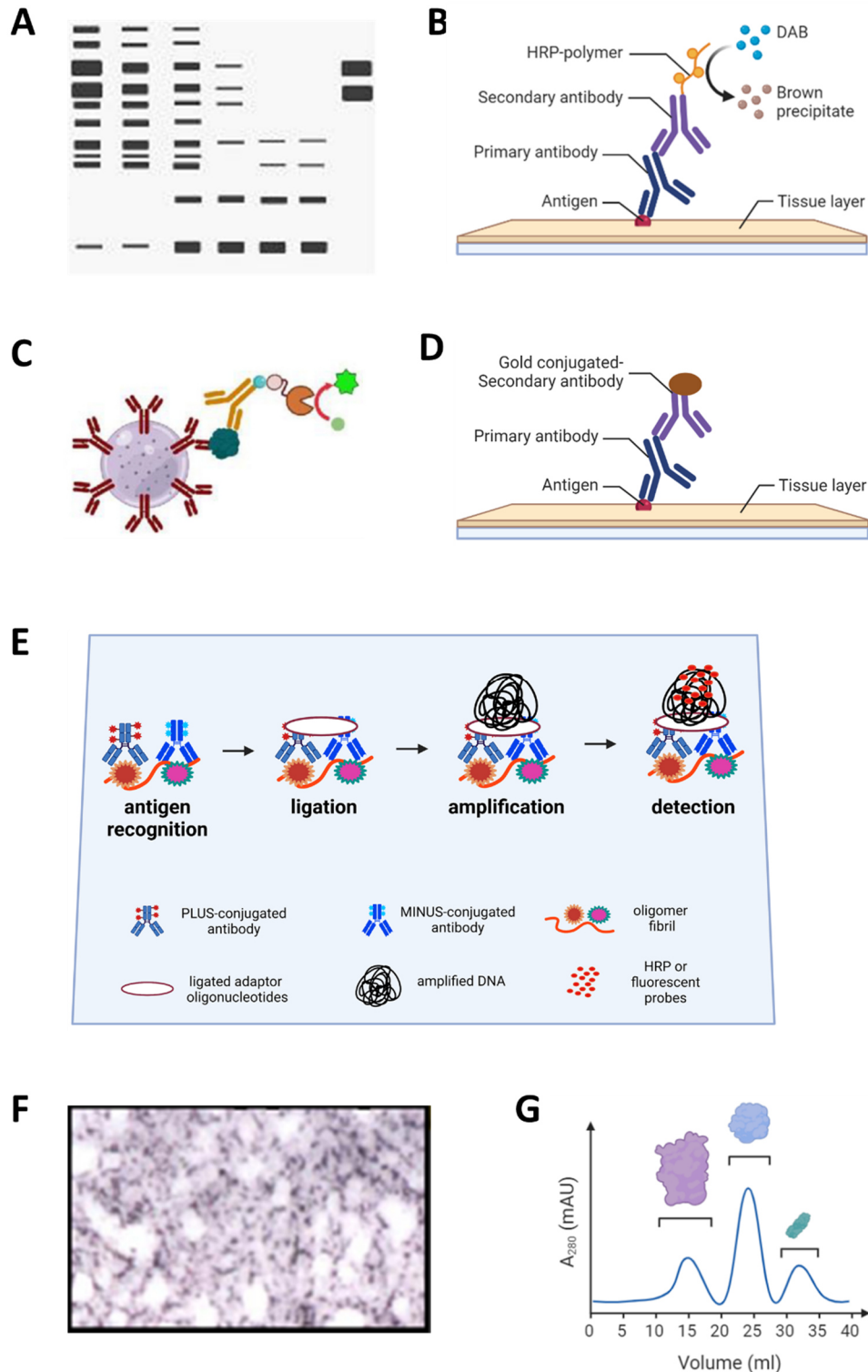


Figure 1.8: Different methods to detect oligomers in the human brain tissues. (A) Western blotting. (B) Immunohistochemistry. (C) enzyme-linked immunosorbent assay (ELISA). (D) Immunogold electron microscopy (EM). (E) proximity ligation assay. (A–E) antibody-based approaches. (F) proteinase K-paraffin-embedded tissue (PK-PET) blot-based method (from ⁵⁵⁰). (G) size-exclusion chromatography (SEC)-based method to separate them according to aSyn species size.

1.4.2 aSyn oligomer toxicity

Most of our understanding of oligomer toxicity (Table 1.5) is based on *in vitro*-generated oligomers and transgenic rodent models that express disease-causing mutations, which have been shown to induce oligomer formation.

1.4.2.1 Membrane disruptions

Several studies over the past two decades support the idea that oligomers can cause membrane disruption thus making membranes more permeable to non-specific cations and disrupting ionic homeostasis^{9,386,552}. This phenomenon is supported by the pore-forming hypothesis wherein oligomers form a membrane-spanning pore, similar to effects induced by α -hemolysin and anthrax toxin⁵⁵³. This hypothesis is further supported by several studies: (1) single-channel electrophysiology in the presence of oligomers causing step wise current flows with pore opening and closing⁵⁵⁴, (2) structural studies using cryo-electron microscopy of annular oligomers in membranes⁵⁵⁵ and solution and solid-state nuclear magnetic resonance techniques demonstrating oligomers strong membrane interactions and their structured region (with β -sheet content) inserted in lipid bilayers disrupting membrane integrity⁵⁵⁶, and (3) oligomer induced permeability is reversed by oligomer-specific A11 antibody⁵⁵⁷ and anti-aggregation compounds⁵⁵⁴.

1.4.2.2 Synaptotoxicity

aSyn is abundantly localized to synaptic terminals, and misfolding and subsequent formation of oligomers might induce synaptic dysfunction, which is believed to be an early event in PD pathogenesis. A study by Choi et al. demonstrated that dopamine-induced oligomers bind to the N-terminal domain of synaptobrevin-2 and inhibit soluble N-ethylmaleimide-sensitive factor attachment protein receptor (SNARE)-mediated lipid mixing and exocytosis. This process has important implications for the inhibition of dopamine release⁵⁵⁸. In addition, aSyn oligomers induced by oligomer-forming mutants (E46K and E57K) in iPSC cells was found to result in axonal transport disruptions and cause a reduction in polymerization (induced by oligomers) of kinesins, tubulin, and microtubule-associated proteins⁵⁵⁹. Interestingly, unmodified and 4-hydroxynonenal (HNE)-induced aSyn oligomers were also shown to impair synaptic transmission through increased activation of N-methyl-D-aspartate (NMDA) receptors, thereby leading to an increase in basal synaptic transmission and long-term potentiation (LTP)⁵⁶⁰. Impairment of LTPs was reported for oligomers prepared in the presence of the polyunsaturated fatty acid, docosahexanoic acid (DHA)⁵⁶¹. In addition, aSyn oligomers were also shown to induce synaptic dysfunction

and spatial memory impairments by targeting GluN2A-NMDA receptors⁵⁰⁷ and causing an increase in NMDA receptor activity in neurons⁵⁶². These studies suggest that aSyn oligomers promote the onset of PD via synapse impairment.

1.4.2.3 ER-stress

Endoplasmic reticulum (ER) stress markers, such as phosphorylated protein kinase RNA-like endoplasmic reticulum kinase (PERK) were shown to be upregulated in the PD brain tissues, and their increased levels were found to be correlated with aSyn aggregates⁴⁰. Using an A53T transgenic mouse model, Colla et al. report that FILA-1 reactive, A11 positive oligomers accumulate in ER/microsomes during disease progression and then promote cell death. Conversely, salubrinal, an anti-ER stress compound that has been shown to reduce the accumulation of FILA-1 reactive oligomers and delay disease onset^{563,564}. Interestingly, in another study it was shown that aSyn oligomers (but not monomers or fibrils) activate ER stress by inducing the X-box binding protein 1 (XBP-1), a transcription factor regulating transcription of chaperones and autophagy components with a profound role in adaptive responses⁵⁶⁵. Therefore, these steps point to ER stress induced by aSyn oligomers.

1.4.2.4 Mitochondrial dysfunction

aSyn oligomers have been shown to cause mitochondrial dysfunction by negatively affecting mitochondrial complex I via several actions: (1) promotion of the opening of mitochondrial permeability transition pore (mPTP) leading to swelling and cell death⁵⁶⁶ and (2) complex I-associated disruptions were also shown to cause change in mitochondrial potential, perturbations in calcium homeostasis, and promotion in the release of cytochrome C⁵⁶⁷. In addition, aSyn oligomers were shown to induce mitochondrial dysfunction through other mechanisms: (1) increased reactive oxygen species (ROS) production by binding to the mitochondrial binding element, TOM 20⁵⁶⁸, (2) mitochondrial fragmentation⁵⁶⁹, and hydrogen peroxide production in astrocytes after mitochondrial dysfunction induction⁵⁷⁰.

1.4.2.5 Proteasomal dysfunction

aSyn aggregation and ubiquitin-proteasomal dysfunction have been implicated in PD⁵⁷¹. In support of this line of thinking, aSyn oligomers were shown to block or impede 20S and 26S proteasome activity by preventing entry of proteasome substrates^{294,572}. In addition, aSyn oligomers could cause nitrosation of

parkin that resulted in parkin level reduction and eventually caused protein accumulation and cell death⁵⁷³.

Table 1.5: Proposed properties of oligomers and their effect on molecular events and cellular systems (modified from ⁵⁷⁴)

aSyn toxic oligomers		
Properties of oligomers	Molecular effects	Cellular systems disrupted
'Pore'-like structure	higher membrane permeability	Disturbed ionic homeostasis
β -sheet rich structures	Glial TLR4 activation	Enhanced neuro-inflammation
Redox active	Free radical generation	Increased oxidative stress
Exposure of hydrophobic patches	Promiscuous binding to multifunctional proteins & membranes	Sequestration of chaperones
		ER Stress and UPR activation
		Impaired proteasome function
		Impaired chaperone mediated autophagy
Altered function	Complex I inhibition	Mitochondrial fragmentation & altered bioenergetics
	Changes to mitochondrial dynamics	
	Less kinesin motility	Disruption of microtubule transport
	Lower tubulin polymerization	
	Reduced SNARE-complex chaperoning	Disturbed vesicle membrane fusion

1.5 Oligomer seeding and spreading: data from *in vitro*, cellular and animal model systems

Neuropathological observations from postmortem brains of PD patients suggest that the aSyn pathology can spread from one brain region to another, and this phenomenon can be observed in PD model systems. Studies on investigating the mechanism of aSyn seeding and pathology spreading have primarily relied on the use of aSyn fibrils. Only sparse evidence exists that supports the action of aSyn oligomeric intermediates as key mediators of aSyn spreading or seeding. This evidence was obtained from *in vitro*, cellular, and animal model systems of PD. A study by Lorenzen and colleagues reported that unmodified oligomers could cause an increase in the lag phase and delay the elongation phase⁷⁸. Interestingly, acetylated oligomers (prepared under similar conditions as unmodified oligomers) were found to delay fibril elongation by acting as auto-inhibitors of acetylated-aSyn fibril formation⁵⁷⁵. In contrast, in another study using single-molecule amplification assay, oligomers were shown to have low seeding potential compared to fibrils⁵⁷⁶. In support of oligomer seeding, Bae and colleagues reported that HNE-induced oligomers act as seeds to induce aggregation of monomeric aSyn, which could be explained by the fact

that HNE-induced oligomers prepared in this study were kept for seven days of incubation at 37 °C without agitation and the resulting HNE-induced oligomers had minimal secondary structure and more of disordered structure that resembled monomers⁵⁷⁷.

Different mechanisms, such as endocytosis³⁸⁸, trans-synaptic transfer⁵⁷⁸, endocytosis, and clathrin mediated pathway⁵⁷⁹ in the cellular model systems of PD, have been proposed for the spreading of extracellular aSyn oligomers. In 2005, Lee et al. reported that aggregated forms of aSyn could be secreted outside (via non-classical endoplasmic reticulum/Golgi-independent exocytosis) in cases in which higher levels of aSyn were expressed in SH-SY5Y cells, and this levels could increase under stress conditions that induce proteasomal dysfunction (such as via the action of MG132, a proteasomal inhibitor)¹³. Although this study demonstrated the presence of higher molecular weight aSyn bands on Western blots, it was not determined whether these bands represent oligomeric or SDS-resistant species that are SDS-induced breakdown products from aSyn fibrils. In a subsequent study, Danzer et al. reported that *in vitro*-generated oligomers (prepared in the presence of iron and ethanol) could induce seeding of aSyn aggregation in neuronal cell lines and in primary neuronal cultures⁵⁸⁰. In a follow-up study, the same group demonstrated that these oligomers could be secreted into exosomes, and their presence in exosomes could facilitate their seeding and pathological transcellular spreading of⁵⁸¹. Seeding induced by iron- and ethanol-induced oligomers could be explained by the presence of proto-fibrillar structures in their AFM analysis^{580,582}.

Although sparse evidence for seeding effect of aSyn oligomers exists, several groups have shown that aSyn oligomers can spread from one brain region to another (Table 1.6). In one study, injection of oligomers into the olfactory bulb resulted in their spreading to other brain regions⁵⁸³. No seeding was observed when rodents were injected with 4-oxo-2-nonenal (ONE)-induced oligomers⁵⁸⁴. In subsequent studies by Peelaerts et al. and Froula et al., it was demonstrated that oligomers are taken up and spread to different brain regions, but no seeding effect was observed in rodents^{408,464}. These findings suggest that cell-to-cell transfer or oligomers occurs, but whether this is the key process driving pathology spreading remains unclear.

Table 1.6: aSyn oligomer spreading *in vivo* model systems

Study by	aSyn protein	Oligomer preparation method	Oligomer character.	Injection site and duration	Amount injected	aSyn species	Uptake	Spreading	Seeding	Brain regions
Fagerqvist et al., 2013 ⁵⁸⁴	WT human aSyn	Molar ratio 30:1 (ONE:aSyn) quiescent incubation for 18hr at 37°C	AFM, ThT	Intracerebral for 4 months	40 ng, 400 ng	O	NI	NI	+/-	Cortex
Rey et al. 2013 ⁵⁸³	S-tagged WT human aSyn	50mM Tris-HCl (pH 7.5, 150 mM KCl) at 4°C for 7 days (Superose 6 HR 10/30)	TEM	Olfactory bulb and few hours to days	800 ng	M, O, F	+	+	NI	Olfactory bulb, piriform cortex, amygdala, striatum
Peelaerts et al. 2015 ⁴⁶⁴	aSyn	aSyn 4°C for 7 days	TEM	Substantia nigra, Striatum And 7day, 4 month	10 µg	M, O, F	+	+	-	Substantia nigra, striatum
Froula et al. 2019 ⁴⁰⁸	Mouse WT aSyn	12mg/ml in PBS at 37°C for 24 hr (filtration by 100kD filters)	AUC, FT-IR, CD, ThT, TEM, AFM	Striatum for 3 months	10 µg	M, O, F	+	+	-	Substantia nigra, amygdala

1.6 Cell-type dependent contributions to PD

1.6.1 Pathology spreading and neurodegeneration in PD: The staging of cell loss in PD

Based on extensive immunohistological analyses of PD brains exhibiting LB pathology, Braak and colleagues proposed a staging hypothesis to describe PD progression, which suggests that LB pathology begins either in olfactory and/or enteric neurons and subsequently spreads to other vulnerable brain regions in a retrograde or anterograde manner^{203,229,230}. The Braak staging hypothesis states that spreading of aSyn pathology from the enteric nervous system (ENS) to the central nervous system (CNS) involves spreading via the vagal nerve and the dorsal motor nucleus (DMV) in the medulla oblongata, and thereafter, from lower brainstem regions to the Substantia nigra (SN), eventually spreading to cortical regions^{203,231} (Figure 1.11A).

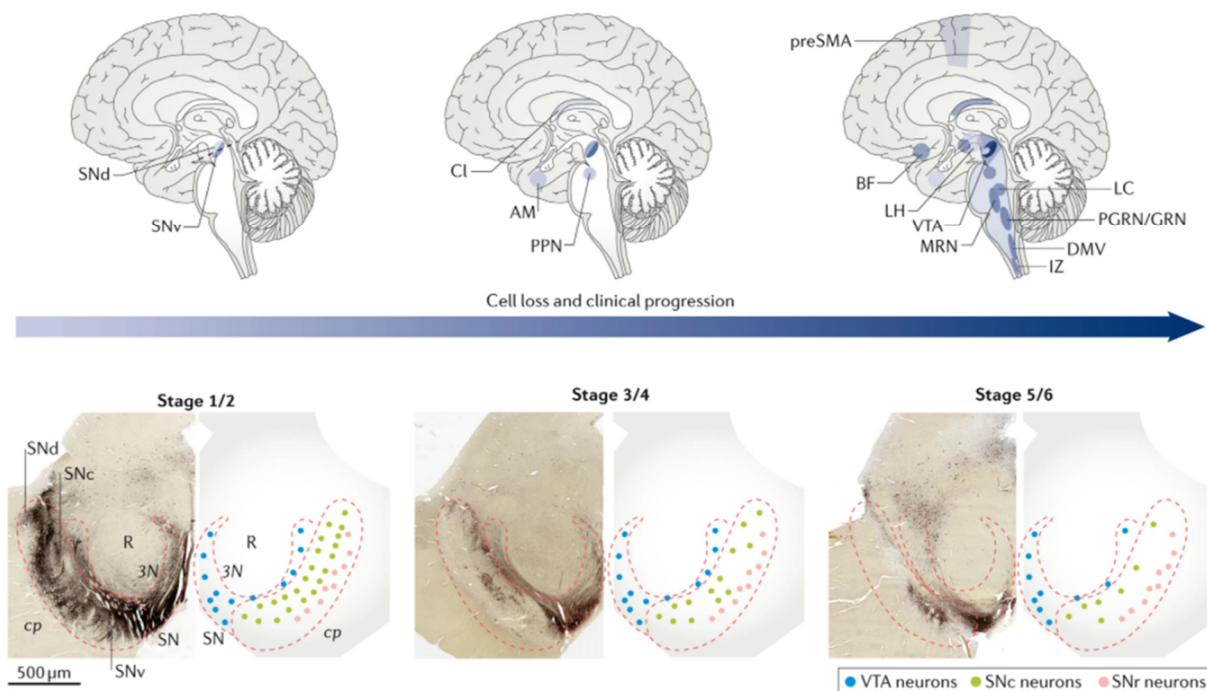


Figure 1.9: Schematics illustrating various stages of neurodegeneration in PD patient brains. The upper panel illustrates the regions affected and cell loss during the progression of the disease and lower panel highlights depigmentation and greater vulnerability of SNc dopaminergic (DA) neurons. Blue dots represent less pigmented ventral tegmental area (VTA) neurons, and green dots represents heavily pigmented Substantia nigra (SN) DA neurons (this figure was adapted from ⁵⁸⁵).

Not all neurons that develop Lewy bodies (LBs) are vulnerable to cell death in PD⁵⁸⁵. Recent studies assessing cell loss in the brains of asymptomatic or pre-symptomatic PD patients (Braak stage 1-2) identified 10%–20% loss of Substantia nigra pars compacta (SNc) DA neurons in the ventral tier of the SNc

but not in any other brain regions with Lewy pathology⁵⁸⁶. In the early symptomatic stages of PD (Braak stage 3-4), a study identified > 90% DA neuron loss (calbindin negative, “nigrosomes”) in the ventral tier of SN⁵⁸⁷; in another study, a ~90% cell loss in the ventral tier was reported⁵⁸⁸. These studies indicate the higher susceptible nature of ventral tier SN DA neurons to the disease process.

Nevertheless, cell loss is not just restricted to the SN since at early symptomatic stages, but it is also observed in other regions: (1) significant loss of cholinergic neurons in the pedunculopontine nucleus (PPN), whereas glutamatergic and gamma aminobutyric acid (GABA)ergic neurons are not affected⁵⁸⁹ and (2) mild loss of glutamatergic neurons in intralaminar nuclei of (IL) and Amygdala (AM) regions in the brains of PD patients⁵⁹⁰. Apart from cell loss in this small number of cell nuclei in other regions, cell loss is not apparent or significant⁵⁸⁵ at an early stage. In the late symptomatic stage (Braak stage 5-6), cell loss is evident and correlates with the presence of LBs⁵⁸⁹ as depicted in Figure 1.11. In contrast, neurons in the supraoptic nucleus that do not develop LB undergo cell death, whereas neighboring region tuberomammillary nucleus of the hypothalamus that develops LBs abundantly do not undergo cell death⁵⁹¹. Similarly, pyramidal neurons in the pre-supplementary motor cortex die in the absence of LBs in the PD patients who do not show dementia symptoms⁵⁹². Therefore, cell loss does not necessarily correlate with the appearance of LBs.

1.6.2 Cell-autonomous factors contributing to cell-type specificity

Not all neurons that develop LBs are susceptible to cell death in PD. Several groups have tried to uncover cell-autonomous factors that may render a specific population of neurons more susceptible to LB pathology and cell death compared to others populations. Some of the common traits among early affected neurons will be discussed in this section (summarized in ^{585,593}). One of the shared features is the presence of long, poorly myelinated, and highly branched axons with several hundred thousand vesicular release sites, namely, SNc DA neurons in the rodents exhibit characteristic profuse axonal ramifications in the striatum^{594,595} thus facilitating coordinated activity in these large networks. One of the hypotheses put forth to explain why this process could be deleterious is that mitochondrial oxidative stress is found to be higher in axons of SNc DA neurons compared to VTA DA neurons⁵⁹⁶.

Many of the early affected regions, such as SN and LC, including other neuromodulatory neurons, have slow tonic pacemaker activity, and the action potentials of these neurons are slow and broad allowing higher calcium ion entry into neurons. This step is followed by slow oscillations in intracellular calcium

concentrations originating from internal ER calcium stores and plasma membrane L-type (Cav1) and T-type (Cav3) voltage-gated calcium channels⁵⁹⁷⁻⁶⁰².

Slow pacemaker activity and calcium oscillations help maintain basal DA levels in the striatum for motor activity, which allows calcium entry into mitochondria and facilitates oxidative phosphorylation and ATP production⁶⁰³⁻⁶⁰⁵. However, this process suggests that adverse effects, such as increased production of reactive oxygen species that are capable of damaging DNA, proteins, and lipids, occur, can cause an increase in the propensity of aSyn aggregation over the course of the disease progression^{598,599,605,606}.

In addition, higher intracellular calcium levels can promote proteasomal dysfunction⁶⁰⁷, lysosomal dependent degradative activity⁶⁰⁸, and aSyn aggregation¹⁰⁵ both directly and indirectly via activation of calcium-dependent activation of cysteine proteases, such as calpain and calcineurin^{609,610}. Moreover, the presence of toxic actors, such as higher calcium levels, aSyn, and DA⁶¹¹ renders SNc dopamine neurons susceptible to earlier cell death compared to other neuronal populations.

The neuronal seeding model has been applied in primary hippocampal⁶¹² and midbrain neuronal cultures⁴⁰⁴. In hippocampal neurons, accumulation of aggregates was found to lead to a decrease in synaptic protein levels and impairment of axonal transport of signaling and degradative machinery and neural network activity^{15,397,612}. A recent study by Luna and colleagues showed that pyramidal neurons are most susceptible to cell death compared to dentate gyrus granule cells thus, correlating cell death with higher expression of aSyn level in pyramidal neurons compared to granule cells⁶¹³. In midbrain dopaminergic cultures, pre-formed aSyn amyloid fibril (PFF) treatment led to accumulation of aSyn in soma and nucleus at nine days post-exposure and caused a decrease in expression of synaptic proteins and axonal transport-related proteins and caused an impairment in mitochondrial functions⁴⁰⁴. However, this study, which used midbrain neurons failed to address the differential susceptibility of dopamine neurons to development of LB-like inclusions and cell loss. Interestingly, in a PFF-based seeding model, it was demonstrated that the special AT-rich sequence-binding protein [SATB] homeobox 2 (SATB2) and CamKII positive excitatory neurons are more susceptible to developing aggregates compared to parvalbumin (PV), calbindin, and calretinin positive inhibitory neurons⁵¹⁹. It is possible that higher expression levels of calcium buffering proteins in inhibitory neurons could have prevented calcium-induced secondary effects, such as mitochondrial dysfunction, calpain-induced cleavage of aSyn, and exacerbation of aSyn aggregation. In addition, buildup of pS129 positive aggregates in excitatory neurons could have occurred because of expression of lower levels of proteins associated with degradative pathways. To explain these phenomena, a mixed model of pathology progression was described in which

cell-autonomous factors and trans-synaptic spread as mediators of pathology progression were considered⁶¹⁴. However, molecular and cellular factors that govern cell susceptibility to developing LB-like inclusions and their responses to aggregate burden in different brain regions are not yet well understood.

1.6.3 Single-cell RNA seq studies in PD model systems

Although the understanding of some phenotypes in highly vulnerable neurons is apparent, this understanding is limited to DA neurons and brain regions involved in neuromodulatory circuits. Especially, the vulnerability of particular cell-types that develop LBs or cell loss that are associated with non-motor symptoms remain poorly understood. To understand these properties, researchers have performed gene expression studies using mainly bulk measurements (either proteomics or RNA sequencing), wherein results were interpreted from average composition of brain tissues. With bulk measurement approaches, it remains difficult to assess which specific cell types are affected. In recent years, with the arrival of single-cell (sc) or single-nucleus (sn) RNA sequencing (RNAseq) and associated techniques, it is becoming possible to sequence up to several hundred thousand cells or nuclei from a single experiment^{615,616}. Recently these sc/snRNAseq methodologies have been applied in some studies to characterize the cellular heterogeneity and cell-type dependent processes that govern PD in model systems. A major limitation of these studies is that they did not use model systems that develop LB-inclusions and that recapitulate features of PD brains. Therefore, these studies do not address the question of how gene expression or pathways are differentially affected in cell-types that develop LB-like inclusions and their surrounding cell types in different brain regions.

Table 7: single-cell transcriptomics studies *in vivo* PD model systems

Study by	sc/sn RNAseq method	Model system	brain region	no. of cells/ nuclei and cell clusters	Characterization of inclusions in their model systems?
Fernandez et al., 2020 ⁶¹⁷	10x	Human iPSC, WT, oxidative stress-induced, SNCA-A53T mutant		15325, 6	No
Tiklova et al. 2019 ⁶¹⁸	Smart-seq2	Th:EGFP BAC transgenic mice	Midbrain, forebrain, olfactory bulb	396, 13	No
Tiklova et al. 2020 ⁶¹⁹	Smart-seq2, 10x	6-OHDA PD rat model	Striatum Brain region	746, 4 7875	No
Lang et al. 2019 ⁶²⁰	Smart-seq2	Human iPSC, WT, PD GBA-N370S patients		146, 6	No
Zhong et al 2020 ⁶²¹	Nucleus	Transgenic	Midbrain, striatum, cerebellum	Total 74493, 11,16, 9	No

1.7 Thesis Objectives

The primary objective of this thesis is to elucidate the structural and cellular determinants of aSyn seeding and toxicity. More specifically, we are interested in understanding the role of aSyn oligomers in regulating aSyn toxicity and pathology formation and spreading. To achieve this goal, it was essential to first identify tools that allow selective detection and monitoring of oligomer formation and cellular properties. Over the past two decades several academic and industry research groups have developed and reported on the use of aSyn oligomer-specific antibodies. Therefore, we initially thought that these tools could be used in our studies. However, it became clear to us that these antibodies have not been thoroughly assessed. Therefore, with the support of the Michael J Fox foundation and in collaboration with ADx neurosciences, we systematically investigated specificity of different conformation-specific antibodies to different forms of aSyn species. In the first chapter of this thesis, we describe an antibody characterization and validation pipeline that allows a systematic investigation of the specificity of aSyn antibodies using well-defined and well-characterized preparations of various aSyn species, including monomers, fibrils, and different oligomer preparations that are characterized by distinct morphological, chemical and secondary structure properties. We then utilized this pipeline to characterize 18 aSyn antibodies, 16 of which have been reported as conformation- or oligomer-specific antibodies, using an array of techniques, including immunoblot analysis (slot blot and Western blot), a digital ELISA assay using single molecule array technology and surface plasmon resonance. This approach enabled us to define a high degree of antibody specificity to different aSyn species (Chapter 2).

Under *in vitro* conditions, oligomers can be detected; however, their presence in the widely used PFF-based neuronal seeding model has not been demonstrated, and whether these obligate intermediates affect the aSyn aggregation process, seeding and toxicity are not well studied. Therefore, in Chapter 3 of this thesis, we systematically addressed two important questions: (1) Whether oligomers are formed in the PFF-based neuronal seeding model? This is investigated using SEC fractionation of soluble fraction isolated from neurons treated with PFFs and then probing for the presence of oligomeric aSyn that might be released in the extracellular media using Western blotting; and (2) Do oligomers exhibit seeding activity and toxicity? This was assessed *in vitro*, primary hippocampal neurons and *in vivo* model system of PD. To overcome the limitations of previous studies, we made use of morphologically, chemically and structurally different types of oligomers such as unmodified oligomers, dopamine-induced oligomers, and HNE-induced oligomers, in the seeding and toxicity studies in an attempt to capture oligomer conformational

diversity that might be present in the brains of PD patients. We also plan to assess the seeding and spreading activity of oligomers in the *in vivo* PFF-based mouse model.

Since we did not identify oligomer specific antibodies and oligomers did not seed, we could not evaluate the cellular determinants of aSyn oligomers seeding and thus focused on fibrils. In Chapter 4 of this thesis, we utilized PFF-based *in vivo* model of PD and single-nucleus RNA sequencing to decipher cellular determinants of aSyn seeding. In PD and DLB cases, different non-motor symptoms are associated with amygdala, which develops LB-like inclusions and have been replicated in PFF-based *in vivo* spreading model. In amygdala, not all neurons develop aggregates suggesting cell-type specificity to vulnerability. We investigated transcriptomics changes in different cell types (neuronal and non-neuronal) in the amygdala brain region of the PFF-injected mice and compared the results with PBS injected mice. We will also aim to identify how expression of PD-risk genes and pathways are affected in different cell types of Amygdala (Chapter 4).

The experimental rational, methods, findings, and conclusions toward achieving these three specific aims are detailed separately in chapters 2-4, respectively.

Chapter 2: Characterization and validation of 16 α -synuclein conformation-specific antibodies using well-characterized preparations of α -synuclein monomers, fibrils and oligomers with distinct structures and morphology: How specific are the conformation-specific α -synuclein antibodies?

2.1 INTRODUCTION

Several neurodegenerative disorders are characterized by the presence of cytoplasmic proteinaceous inclusions termed Lewy bodies (LBs), which are enriched in misfolded and aggregated forms of the presynaptic protein alpha-synuclein (aSyn)⁶²². These diseases include Parkinson's disease (PD), dementia with Lewy bodies (DLB), and multiple system atrophy (MSA), which are collectively referred to as synucleinopathies. Early studies of the ultrastructural properties and compositions of LBs revealed that they are highly enriched in filamentous structures^{225,623}, which were later shown to be composed of aSyn^{5,624}. These findings, combined with the discovery that mutations in the gene that encodes aSyn causes early-onset forms of PD⁴, led to the hypothesis that the process of aSyn fibrillization and LB formation plays a central role in the pathogenesis of PD and other synucleinopathies. However, the failure of this hypothesis to explain several neuropathological and experimental observations prompted the possibility that intermediates generated on the pathway to aSyn fibrillization and LB formation, rather than the fibrils or LBs themselves, are the primary toxicity-inducing and disease-causing species. These observations include 1) the lack of a strong correlation between Lewy pathology burden, neurodegeneration and disease severity^{625,626}; 2) the presence of LBs in the brains of individuals who do not show any symptoms of PD or other synucleinopathies at the time of death^{627,628}; and 3) the identification of patients who exhibit Parkinsonian symptoms in the absence of LBs e.g. PD patients harboring parkin and LRRK2 G2019S mutations⁶²⁹⁻⁶³². These observations are similar to those demonstrating the lack of a correlation between amyloid-plaque burden and cognitive decline in Alzheimer's disease (AD)⁶³³⁻⁶³⁵, which have supported the toxic oligomer hypothesis of AD.

Several lines of evidence support the aSyn oligomer hypothesis. Both on- and off-pathway soluble and nonfibrillar aSyn oligomers of different sizes and morphologies were consistently observed during the *in vitro* aggregation of aSyn under different conditions^{536,636,637}. Subsequent studies over the past decade have also provided evidence for the presence of aSyn oligomers in biological fluids such as saliva, blood plasma, basal tears, and cerebrospinal fluid (CSF) from patients suffering from PD and other synucleinopathies^{540,544,638-642}. Several of these studies suggested that the level of oligomers is correlated with the diagnosis of PD and/or disease progression^{538,540,643}. One major caveat of these studies is that they were potentially carried out using tools and immunoassays that do not distinguish between oligomers and other higher-order aggregated forms of aSyn (fibrils or amorphous aggregates). Nonetheless, they paved the way for further studies demonstrating that aSyn oligomers/aggregates are secreted by neurons^{538,544,638,644,645} in the brain, and could mediate the propagation of aSyn pathology and cause neurodegeneration. Indeed, several studies have reported that aSyn oligomers are released by neurons via exocytosis⁶⁴⁵ and are then taken up by other cells via different mechanisms, including endocytosis³⁸⁸, trans-synaptic propagation⁵⁸¹ or receptor-mediated uptake⁶⁴⁶. Furthermore, aSyn oligomers have been shown to directly or indirectly contribute to aSyn-induced toxicity and neurodegeneration via different mechanisms, including but not limited to i) the disruption of cell membrane integrity by the formation of pores in the membrane^{9,386}; ii) synaptic toxicity or neuronal signaling dysfunction^{561,647-649}; iii) the failure of protein degradation pathways⁶⁵⁰⁻⁶⁵²; iv) endoplasmic reticulum dysfunction⁶⁵³; v) mitochondrial dysfunction^{654,655}; and vi) the enhancement of inflammatory responses⁶⁵⁶. These observations, combined with the overwhelming evidence that oligomer-induced toxicity is a key contributor or driving force leading to neurodegeneration in Alzheimer's disease (AD), fueled greater interest in the development of tools, therapies and diagnostics that specifically target aSyn oligomers. This includes the development of various protocols for the preparation of oligomers, the generation of oligomer-specific antibodies, and immunoassays for quantifying oligomers.

Oligomers can be broadly defined as all the soluble multimeric species that exist before the formation of aSyn fibrils, including a) dimers, trimers and low molecular weight assemblies, which are not easily discernable by electron microscopy (EM) and atomic force microscopy (AFM)), and b) higher molecular weight oligomers with different morphologies that are composed of >10 monomers, which are easily detectable by EM, AFM and other imaging techniques^{536,657-661}. Our current knowledge of the biophysical properties of aSyn oligomers has been shaped primarily by results obtained by investigating aSyn aggregation and fibril formation *in vitro*. The propensity of aSyn to form oligomers is highly dependent on several factors, such as the protein concentration and sequence (including the presence of disease-

associated mutations and post-translational modifications)^{536,662,663}, interactions with metals, other proteins and small molecules, and chemical modification by specific molecules (e.g. dopamine, 4-oxo-2-nonenal, 4-hydroxy-2-nonenal (HNE), and epigallocatechin gallate)^{386,664-666}. Depending on the conditions used, different types of aSyn oligomers have been consistently observed *in vitro*, including globular, spherical, amorphous, curvilinear and pore-like oligomers (Figure 2.1)^{536,661}. It remains unknown to what extent these oligomers resemble the oligomers that form in different cell types in the brains of patients. Several studies have reported the detection of oligomers in cell cultures, in the brains of animal models of synucleinopathies, and during the analysis of cerebrospinal fluids (CSF) and postmortem examinations of brains of PD, DLB and MSA patients^{538,544,638,644,645}. However, the evidence to support the presence of specific oligomers in these studies has been based for the most part on the detection of SDS-resistant oligomeric bands by Western blotting^{149,538,667}, the use of proximity ligation assays⁴²⁷, or the reliance on “oligomer-specific” antibodies or immunoassays. Thus, much of the knowledge and many of the hypotheses in the field today are based on conclusions drawn from studies relying on antibodies.

One major untested assumption related to the use of oligomer-specific antibodies and immunoassays is that the antibodies used are capable of capturing the structural and morphological diversity of aSyn oligomers *in vivo*. Notably, all these antibodies were generated using specific recombinant aSyn aggregates, fibrils or oligomers generated under *in vitro* conditions. Some of the limitations of existing antibody validation approaches include the following: 1) the lack of detailed characterization of *in vitro* oligomer preparations with respect to their purity, homogeneity and structural properties; 2) the use of oligomer preparations that may not reflect the conformational, biochemical and morphological diversity that exists in the brain; and 3) the lack of research that establishes whether the specificity of antibodies is driven by their high affinity for oligomers, or by the avidity binding characteristics of the antibodies.

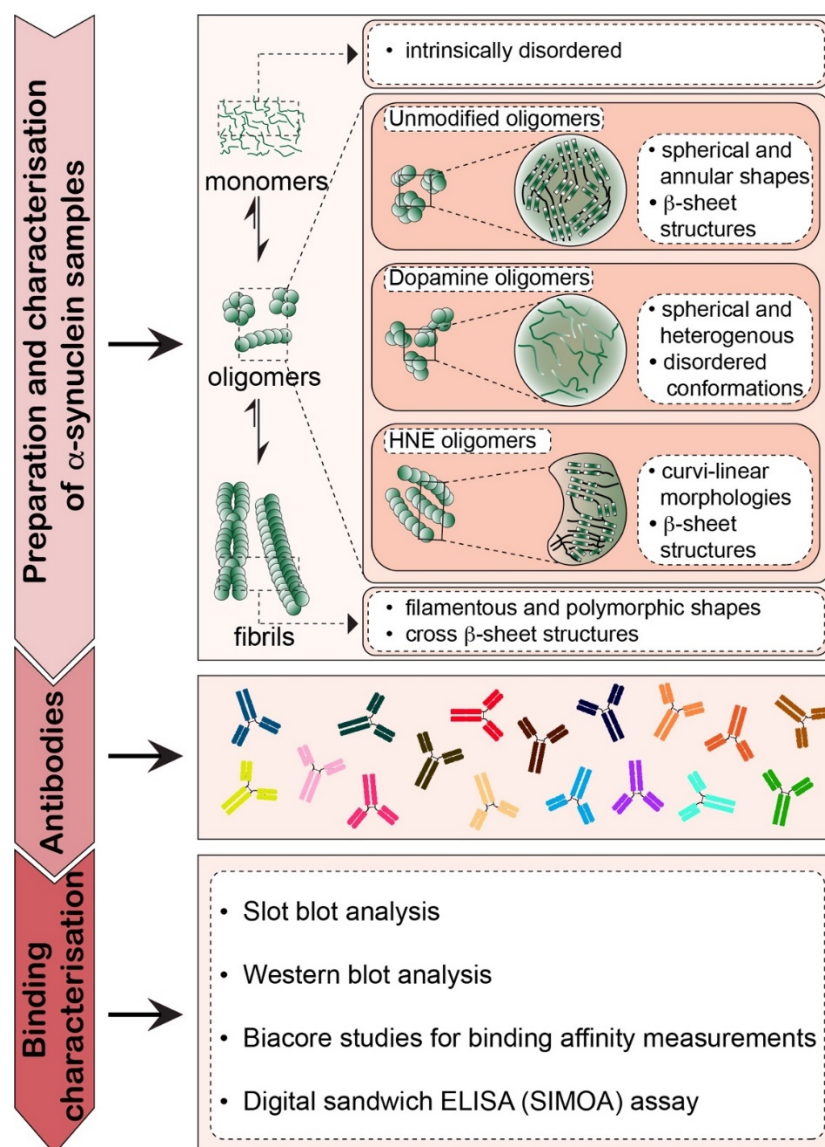


Figure 2.1: A schematic illustration of our antibody validation strategy. In brief, the pipeline included the preparation of well-defined preparations of aSyn monomers, oligomers, and fibrils. Oligomers were generated from three different protocols in an attempt to partially capture the morphological, chemical and structural heterogeneity of oligomers *in vivo*. The aSyn conformation-specific antibodies were procured from different sources. The immunoreactivity of these antibodies was assessed using slot blot, Western blot, a digital sandwich ELISA (SIMOA) assays and SPR. (This figure was adapted from⁶⁶⁸)

Given the impact of the use of antibodies on shaping our knowledge of aSyn and its role in health and disease, and on developing diagnostics and therapies for PD and synucleinopathies, we developed a protocol that enables systematic assessment of the specificity of aSyn antibodies using well-defined and well-characterized preparations of aSyn fibrils, oligomers, and monomers. This approach was then used to evaluate a library of 18 aSyn antibodies, 16 of which were reported to be aggregate-specific (Table 2.1).

These antibodies can be broadly classified depending on the immunogens used for their generation: oligomers based on the use of i) a modified version of full-length aSyn (antibody clones 24H6, 12C6, 26F1, and 26B10); ii) *in vitro* generated aSyn fibrils (antibody clones 7015, 9029, SYNO2, SYNO3, and SYNO4); iii) recombinant aSyn aggregates (antibody clones A17183A, A171183B, A17183E, and A17183G); iv) synthetic aSyn peptides encompassing amino acids 44 to 57 (5G4) or filaments derived from recombinant “exact sequence is not disclosed by the vendor” (MJFR-14) or amino acids 115-125 (ASyO5) ; vi) recombinant full-length aSyn monomers (SYN211); and vi) a recombinant truncated aSyn variant consisting of residues 15-123 (SYN-1) (Table 2.1). To verify the specificity of these antibodies, we first screened them all against well-characterized preparations of aSyn species (monomers, oligomers, and fibrils) using immunoblot analysis (slot blotting and Western blotting) and a digital enzyme-linked immunosorbent assay (ELISA) using single molecule array (SIMOA) technology (Figure 2.1). To further scrutinize the conformational specificity of the antibodies, we tested them against different types of oligomer that exhibit distinct morphological, chemical and secondary structure properties. Finally, the binding affinity of selected antibodies was determined using surface plasmon resonance (SPR). This approach enabled us to define the specificity of the antibodies to a high degree and show that although some antibodies were specific for aggregated forms of aSyn and did not recognize monomers, all antibodies that were reported to be oligomer-specific also recognized fibrillar aSyn. Furthermore, some of the antibodies that were reported to be oligomer- or fibril-specific also recognized aSyn monomers. We also identified an antibody that showed a preference for β -sheet-enriched fibrils and oligomers, but not for disordered oligomers or monomers. Our studies reveal that none of the antibodies tested (Table 2.1) showed any unique preferential specificity for one particular form of aSyn species, including monomers, oligomers or fibrils, and that it is possible to develop antibodies that recognize diverse aSyn oligomers and fibrils. Our work underscores the importance of using well-characterized tools (*in vitro*-produced calibrants) and multiple methods to define the specificity of antibodies. This will not only help us to advance PD research, but will also improve the selection of promising antibody candidates and reduce the number of failures in advanced clinical trials of PD therapeutics.

Table 2.1: List and details of antibodies used in this study (This table was adapted from ⁶⁶⁸)

Antibody (clones)	Source	Specificity	Immunogen	Epitope	Isotype	Host	Original Reference	Characterization by purified aSyn standards in the original reference
24H6	MJFF DOSAB*	conformational	HNE-induced oligomers	not reactive towards recombinant FL aSyn nor synthetic peptides in the amino acid region 96-140	IgG2a, κ	Mouse monoclonal	⁵⁶¹ #	NA
26B10					IgG2a, κ			
26F1					IgG2a, κ			
12C6			DHA induced oligomers	reacts with synthetic peptide in the amino acid region 113-140	IgG2a, κ			
7015	UPenn	conformational	Strain A, <i>in vitro</i> aSyn PFF	recognizes a discontinuous epitope with binding elements in the extreme C-terminus and near amino acid 50	NA	Mouse monoclonal	⁶⁶⁹ ⁶⁷⁰	Yes, Sandwich ELISA using Strain A fibrils, Strain B fibrils and monomer
9029			Strain B, <i>in vitro</i> aSyn PFF	amino acids 32 – 58				
SYNO2	Biolegend	conformational	aSyn fibrils (50 µg/mouse)	Weak signal for amino acids 127-140 detected by ELISA	IgG1	Mouse monoclonal	⁶⁷¹	Yes, dot blot, inhibition ELISA, sandwich ELISA using fibrils and monomers
SYNO3					IgG1			
SYNO4					IgG1			
A17183A	Biolegend	conformational	Recombinant aSyn aggregate	NA	IgG2a, κ	Rat monoclonal	BioLegend Cat. No. 864901	NA
A17183E					NA		NA	
A17183G					IgG1, κ		BioLegend Cat. No. 865103	
A17183B					IgG2a, κ		BioLegend Cat. No. 865001	
MJFR-14	MJFF/Abcam	conformational	Recombinant aSyn filament amino acids 1 to the C-term	amino acids 133 – 138	NA	Rabbit monoclonal	Martinez et al., 2016, Poster 413.21, Abcam Cat. No. ab209538	Yes, dot blot using filament, oligomer and monomer Luminex assay using monomer, oligomer and fibrils
5G4	Kovacs (Merck Millipore)	Aggregated aSyn	TKEGVVHGVATVA E (44 – 57)	amino acids 46 – 53	IgG1, κ	Mouse monoclonal	⁶⁷²	No
ASyO5	Agrisera	conformational	Human aSyn (111-125)	NA	IgG1	Mouse monoclonal	Agrisera Cat. No. AS13 2718	Yes, dot blot using monomer, oligomer, and fibrils
SYN211	Abcam	sequence	Recombinant full-length Human aSyn	amino acids 121 – 125	IgG1	Mouse monoclonal	⁶⁷³ , Abcam Cat. No. ab80627	Yes, Western blot using monomer
SYN-1	BD-biosciences	sequence	Rat Synuclein-1 amino acids 15-123	amino acids 91 – 99	IgG1	Mouse monoclonal	⁶⁷⁴ BD-biosciences Cat. No. 610787	Yes, Western blot using monomer

*Antibodies were generated by ADx NeuroSciences in a MJFF sponsored project (DOSAB) in collaboration with Crossbeta.

Reference contains the information of the immunogen used for the generation of antibodies., DHA: docosahexaenoic acid; NA: informations not available

2.2 RESULTS

2.2.1 Preparation and characterization of aSyn monomers, oligomers and fibrils

To investigate the specificity of the antibodies listed in Table 2.1, we first assessed their specificity towards aSyn monomers, oligomers, and fibrils. To accomplish this goal, we generated well-characterized preparations of human aSyn 1) fibrils, 2) oligomers and 3) monomers that were “free” of cross-species contamination. The purity of each preparation was verified using our recently described centrifugation-filtration protocol⁶⁶¹ (Figure 2.2A). Given that aSyn oligomers and fibrils are always in equilibrium with monomers, it is difficult to eliminate the presence of monomers completely. To eliminate or minimize the amount of monomers (<5%), all fibril and oligomeric samples were subjected to centrifugation-filtration protocol immediately prior to their use in our studies, as previously described⁶⁶¹. Similarly, to ensure that the aSyn monomeric preparations were free of any preformed aggregates, the monomeric samples were filtered through a 100 kDa filter, and the flow-through (aggregate-free monomers) was collected and kept on ice and used immediately.

Several procedures have been developed with the aim of generating homogenous preparations of oligomers *in vitro*, but all were shown to result in preparations that contain mixtures of oligomers that are structurally and morphologically diverse. However, it is possible to generate preparations that are enriched in specific oligomeric species by subfractionating these preparations using size exclusion chromatography or other separation methods^{536,657}. The protocols involve the generation of oligomers either by incubating recombinant aSyn monomers at high concentrations in buffers with or without additional components such as dopamine^{637,675-680}, lipids^{647,664,666,681-686}, metals^{386,580,687-690}, alcohols^{386,580,665,691}, or by using methods that are based on the use of chemical cross-linking agents⁶⁹².

In the absence of additional components, oligomers are found to exhibit heterogeneous morphologies, such as globular, spherical, annular pore-shaped, rectangular and tubular-shaped, and are usually but not always enriched in β -sheet structures⁵³⁶. In the presence of additional components such as dopamine, lipids or alcohols, oligomers are found to have spherical, globular, rod-shaped or curvilinear morphologies, which are structurally different from primarily disordered, α -helical or β -sheeted structures, suggesting that the formation of oligomers is strongly influenced by the environment in which they form^{386,647,675,676,678-681,683-685,687,693,694}.

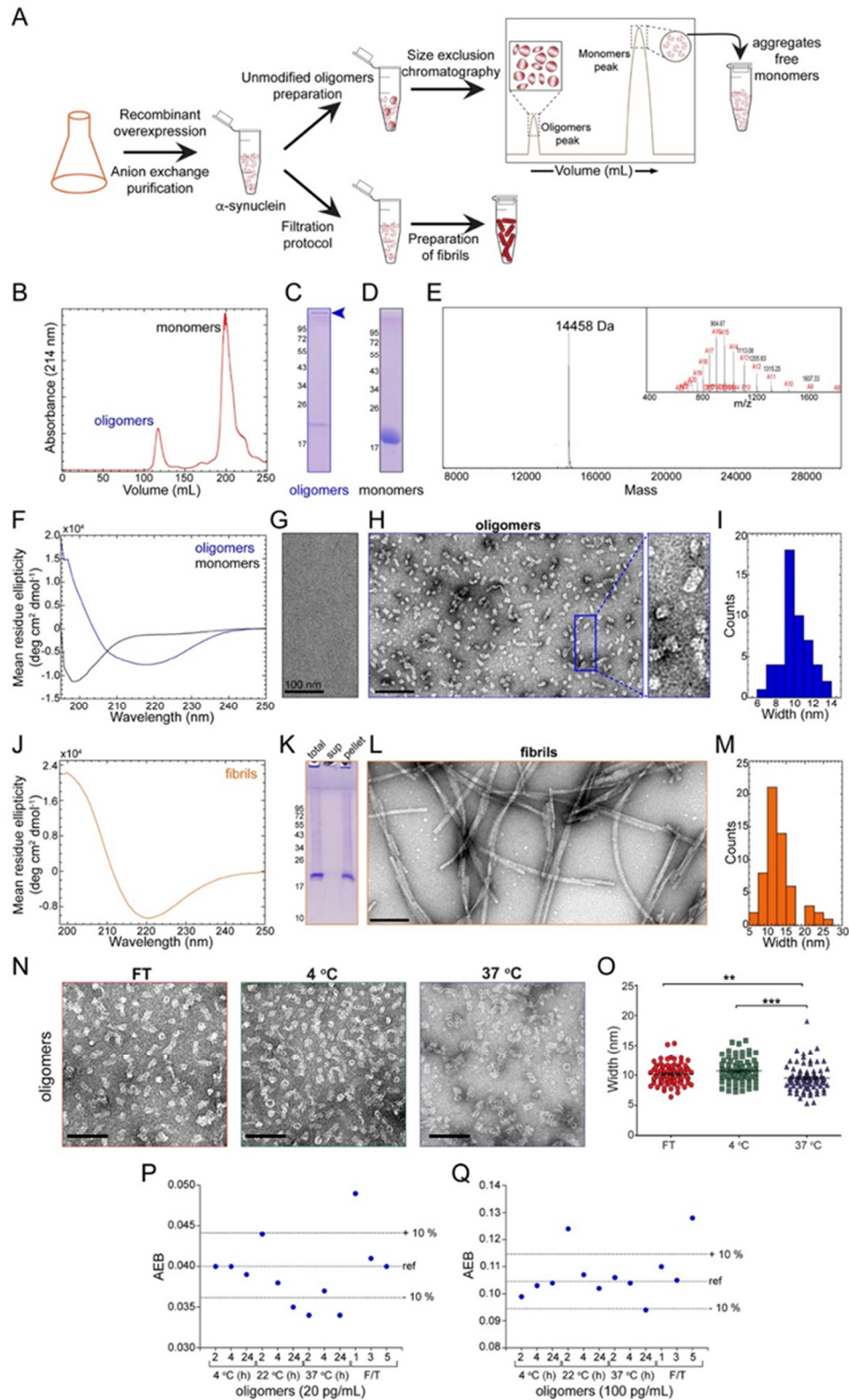


Figure 2.2: Preparation and characterization of aSyn monomers, oligomers, and fibrils. (A) A scheme depicting the preparation of aSyn monomers, oligomers, and fibrils. (B) SEC purification of monomers and oligomers. (C and D) SDS-PAGE analysis followed by Coomassie staining of oligomers (C) and monomers (D) purified from B. (E) ESI-MS

spectra of monomers separated by SEC. (F) Comparison of the CD spectra of monomers and oligomers. Oligomers were predominantly enriched in β -sheet structures and monomers showed a predominantly disordered structure. (G) Negatively stained EM analysis performed on monomers. (H) Negatively stained EM analysis performed on oligomers. (I) Width distribution of oligomers. (J) CD spectra of fibrils. (K) SDS-PAGE analysis followed by Coomassie staining of the total, supernatant, and pellet fractions obtained during fibril preparation. The pellet fraction is the fibril fraction devoid of monomers and oligomers that was used for further binding studies. (L) Negatively stained EM analysis performed on fibrils. (M) Width distribution of the fibrils. (N) EM images and width distribution (O) of oligomers subjected to different temperature conditions, freeze-thawing cycles and incubation at 4°C and 37°C, these were quantified from three TEM images from each of the conditions (FT, 4°C and 37°C). Scale bar = 100 nm in Figure 2.2G, H, L, N. (P and Q) Assessment of the stability of the oligomeric preparation by ELISA. Two concentrations of oligomers (20 pg/mL (P) and 100 pg/mL (Q)) were incubated at three different temperatures ranges (2-8°C, 20-25°C and 36-38°C) for varying times (2 h, 4 h and 24 h) or subjected to multiple freeze-thaw (F/T) cycles (1x, 3x, and 5x) (X-axis). The signals (AEB) from the immunoassay with the antibody A17183B were plotted on the Y-axis. The dashed lines represent the reference condition "ref" and a 10% decrease/increase in the AEB signal as arbitrary thresholds. (This figure was adapted from⁶⁶⁸)

Recombinant aSyn was used for the preparation of oligomers and fibrils. For the preparation of oligomers^{536,695}, 12 mg/mL aSyn monomer was dissolved in PBS and incubated at 37°C and 900 rpm for 5 h. After incubation, the sample was centrifuged, and the supernatant was applied to a size exclusion chromatography (SEC) column (Hiload 26/600 Superdex 200 pg) to separate the monomers from the oligomers (Figure 2.2B). Analysis of these fractions by SDS-PAGE under denaturing conditions showed the expected profile of monomeric and high molecular weight (HMW) bands, suggesting that the oligomer preparations contained a mixture of SDS-resistant and SDS-sensitive oligomers. An alternative explanation could be that the observed monomers were released from the ends/surfaces of the oligomers in the presence of SDS. The HMW species (with a molecular weight distribution of up to 1 MDa) could be visualized at the top of the resolving portion of the gel (Figure 2.2C). As expected, the monomers that were separated using SEC, it appeared in the gel around 15 kDa (Figure 2.2D), which was consistent with the expected MW of aSyn of 14461 Da (Figure 2.2E). The samples were analyzed by CD spectroscopy to ensure that each of the preparations exhibited the expected secondary structure signatures of oligomers and monomers. Oligomers exhibited a CD spectrum with a broad minimum peak centered at 219 nm, indicating the presence of mixed secondary structure contents dominated by β -sheet structures (Figure 2.2F). Monomers possessed a peak with the minimum at 198 nm consistent with their predominantly disordered structures (Figure 2.2F). Next, we performed EM studies on monomer and oligomer preparations. Because of their small size (~14 kDa), the monomers are not visible by electron microscopy (Figure 2.2G). In contrast, the EM of the oligomer preparations showed heterogeneous morphologies consisting of annular pore-like structures and spherical and rectangular tubular-like shaped

particles (Figure 2.2H)⁵³⁶ with a mean width of approximately 10 nm (Figure 2.2I). To prepare the fibrils, we followed the protocol described in Kumar et al., 2020. In brief, the lyophilized aSyn were dissolved in PBS to a final concentration of ~300 μ M and incubated with shaking at 37 °C for five days at 1000 rpm. Next, we used our filtration protocol⁶⁶¹ to remove any remaining monomers and oligomers from the fibril preparations. The fibrils are enriched in β -sheet structures, as evidenced by the minimum peak at 221 nm in the CD spectrum shown in Figure 2.2J and the characteristic streaking pattern in the SDS-PAGE analysis, which confirmed the presence of SDS-resistant high molecular weight species of aSyn (Figure 2.2K). Ultrastructural analysis by EM revealed that these fibrils were polymorphic with fibril morphologies, including straight, twisted, or stacked fibrillar structures (Figure 2.2L), with a mean width of approximately 13 nm (Figure 2.2M).

2.2.2 Stability of aSyn preparations

Since these preparations were to be characterized in different labs, we investigated their stability to ensure that they would not change their properties due to the shipping and storage conditions. Therefore, we subjected the oligomers to several cycles of freezing and thawing by snap-freezing them 3-4 times followed by room temperature thawing and incubation at temperatures of 4°C and 37°C for 2 days (Figure 2.2N). Interestingly, we found that the morphological distribution of the oligomers was not significantly altered when the oligomers were subjected to up to 3-4 freeze-thaw cycles or incubated at 4°C for 2 days (Figure 2.2O and 2.2I). However, the oligomeric mean width was slightly reduced by approximately 6% after incubation at 37°C (Figure 2.2O), which could be due to the release of aSyn monomers from the oligomeric structures.

We also tested the stability of the oligomer preparations using the digital ELISA assay based on the differences in the level of detection of oligomers at known concentrations under different solution conditions. Oligomers at 20 and 200 pg/mL were incubated at three different temperatures (2-8°C, +20-25°C or 36- 38°C) for different durations (2, 4 and 24 h). In parallel, the effect of freezing and thawing (F/T) the samples 1x, 3x, and 5x was also tested. These samples were analyzed by the SIMOA sandwich assay using the A17183B antibody, which was captured on beads. The oligomer preparations are stable at 4°C for up to 24 hours and at 22°C for up to 4 hours. At temperature (37°C) for long incubation time (24 h), there was a significant decrease in the signal. When subjected to freeze/thaw cycles, a decrease in the signal was observed at lower (20 pg/mL) but not at higher concentrations (100 pg/mL) of oligomers. This evaluation did not include any optimization regarding the formulation of the oligomeric aSyn to ensure optimal stability in the follow-up experiments shown in Figure 2.5. However, these data, as well as the

results of the EM analysis did not indicate any significant changes in the stability of the oligomers that could influence the interpretation of the results from the experiments performed in this study.

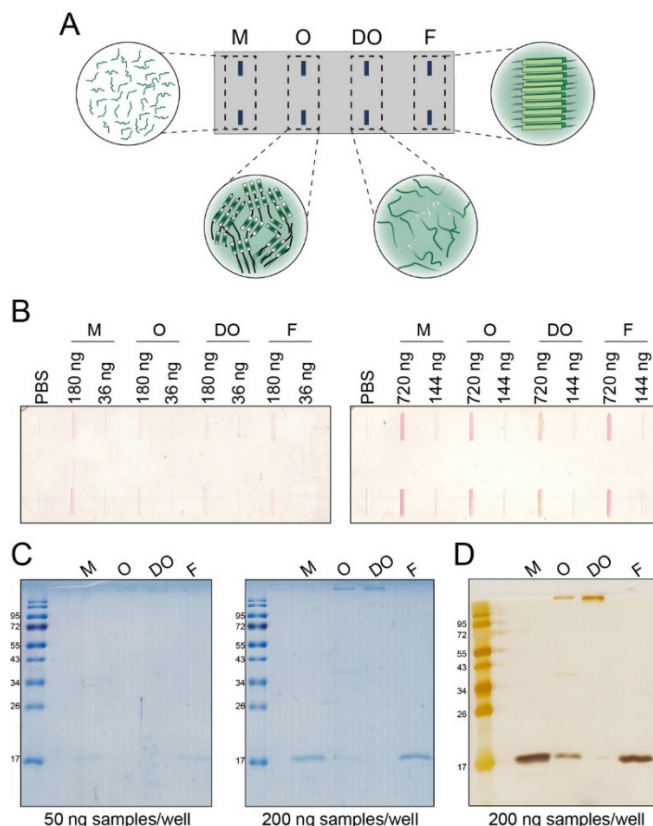


Figure 2.3: A) A Schematic illustration of slot blot performed with different aSyn monomers (**M**, unstructured), β -sheet rich oligomers (**O**), dopamine-induced unstructured oligomers (**DO**) and fibrils (**F**, beta-sheet rich). B) Ponceau S staining on nitrocellulose membranes loaded with different aSyn samples used at varying concentration to ensure equal loading on the membranes for slot blot experiments. C and D) SDS-PAGE analysis followed by Coomassie staining (C) and silver staining (D) of aSyn samples (monomers, O, DO and fibrils) Abbreviations: M: Monomers; O: Unmodified Oligomers; DO: Dopamine-induced oligomers; F: Fibrils. (This figure was adapted from⁶⁶⁸)

2.2.3 Profiling the immunoreactivity of antibodies to different aSyn species by immunoblotting

Prior to our immunoblot experiments, we ensured equal amount of protein loading on the nitrocellulose membranes using a combination of Ponceau S staining (for slot blot analysis), Coomassie staining and silver nitrate staining (for Western blot analysis) (Figure 2.3). To assess the specificity of the antibodies, we first performed slot blot analysis of all the antibodies listed in Table 2.1 using pure preparations of aSyn monomers, oligomers, and fibrils under non-denaturing conditions (Figure 2.4A). Among the 18

antibodies tested (Figure 2.4B), 16 were reported in the literature to be conformation- or aggregation-state (oligomers or fibrils) specific; see Table 2.1^{561,669,671,672}. The remaining two antibodies, Syn 211 (which recognizes an epitope in the C-terminus region spanning residues 121-125)⁶⁷³ and SYN-1 (which recognizes an epitope in the NAC region spanning residues 91-99 of aSyn)⁶⁷⁴, are sequence-specific and recognized all three species. Surprisingly, we found that none of the antibodies tested (Table 2.1) had specific immunoreactivity towards only one particular species of aSyn (either the monomer, oligomers or fibrils). All 16 reported conformation-specific antibodies detected both oligomers and fibrils. Interestingly, among these, 1) the antibody clone 5G4 showed exceptional immunoreactivity towards oligomers and fibrils in a concentration-dependent manner (increased dose dependency) and almost no immunoreactivity towards monomers at both concentrations tested; 2) the antibodies SYNO3 and A17183E showed stronger immunoreactivity towards oligomers and fibrils but very weak (only at high concentrations) or no immunoreactivity towards monomers. Except for these three antibodies, the rest of the antibodies fell into one of the following three categories: i) antibodies that recognized oligomers and fibrils (even at low concentrations) with higher specificity than monomers (clones 26F1, SYNO2, and A17183B; ii) antibodies that recognized oligomers and fibrils in a concentration-dependent manner (high concentration → stronger detection) but also showed weak immunoreactivity towards monomers at high concentrations (clones 24H6, A17183A, SYNO4, 7015, 26B10, and A17183G); and 3) antibodies that were non-specific and recognized all three forms of aSyn (clones 9029, 12C6, ASyO5, and MJFR-14) (Figure 2.4A; summarized in Table 2.2).

Given that many of these antibodies are also commonly used to assess the presence or formation of aSyn aggregates in cellular and animal models of synucleinopathies or in postmortem brain tissues using Western blot analysis, we assessed their immunoreactivity toward aSyn monomers, oligomers, and fibrils using this technique (Figure 2.4C). Although the samples are mixed and boiled in Laemmli buffer which contains SDS prior to loading into the SDS-PAGE gels, it is not clear whether this treatment is sufficient to denature all the aSyn aggregates, i.e. the conformational state of the various aSyn species detected by Western blot remains undefined.

As expected, the sequence-specific antibodies SYN211 and SYN-1 showed stronger immunoreactivity towards monomers, oligomers and the high molecular weight bands in the fibrillar samples^{673,674}. This is consistent with the fact that the epitopes of these antibodies are outside of the domains that form the cores of oligomers and fibrils. Interestingly, antibodies such as 5G4, A17183E, 24H6, 26F1, A17183A, A17183G, SYNO2 and SYNO4 showed no or very weak immunoreactivity towards any of the three aSyn

species when 36 ng the samples was used, suggesting that these antibodies recognize a native conformation that is lost upon treatment with SDS. Specifically, 5G4 and A17183A did not detect any of the aSyn bands. The 24H6 antibody reacted weakly only with the oligomeric band (at the top of the resolving gel). A17183E and 26F1 weakly detected monomers along with the detection of HMW bands. In contrast, several antibodies, including SYNO3, A17183B, 26B10, 9029, 12C6, ASyO5, MJFR-14 and 7015, which were reported to be oligomer/aggregate-specific, showed cross-reactivity and detected SDS-denatured monomers, SDS-resistant oligomers and HMW bands in the fibrillar samples without any preference for one form of aSyn.

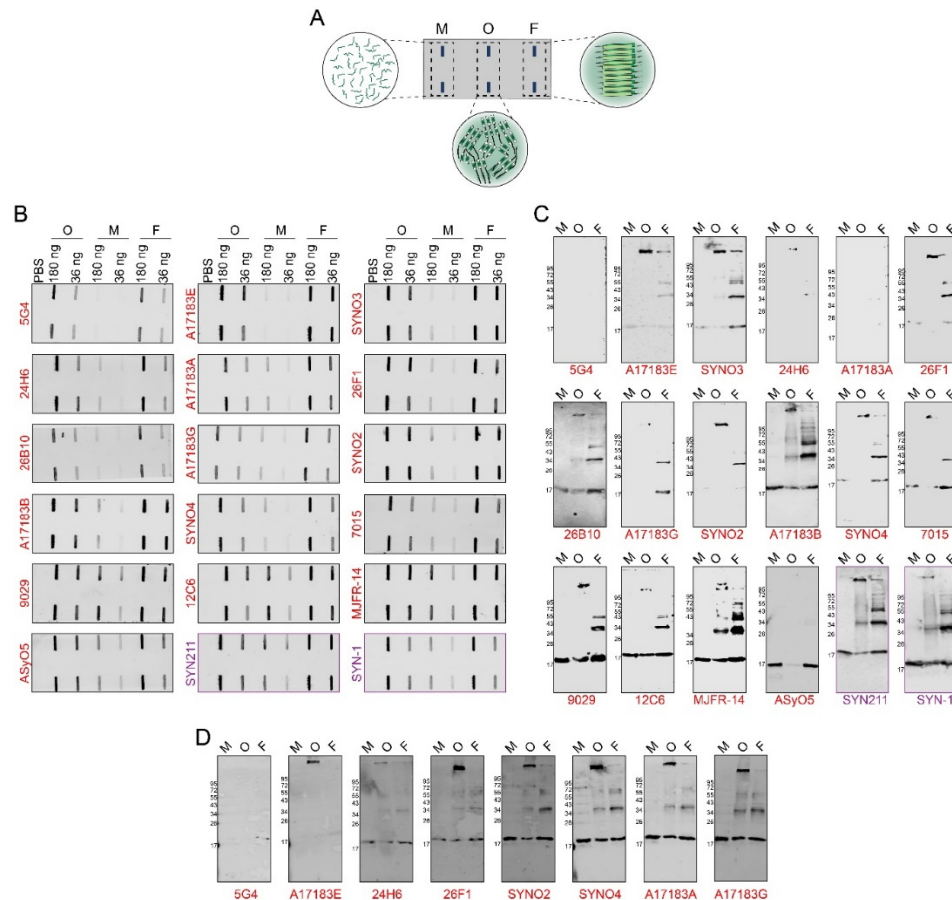


Figure 2.4: *In vitro* binding analysis of antibodies against aSyn monomers, oligomers and fibrils using slot blots and Western blots. (A) A schematic illustration of slot blot showing the blotting with different aSyn samples on the nitrocellulose membrane. (B) Slot blot analysis of the immunoreactivity of aSyn antibodies against aSyn monomers (M), β -sheet rich oligomers (O), and fibrils (F) under native conditions, spotted in duplicates at two different concentrations: 180 ng and 36 ng. (C and D) Assessment of the immunoreactivity of antibodies against SDS and heat treated aSyn samples loaded at concentration of 36 ng (C) and 180 ng (D). (This figure was adapted from⁶⁶⁸)

Table 2.2: Immunoreactivity and binding specificity of antibodies against native structures of aSyn species by different techniques (This table was adapted from ⁶⁶⁸)

Immunogen	Antibodies	Slot blot analysis					ELISA assay			SPR	
		M	O	DO	HO	F	M	O	F	M	O
oligomers	26F1	+	+++	--	+++	+++	--	++	++	*	***
	12C6	+++	+++	+++	+++	+++	+++	+++	+++	***	***
	24H6	+	+++	+++	+++	+++	--	++	+++	∅	∅
	26B10	+	++	+++	+++	++	--	++	+++	∅	∅
fibrils	7015	++	+++	+++	+++	+++	+	+++	+++	∅	∅
	9029	++	+++	+++	+++	+++	++	+++	+++	∅	∅
	SYNO2	+	+++	+++	+++	+++	+	+++	+++	∅	∅
	SYNO3	+	+++	+++	+++	+++	+	+++	+++	∅	∅
	SYNO4	+	+++	+++	+++	+++	--	+++	+++	*	***
recombinant aSyn aggregates	A17183A	+	+++	+++	+++	+++	--	+++	+++	*	***
	A171183B	+	+++	+++	+++	+++	+	+++	+++	∅	∅
	A17183E	+	+++	+++	+++	+++	--	+	+++	∅	∅
	A17183G	+	++	+++	+++	+++	+	+++	+++	∅	∅
a.a. (44-57)	5G4	+	+++	++	+++	+++	--	--	+++	∅	∅
a.a. (1-140)	SYN211	+++	+++	+++	+++	+++	∅	∅	∅	***	∅
a.a. (15-123)	SYN-1	+++	+++	+++	+++	+++	∅	∅	∅	∅	∅
a.a. (111-125)	ASyO5	++	+++	++	+++	+++	∅	∅	∅	∅	∅
aSyn filaments	MJFR-14	+++	+++	+++	+++	+++	--	++	+++	*	***

M: monomers; O: oligomers; DO: DA induced oligomers; HO: HNE induced oligomers; F: fibrils.

-- : no detection; + : faint detection; ++ : medium detection; +++ : strong detection; ∅ : data not available

*** : strong affinity; * : weak affinity

Given that some antibodies (5G4, A17183E, 24H6, 26F1, A17183A, A17183G, SYNO2 and SYNO4) had weak or no reactivity against aSyn at 36 ng, we repeated the Western blot analysis using a high concentration (180 ng) of aSyn . Interestingly, we observed similar results for 5G4 and A17183E (Figure 2.4D and Table 2.3), whereas 26F1 and 24H6 showed concentration-dependent reactivity to aSyn species (high concentration → stronger detection). However, the antibodies A17183A, A17183G, SYNO2 and SYNO4 which showed minimal detection at 36 ng (Figure 2.4C) displayed strong reactivity to aSyn bands at 180 ng (Figure 2.4D). Taken together, these results suggest that all the antibodies tested here do not preferentially detect one particular aSyn species (consistent with the slot blot analysis). Furthermore,

Western blot analysis showed that many of the reported conformational- and aggregate-specific antibodies detected SDS-resistant HMW aSyn species and monomeric in SDS-PAGE gels (summarized in Table 2.3). These findings highlight the limitation of using selected antibodies to profile aSyn species by Western blot and underscore the critical importance of using multiple antibodies to capture the diversity of aSyn species.

Table 2.3: Immunoreactivity of antibodies against SDS and heat treated aSyn samples by Western blot analysis (This table was adapted from ⁶⁶⁸)

Immunogen	Antibodies	Western blot analysis ^Δ					
		M		O		F	
		36 ng	180 ng	36 ng	180 ng	36 ng	180 ng
oligomers	26F1 [#]	+	++	+++	+++	+	++
	12C6	+++	∅	+++	∅	+++	∅
	24H6 [#]	--	++	+	++	--	++
	26B10	++	∅	++	∅	+++	∅
fibrils	7015	+	∅	+	∅	++	∅
	9029	+++	∅	+++	∅	+++	∅
	SYNO2 [#]	--	+++	+++	+++	+	+++
	SYNO3	+++	∅	+++	∅	+++	∅
	SYNO4 [#]	+	+++	+++	+++	+	+++
recombinant aSyn aggregates	A17183A [#]	--	+++	--	+++	--	+++
	A171183B	+++	∅	+++	∅	+++	∅
	A17183E [#]	+	--	+++	+++	+	+
	A17183G [#]	--	+++	--	+++	+	+++
a.a. (44-57)	5G4 [#]	--	--	--	--	--	+
a.a. (1-140)	SYN211	+++	∅	+++	∅	+++	∅
a.a. (15-123)	SYN-1	+++	∅	+++	∅	+++	∅
a.a. (111-125)	ASyO5	+++	∅	+	∅	+++	∅
aSyn filaments	MJFR-14	+++	∅	+++	∅	+++	∅

M: monomers; O: oligomers; F: fibrils.

-- : no detection; + : faint detection; ++ : medium detection; +++ : strong detection; ∅ : data not available

^Δ Western blot analysis against aSyn at 36 ng (for all antibodies) and 180 ng (# selected antibodies) concentrations.

Next, we assessed the antibody specificity towards aSyn monomers, oligomers and fibrils using a sandwich ELISA assay. We employed this assay for the detection of antibody specificity against low picogram concentrations of aSyn species under soluble conditions. The assay format utilizes the covalent capture of conformation-specific antibodies by a microsphere (Figure 2.5A). The three aSyn species described above were used as analytes at two concentrations (100 and 1000 pg/mL). A pan-synuclein antibody was included as a pairing antibody with the oligomer-specific antibody.

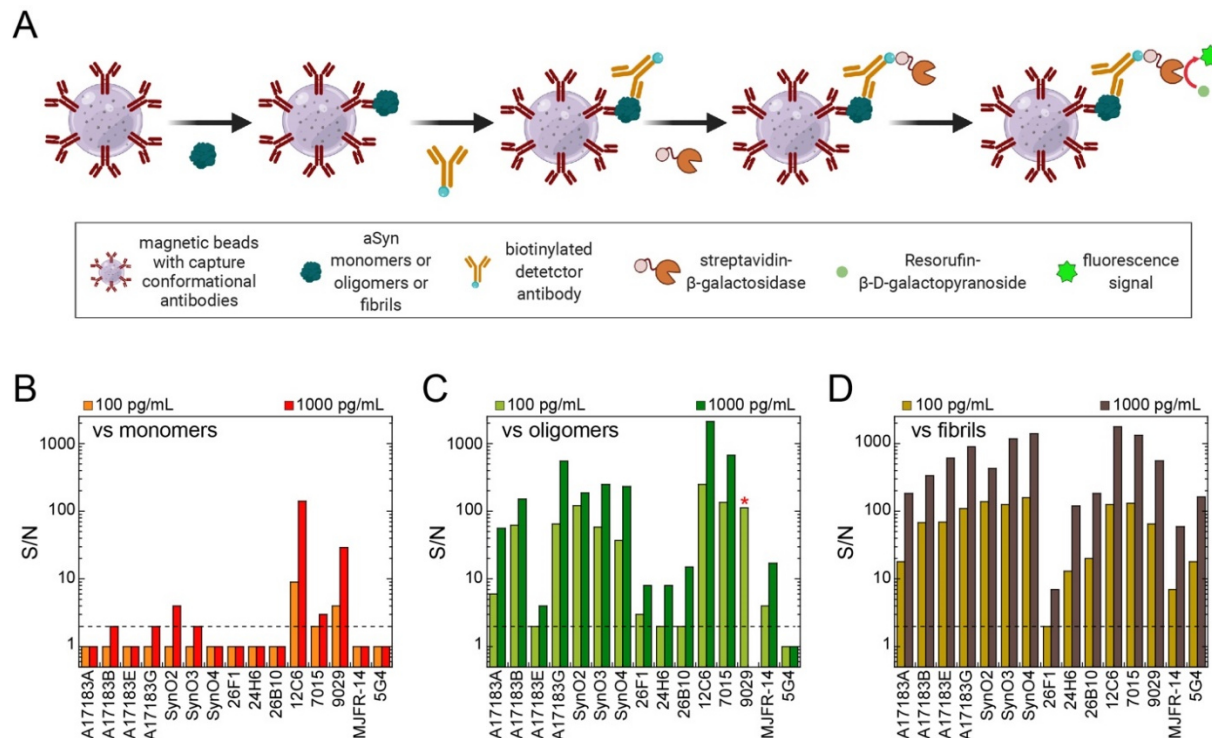


Figure 2.5: ELISA Simoa assay of antibodies against monomers, oligomers and fibrils. A) An illustration of ELISA Simoa assay and its experimental steps. The 15 aSyn conformation specific antibodies were coupled to the beads as capture monoclonal antibodies (X-axis), respectively. aSyn monomers (B), oligomers (C), and fibrils (D) were used as the analyte (100 and 1000 pg/mL). The detector antibody was a C-terminal monoclonal antibody (clone SYN211) with an epitope in the amino acid region from 121-125. The signal-to-noise values (S/N) are indicated on the Y-axis for the three aSyn forms. * indicates the availability of only 100 pg/mL oligomer data for antibody clone 9029 (C). (This figure was adapted from ⁶⁶⁸)

When monomeric aSyn was used as the analyte, 12 of the 15 antibodies yielded lower than signal-to-noise S/N = 2, which is used as a threshold (Figure 2.5B). Three antibodies (clones 12C6, 7015 and 9029) showed S/N values higher than 2. In terms of immunoreactivity against oligomeric aSyn, 14 antibodies yielded S/N values higher than 2, although four antibodies (A17183E, 26F1, 24H6, and 26B10) possessed S/N values close to 2 in the presence of low concentrations of oligomers (100 pg/mL), but the immunoreactivity was

enhanced at high concentrations (1000 pg/mL). The antibody 5G4 yielded the lowest S/N value of 1 at both concentrations (Figure 2.5C). When using fibrillar aSyn as an analyte, 14 antibodies resulted in S/N values higher than 2, while 26F1 showed immunoreactivity in the presence of high concentrations (1000 pg/mL) but had lower than borderline immunoreactivity toward 100 pg/mL of fibrils (Figure 2.5D). These experiments revealed that several antibodies reacted with monomeric aSyn, including 12C6 and 9029, whereas 7015 was borderline reactive. Those antibodies with strong immunoreactivity toward oligomers (10 antibodies: A17183A, A17183B, A17183G, SYNO2, SYNO3, SYNO4, 12C6, 7015, 9029 and MJFR14) also had strong immunoreactivity toward fibrils. The antibody 26F1 showed concentration-dependent immunoreactivity toward oligomers and fibrils (high concentration → stronger immunoreactivity), while the antibodies A17183E, 24H6, 26B10 and 5G4 showed greater fibril specificity. No antibodies could be identified that were solely oligomer-specific with no immunoreactivity toward aSyn monomers or fibrils, as observed by the slot blot analysis (Figure 2.5B) (summarized in Table 2.2).

2.2.4 Characterization of the specificity of the antibodies toward morphologically and structurally different forms of oligomeric aSyn

Since our knowledge of the morphological and conformational properties of native oligomers in the brain is unknown, we sought to further assess the specificity of the antibodies toward different preparations of oligomers that exhibited distinct structurally, chemical and morphologically properties. The use of these different oligomer preparations allowed us to test whether differences in the morphologies/structures of aSyn oligomers could influence the immunoreactivity or binding specificities of the antibodies. We employed dopamine (DA) (Figure 2.6A) and 4-hydroxy-2-nonenal (HNE) (Figure 2.6B) to prepare cross-linked human WT aSyn oligomers. Several studies have shown that the interaction of DA with aSyn promotes the formation of aSyn oligomers and influences aSyn aggregation propensity and neurotoxicity^{675,696}, raising the possibility of the presence of DA-modified aSyn oligomeric species in PD patient brains. Similarly, HNE, a physiological byproduct of lipid peroxidation, has been shown to play roles in oxidative stress responses and to alter the aggregation of aSyn in PD^{12,664}.

The DA- and HNE-induced oligomers (Figure 2.6C and 2.6D) were prepared by the incubation of DA or HNE with aSyn, followed by the isolation of the oligomers using SEC as described above. Mass spectrometry analysis of the monomeric fractions from the SEC purifications (in both DA- and HNE-induced oligomer preparations; Figure 2.6C and 2.6D) showed masses that are higher than the expected mass of monomeric aSyn (14460 Da). In the samples where aSyn was co-incubated with dopamine, we observed an increase in mass by 65 Da (14525 Da; Figure 2.7A), which may correspond to the oxidation of the four methionine

present in aSyn (4*16=64 Da). For the aSyn monomers isolated by SEC from the HNE-aSyn sample mixtures, we observed several peaks reflecting the addition of single or multiple modification of 156 Da each (14615 Da, 14771 Da, 14928 Da and 15084 Da; Figure 2.7B), corresponding to the formation of HNE-aSyn adducts. The DA-induced oligomers exhibited CD spectra with a minimum at 198 nm, revealing the presence of species with predominantly disordered conformations and little structure (Figure 2.6E, Table 2.4). However, the HNE-induced oligomers showed a broad CD spectrum centered at 219 nm that is more similar to the CD spectrum of the oligomers (Figure 2.6F), indicating these oligomers are rich in β -sheet structure (Figure 2.6J, Table 2.4). Analysis of these fractions by SDS-PAGE analysis under denaturing conditions (Figure 2.6F: DA oligomers, Figure 2.6K: HNE-induced oligomers) showed a very similar gel profile for both types of oligomers, with the presence of HMW bands at the top of the resolving part of the gel and a light band of monomers at 15 kDa that may have been released from the oligomers in the presence of SDS.

Table 2.4: Morphologies and structural properties of oligomers used in this study (This table was adapted from ⁶⁶⁸)

Oligomers	Morphologies	Width/diameter	Secondary structure composition (%)		
			α -helix	β -strand	irregular
Oligomers	annular pore, spherical, tubular	6-14 nm	27	38	32
DA oligomers	near-spherical, globular	5-20 nm	11	11	78
HNE oligomers	curvi-linear	5-11 nm	27	26	49

EM ultrastructural analysis of the DA-induced oligomers showed the presence of oligomers with near-spherical morphologies of different shapes and sizes (Figure 2.6G), as previously shown^{637,675,697}. These oligomers exhibited a mean width of approximately 13 nm (Figure 2.6I). However, the HNE-induced oligomers appeared to be more homogenous and displayed a curvilinear (chain-like) morphologies with a mean width of approximately 8 nm (Figure 2.6L and 2.6N). Next, we tested the stability of these oligomers by monitoring changes in their sizes and oligomeric morphologies as described above for the oligomers shown in Figure 2.6. Neither repeated cycles of freeze-thaw conditions or longer incubations at 4 °C seem to influence the morphologies of the DA oligomers. The number/density of the oligomeric particles on the EM grids was significantly reduced for the DA oligomeric sample incubated at 37 °C (Figure 2.6H), and a decrease in the mean width to approximately 10 nm was also observed (Figure 2.6I). Under identical

conditions, the HNE oligomers did not show major changes in their morphologies or mean width (Figure 2.6M and 2.6N).

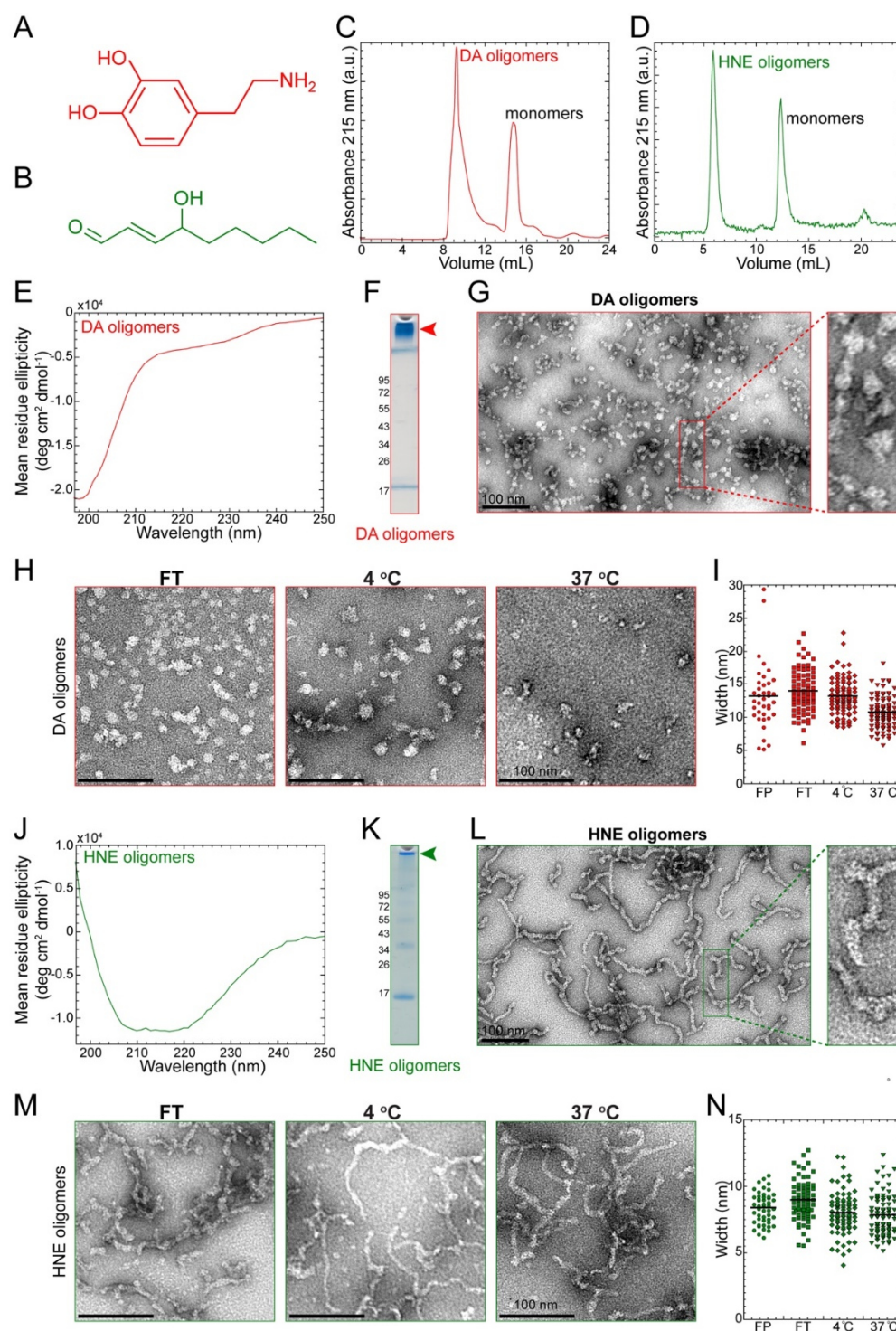


Figure 2.6: Preparation of dopamine- and HNE-induced oligomers and analysis of their stability. Chemical structures of dopamine (A) and HNE (B). SEC purification of DA-induced oligomers (C) and HNE-induced oligomers

(D) separated from monomers. (E) CD spectra of DA-induced oligomers. (F) Coomassie staining of dopamine and DA-induced oligomers. (G) Negatively stained EM analysis performed on DA-induced oligomers. DA-induced oligomers showed mainly spherical, undefined morphologies. (H) Assessment of the stability of the DA-induced oligomers subjected to different temperature conditions incubation (4 °C and 37 °C) and freeze-thawing as determined by analysis of their width distribution (I). (J) CD spectra of HNE-induced oligomers. (K) Coomassie staining of HNE-induced oligomers. (L) Negatively stained EM analysis performed on HNE-induced oligomers. (M) Assessment of the stability of HNE-induced oligomers incubation (4 °C and 37 °C) and and freeze-thawing as determined by analysis of their width distribution (N). (This figure was adapted from⁶⁶⁸)

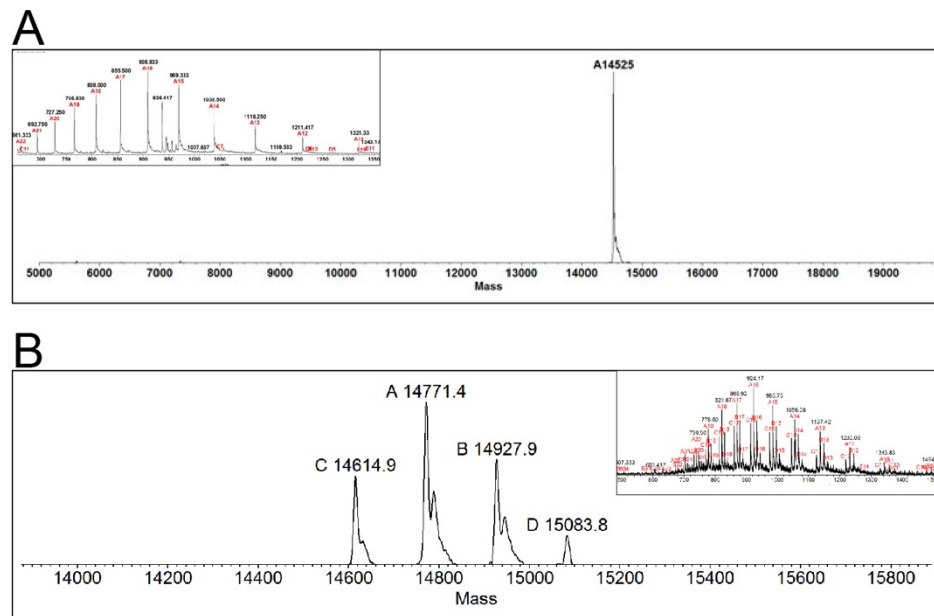


Figure 2.7: Mass spectrometry analysis of aSyn monomers purified by size exclusion chromatography. aSyn monomers purified from preparation of Dopamine-induced oligomers(A) and HNE-induced oligomers (B). (This figure was adapted from⁶⁶⁸)

To investigate whether the antibodies in Table 2.1 show differential immunoreactivity to morphologically, chemically and conformationally distinct oligomer preparations under native conditions, we performed slot blot analysis using DA- and HNE-induced oligomers and monomers as a control (Figure 2.8A). The majority of the antibodies we tested detected DA- and HNE-induced oligomers and monomers irrespective of their morphological or structural differences (Figure 2.8B). Strikingly, among all the antibodies tested, 26F1 showed no immunoreactivity toward DA-induced oligomers, weak immunoreactivity toward monomers but very strong immunoreactivity toward HNE-induced oligomers, which is consistent with the data shown in Figure 2.4B. 26F1 was generated against oligomerized HNE-modified aSyn. The 5G4 antibody, which does not recognize aSyn monomers, also showed strong immunoreactivity toward HNE-induced oligomers but exhibited weak immunoreactivity toward DA-induced oligomers, which could be due to the presence of small population of structured DA oligomers (Table 2.4) or due to the weak affinity of 5G4 to the ensemble of DA-induced oligomers. As expected, the

sequence-specific antibodies SYN211 and SYN-1 detected both DA- and HNE-induced oligomers and monomers.

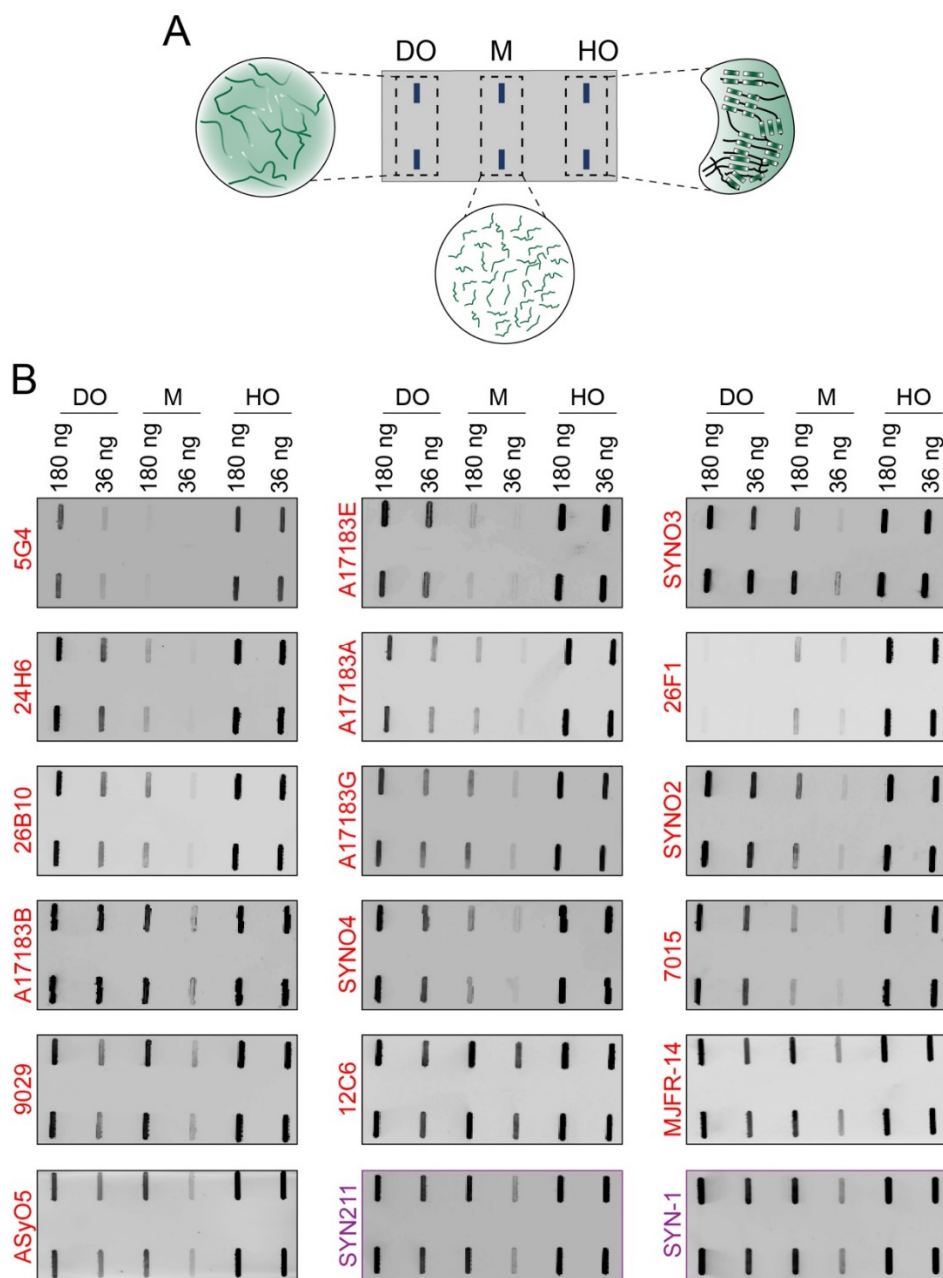


Figure 2.8: Slot blot analysis of antibodies against aSyn monomers and DA- and HNE-induced oligomers. (A) A scheme illustrating the slot blot analysis showing the different aSyn samples blotted in the nitrocellulose membrane. (B) Assessment of the immunoreactivity of antibodies by slot blot against dopamine-induced unstructured oligomers (DO), aSyn monomers (M) and HNE-induced oligomers (HO), and fibrils (F) under native conditions and spotted in duplicates at two different concentrations: 180 ng and 36 ng. (This figure was adapted from ⁶⁶⁸)

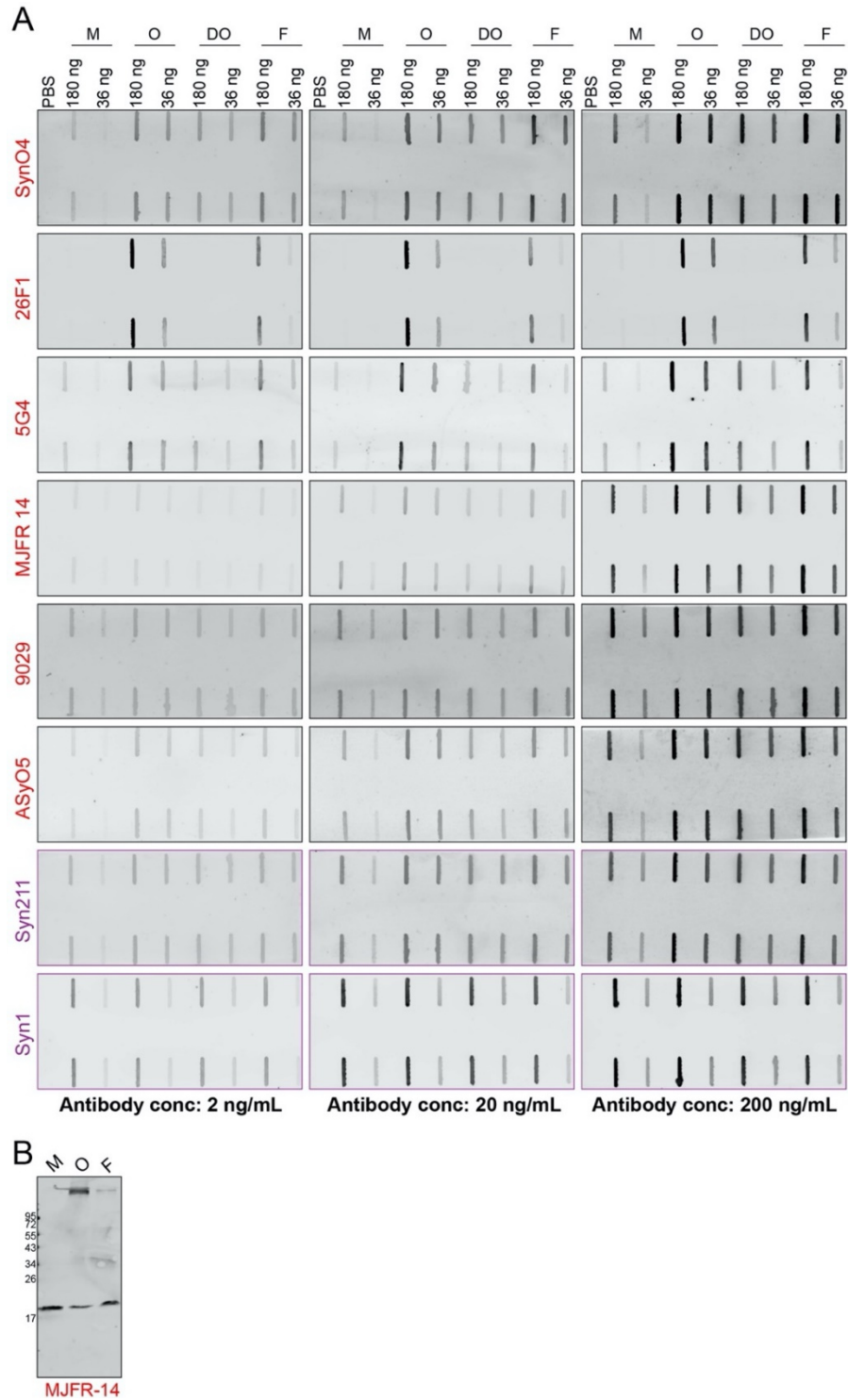


Figure 2.9: (A) Specificity of antibodies against aSyn monomers (M), unmodified oligomers (O), Dopamine-induced oligomers (DO), and fibrils (F) using increasing concentrations of antibodies (2 ng/mL, 20 ng/mL, 200 ng/mL and). (B) WB assessment of the immunoreactivity of MJFR-14 (2 ng/mL) against aSyn samples (180 ng). (This figure was adapted from ⁶⁶⁸)

The antibodies that showed stronger immunoreactivity toward HNE-induced oligomers can be categorized further depending on their immunoreactivity toward DA-induced oligomers and monomers as follows: i) A17183E showed enhanced detection of DA- and HNE-induced oligomers compared to monomers; ii) 24H6, 9029, ASyO5, A17183A, 26B10, MJFR-14 and A17183G showed stronger immunoreactivity to HNE-induced oligomers (even at a low concentration of protein of 36 ng per spot) and concentration-dependent detection of DA-induced oligomers and monomers; iii) SYNO2, SYNO3, SYNO4, A17183B, 7015 showed enhanced detection of HNE- and DA-induced oligomers and concentration-dependent immunoreactivity toward monomers (weak binding at a low concentration of monomers, 36 ng of protein per spot). In contrast, 12C6 showed very strong nonspecific detection of DA- and HNE-induced oligomers as well as monomers irrespective of the concentration of proteins loaded in each spot in the slot blot analysis, consistent with the ELIA results.

Next, we investigated whether the concentration of antibodies may influence their immunoreactivities towards different aSyn species. To do this, we selected few antibodies that were shown to be aggregate specific (26F1, 5G4) and others that are nonspecific and recognize different aSyn forms (Syn211, SYN-1, 9029, SynO4, MJFR-14 and ASyO4). We reassessed their specificity over antibody concentrations ranging from 2 to 200 ng/mL and observed similar results (Figure 2.9) as reported in (Figure 2.4B, Figure 2.8B) at all the antibody concentrations tested.

In summary, our immunoblotting studies (Figure 2.4, Figure 2.8 and Figure 2.9) demonstrate that none of the antibodies showed any preferential specificity toward one particular aSyn species, including monomers, oligomers and fibrils. However, we observed some exceptions: i) the antibody clone 26F1 did not show any immunoreactivity toward the largely unstructured DA-induced oligomers but was highly specific for β -sheet-enriched oligomers, HNE-induced oligomers and fibrils; ii) the antibody 5G4 showed weak immunoreactivity toward the largely unstructured DA-induced oligomers but stronger immunoreactivity towards β -sheet-enriched oligomers, HNE-induced oligomers and fibrils (summarized in Table 2.2). These differences in immunoreactivity emphasize the importance of using many antibodies in parallel rather than a single antibody for the identification of pathological oligomers in the brain given the heterogeneous nature and structural properties of such oligomers.

2.2.5 Kinetics of the binding of aSyn monomers and oligomers to immobilized antibodies

To further characterize and validate the specificity of the antibodies, we assessed their binding affinity and kinetics to monomeric and oligomeric aSyn species using SPR (Figure 2.10A). The antibodies were immobilized on the SPR chip surface at low densities. Figure 2.10 and Figure 2.11 show the SPR sensorgrams of selected antibodies (seven in total; six conformational and one sequence-specific) as a function of time as obtained by the successive injection of monomers or oligomers at concentrations ranging from 30 to 2000 nM. Sensorgram plots were fitted to extract the kinetic parameters, such as the binding affinity (KD) and association (k_a) and dissociation (k_d) rate constants of the binding between antibodies and monomer or oligomer complexes. The fitting of the plots was based on either a 1:1 binding model or by a global heterogeneous ligand binding model, which provides kinetic parameters for two binding sites. Collectively, all of the tested antibodies showed binding responses to both aSyn monomers and oligomers with varying binding affinities. Interestingly, many of the antibodies that were found to be highly specific for oligomers/fibrils (Figure 2.4B) also showed some binding to monomers. However, the binding affinities (KD) of the antibodies A17183A, SYNO4, and 26F1 reflected μ M affinities toward monomers, which was consistent with the slot blot data (Figure 2.4B). The kinetic parameters obtained from the sensorgrams are summarized in Table 2.5.

The shape of the dissociation portion of the SPR sensorgrams (after 120 seconds) provides clues about the binding affinity of the antibodies toward monomers or oligomers; a stronger affinity is reflected by a flatter slope of the dissociation curve (slower off-rate), but a weaker affinity is reflected by a steeper curve (faster off-rate). Figure 2.10 and Figure 2.11 show the SPR sensorgrams of the antibodies upon titration of monomers and oligomers. Fitting with a 1:1 binding model was possible for the binding of a few antibodies to aSyn monomers. These antibodies showed weak binding affinities to monomers with KD values of 3.61 μ M (A17183A), 5.67 μ M (SYNO4) and 76 μ M (26F1). However, the same antibodies exhibited stronger binding affinities towards oligomers as evident by the fitting of the raw data which was possible only by heterogeneous binding model, suggesting two possible oligomer binding sites: A17183A (KD1: 3.67 μ M, KD2: 45 nM), SYNO4 (KD1: 249 nM, KD2: 2.14 pM) and 26F1 (KD1: 2.12 μ M, KD2: 279 pM) (Figure 2.10B and Figure 2.11, Table 2.5). A stronger binding affinity for oligomers by antibodies A17183A, SYNO4 and 26F1, is in agreement with our slot blot analyses (Figure 2.4B), confirming that these antibodies bind with greater specificity to oligomers than monomers. 12C6 and 9029 showed stronger binding toward oligomers (Figure 2.10C and Figure 2.11, Table 2.5), but also exhibited good binding to monomers. This is consistent with the fact that these antibodies showed binding to monomers by slot

blots and ELISA (Figure 2.5B) and detected aSyn under denaturing conditions. However, it was not possible to fit the data and calculate the kinetic rate constants and binding affinities for 9029. Both antibodies showed a slow dissociation of monomers as evidenced by the fact that the dissociation portion of the sensorgrams (after 120 seconds) returns slowly to the baseline response units (RU, y-axis) but not as rapidly as seen with A17183A, 26F1 and SynO4. These observations suggest that the antibodies 9029 and 12C6 possessed a stronger affinity to monomers, in comparison to A17183A, 26F1 and SynO4, which exhibit weak binding affinity to monomers.

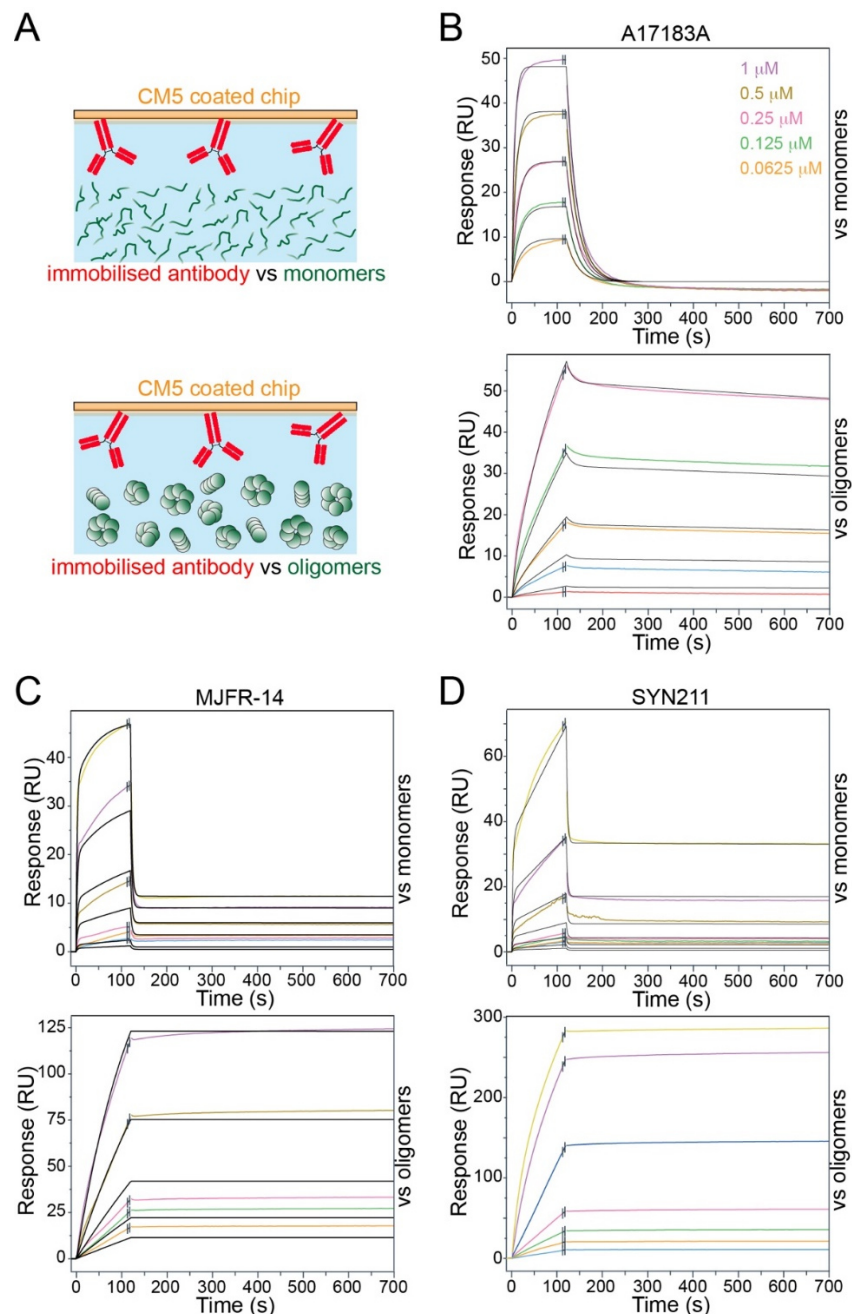


Figure 2.10: SPR-based kinetic analysis of different immobilized monoclonal antibodies (A17183A (B), MJFR-14 (C), and SYN211 (D)) binding to aSyn monomers (top) and oligomers (bottom) at 30, 60, 120, 250, 500, 1000 and 2000 nM concentrations. The antibodies were immobilized at a ligand density of approximately 3000-4000 RUs. The aSyn monomers or oligomers were injected for 2 min, followed by 5 min dissociation with injection of PBS buffer at a 30 $\mu\text{L}/\text{min}$ flow rate. The sensorgrams are shown as colored lines representing varying concentrations of aSyn monomers or oligomers, and the fits are shown as black lines. The kinetic parameters obtained from the fitting are shown in Table 2.5 (This figure was adapted from ⁶⁶⁸).

Table 2.5: Kinetic parameters of the antibodies binding to aSyn monomers or oligomers (This table was adapted from ⁶⁶⁸)

Immobilized antibodies	Injected aSyn	$k_a(\text{M}^{-1}\text{s}^{-1})$	$k_d(\text{s}^{-1})$	KD
A17183A	monomers	1.18×10^4	4.26×10^{-2}	3.61 μM
	oligomers	$k_{a1}:2.31 \times 10^4$ $k_{a2}:2.99 \times 10^3$	$k_{d1}:8.46 \times 10^{-2}$ $k_{d2}:1.35 \times 10^{-4}$	KD1: 3.67 μM KD2: 45 nM
SYNO4	monomers	1.22×10^4	6.93×10^{-2}	5.67 μM
	oligomers	$k_{a1}:4.25 \times 10^5$ $k_{a2}:2.34 \times 10^4$	$k_{d1}:1.06 \times 10^{-1}$ $k_{d2}:5.01 \times 10^{-7}$	KD1: 249 nM KD2: 2.14 pM
26F1	monomers	2.58×10^2	1.97×10^{-2}	76 μM
	oligomers	$k_{a1}:1.01 \times 10^4$ $k_{a2}:7.94 \times 10^3$	$k_{d1}:2.13 \times 10^{-2}$ $k_{d2}:2.22 \times 10^{-6}$	KD1: 2.12 μM KD2: 279 pM
12C6	monomers	$k_{a1}:5.87 \times 10^4$ $k_{a2}:4.60 \times 10^4$	$k_{d1}:4.32 \times 10^{-2}$ $k_{d2}:3.86 \times 10^{-3}$	KD1: 737 μM KD2: 8.4 nM
	oligomers	$k_{a1}:4.43 \times 10^7$ $k_{a2}:1.32 \times 10^4$	$k_{d1}:3.29 \times 10^{-1}$ $k_{d2}:9.83 \times 10^{-6}$	KD1: 7.4 nM KD2: 0.74 nM
MJFR-14	monomers	$k_{a1}:1.04 \times 10^5$ $k_{a2}:2.22 \times 10^4$	$k_{d1}:3.43 \times 10^{-1}$ $k_{d2}:5.7 \times 10^{-6}$	KD1: 3.29 μM KD2: 0.25 nM
	oligomers	$k_{a1}:9.07 \times 10^5$ $k_{a2}:1.54 \times 10^4$	$k_{d1}:6.95 \times 10^{-4}$ $k_{d2}:4.31 \times 10^{-7}$	KD1: 0.76 nM KD2: 2.8 pM
9029	monomers	No fitting	No fitting	No fitting
	oligomers	No fitting	No fitting	No fitting
SYN211	monomers	$k_{a1}:1.52 \times 10^4$ $k_{a2}:8.37 \times 10^2$	$k_{d1}:4.10 \times 10^{-1}$ $k_{d2}:1.81 \times 10^{-5}$	KD1: 271 μM KD2: 217 nM
	oligomers	No fitting	No fitting	No fitting

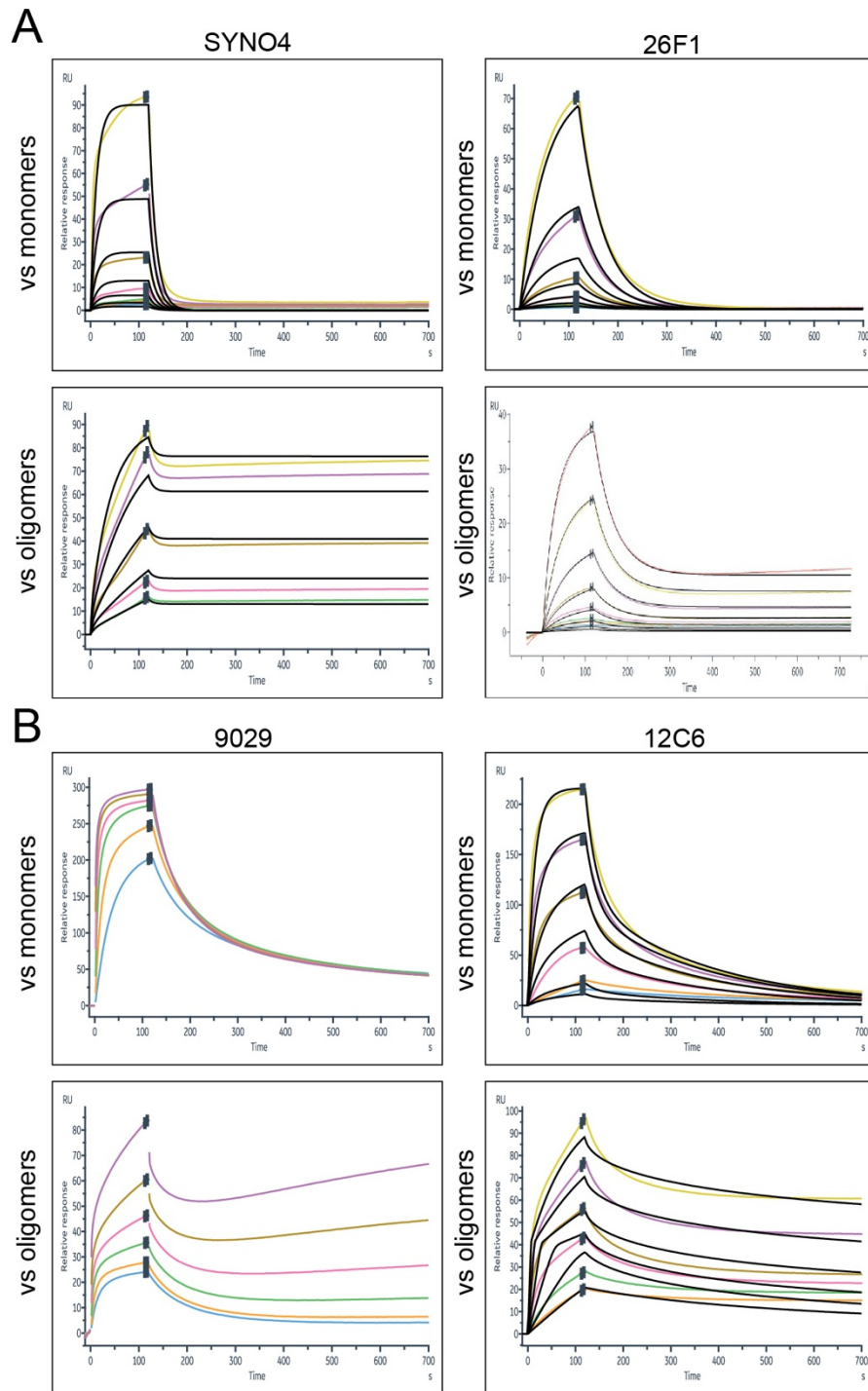


Figure 2.11: SPR-based kinetic analysis of different immobilized monoclonal antibodies (SynO4, 26F1, 9029 and 12C6) binding to aSyn monomers (A) and unmodified oligomers (B) (This figure was adapted from ⁶⁶⁸).

The MJFR-14 antibody also showed preference for binding oligomers, but still showed binding to monomers. The SPR sensograms suggested two distinct kinetics events on the dissociation portion with a

rapid drop (after 120 seconds) indicating a major fraction of monomers dissociating fastly because of the weak affinity to MJFR-14 (KD1: 3.29 μ M). However, the RU values did not return to baseline, suggesting that MJFR-14 might have a second binding to another conformation of monomers (KD2: 0.25 nM) or binds strongly to a small population of aSyn aggregates which might have formed from the monomers during the SPR experimental timeframe. MJFR-14 also showed two binding kinetics against oligomers, but, both exhibited very stronger affinity (KD1: 0.76 nM and KD2: 2.8 pM). As expected, SYN211, which recognizes all three forms of aSyn, showed a stronger affinity for monomers (Figure 2.10D). The fitting of SYN211 binding to oligomers was not possible but indicated stronger binding to oligomers, as reflected by the shape of the curves.

2.3 DISCUSSION

Increasing evidence supports the hypothesis that different forms of aSyn aggregates (e.g. fibrils and oligomers) play an important role in the pathogenesis of PD. Testing this hypothesis requires the development of therapeutic drugs or antibodies that target the different species and assays that enable the accurate assessment of changes in their levels during disease progression and in response to therapies. Although there are several biochemical, structural and imaging-based approaches for the direct and indirect visualization and characterization of aSyn fibrils^{623,698}, detection of nonfibrillar oligomeric aSyn species in cells or postmortem brain tissues remains challenging. The existing methods and techniques, such as Western blotting and proximity ligation assays, provide indications of the presence of oligomers but not information about their size, conformation and/or morphology. The instability and low abundances of native oligomers make the isolation and characterization of their structural properties using NMR and Cryo-EM very challenging. Due to these challenges, researchers in the field have resorted to the development of conformation- or aggregate-specific antibodies.

One of the major untested assumptions about conformation-specific antibodies is that they are capable of capturing the structural and morphological diversity of aSyn aggregates *in vivo* or to target specific aSyn aggregates. However, these assumptions are rarely experimentally tested. Therefore, there is a need to develop protocols and pipelines that enable systematic characterization of antibodies using a well-characterized and validated set of aSyn reagents representing, to the extent possible, the diversity of aSyn *in vivo*. Towards this goal, we developed such a validation pipeline and used it to evaluate the binding specificity of 18 aSyn antibodies, 16 of which were reported to be conformation- or aggregation state-

specific (Table 2.1). First, the antibodies were screened against disordered monomers and preparations of β -sheet rich aSyn oligomers and fibrils. This enabled us to test the specificity of the antibodies to monomers, oligomers and fibrils. To further assess whether antibody binding was indeed driven by conformational specificity or avidity, the antibodies were screened against three preparations of aSyn oligomers with distinct biochemical, conformational and morphological properties (disordered oligomers and oligomers with different β -sheet and secondary structure contents) (Table 2.4). In parallel, we also tested the specificity and binding affinities of various aSyn antibodies by SIMOA assays and SPR, respectively.

2.3.1 None of the antibodies specifically detect either monomers, oligomers or fibrillar aSyn species

Surprisingly, we found that none of the antibodies tested in our study had unique specific immunoreactivity toward one particular aSyn species (monomers, oligomers or fibrils). All 16 reported conformational-specific antibodies detected both unmodified β -sheet rich oligomers and fibrils, demonstrating that they could not differentiate between oligomers and fibrils and are not specific for a particular conformation or aSyn aggregation state.

In an attempt to assess the specificity of the antibodies against a diverse set of oligomers, we also produced oligomeric preparations (DA and HNE oligomers) possessing structurally, chemically and morphologically distinct properties (Figure 2.6). The dopamine-induced oligomers were predominantly disordered, whereas the HNE-induced oligomers were rich in β -sheet structure. The immunoreactivity toward these oligomers was compared to that toward the unmodified oligomers, which are enriched in β -sheet structures (Figure 2.4 and Figure 2.8). Despite the similarity of the CD signatures of HNE-induced and unmodified aSyn oligomers, the two types of oligomers exhibited distinct morphological features (Figure 2.2 and Figure 2.6). The structural and morphological diversity of the different oligomer preparations provided a unique opportunity to assess the specificity of the conformational-specific antibodies.

As expected, the Syn 211 and SYN-1 antibodies detected all three forms of aSyn species (monomers, oligomers and fibrils) as well as the DA- and HNE oligomers in both slot blots and Western blots (Figure 2.4)^{673,674}. This could be attributed to the fact that their epitopes are located in regions that do not constitute the core of aSyn oligomers or fibrils^{533,663,699} and are thus likely to be exposed in both aggregation states. Our results are consistent with previous studies in which Syn 211 was shown to detect monomers and HNE-induced oligomers⁵⁶¹ and the detection of monomers and fibrils by SYN-1^{671,700}.

Interestingly, the antibody clone 5G4 showed increased immunoreactivity with high conformational specificity for all forms of aSyn aggregates but showed very weak immunoreactivity toward monomers. We can not rule out the possibility that the binding to the DA oligomers could arise from the presence of partial β -sheet structure or small population of oligomers with β -sheet structure in these preparations, as suggested by the analysis of the CD data (Table 2.4). Previous studies reported that 5G4 detects widespread and distinct aSyn-induced pathology in the cortical and brain stem brain regions in postmortem synucleinopathic brain tissues⁶⁷² but only weakly detects monomeric bands in brain homogenate samples from Lewy body dementia patients. Furthermore, van Diggelen et al. found that 5G4 antibody detected HNE-induced oligomers and showed no immunoreactivity toward monomers⁵⁶¹.

However, several of our observations with a number of antibodies were not consistent with previously published reports or data provided by the manufacturers of the antibodies. Previous reports indicated that the antibody MJFR-14 is a conformational-specific antibody that detects filamentous aSyn aggregates⁷⁰¹⁻⁷⁰³, but not monomeric form of the protein. Martinez *et al.* reported that MJFR-14 is a conformation-specific with enhanced immunoreactivity towards filaments but not to the denatured filaments or monomers by dot blot analysis^{704,705}. Until the publication of a preprint version of this report in bioRxiv⁶⁶⁸, the antibody was sold by⁷⁰⁵ as “Anti-Alpha-synuclein filament antibody [MJFR-14-6-4-2] - Conformation-Specific”. Furthermore, data obtained using Luminex assay demonstrated an increased specificity of MJFR-14 antibody towards aSyn oligomers compared to monomers and filaments⁷⁰⁴ (at low ng concentrations). Interestingly, it was previously shown that MJFR-14 exhibits weaker binding to monomers, which could be eliminated by preabsorbing the antibodies with recombinant aSyn⁷⁰⁴. MJFR-14 has also been described as an oligomer-specific antibody. For example, Lassen *et al.* reported that MJFR-14 is highly specific for oligomers but not to monomers⁷⁰⁶. Direct comparison to fibrils was not performed in this study. In line with these evidences, our ELISA Simoa assay showed that MJFR-14 does not bind to monomers at low picogram concentrations (Figure 2.5B) and although it binds to both to fibrils and oligomers, it exhibits preferential binding to fibrils compared to oligomers (Figure 2.5C and 2.5D). In addition, our slot blot analysis (Figure 2.4B and Figure 2.8B) showed stronger and similar immunoreactivity towards oligomers and fibrils but a weaker immunoreactivity to monomers at 36 ng concentrations. Collectively, our studies show that MJFR-14 shows high immunoreactivity toward all aggregated forms of aSyn, including unmodified oligomers, DA- and HNE-induced oligomers and fibrils, suggesting that this antibody is neither fibril- or oligomer-specific. Furthermore, MJFR-14 binds to both β -sheet rich and disordered aSyn oligomers. Altogether, our findings confirm previous reports suggesting preferential binding of MJFR-14 to aggregate forms of aSyn, but also show that it still binds to monomers

in a concentration-dependent manner (Figure 2.4, Figure 2.5, Figure 2.8, Figure 2.10C and Figure 2.9) and recognizes aSyn monomeric bands in SDS-PAGE gels (Figure 2.4C). These observations combined with MFJR-14 strong immunoreactivity towards disordered oligomers (DA oligomers) suggest that its preferential binding to oligomers and fibrils could be driven by avidity rather than by its conformational specificity.

Similarly, Vaikath et al. reported that SYNO2, SYNO3, and SYNO4 can bind to aSyn oligomers and fibrils but not monomers⁶⁷¹. However, in our study, SYNO2 and SYNO3 recognized strongly oligomers and fibrils and detected aSyn monomers in a concentration-dependent manner (higher concentration of monomer → better immunoreactivity) (Figure 2.4 and Figure 2.8). Again, all three antibodies recognized equally β -sheet rich (oligomers and HNE oligomers and disordered oligomers (DA oligomers)), suggesting that their specificity to aSyn aggregates could be driven by avidity rather than conformational specificity. Interestingly, all three antibodies SYNO2, SYNO3, and SYNO4 recognized monomeric aSyn bands in SDS-PAGE gels (Figure 2.4C and 2.4D).

ASyO5 is another commercial antibody (Agrisera: AS13 2718) that has been reported to exclusively detect oligomers, but not monomers or fibrils (using dot blot⁷⁰⁷). However, in our hand and using the aSyn samples described above, we found that ASyO5 antibody binds non-specifically to aSyn monomers, different types of oligomers and fibrils (Figure 2.4B, Figure 2.8B and Figure 2.9).

Among the 18 antibodies in Table 2.1, the binding affinity and kinetics of only three antibodies (SYNO2, SYNO3, and SYNO4) against aSyn fibrils but not monomers or oligomers have been described in the literature or in the material provided by the manufacturer⁶⁷¹. Most importantly, we could not find any comparative SPR or binding studies using well-characterized preparations of aSyn monomers or different types of oligomers.

The comparison of the kinetics data and binding affinities of various antibodies for monomers and oligomers showed a significant degree of variation in the values of k_a , k_d , and K_D (Table 2.5). Antibody clones A17183A, 26F1, and SYNO4 showed high binding affinities for oligomers and weak binding affinities for monomers (Figure 2.10, Figure 2.11 and Table 2.5). This suggests that these antibodies are highly conformationally specific, which is in agreement with the slot blot and Western blot data (Figure 2.4B and 2.4C). Interestingly, the A17183A antibody showed stronger immunoreactivity to unstructured DA oligomers (Figure 2.8), which may hint that the binding is, perhaps, driven by avidity rather than affinity.

However, the 26F1 antibody showed specificity for β -sheet-enriched oligomers but not for unstructured DA oligomers, suggesting that it could be truly conformationally specific. The very weak affinity of 26F1 with a K_D of 76 μ M for monomers is also in line with all our analyses, including the ELISA analysis, suggesting that 26F1 is highly conformationally specific for β -sheet-enriched aSyn aggregates.

Other antibodies, such as 7015, 12C6, 9029 showed strong binding and immunoreactivities for monomers, oligomers and fibrils, although 7015 showed higher binding and immunoreactivity to oligomers and fibrils. By ELISA, the antibodies 12C6, 7015, and 9029 exhibited high immunoreactivity towards monomers at low pg concentrations (Figure 2.5B; 100 and 1000 pg/mL concentration of monomers used). This is consistent with both the slot blot and Western blot analyses, where these antibodies showed high immunoreactivity to monomers (Figure 2.4B) and detection of monomeric aSyn bands in denaturing gels (Figure 2.4C).

2.4 MATERIALS AND METHODS

2.4.1 Recombinant overexpression and purification of human WT aSyn

Recombinant overexpression and purification of human WT aSyn was performed as described previously⁷⁰⁸ with slight modifications. pT7-7 plasmids encoding human WT aSyn were used for transformation in BL21 (DE3) *E-Coli* cells on an ampicillin agar plate. A single colony was transferred to 400 mL of Luria broth (LB) medium containing 100 μ g/mL ampicillin (AppliChem, A0839) (small-scale culture) and incubated overnight at 37 °C and 180 rpm. On the next day, the pre-culture was used to inoculate 3-6 liters of LB medium having 100 μ g/mL ampicillin (large-scale culture). Upon A_{600} approaching 0.4 to 0.6, aSyn protein expression was induced by the addition of 1 mM 1-thio- β -D-galactopyranoside (AppliChem, A1008) and the cells were further incubated at 37 °C and 180 rpm for four hours. This incubation step was followed by harvesting cells by centrifugation at 4000 rpm using JLA 8.1000 rotor (Beckman Coulter, Bear, CA) for 30 minutes at 5 °C. The harvested pellets were stored at -20 °C until the next step. The cell lysis was performed by dissolving the bacterial pellet in buffer A (20 mM Tris-HCl, pH 7.5) containing protease inhibitors (1 mM EDTA (Sigma-Aldrich, 11873580001) and 1 mM PMSF (Applchem, A0999) followed by ultrasonication (VibraCell VCX130, Sonics, Newtown, CT) time: 5 min; cycle: 30 sec ON, 30 sec OFF; amplitude 70%. After lysis, centrifugation at 12000rpm and 4°C for 30minutes was performed to collect the supernatant. This supernatant was collected in 50 mL Falcon tube and placed in boiling water (100 °C) for about 15 minutes. This solution was subjected to another round of centrifugation at 12000 rpm and 4 °C for 30 minutes. The supernatant obtained at this step was filtered through 0.45 μ m filters and injected into a sample loop connected to HiPrep Q FF 16/10 (GE healthcare, 28936543). The supernatant was

injected at 2 mL/min and eluted using buffer B (20mM Tris-HCl, 1M NaCl, pH 7.5) from gradient 0 to 70% at 3 mL/min. All fractions were analyzed by SDS-PAGE, and the fractions containing pure aSyn were pooled and concentrated using a 30 kDa molecular weight cut-off (MWCO) filters (MERCK, UFC903008) at 4 °C. The retentate was collected and dialyzed using 12-14 kDa MWCO Spectrapor dialysis membrane (Spectrum Labs, 9.206 67) against deionized water at 4 °C overnight to remove salts. Dialyzed solution was collected, snap-frozen, and lyophilized.

2.4.2 Preparation of WT aSyn oligomers

To generate monomer and fibril free aSyn oligomeric preparations, 60 mg of lyophilized recombinant aSyn protein was dissolved in 5 mL PBS (10 mM disodium hydrogen phosphate, 2 mM potassium dihydrogen phosphate, 137 mM NaCl and 2.7 mM potassium chloride, pH 7.4) (final concentration: 12mg/mL) containing 5 µL Benzonase (final concentration: 1 µL benzonase/mL (MERCK, 71205-3)). After dissolving, the solution is filtered through 0.22 µm filters (MERCK, SLGP033RS) and transferred to five low-protein binding 1.5 mL tubes, each containing 1 mL solution. These tubes were incubated in a shaking incubator at 37 °C and 900 rpm for five hours. The samples were centrifuged at 12000g for 10 min at 4 °C to remove any insoluble aSyn aggregates. 5 mL of supernatant was loaded into a sample loop of the chromatography setup. This sample was run through Hiload 26/600 Superdex 200pg (GE Healthcare, 28-9893-36) column equilibrated with PBS and eluted as 2.5 mL fractions at a flow rate of 1 mL/min. The elution of protein was monitored by UV absorbance at 280nm. Different fractions were visualized by SDS-PAGE analysis, and fractions of interest (oligomer) corresponding to the void volume peak were aliquoted (500 µL), snap-frozen, and stored at -20 °C.

2.4.3 Preparation of DA-induced oligomers

DA-induced oligomers were prepared as described previously⁶⁹⁷. Briefly, the recombinant aSyn protein was dissolved in 20mM Tris and 100mM NaCl to have a final concentration of 140 µM (pH 7.4). After dissolving, the protein solution was filtered through a 100 kDa filter (MERCK, MRCFOR100). The filtrate was transferred to a low-protein binding tube and 20 equivalents of dopamine (final concentration: 2.8 mM) (Sigma-Aldrich, H8502) was added. This tube was covered with aluminum foil and incubated in a shaking incubator at 37 °C and 200 rpm for five days. The sample was centrifuged at 12000g for 10 min at 4 °C to remove any insoluble aSyn aggregates. The supernatant was loaded into a sample loop of the chromatography setup. This sample was then run through Superdex 200 Increase 10/300 GL (GE

healthcare, 28990944) column equilibrated with PBS and eluted as 0.5 mL fractions at a flow rate of 0.4 mL/min. The elution of protein was monitored by UV absorbance at 280 nm. The SEC fractions were analyzed by SDS-PAGE analysis, and fractions of interest (oligomer) were collected and stored at 4 °C.

2.4.4 Preparation of HNE-induced oligomers

HNE-induced oligomers were prepared as described previously⁶⁸⁴. Briefly, the recombinant aSyn protein was dissolved in 20 mM Tris and 100 mM NaCl to have a final concentration of 140 µM (pH 7.4). After dissolving, the protein solution was filtered through 100 kDa filter (MERCK, MRCFOR100). The filtrate was transferred to a low-protein binding tube and 30 equivalents of HNE (Cayman Chem, 32100) (final concentration: 4.2mM) was added. This tube was incubated in an incubator at 37°C under quiescent conditions for 18 hours. Following incubation, the sample was centrifuged at 12000g for 10 min at 4 °C to remove any insoluble aSyn aggregates. The supernatant was loaded into a sample loop of the chromatography setup. This sample was run through Superdex 200 Increase 10/300 GL (GE healthcare, 28990944) column equilibrated with PBS and eluted as 0.5 mL fractions at a flow rate of 0.4 ml/min. The elution of protein was monitored by UV absorbance at 280nm. The SEC fractions were analyzed by SDS-PAGE analysis, and fractions of interest (oligomer) were collected and stored at 4 °C.

2.4.5 Protein concentration estimation

The concentration of aSyn samples such as monomers, oligomers, and fibrils were estimated using BCA assay and amino acid analysis. For BCA assay, microplate measurements were carried out using BCA protein assay reagents (Pierce, catalog number: 23227). Briefly, triplicates of known concentrations (from 10 µg/mL-1000 µg/mL) of bovine serum albumin (concentration standard) and an equal volume of aSyn samples were pipetted into microplate wells. To which, 200 µL of BCA working reagent was added and incubated at 37 °C for 30 minutes. Absorbance at 562 nm was measured using a Tecan plate reader. Using BCA assay based concentration estimation as standards, known concentrations (2-3 µg) of aSyn samples were pipetted into a conical insert, flash-frozen, and lyophilized. The dried form of aSyn samples was shipped to Functional Genomic Center Zurich for subjecting for amino acid analysis (AAA) for absolute quantification of aSyn samples concentrations.

2.4.6 Preparation of WT aSyn fibrils

WT aSyn fibrils were prepared as described in¹⁶. Briefly, 4 mg of lyophilized recombinant aSyn was dissolved in 50 mM Tris, and 150 mM NaCl and pH was adjusted to 7.5. The solution is filtered through

0.2 μm filters (MERCK, SLGP033RS), and the filtrate is transferred to black screw cap tubes. This tube was incubated in a shaking incubator at 37 °C and 1000 rpm for five days. After five days, the formation of fibrils was assessed by TEM and SDS-PAGE, followed by Coomassie staining as described in⁸⁹.

2.4.7 Characterization of oligomers by SDS-PAGE analysis

Human WT aSyn monomers, unmodified WT, DA-induced, and HNE-induced oligomers were run on 15% polyacrylamide gels, and Coomassie blue staining was performed as described previously⁶⁶¹. Before carrying out Western blot analysis, equal loading on the gel was also confirmed using Coomassie staining or silver staining (Invitrogen, LC6100) as per manufacturers protocol.

2.4.8 Characterization of oligomers by TEM analysis

TEM analysis of protein samples were performed as described previously⁶⁶¹. Briefly, 5 μL protein samples were placed on glow discharged Formvar and carbon-coated 200 mesh-containing copper EM grids. After about a minute, the samples were carefully blotted using filter paper and air-dried for 30 s. These grids were washed three times with water and followed by staining with 0.7% (w/v) uranyl formate solution. TEM images were acquired by Tecnai Spirit BioTWIN electron microscope, and image analysis was performed by ImageJ software as described previously⁶⁶¹.

2.4.9 Far-UV circular dichroism (CD) spectroscopy

Approximately 150 μL of protein samples were loaded onto 1 mm path length quartz cuvette, and CD spectra were obtained on Chirascan spectropolarimeter (Applied Photophysics) with the following parameters as described in⁶⁶¹. Temperature: 20 °C; wavelength range: 198 to 250 nm; data pitch: 0.2 nm; bandwidth: 1 nm; scanning speed: 50 nm/min; digital integration time: 2 s. The final CD spectra was a binomial approximation on an average of 10 repeat measurements. The secondary structural content of the oligomers was estimated using the online CD analysis tool known as CAPITO⁷⁰⁹.

2.5.0 Mass spectrometry analysis

Mass spectrometry (MS) analysis of proteins were performed by liquid chromatography-mass spectrometry (LC-MS) on the LTQ system (Thermo Scientific, San Jose, CA). Before analysis, proteins were desalted online by reversed-phase chromatography on a Poroshell 300SB C3 column (1.0x75mm, 5 μM , Agilent Technologies, Santa Clara, CA, on the LTQ system). 10 μL protein samples were injected on the column at a flow rate of 300 $\mu\text{L}/\text{min}$ and were eluted from 5 % to 95 % of solvent B against solvent A,

linear gradient. The solvent composition was, Solvent A: 0.1% formic acid in ultra-pure water; solvent B: 0.1% formic acid in acetonitrile. MagTran software (Amgen Inc., Thousand Oaks, CA) was used for charge state deconvolution and MS analysis.

2.5.1 Temperature stability analysis of oligomers

Human WT aSyn unmodified WT, DA-induced and HNE-induced oligomers were tested for their stability at different temperature conditions. Morphological characteristics were assessed by TEM under conditions such as freeze-thaw cycles, storage at 4°C or 37°C for 5 days.

2.5.2 Binding characterization of aSyn species to different antibodies by Slot blot analysis

Nitrocellulose membranes (Amersham, 10600001) were spotted with 5 µL and 1 µL samples volumes corresponding to 180 ng and 36 ng of aSyn proteins in duplicates (monomers, oligomers, DA-induced oligomers, HNE-induced oligomers and fibrils) per sample spot. The membranes were blocked for 1 hour with Odyssey blocking buffer (LiCoR, 927-40000), and then incubated overnight with different primary antibodies (Table 2.1) diluted in PBST at 2 µg/mL concentration for all the antibodies except SYN-1 antibody at 1 µg/mL concentration (Figure 2.4 and 2.8). Varying concentrations of primary antibodies (200, 20 and 2 ng/mL) were used in the Figure 2.9. The membranes were washed three times, with 0.1% PBS-Tween (3x10minutes) and incubated with IRdye conjugated secondary antibodies (1:7500) (Table 2.6) for 1 hour at RT. Thereafter, the membranes were washed three times, with 0.1% PBS-Tween (3x10minutes). The visualization was performed by fluorescence using Odyssey CLx from LiCor. Equal loading of protein samples on the membrane was confirmed using Ponceau S (MERCK, P3504) staining (2% Ponceau S (w/v) in 5% acetic acid).

Table 2.6: Materials and Reagents

Equipment/Material description	Supplier	Catalogue/Reference
Chromatography columns		
HiPrep Q FF 16/10	GE healthcare	28936543
Hiload 26/600 superdex 200pg	GE healthcare	28-9893-36
Superdex 200 Increase 10/300 GL	GE healthcare	28990944
Tubes and Filters and dialysis membrane		
Low protein binding tubes	Eppendorf	022431081
30 kDa MWCO	MERCK	UFC903008
100 kDa MWCO	MERCK	MRCFOR100
0.22 µm filters	MERCK	SLGP033RS
0.45 µm filters	MERCK	SLFH05010
12-14 kDa MWCO dialysis membrane	Spectrum Labs	9.206 67

Chemicals and Reagents		
TRIS	Biosolve	200923
Ampicillin	AppliChem	A0839
IPTG	Biochemica	A1008
EDTA-free Protease Inhibitor Cocktail	SIGMA	11873580001
PMSF	Applchem	A0999
Dopamine	Sigma Aldrich	H8502
4-hydroxy Nonenal (HNE)	Cayman Chem	32100
Benzonase® Nuclease HC	MERCK	71205-3
Ponceau S	MERCK	P3504
SilverXpress Silver staining kit	Invitrogen	LC6100
Centrifuges and Sonicator		
Ultrasonicator	VibraCell, Sonics	VCX130
Benchtop centrifuge	Eppendorf	5417R
Ultracentrifuge	Beckmann Coulter	Optima Max XD
Blocking Buffer and Secondary Antibodies		
Odyssey blocking buffer	LiCoR	927-40000
Goat anti-mouse AF680	Invitrogen	A21058
Goat anti-rabbit AF800	Invitrogen	926-32211
Goat anti-rat IRDye 680RD	LiCoR	P/N 926-68076

2.5.3 Western blot analysis

Approximately 36 ng (Figure 2.4C) and 180 ng (Figure 2.4D) of proteins (monomers or oligomers or fibrils) were loaded onto 15 % SDS-PAGE gels (prior to loading samples were boiled at 95°C for 10 minutes) and run at 180 V for 1 hour in running buffer (25 mM Tris, 192 mM Glycine, 0.1% SDS, pH 8.3). Gels were transferred onto nitrocellulose membranes (Amersham, 10600001) at 25 V, 0.5 A, and 45 minutes using Trans-Blot Turbo (Bio-Rad, 170-4155). The membranes were blocked for 1 hour with Odyssey blocking buffer (LiCoR, 927-40000), and then incubated overnight with different primary antibodies (Table 2.1) diluted in PBST at 2 µg/mL concentration for all the antibodies except SYN-1 antibody at 1 µg/mL concentration. The specificity of MJFR-14 was also assessed at 2 ng/mL against 180 ng of aSyn monomer, oligomers and fibrils (Figure 2.9B). The membranes were washed three times, with 0.1% PBS-Tween (3x10minutes) and incubated with IR dye conjugated secondary antibodies (1:7500) (Table 2.6) for 1 hour at RT. After that, the membranes were washed three times, with 0.1% PBS-Tween (3x10 minutes). The visualization was performed by fluorescence imaging using Odyssey CLx from LiCoR.

2.5.4 Determination of antibody affinities by surface plasmon resonance (SPR, BIACORE)

SPR data were collected on a Biacore 8K device (GE Healthcare). Selected antibodies were immobilized on a CM5 biosensor chip (GE Healthcare) at 10-20 $\mu\text{g/mL}$ concentration in 10 mM acetate solution (GE Healthcare) at pH 4.5 to reach a final surface ligand density of around 2000-4000 response units (RUs). In short, the whole immobilization procedure using solutions of 1-ethyl-3-(3-dimethyl aminopropyl) carbodiimide (EDC) and N-hydroxy succinimide (NHS) mixture, antibody sample and ethanolamine, was carried out at a flow rate of 10 $\mu\text{L/min}$ into the flow cells of the Biacore chip. Firstly, the carboxyl groups on the sensorchip surface were activated by injecting 200 μL of 1:1 (v/v) mixture of EDC/NHS (included in the amine coupling kit, Cytiva life sciences) into both flow cells 1 and 2 and followed by the injection of antibodies overflow cell 2 for 180 s. The remaining activated groups in both the flow cells were blocked by injecting 129 μL of 1 M ethanolamine-HCl pH 8.5. The sensor chip coated with antibodies were equilibrated with PBS buffer before the initiation of the binding assays. Serial dilutions of analytes such as aSyn monomers or oligomers (oligomers) at a concentration ranging between 2 μM to 0.030 μM in PBS buffer were injected into both flow cells at a flow rate of 30 $\mu\text{L/min}$ at 25 $^{\circ}\text{C}$. Each sample cycle has the contact time (association phase) of 120 seconds and followed by a dissociation time of 600 seconds. After every injection cycle, surface regeneration of the Biacore chips was performed using 10 mM glycine (pH 3.0). The obtained data were processed and analyzed using Biacore 8K evaluation software for the calculation of the binding kinetics (association rate constant (K_a) and dissociation rate constant (K_d)) and binding affinity (KD). The fitting of the data was based on either 1:1 binding model (mostly for the monomers) or heterogeneous ligand binding model (for oligomers) using global kinetic fitting unless otherwise noted.

2.5.5 Antibody characterization and stability analysis of oligomers by digital sandwich ELISA using Simoa technology

The Quanterix Simoa platform is a highly sensitive platform that allows detection at the sub pg/mL concentration range⁷¹⁰. Attempts to measure for example neurofilament light into plasma matrix were successful by Simoa technology as described before⁷¹¹. Kuhle et al compared three immunoassays for neurofilament light chain measurements into blood. The analytical sensitivity was 78 pg/mL and 0.62 pg/mL for the conventional ELISA and the Simoa based assay, respectively. The presence of conformational synuclein forms (oligomers and fibrils) into body fluids like CSF is expected to be low abundant making the Simoa platform the preferred technology platform for our experimental work.

A sandwich ELISA Simoa immunoassay was used to assess the immunoreactivity of different aSyn antibodies towards aSyn uclein forms such as monomers, oligomers, and fibrils. To prepare the conjugated

beads, paramagnetic carboxylated particles/beads were activated for 15 minutes at 4 °C using 0.05 mg/mL of 1-ethyl-3-[3-dimethylaminopropyl]carbodiimide hydrochloride (EDAC) (ThermoScientific, Cat N°A35391) added to 1.40×10^9 beads/mL. The beads were washed using a magnetic separator, and 0.1 mg/mL of the oligomeric aSyn uclein specific monoclonal capture antibody was added. After 2 hours of incubation on a mixer-shaker at 4 °C, the conjugation reaction was blocked (Quanterix blocking buffer, Cat N°101356) for 30 minutes at room temperature. The conjugated beads were washed and stored at 4 °C. The biotinylated detector antibody (SYN211) was used with an antibody/biotin ratio of 64. The assay was performed on the fully automated Quanterix Simoa HD-1 with a 2-step protocol. The undiluted samples were tested, which required 300 µL volume of samples without accounting for dead volume (duplicate testing). The calibrator diluent consists of 1xPBS with 0.1% milk, 0.1% Tween. The first incubation step of the sample with the beads was 60 minutes. After washing, the second incubation step with streptavidin-β-galactosidase (Quanterix, Cat N° 103397) was 5 minutes. Prior to reading Resorufin-β-D-galactopyranoside (Quanterix, Cat N° 101736) was added. The resulting fluorescence signal is captured and translated into an AEB value (Average Enzymes per Bead) that is proportional to the analyte concentration in the measured sample.

2.5 Contributions of the authors

Somanath Jagannath (SJ) and Senthil T. Kumar (STK) designed, performed and analyzed all experiments except ELISA. Cindy Francois (CF) carried out the ELISA assay. Hilal A. Lashuel (HAL), Hugo Vanderstichele (HV), and Erik Stoops (ES) conceived and conceptualized the study. STK, SJ, ES and HAL analyzed the data. STK, SJ and HAL wrote the chapter, with inputs from CF and ES.

This chapter is published in Neurobiology of disease journal: **Kumar S.T.*; Jagannath S.***; Francois C, Vanderstichele H.; Stoops E.; Lashuel H.A[#]. “How specific are the conformation-specific α-synuclein antibodies?” Neurobiology of Disease, 2020 (* equal contributions; # corresponding author)

Chapter 3: a-synuclein fibrils are the key mediators of seeding and pathology spreading in the PFF-based seeding model

3.1 INTRODUCTION

Parkinson's disease (PD) is a progressive neurodegenerative disease characterized by the loss of dopaminergic neurons in the substantia nigra and other brain regions in the advanced stages of the disease⁷¹². The presence of intracellular proteinaceous accumulations composed of misfolded and aggregated forms of the presynaptic protein, alpha-synuclein (aSyn), in surviving neurons, is one of the defining pathological hallmarks of PD and other neurodegenerative disorders, also known as synucleinopathies^{5,7}. Several mutations in aSyn or multiplications in the gene that code of the aSyn protein cause early onset PD and enhance aSyn aggregation *in vitro* and *in vivo*. This led some to hypothesize that aSyn fibrillization and LB formation are the primary drivers for neurodegeneration in PD and related synucleinopathies. However, this hypothesis failed to explain several neuropathological and clinical observations – these include: 1) The presence of LBs in postmortem brains of individuals with no Parkinsonian symptoms^{627,628,713}; 2) Appearance of Parkinsonian symptoms in patients in the absence of LBs⁶²⁹⁻⁶³²; 3) The lack of correlation between Lewy pathology burden or levels of LB-associated proteins in plasma, neurodegeneration and diseases severity in some cases of synucleinopathies^{625,626,714}. To reconcile these observations, it was suggested that early events in the process of aSyn aggregation, i.e., formation of aSyn oligomers, rather than aSyn fibrillization and LB, could be the primary initiator and driver of aSyn toxicity and neurodegeneration.

Similarly, several studies supported the aSyn oligomer hypothesis in PD. These include: 1) consistent detection of oligomer formation during the *in vitro* aggregation of aSyn under various conditions^{536,636,637}; 2) the observation that oligomeric forms of aSyn exhibit membrane permeabilizing properties^{8,9,657}; induced toxicity in cellular models and *in vivo*^{386,715,716}; 3) Presence of oligomers in the biological fluids such as saliva, blood plasma, cerebrospinal fluid^{540,541,544,639,641,642,717,718}. Furthermore, several of these studies reported increased levels of aSyn oligomers in PD patients and suggested that they correlate with the diagnosis and progression of PD^{540,544,641,719-722}.

aSyn aggregation is a dynamic process during which various oligomeric and fibrillar forms of aSyn can co-exist and be in dynamic equilibrium⁷²³. Oligomers are the soluble, intermediate, multimeric species that form prior to the formation of aSyn fibrils but can also co-exist with fibrillar and other aggregated forms of aSyn within pathological aggregates in the brain. Under *in vitro* conditions, on- and off-pathway soluble, and non-fibrillar aSyn oligomers of different sizes and morphologies have been detected and characterized *in vitro*^{536,636,637}. In the absence of monomers, converting oligomers to fibrils is very slow. However, in the presence of excess monomers, both on- and off-pathway oligomers convert to fibrils. In the case of the off-pathway oligomers, this occurs through their disassociation to monomers which are then integrated into growing oligomeric or fibrillar forms of aSyn. Different types of oligomers have been implicated in various purported mechanisms of aSyn toxicity, including in membrane damage^{9,386,716}, mitochondrial defect^{568,654,724}, ER stress⁶⁵³, proteasomal dysfunction, autophagy and lysosomal dysfunction⁶⁵⁰⁻⁶⁵², synaptic dysfunction^{507,560,648,725}.

Increasing evidence suggests that aSyn pathology spreading in the brain and the progression of PD are mediated, at least in part, by the transfer of seeding-competent aSyn species from one cell to another. To investigate these mechanisms, aggregated forms of aSyn are usually injected into mice brains or muscles and pathology formation and spreading are monitored using antibodies against phosphorylated aSyn at S129, which is the dominant post-translational modification in LBs and LNs. Several studies have also suggested that oligomeric forms of aSyn could be the primary species that are secreted by neurons and mediate aSyn cell-to-cell propagation in neighboring cells and from one brain region to another^{464,583,584,726,727}. Interestingly, despite these claims, the great majority of the published work on aSyn seeding and propagation in neuronal and animal models of pathology spreading has relied on using preformed fibrils (PFFs), wherein PFFs act as seeds and recruit endogenous aSyn to form aSyn aggregates. This is in part because of the limited knowledge about on the *in vitro* seeding activity of different types of oligomers and their relation to aSyn fibrils and pathology in diseased brains. Furthermore, whether intermediate aSyn oligomers are formed in aSyn seeding models remains unknown and our understanding of their role in pathology formation and spreading in the PFFs-based neuronal seeding models is incomplete.

Some of the limitations of some of the previous studies include: i) the use of one type of aSyn oligomers and thus are may not capture the diversity of aSyn oligomers that might exist in the diseased brains; 2) assessing aSyn oligomer toxicity under nonphysiological concentrations; 3) use of model systems, such as overexpression systems, that do not recapitulate PD pathology to assess the seeding or spreading

properties of oligomers^{386,728}; 4) many of the conclusions on the existence of oligomers were based on tools (e.g., antibodies) that do not distinguish between oligomers and fibrils⁵³⁸; 5) lack of validation of oligomer presence or accumulation using independent techniques; 6) use of fluorescently tagged proteins with poor solubility^{728,729}; vii) no isolation and characterization of oligomers; viii) No information about the biochemical and biophysical properties of the oligomers.

In this chapter, we sought to systematically address the current knowledge gaps on the role of aSyn oligomers in the initiation, seeding and pathology spreading of aSyn. Towards this goal, we used different biophysical approaches to investigate aSyn seeding *in vitro* and in neurons and animal models of aSyn seeding and pathology spreading. More specifically we sought to determine whether oligomers are formed in the PFF-based neuronal seeding model? This was achieved using SEC fractionation of soluble fraction isolated from neurons treated with PFFs to probe intracellular aSyn oligomers and Western blotting analysis of the extracellular media to probe for secreted aSyn species. Next, we investigated if aSyn oligomers are seeding competent. This was assessed in primary hippocampal neurons, in cell free systems and *in vivo*. To determine if different types of oligomers exhibit differential neuronal seeding activity, all of the experiments were carried out using three distinct preparation of aSyn oligomers with distinct morphological and structural properties: unmodified oligomers (UO), dopamine-induced oligomers (DO) and HNE-induced oligomers (HO). To gain mechanistic insight into the dynamic equilibrium between aSyn monomers, oligomers and fibrils during aSyn seeding and fibrillization, we also conducted systematic studies to compare the seeding activity of the different preparation of oligomers in the presence of aSyn monomers or mixtures of aSyn monomers and fibrils (Figure 3.1).

Our results demonstrate that oligomeric forms of aSyn do not form in the PFF-based neuronal seeding model, where the process is dominated by fibril-mediated seeding and fibril growth. We also demonstrate that the different types of oligomers (UO, DO, and HO) do not have seeding activity *in vitro* and primary hippocampal neurons, and their presence slows rather than accelerates aSyn fibrillization. Our studies reveal that fibrils and oligomer growth occur through monomer addition, and fibrils compete more efficiently for monomer addition. Also, depletion of monomers might favor more oligomer dissociation to monomers which could be cleared or re-enter the aggregation pathway through addition to fibrils. Altogether, our work points to fibrils as the most seeding competent species and suggest that they are the key mediators of pathology spreading in PD and other synucleinopathies. The implications of our finding for future mechanistic studies and current aSyn targeting therapies are discussed.

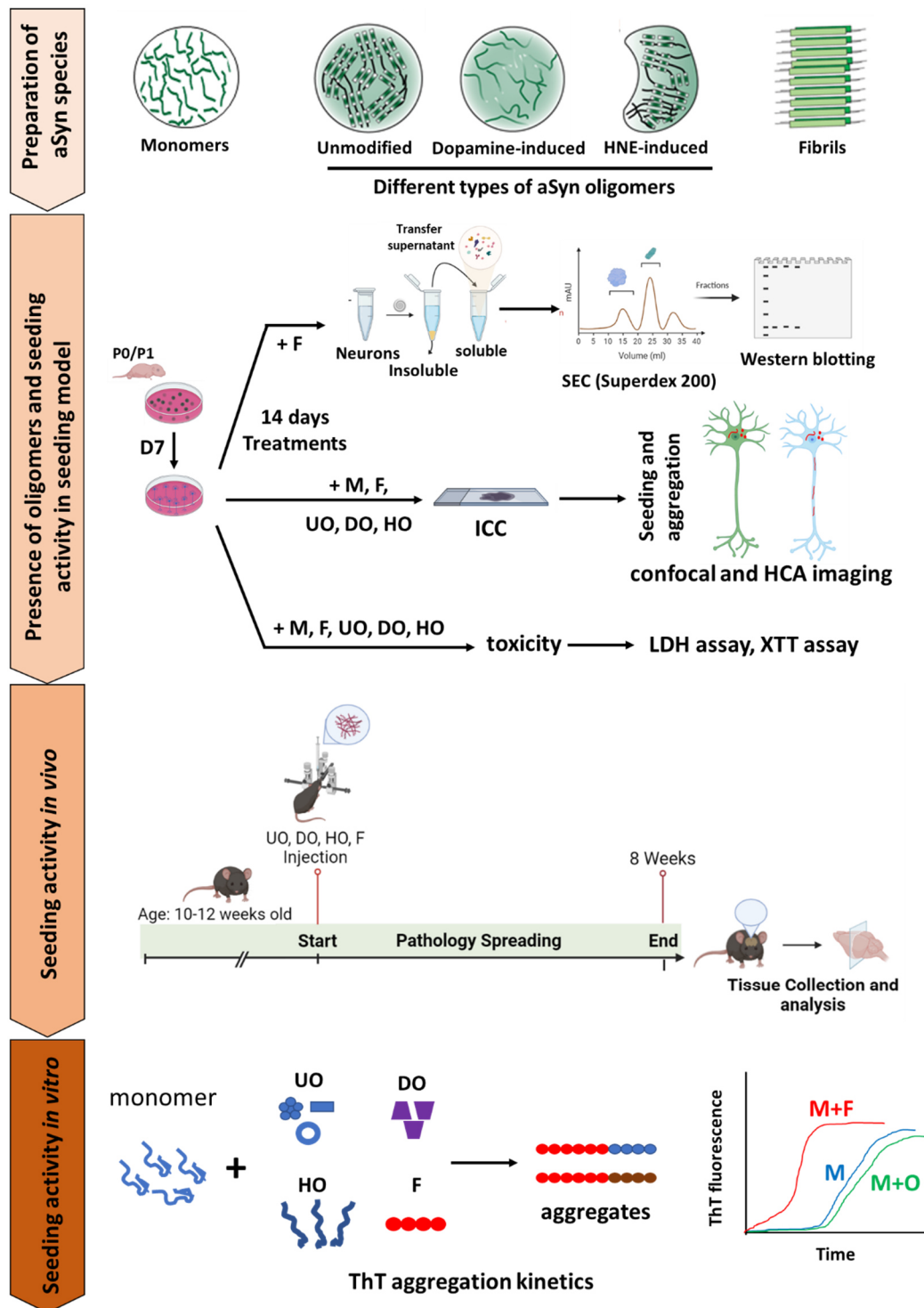


Figure 3.1: A schematic illustration of our workflow to investigate the role of aSyn oligomers in the aggregation process and toxicity. In brief, the pipeline included the preparation of well-defined preparation of aSyn monomers, fibrils and three different types of oligomers. The presence of oligomers is investigated in the neuronal seeding model by biochemistry. Oligomer seeding activity is assessed in primary hippocampal neurons *in vivo*. In addition, our workflow included toxicity by different types of oligomers in primary hippocampal neurons and *in vitro* approaches to study the seeding activity of different types of oligomers in relation to fibrils.

3.2 RESULTS

3.2.1 oligomeric aSyn do not accumulate in the PFF-based neuronal seeding model of aSyn pathology formation

To investigate whether aSyn oligomers form and populate during PFF seeding-mediated aSyn aggregation and pathology formation, we sought to monitor their formation in primary hippocampal neurons treated with PFFs or with PBS. After 14 days post-treatment with PFFs, the lysates were separated into soluble and insoluble fractions. The soluble fraction (approx. 1000 ul) of treated and non-treated neurons was injected into the size exclusion chromatography (SEC) column (Superdex 200 10/300 GL) (Figure 3.2A, 3.2D). The elution pattern of aSyn (distribution of aSyn species of different sizes) was then assessed by analyzing all the fractions by Western blotting (WB), using aSyn antibodies targeting 134-138 amino acids of aSyn.

In the case of primary neurons treated with +PFFs, aSyn eluted with an elution volume corresponding to that expected for the unfolded monomer and no aSyn was detected in the void volume peak (Figure 3.2B). Similar findings were obtained when primary neurons were treated with PBS only (Figure 3.2E). To verify if our inability to detect oligomers is arising from possible dissociation of oligomers in the column, we carried out a similar experiment where we spiked-in (75 ug of UO) into the soluble fractions of PFF and PBS treated neurons before injection onto the Superdex 200 gel-filtration column (Figure 3.3A). As expected, for the “spiked” samples, native brain-derived aSyn monomer eluted at the same position as before. However, we also observed oligomeric SDS-resistant bands, which co-elutes the same position as the recombinant oligomer (Figure 3.3B and 3.3C), which is about one-third of the column volume (between 7 to 11 ml) of the Superdex 200 10/300GL.

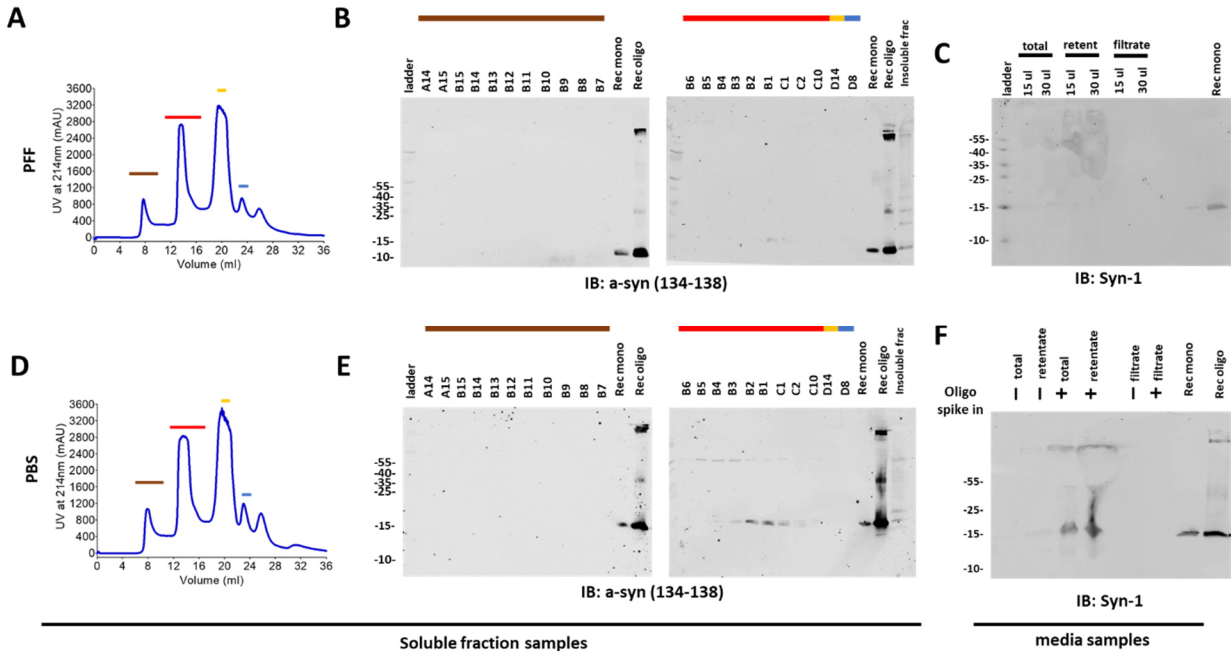


Figure 3.2: Probing the presence of oligomers in the PFF-based neuronal seeding model in primary hippocampal neurons. (A-D) SEC of soluble fractions of primary hippocampal neurons treated with PBS and PFFs. (E, F) Detecting the presence of oligomers before and after spike in the media samples.

Previous studies have suggested that aSyn oligomers could be secreted and contribute to the cell-to-cell propagation of aSyn and pathology spreading of in the brain^{581,730}. Therefore, we considered the possibility that the absence of intracellular oligomers could be due to their rapid secretion. To test this hypothesis, we collected the media from the neurons treated with PFFs and subjected it to a filtration protocol⁶⁶¹ to separate monomeric (flow-through) and oligomeric fractions (retentate) using a 100 kDa filters, which we have shown previously to allow for isolation of minute amounts of oligomers from aSyn samples⁶⁶¹. The flow through and retentate samples were then analyzed by Western blotting and probed with SYN-1 antibody (Figure 3.2C).

Surprisingly, no oligomeric or monomeric bands were detected in the retentate samples. We also performed a similar experiment with oligomers spiked into the culture media to validate our filtration protocol. Under these conditions, we detected oligomeric bands in total and retentate fractions but not in the flow through fractions (Figure 3.2F), thus demonstrating the robustness of our method to isolate monomeric and oligomeric fractions from the media samples. Our SEC fractionation results on soluble fractions from neuronal lysates suggest that aSyn oligomers do not populate during PFF-mediated seeding in neurons, which is consistent with the absence of oligomers in the extracellular culture media. The

absence of oligomers in both samples suggests that oligomers either do not form or populate in seeding-mediated fibrillization conditions and thus may not play important role in the formation of aSyn pathology in the PFF-based neuronal seeding models of aSyn pathology formation and cell-to-cell propagation.

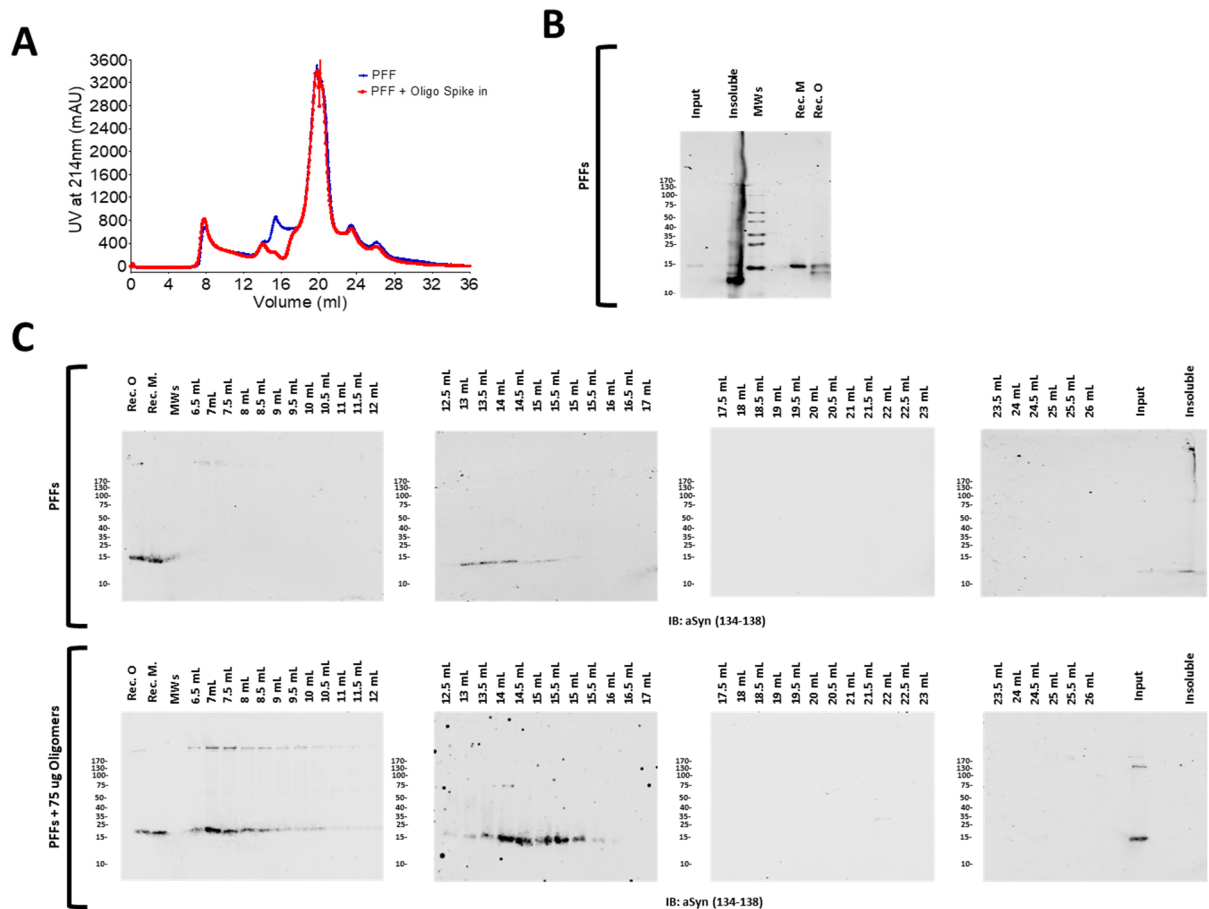


Figure 3.3: Oligomeric aSyn with oligomer spike-in of soluble fractions of neurons treated with PFFs. (A) SEC chromatograms with or without oligo spike in of neurons treated with PFFs. (B) Western blotting of insoluble fraction showing streaks confirming successful seeding upon PFF treatment in primary neurons. (C) SEC of soluble fractions without or with 75ug oligo spike in.

3.2.2 Preparation and characterization of morphologically and structurally different types of aSyn oligomers

The experiments in Figure 3 did not address the important question of whether aSyn oligomers have the capacity to seed the aggregation of endogenous aSyn in primary neurons. Therefore, to investigate specifically the role of oligomers in the initiation of aSyn aggregation process, we generated highly pure and well-characterized preparations of three morphologically and structurally distinct types of aSyn oligomers as previously described in⁶⁶⁸. Oligomers prepared in the absence of any chemical reagent are

termed as unmodified oligomers (UO), and oligomers prepared in the presence of HNE and dopamine are termed as HO and DO, respectively. All three oligomeric were purified using size exclusion chromatography (SEC) (Figure 3.4A, 3.4E, 3.4I). Transmission electron microscopy (TEM) analysis of i) UO showed the presence of heterogeneous structures ranging from spherical to tubular to rectangular structures (Figure 3.4B); ii) HO showed the presence of curvilinear morphologies (Figure 3.4F); iii) DO showed the presence of spherical and un-structured morphologies (Figure 3.4J). Sodium dodecyl sulfate–polyacrylamide gel electrophoresis (SDS-PAGE) analysis of i) UO showed the presence of high molecular weight bands that do not enter resolving gel corresponding to oligomeric fractions (Figure 3.4C); ii) HO and DO showed very high molecular weight streaks in the stacking gels (Figure 3.4G, 3.4K). UO and HO exhibited a CD spectrum with a broad minimum peak centered at 219 nm (Figure 3.4D, 3.4H), indicating the presence of mixed secondary structure contents dominated by β -sheeted structures. DO exhibited CD spectra with a minimum at 198 nm, revealing the presence of species with predominantly disordered conformations (Figure 3.4L).

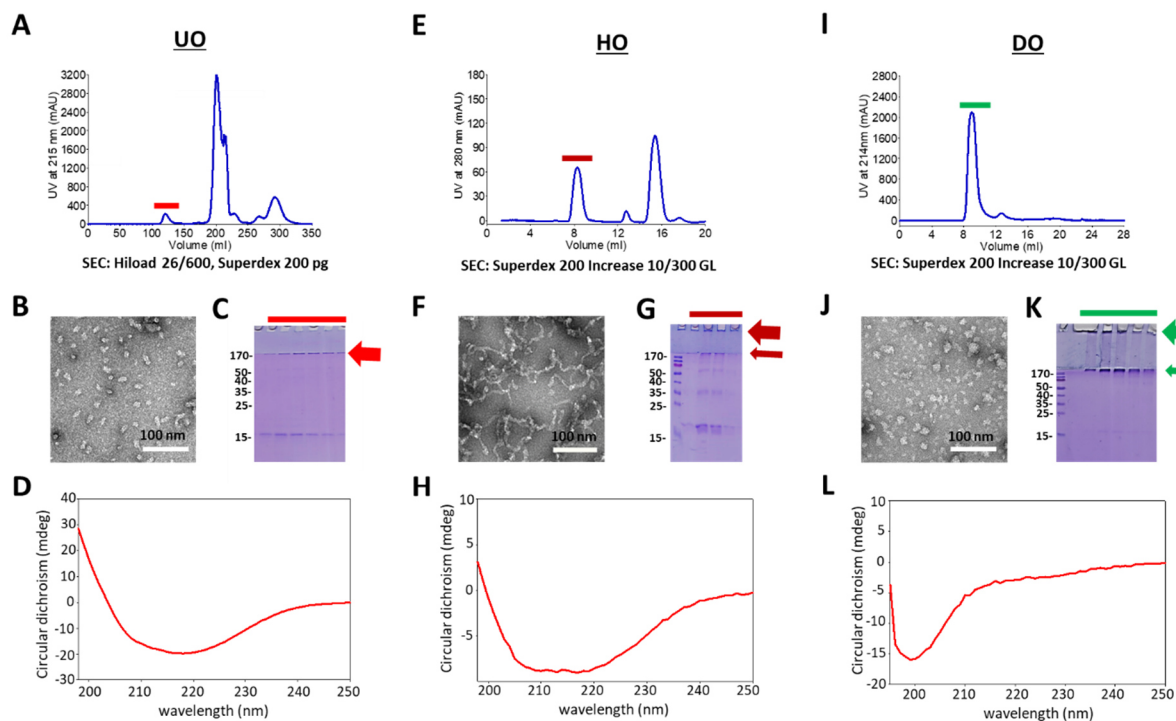


Figure 3.4: Preparation and characterization of morphologically and structurally different human aSyn oligomers. (A) SEC purification of UO oligomers by HiLoad 26/600, Superdex 200pg. (B) TEM analysis of UO fraction showing morphologically different structures. (C) SDS-PAGE Coomassie analysis of UO showing SDS-resistant bands that do not enter resolving gel. (D) CD spectra of UO showing majorly β -sheeted structure. (E) SEC purification of HO oligomers by Superdex 200 increase 10/300 GL. (F) TEM analysis of HO fraction showing curvilinear morphologies. (G) SDS-PAGE Coomassie analysis of HO showing high molecular weight bands. (H) CD spectra of HO. Showing majorly β -sheeted secondary structures (I) SEC purification of DO oligomers by Superdex 200 increase 10/300 GL. (J) TEM

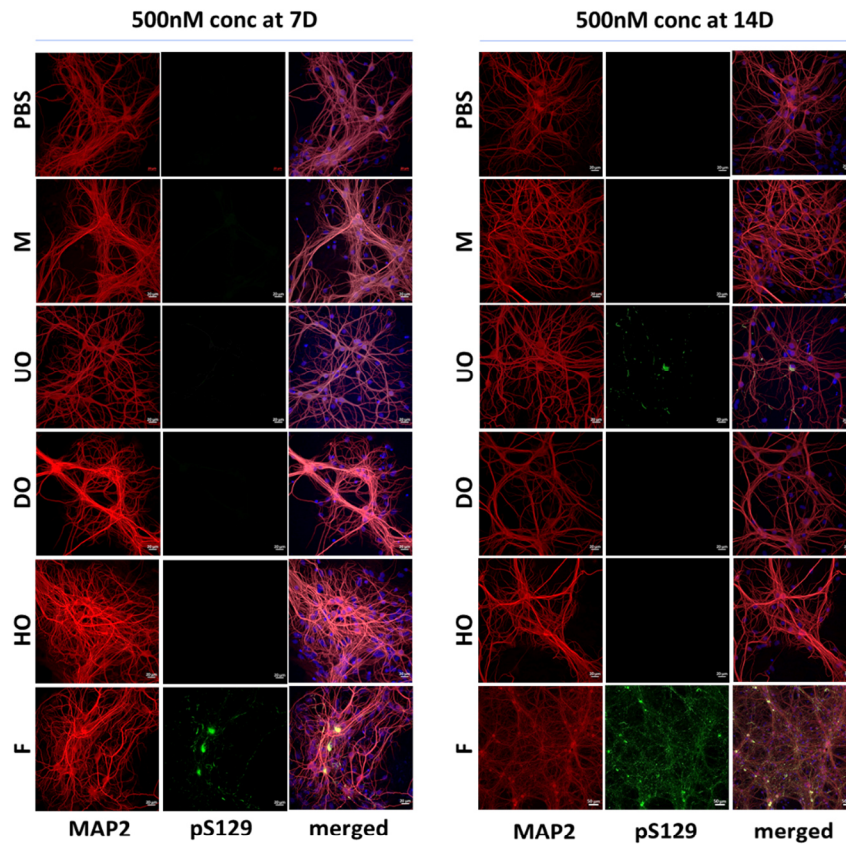
analysis of DO fraction showing mainly spherical and undefined morphologies. (G) SDS-PAGE Coomassie analysis of DO. (H) CD spectra of DO showing majorly disordered structures. Abbreviations: UO- Unmodified oligomers; HO- HNE-induced oligomers; DO- dopamine-induced oligomers

3.2.3 Unmodified aSyn oligomers, but not DO or HO oligomers, exhibited marginal seeding activity only at higher concentrations.

We next investigated whether the different types of oligomers act as seeds capable of recruiting or inducing endogenous aSyn to fibrillize and form LB-like inclusions, as consistently observed for aSyn PFFs. We treated primary hippocampal neurons with different concentrations (70 nM, 140 nM, 250 nM, 500 nM) of aSyn oligomeric species (UO, DO, HO) or aSyn monomers or PFFs (conc 70 nM) as negative and positive controls. The extent of seeding was assessed by quantification of pS129 positive aggregates at two different time points, 7 days and 14 days after the treatment (Figure 3.5A, Figure 3.6). Immunohistochemical analysis at the 7 days and 14 days post-treatment revealed that none of the oligomer preparations exhibited seeding activity over the concentration range of 70-250 nM. Interestingly, at an oligomer concentration of 500 nM, only the UO oligomers showed marginal seeding activity. As expected, we observed robust seeding activity for aSyn PFFs at 70 nM but not aSyn monomers (70 nM, 140 nM, 250 nM, 500 nM). For a more quantitative assessment of oligomer seeding activity, we performed similar experiments and quantified the level of pS129 aggregates using high-throughput content imaging, as described previously¹⁶. We observed similar results as shown in (Figure 3.5B). These findings further support the idea that aSyn fibrils but not oligomers are the primary seeding-competent species capable of inducing the formation of pS129 positive aggregates.

A

ICC at 7 and 14 days after treatment



B

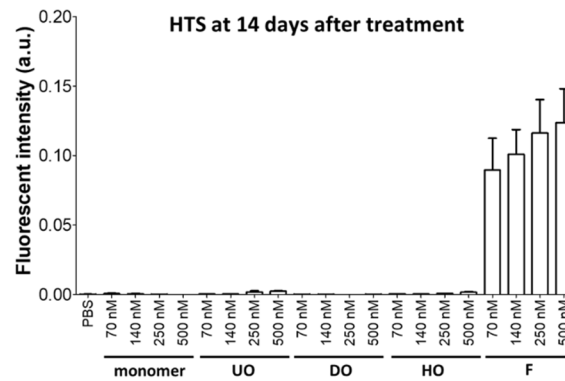


Figure 3.5: Fibrils are the major seeds to induce the formation of pS129 positive aggregates in the primary hippocampal neurons. (A) A schematic workflow. (B) Probing for the formation of pS129 positive aggregates by ICC at 7 and 14 days post treatment with different types of oligomers and fibrils (N=3). Scale: 20 μ m. (C) Formation of pS129 positive aggregates detected by high content imaging (HTS) at 14 days post treatment of different types of oligomers and fibrils at different concentrations (N=3). Note that very minimal pS129 aggregate formation by UO and none by DO and HO.

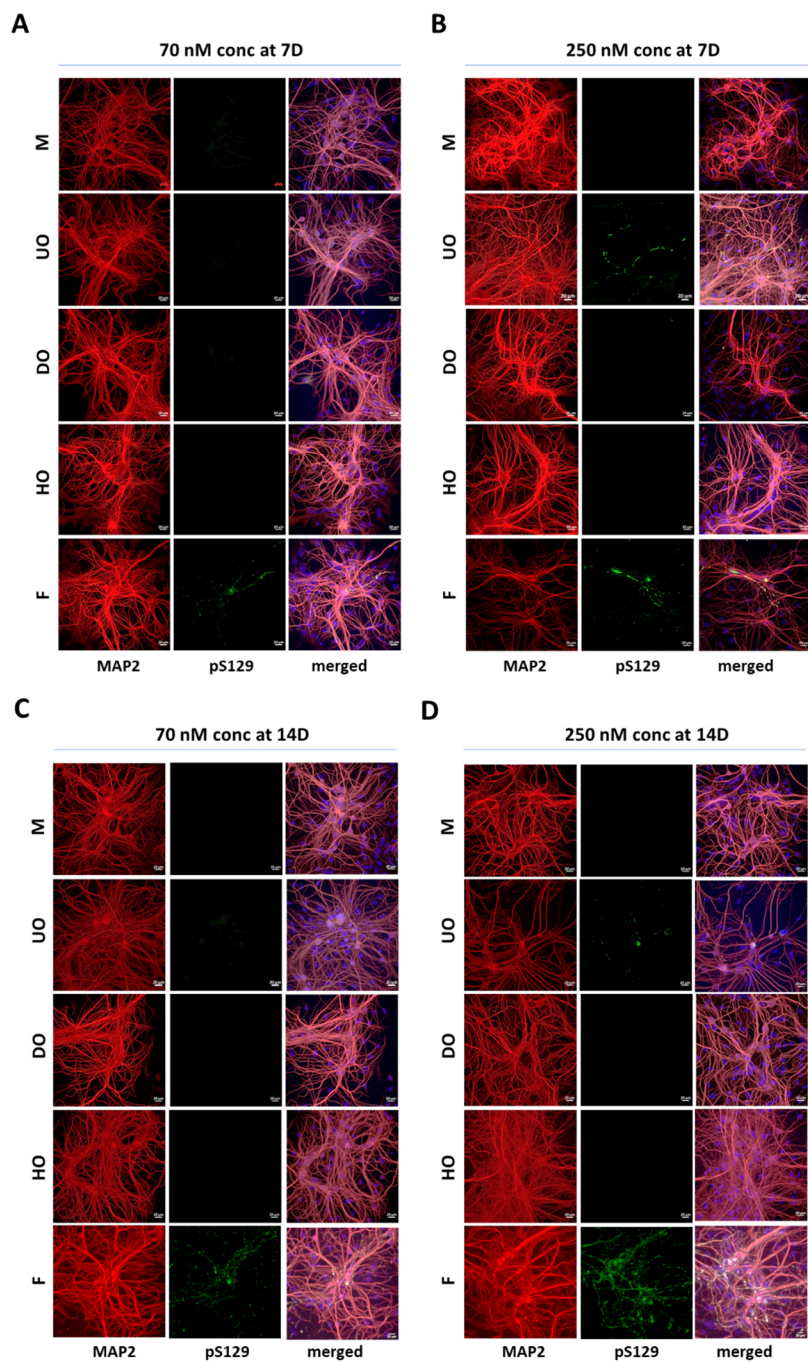


Figure 3.6: Fibrils act as seeds majorly to induce the formation of pS129 positive aggregates in the primary hippocampal neurons at different concentrations and different time points tested. Various samples tested – 70nM concentration at 7D (A), 250 nM concentration at 7D (B), 70 nM concentration at 14D (C), 250 nM concentration at 14D. Scale bar: 20 μ m

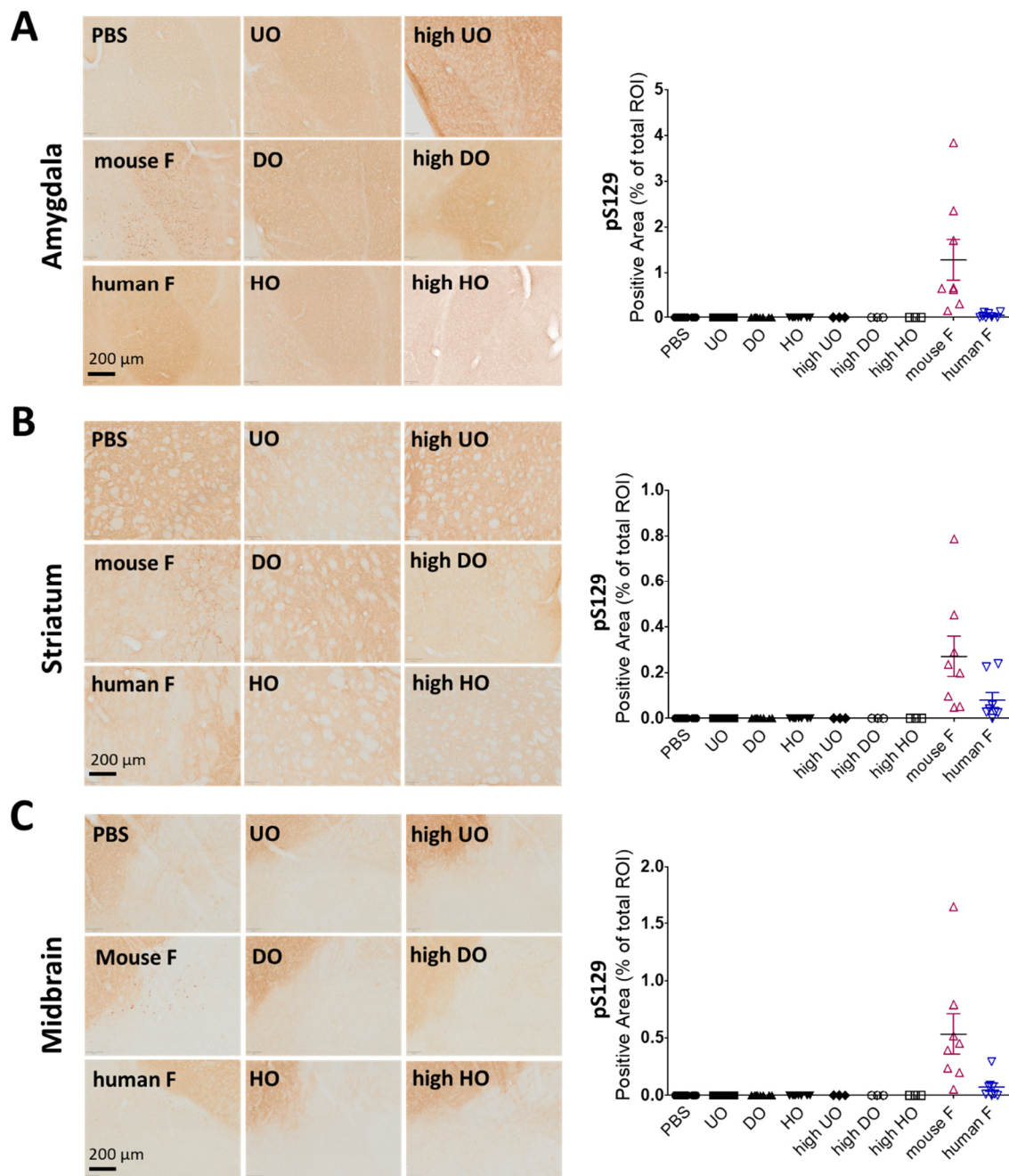


Figure 3.7: Oligomers do not induce pS129 aggregate formation *in vivo*. pS129 (EP1536Y) stained sections and quantifications from Amygdala (A), Striatum (B), and Midbrain (C). Scale bar: 200 μ m. Abbreviations: M- Monomers; UO- Unmodified oligomers (2.5 μ g); HO- HNE-induced oligomers (2.5 μ g); DO- dopamine-induced oligomers (2.5 μ g), F- pre-formed fibrils (2.5 μ g), High = 5 μ g.

3.2.4 Investigating *in vivo* seeding by different types of oligomers

To further understand the seeding potential of oligomers under *in vivo* conditions, we performed intrastriatal injections in mice with different aSyn species and quantified pS129 levels in striatum, amygdala and midbrain regions. Different aSyn species included 2.5 µg of different types of aSyn oligomers (unmodified oligomers, dopamine-induced oligomers and HNE-induced oligomers) and compared them with mouse and human WT aSyn PFFs as positive control and PBS injected mice as a negative control. We also injected mice with higher doses of oligomers (5 µg for each type of oligomers). After 2 months, we collected brains from all injected mice and performed serial sectioning and pS129 staining. Interestingly, pS129 level quantifications in Amygdala, striatum and midbrain region indicated that oligomers do not induce pS129 positive aggregate formation unlike mouse and human fibrils under *in vivo* conditions.

3.2.5 None of the aSyn oligomers seed aSyn aggregation *in vitro*

To gain better insight into the lack of accumulation of aSyn oligomers in neurons and their failure to induce seeding and aggregation of endogenous aSyn, we performed a series of studies to determine whether different types of oligomers can seed the aggregation of monomeric aSyn *in vitro*. We tested different conditions, including 20 µM monomers with or without 2 µM (10%) of different types of seeds (UO, DO, HO, fibrils) and equimolar combination of oligomers and fibrils (Figure 3.8A, 3.8G, 3.8M). In the absence of UO, DO or HO, monomeric aSyn (20 µM) showed ThT kinetics with a typical sigmoidal growth curve characterized by an initial lag phase followed by an elongation phase before reaching a plateau. In the presence of fibril seeds, we observed a decrease in the lag phase, suggesting a faster rate of aggregation and fibril formation. Interestingly, the kinetics of aggregation differed markedly in the presence of different types of oligomers. In the presence of 10% (2µM) of different types of oligomers, we did not observe any significant changes in the lag phase (Figure 3.8D, 3.8J, 3.8P), but we observed slow rate of aggregation (higher slope value corresponding to a slower rate of aggregation) compared to monomer alone and monomer plus fibril combination (Figure 3.8E, 3.8K, 3.8Q). However, there was no significant change in fluorescence intensity for the plateau in all the conditions tested (Figure 3.8F, 3.8L, 3.8R), suggesting that the presence of oligomers does not influence early oligomerization events or the extent of fibril formation, but seems to slow the elongation phase. These results are consistent with previous findings⁷⁸, where they reported that one type of oligomers (unmodified oligomers, same preparation protocol as ours) slightly slow the rate of the aggregation process.

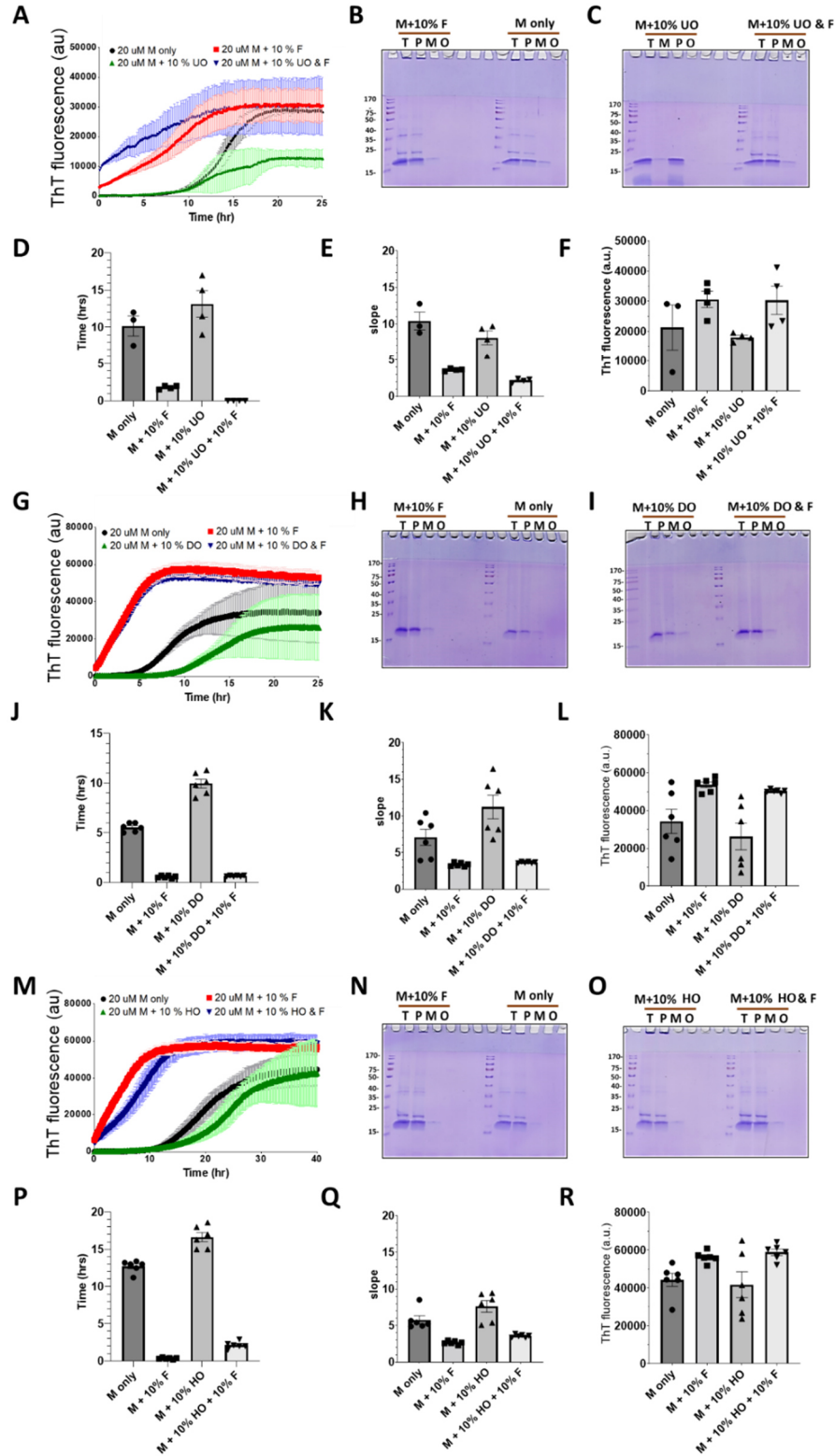


Figure 3.8: ThT aggregation kinetics in the presence of human aSyn UO, DO, HO alone or in combination with fibrils. (A, G, M) ThT aggregation kinetics curves of tested conditions with monomers only, 10% fibril seeds, 10% seeds of oligomers (UO, DO, HO), 10% seeds of oligomers and 10% seeds of fibrils in combination. (B, C, H, I, N, O)

SDS-PAGE analysis of samples collected at the end of the ThT kinetics experiment following filtration protocol⁶⁶¹ under different conditions. (D, J, P) Lag phase, (E, K, Q) rate of aggregation, (F, L, R) ThT plateau intensity quantifications of various conditions tested (Abbreviations: UO- unmodified oligomers; DO- Dopamine-induced oligomers; HO- HNE-induced oligomers; F- fibrils; T: total; P: pellet; M: monomer; O: oligomer)

3.2.6 aSyn fibrils outcompete oligomers for aSyn monomers

Since different species of aSyn (monomers, oligomers and fibrils) co-exist during aSyn aggregation process, we also investigated the seeding activity of aSyn PFFs in solutions containing a mixture of aSyn monomers and oligomers. Interestingly, in all of these tested conditions in the presence of fibrils and oligomers (2 μ M, 10% seeds), the fibril formation process was unaffected by the presence of different types of oligomers. These findings suggest that fibril seeds compete more efficiently for monomers leading to fibril formation and depletion of monomers, thus further supporting the hypothesis that aSyn fibrils are major seeding competent and aggregation inducing agents.

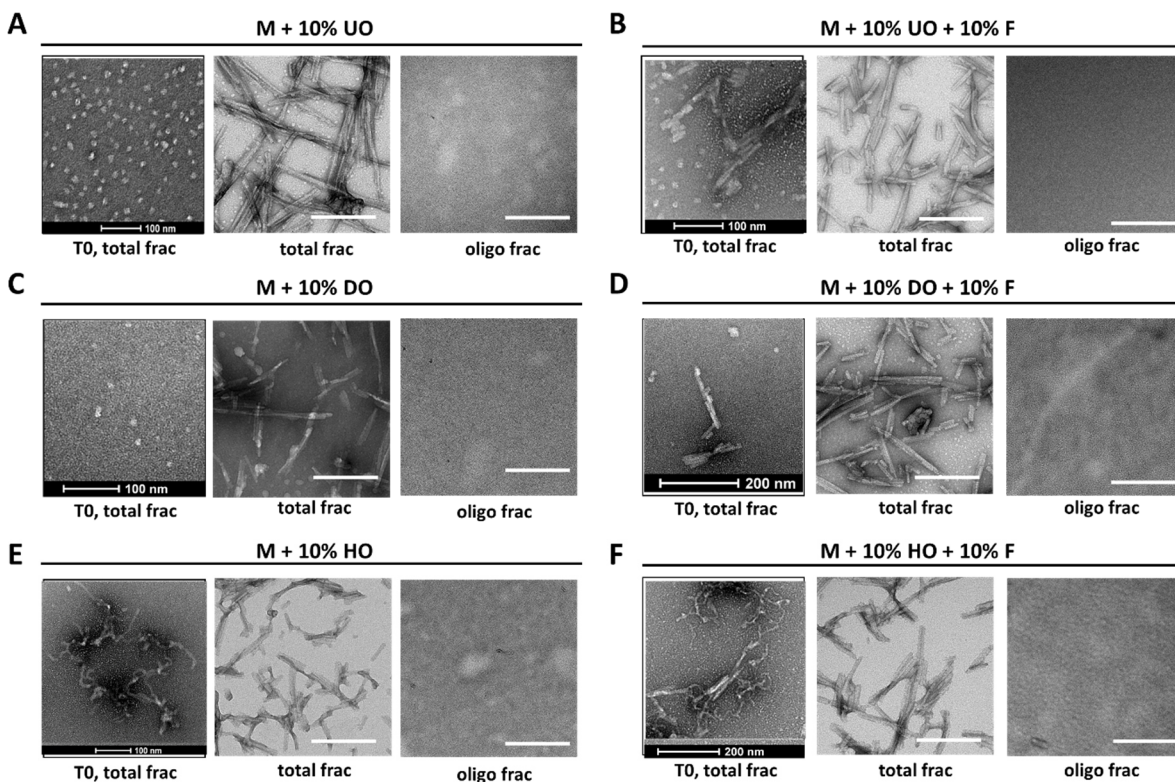


Figure 3.9: TEM images of different conditions with or without fibril seeds after the filtration protocol: total and oligomeric fractions. (A) 20 μ M M only condition. (B) 20 μ M M + 10% F seeds. (C) 20 μ M M + 10% UO seeds. (D) 20 μ M M + 10% UO + 10% F seeds. (E) 20 μ M M + 10% DO seeds. (F) 20 μ M M + 10% DO + 10% F seeds. (G) 20 μ M M + 10% HO seeds. (H) 20 μ M M + 10% HO + 10% F seeds. White Scale bar: 200 nm unless labeled.

In addition to performing the ThT kinetics assay, we also quantified the amount of monomers, oligomers and fibrils present at the end of the aggregation process in samples containing monomer alone, monomer with oligomers or fibrils seeds, and monomers with different types of oligomers and fibrils together. To understand the different species that could be present in this process, we collected samples and performed filtration⁶⁶¹ protocol and TEM analysis. We quantified the levels of monomers, oligomers and fibrils at the end of ThT kinetics assay. In all the conditions tested, more than 90% of monomers were converted to fibrils and no oligomers were detected by sedimentation assay (Figure 3.8B, 3.8C, 3.8H, 3.8I, 3.8N, 3.8O) at the end of ThT kinetics experiment. In addition, we performed TEM analysis (total and retentate (oligomeric) fractions after filtration protocol) of the various samples collected at the beginning and at the end of the experiment (Figure 3.9), and we confirmed the findings obtained by SDS-PAGE Coomassie staining upon filtration protocol. We found by TEM analysis that in none of the tested conditions we detected oligomeric structures in the retentate fractions at the end of the ThT kinetics assay. Our sedimentation and TEM analysis suggest that oligomeric species are intermediates that most likely re-enter the aggregation pathway through dissociation to monomers that are then more efficiently sequestered by the growing fibrils.

3.2.7 Different types of oligomers disrupt plasma membrane and reduce metabolic activity

Since oligomers do not induce pS129 aggregate formation in primary hippocampal neurons and *in vivo*, we assessed whether these oligomers induce toxicity in primary hippocampal neurons. To investigate this, we quantified LDH release (Figure 3.10A) and XTT metabolization (Figure 3.10B) after 14 days treatment with aSyn forms such as monomers, different types of oligomers and fibrils. Human and mouse aSyn pre-formed fibrils induced a concentration-dependent decrease in the cell viability indicating reduced metabolic activity, while triggering a prominent rise in the LDH content within the culture supernatant indicating disrupted plasma membrane. Similarly, in the presence of different types of oligomers we observed prominent increase in LDH release and reduced cell viability – this effect was robust with 500 nM conc compared to 140 nM conc of oligomers, in contrast no such effects were observed when treated with monomers. Our results suggest that irrespective of morphological, structural and conformational properties of oligomers, they cause toxicity by plasma membrane disruptions and reducing metabolic activity thereby cellular viability. Our results are consistent with previous findings where they reported oligomer induced toxicities assessed by different assays such as propidium iodide assay, MTT assay, calcein release ^{684,686,689,694,731-734}.

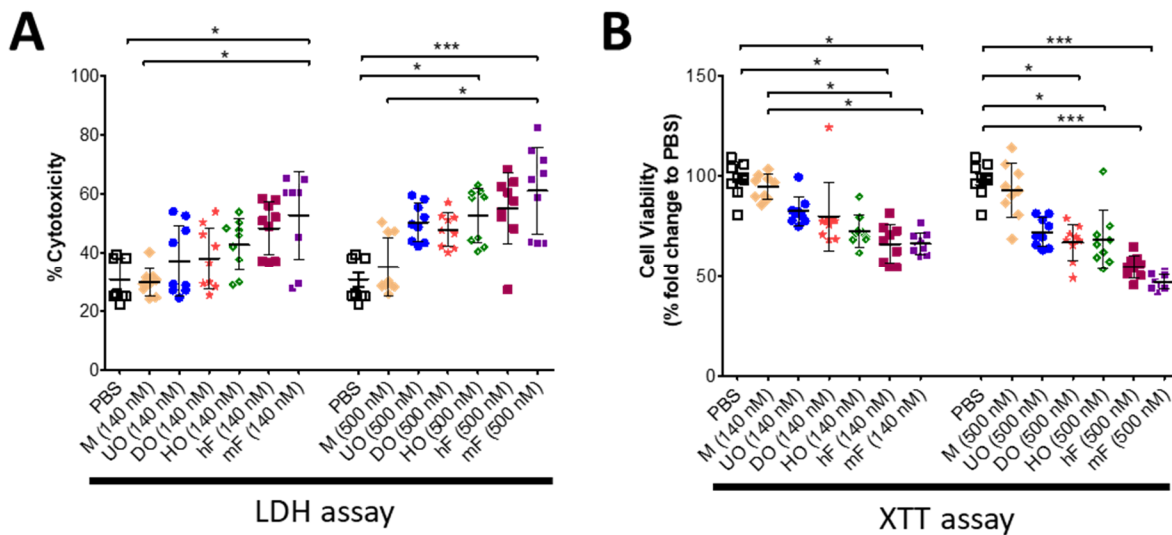


Figure 3.10: Oligomers and fibrils reduce cellular viability metabolic activity. (A) % cytotoxicity quantified from LDH release, (B) cell viability quantified from XTT assay upon treatment with two concentrations (140 nM and 500 nM) of different forms of aSyn. Abbreviations: M- Monomers; UO- Unmodified oligomers; HO- HNE-induced oligomers; DO- dopamine-induced oligomers, mF- mouse pre-formed fibrils; hF- human pre-formed fibrils. Statistical analysis: non-parametric ANOVA, Kruskal-Wallis Test with Dunn's multiple comparison test.

3.3 DISCUSSION

There has been a growing interest in developing antibodies and therapeutic strategies explicitly focused on targeting aSyn oligomers, which have increased in the past few years due to studies implicating aSyn oligomers as the critical mediator of aSyn cell-to-cell transfer and pathology spreading during the progression of PD and other synucleinopathies^{386,409,464,536,578,580,583,584,727}. aSyn oligomers have also been implicated in aSyn-induced synaptic dysfunction^{561,562,647,725,727} and toxicity^{9,386,564,651,679,716,729}. However, the precise mechanisms by which aSyn oligomers regulate pathology formation and spreading remains unknown. This is partially because a majority of studies on aSyn pathology spreading have relied on the use of preformed fibrils^{15,16,89,411,735}. Limited studies have explored the role of aSyn oligomers in initiating aSyn pathology in model systems that reproduce LB-like inclusions. For the most part, studies on aSyn oligomer toxicity^{9,386,558,564,651,729,716} or cell-to-cell propagation^{386,409,464,578,580,583,584,727} focus on investigating one type of aSyn oligomers. Other studies on the role of *de novo* aSyn oligomerization relied on the use of aSyn fused to split GFP/YFP constructs^{728,729}, which we recently shown to exhibit a high tendency to misfold and form off-pathway aggregates⁴¹⁹. Therefore, whether aSyn oligomers are sufficient to mediate aSyn transmission and pathology formation and spreading remains unknown. The work in this chapter

aims to address this knowledge gap and examine the complex dynamics between aSyn monomers, oligomers, and fibrils during neurons' aSyn fibrillization, pathology formation and toxicity.

Towards this goal, we first sought to systematically reassess the role of aSyn oligomers in the initiation of aSyn fibrillization, LB formation and toxicity. Given that we have limited knowledge about the biochemical and structural properties of aSyn oligomers in the brain, we did not rely on a single oligomer preparation. Instead, we used three different types of well-characterized aSyn oligomers (unmodified oligomers, dopamine-induced oligomers, and HNE-induced oligomers)⁶⁶⁸ that might form under disease-relevant conditions and exhibit distinct morphological and structural properties. We reasoned that this would enable us to explore, to the extent possible, the diversity of aSyn oligomers and rule out the possibility that what we observe is specific to one type of oligomers.

aSyn oligomers have been reported to be obligate intermediate species that form before the formation of fibrils. However, the ability of oligomers to seed and accelerate the aggregation of monomeric aSyn has not been extensively studied. Herein, we showed that none of the three types of aSyn oligomers are capable of seeding aSyn fibrillization *in vitro* or in neuronal models of aSyn pathology formation. Instead, our ThT aggregation kinetics studies demonstrate that different types of oligomers cause delayed elongation phase and slower aggregation process compared to fibril seeds irrespective of their structural, chemical, and morphological properties. When fibrils are added to a mixture of oligomers and monomers, they compete more effectively for the monomers and the oligomer-induced delayed in aggregation is no longer observed.

Our results with unmodified oligomers are consistent with a study by Lorenzen and colleagues where they reported increased lag phase and delayed elongation phase with unmodified oligomers (Lorenzen et al., 2014). In another study by Yang et al. acetylated oligomers (prepared in similar conditions as unmodified oligomers) also delayed fibril elongation by acting as auto-inhibitors of acetylated-aSyn fibril formation⁵⁷⁵. In a separate study using a single-molecule amplification assay, oligomers have been shown to have low seeding potential compared to fibrils⁵⁷⁶. However, our results are not consistent with a study by Bae and colleagues wherein they reported that HNE-induced oligomers act as seeds to induced aggregation of monomeric aSyn. This discrepancy can be explained by differences in the methods to prepare the HNE-induced aSyn oligomers and the secondary structure properties of the oligomers used in the two studies. The HNE-induced oligomers prepared in this study were kept for 7 days of incubation at 37°C without agitation, and they exhibited a predominantly disordered structure similar to monomers⁵⁷⁷, whereas our HNE-oligomers (HO) and those prepared in previous studies exhibit a predominantly β -sheeted rich

secondary structure of HNE-induced oligomers^{668,684}. Moreover, Bae et al., report the presence of heterogeneous morphologies (spherical, ring-like, and curvilinear) of HNE-induced oligomers in their preparation compared to curvilinear morphologies that we observed in our study. Therefore, these morphological, and structural features might explain the differences that we observed in our study. In addition, other studies report the seeding ability of oligomers by *in vitro* ThT kinetics. However, we found these oligomer preparation steps are very different compared to ours and the initial concentration of oligomers used are very high e.g., Celej et al. report *in vitro* seeding properties of oligomer which are prepared in the absence or presence of HEPES buffers and without any additional purification steps other than a simple 100 kD filtration protocol to separate oligomers and monomers; oligomers prepared with such procedures might not be pure. In addition, seeding ability of these oligomers were tested with initial high concentration (8 μ M) of oligomers⁷³⁶.

To explain our findings, we describe here several possibilities that might explain our findings (Figure 3.11). In the presence of fibril seeds, fibrils recruit monomers efficiently, leading to rapid fibril growth and depletion of monomers, resulting in a short lag phase (Figure 3.11A). In contrast, oligomers do not seed efficiently and delay the aggregation process by initially sequestering monomers, thus delaying the initial nucleation events and/or slowing initial fibrillization events, i.e., reducing the amount of monomers available for fibrils for further growth (Figure 3.11B). This sequestration of monomers by oligomers appears to be more efficient for disordered dopamine-induced oligomers than β -sheeted unmodified and HNE-induced oligomers, as there is a greater lag-phase for dopamine-induced oligomers than for unmodified and HNE-induced oligomers. In the presence of both oligomers and fibrils, the fibrils always compete more efficiently for aSyn monomers (Figure 3.11C), thus favoring fibrils growth and accelerated aSyn fibrillization. The absence of oligomers at the end of the reaction could be explained by the fact that depletion of the monomers due to fibril formation shifts the oligomer to monomer equilibrium towards the monomers, which are then quickly sequestered by the growing fibrils (Figure 3.11D). These findings show that the oligomers we studied here represent off-pathway oligomers capable of re-entering the aggregation pathway through disassociation with monomers. It also suggests that lowering aSyn levels may provide a mechanism for reversing aSyn oligomers formation and toxicity. Essentially our study uncovers that fibrils display the highest seeding activity and propensity to induce aggregate formation.

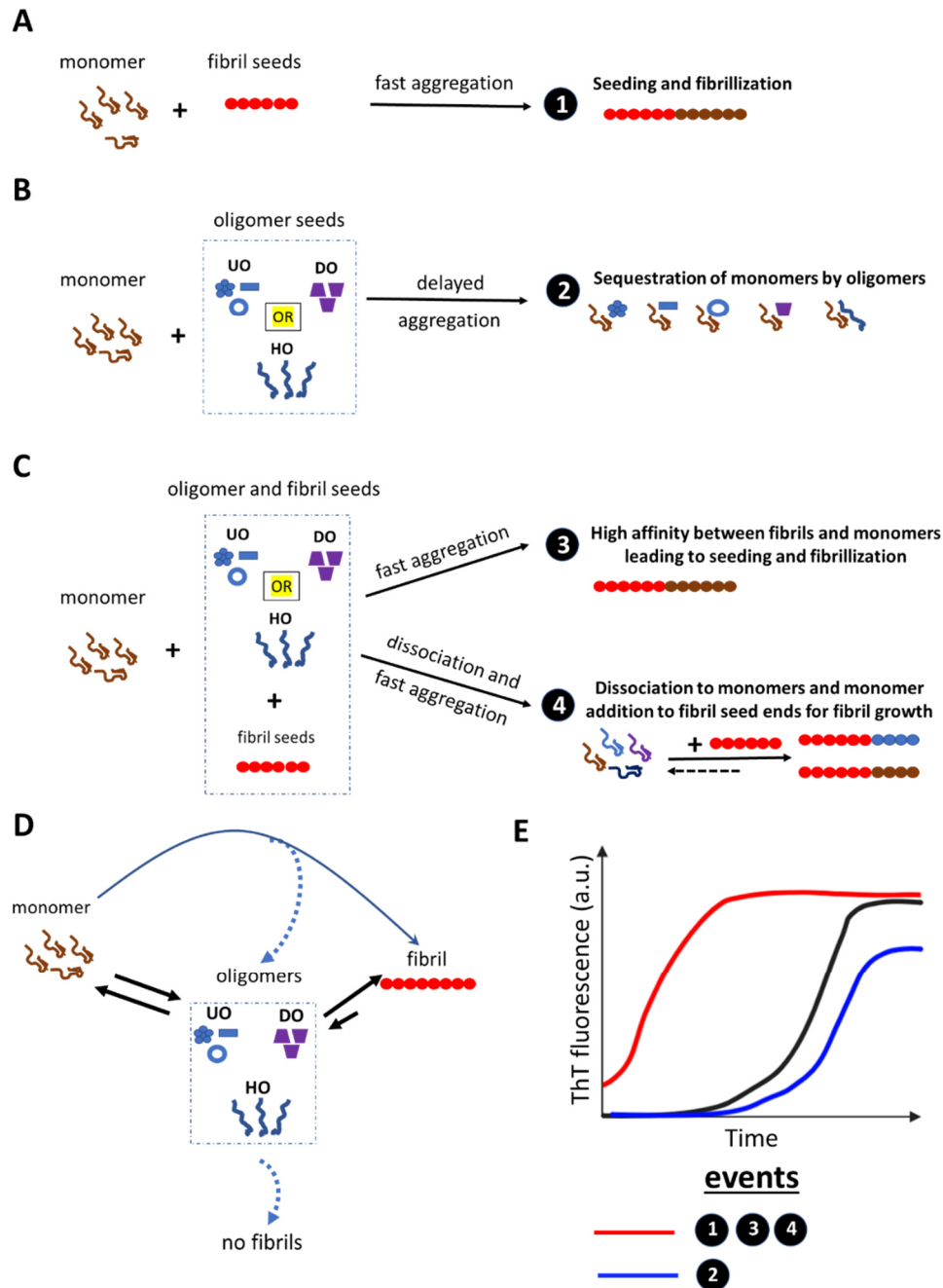


Figure 3.11: Schematic representation and model of various events that are related to the aggregation process in the presence of different seeds. (A) monomers in the presence of fibrils as seed. (B) monomers in the presence of different types of oligomers, wherein the aggregation process is delayed or slowed – this could be mainly due to the interaction of off-pathway oligomers and monomeric aSyn. (C) monomers in the presence of both oligomers and fibrils, wherein higher affinity between fibrils and monomers or dissociation of monomers from oligomers could be acting to boost the faster aggregation process. (D) A schematic representation to show the aggregation process. (E) a schematic representation to show ThT kinetic curves with possible events that drive their aggregation process. ThT kinetics curve color -- i) red is for monomer plus fibril seeds or with fibril and oligomer seed; ii) black is for monomer only condition; iii) blue is for monomers plus oligomers condition.

A vast amount of literature suggests the presence of oligomers in the postmortem PD brains and in CSF of patients, indicating that aSyn oligomers could be secreted and contribute to seeding and spreading. To test this hypothesis, we investigated the ability of different types of aSyn oligomers to seed and induce fibril formation in neurons. To our surprise, only unmodified oligomers at higher concentrations (250 nM and 500 nM) induced a marginal level of pS129 positive aggregate formation but neither dopamine-induced nor HNE-induced oligomers induced any pS129 positive aggregation in neurons at different concentrations over a period of 7-14 days post treatment. These results suggest oligomers are not seeding competent and that aSyn seeding activity is primarily driven by fibrils.

Previously, a few studies investigated the propensity of oligomers to seed and induce intracellular aSyn aggregation in cellular model systems. Iron- and ethanol-induced aSyn oligomers have been shown to exhibit seeding properties and inducing aSyn aggregation formation in SH-SY5Y cells overexpressing A53T mutant aSyn^{386,580,691} and in primary cortical neurons⁵⁸⁰. Here, they looked at immunopositivity to aSyn antibody (Asy-1, epitope not available) alone was used to determine the seeding activity of oligomers and failed to perform any immunohistochemical or CLEM studies to determine whether these aSyn positive aggregates are fibrillar in nature. These oligomers are structurally and chemically different from the ones we used in our study. The seeding effect claimed by these oligomers in these studies could be explained: i) by the fact that these iron- and ethanol-induced aSyn oligomers reveal protofibrillar morphology by AFM imaging; ii) these studies were performed using an over-expression cellular model system, wherein the aggregation could be favored because of supra-physiological levels of aSyn^{386,691}; iii) these studies failed to purify oligomers by chromatographic techniques (such as size-exclusion) therefore, the oligomers used for testing seeding might not be pure; iv) And these studies used very high concentrations (7 μ M) of oligomers for testing the seeding effect. Therefore, higher concentrations of oligomers, over-expression cellular model system and absence of pure preparation of oligomers might explain their detection of immunopositivity to ASy-1 antibody (epitope not described) for aSyn aggregates. However, in our study, we used purified, well-characterized oligomers and a wide-range of concentrations (from 70 nM to 500 nM) of oligomers in the primary neuronal model, a well-established model of fibril formation and LB-like inclusion formation¹⁶, for assessing the seeding activity of different types of oligomers that are morphologically and structurally different.

A study by Pieri and colleagues reported seeding induced by large stable dopamine-induced and Glutaraldehyde induced oligomers in Neuro2A cells stably expressing ChFP-aSyn⁷²⁸. However, we have recently shown that fluorescent-tagged proteins exhibit a high tendency to misfold and form off-pathway

aggregates⁴¹⁹. In their study, the seeding propensity of these oligomers is assessed solely based on fluorescence measurements upon aSyn aggregate formation, and no further characterization of aSyn aggregates using markers of LBs such as immunopositivity to ubiquitin, pS129, p62 or positivity to amyloid dyes, their insolubility and PK resistance properties and ultrastructural characterization of aSyn positive aggregates is investigated. Dopamine-induced oligomers are structurally and chemically similar to the ones we prepared; it is possible that supra-physiological levels of aSyn might induce aggregate formation in their cell lines. Though these studies report seeding based on aSyn overexpression or aSyn fused with ChFP constructs, these model systems do not recapitulate LB-inclusion formation and maturation.

Though sparse evidence exists for the seeding effect of aSyn oligomers, several groups have shown that aSyn oligomers can spread from one cell to another or from one brain region to another. In 2005, Lee et al. reported that aggregated forms of aSyn could be secreted outside (via non-classical endoplasmic reticulum/Golgi-independent exocytosis) when higher levels of aSyn is expressed in SH-SY5Y cells, and the levels could be increased under stress conditions that induce proteasomal dysfunction (e.g., MG132, a proteasomal inhibitor)¹³ and mitochondrial dysfunction (rotenone)⁷³⁷. Though this study shows the presence of higher molecular weight aSyn bands in their Western blots, it is not clear whether these are oligomeric or fibrillar in nature. In another study, Danzer and colleagues demonstrated that ethanol and iron-induced oligomers could be secreted in exosomes, and their presence in exosomes could facilitate their seeding and transcellular spreading of pathology⁵⁸¹. Studies *in vivo* support these spreading results. In one study, injection of oligomers in the olfactory bulb resulted in their spreading to other brain regions⁵⁸³. In a subsequent study Peelaerts et al. and Froula et al. demonstrated that oligomers are uptaken and spread to different brain regions^{464,727}. The majority of these studies suggest that oligomers could be involved in spreading. Therefore, we investigated whether these could be forming *de novo* in the PFF-based neuronal seeding model and act as spreading agents for disease propagation. To our surprise, no oligomeric bands were detected by Western blots upon SEC fractionation (of neuronal lysates) and filtration protocol (performed on extracellular media) – this confirms that oligomeric aSyn may not be the major species formed during the LB-like inclusion formation and maturation and the cellular dysfunction seen in this model system are mainly attributed to the LB formation and maturation process¹⁶ but not majorly mediated by oligomeric intermediate species. Importantly, our findings highlight a key limitation of the PFF-based neuronal seeding model – that it is not a model of *de novo* aSyn aggregation, and it only models aSyn fibril growth and LB formation, but not early events associated with aSyn oligomerization. In addition, we also investigated whether different types of oligomers induce seeding and pS129 aggregate formation in different brain regions *in vivo*. To the best of our knowledge, this is the first study which

conclusively show that irrespective of morphological, chemical and structural properties different types of oligomers do not induce seeding and pS129 aggregate formation in Amygdala, striatum and midbrain regions. A limitation of our study is the caveat that cross-species seeding might be inhibited since our study utilized human aSyn oligomers in mouse brains. In the future, *in vivo* studies with mouse aSyn variants of different types of oligomers are required to overcome this limitation.

Although there are several studies which suggest intermediate species such as oligomers to be toxic toxicity^{9,386,564,651,679,716,729}. These studies used majorly one type of oligomers. In our study we made use of three different types of oligomers and compared their toxicity to monomers and fibrils. Our results demonstrate that irrespective of different morphological, structural and chemical properties, oligomers cause membrane permeability as evident by increased LDH release and reduced metabolic activity quantified by XTT metabolization. These toxicity properties of oligomers are similar to fibril-induced LDH release and metabolic activity. Therefore, these results might indicate that in the presence of oligomers there could be exacerbated cellular death. Future studies are required to address exact mechanism of toxicities induced by oligomers.

In summary, our work demonstrates that fibrils are the most seeding competent species and suggest that fibrils are the critical mediators of pathology spreading in PD and other synucleinopathies and also oligomers induce toxicity similar to fibrils. Therefore, the oligomer hypothesis and results obtained from immunotherapy studies targeting oligomer-specific antibodies to reduce aSyn aggregates in the brain need to be revisited. Better therapeutic approaches are required to target fibrils to control the LB pathology spread to different brain regions in model systems of PD and clinical trials.

3.4 METHODS

3.4.1 Primary culture of hippocampal neurons and treatment with aSyn oligomers and fibrils

The primary hippocampal neurons were cultured from P0 pups of WT mice (C57BL/6JRj, Harlan) and cultured as previously described in¹⁶. The neurons were seeded in 6 well plates (for SEC fractionations) at 600000 cells/well and in 24 well plates (for ICC) at 125000 cells/well and in 96 well plates at 30000 cells/well (for HCA imaging). For ICC, the cells were plated on coverslips (VWR, Switzerland) which were previously coated with poly-L-lysine 0.1% w/v in water (Brunschwig, Switzerland). For ICC and HCA analysis, after 5 days in culture, the WT hippocampal neurons were treated exogenously with different concentrations (70 nM, 140 nM, 250 nM, 500 nM) of human monomers (M), unmodified oligomers (UO), dopamine-induced oligomers (DO), HNE-induced oligomers (HO) and preformed fibrils (F). For SEC

fractionation experiments, after 7 days in culture, the WT hippocampal neurons were treated with 140 nM human aSyn preformed fibrils. Primary neuronal culture procedures were approved by Swiss Federal Veterinary Office (animal license number VD 3392).

3.4.2 Preparation of aSyn monomers, fibrils and different types of oligomers

The preparation of human aSyn species such as monomers, different types of oligomers (UO, DO, HO) and fibrils (F) were performed and characterized by SDS-PAGE, TEM analysis and CD spectroscopy as described in ⁶⁶¹.

3.4.3 Immunocytochemistry (ICC)

After aSyn species treatment, primary hippocampal neurons on coverslips were washed with PBS twice and fixed in 4% PFA for 15 min at RT until the immunocytochemical (ICC) procedure. After fixation, the coverslips were blocked with 3% BSA and 0.01 % Triton X-100, followed by incubation with primary antibodies and secondary antibodies with intermitted washing with PBS. The coverslips were mounted with a mounting medium and then were examined with a confocal laser-scanning microscope (LSM 700, Carl Zeiss Microscopy, Germany).

3.4.4 Quantitative high-content wide-field imaging analysis (HCA)

After treatment with different concentrations of aSyn monomers, oligomers and fibrils, primary hippocampal neurons plated in black, clear bottom 96-well plates (BD) were washed twice with PBS and fixed in 4% PFA for 15 minutes at RT and immunostained as performed for ICC. In addition, HCA analysis was performed as described in¹⁶. Briefly, images were acquired with IN Cell Analyzer 2200 (GE Healthcare) using Nikon 10x/0.45 Plan Apo objective lens and a high-throughput and high-resolution camera (16-bit sCMOS camera, 2048x2048 pixels) system with bin size 2 x 2. Nine fields of view were imaged in each duplicated well for each independent test condition. Image analysis was carried out using Cell Profiler 3.4 software to identify and quantify the level of pS129 positive aggregates formed in MAP2-positive neurons.

3.4.5 Cell lysis and WB analyses of SEC fractionation

After treatment with 140 nM human aSyn fibrils for 7 and 14 days, primary hippocampal neurons were lysed as described in ⁶¹². For SEC fractionation studies, neurons from each well (of a 6-well plate) were lysed in TBS lysis buffer (50 mM Tris, 150 mM NaCl, pH 7.5) containing 1% Triton X-100 and supplemented

with phosphatase inhibitor cocktail 2 and 3 (Sigma-Aldrich, Switzerland), protease inhibitors cocktails, 1 mM phenyl methane sulfonyl fluoride (PMSF). Lysed neurons from 6 wells were pooled together and subjected to sonication using a fine probe [(0.5-sec pulse at an amplitude of 20%, 10 times (Sonic Vibra Cell, Blanc Labo, Switzerland)], cell lysates were incubated on ice for 30 mins and centrifuged at 100,000 g for 30 min at 4°C. The supernatant (soluble fraction) was collected. For insoluble fraction pellet, the pellet after the first ultracentrifugation step was washed in TBS lysis buffer and sonicated with a fine probe [(0.5-sec pulse at an amplitude of 20%, 10 times (Sonic Vibra Cell, Blanc Labo, Switzerland)] and centrifuged for 30 min at 100,000 g. After the ultra-centrifugation step, the supernatant was discarded, and the pellet (insoluble fraction) was resuspended in 2% sodium dodecyl sulfate (SDS)/TBS supplemented with phosphatase inhibitor cocktail 2 and 3 (Sigma-Aldrich, Switzerland), protease inhibitors cocktails, 1 mM phenyl methane sulfonyl fluoride (PMSF) and sonicated using a fine probe (0.5-sec pulse at an amplitude of 20%, 15 times). To assess the presence of aSyn oligomers in the preformed fibrils (PFFs)-based neuronal seeding model, soluble fraction, either supplemented with or without 75 ug WT aSyn oligomers, was analyzed by size-exclusion chromatography (SEC). SEC fractionation was performed using a Superdex 200 10/300 GL column (GE Lifesciences), equilibrated with PBS, pH 7.4. Different fractions (vol. = 500 ul) were collected and analyzed by western blotting analysis using 16% Tricine gels and probed with aSyn antibodies recognizing different epitopes: aSyn 91-99 (Syn-1) and aSyn 134-138. GraphPad PRISM software was used to plot the SEC chromatograms.

3.4.6 WB analysis of extracellular media

To probe for the presence of oligomeric aSyn species that might be released in the extracellular media WB analysis on the media samples was carried out. First, 3ml of neuronal media (treated with PBS or preformed fibrils) was isolated and subjected to centrifugation at 10000g for 10 min at 4°C, and the pellet was discarded to remove any cellular debris and insoluble aSyn fibrils. Then, the supernatant was subjected to filtration protocol⁶⁶¹ to separate filtrate and retentate that constitute monomer and oligomer, respectively. Two different amounts of total filtrate and retentate samples were loaded onto 16% tricine gels, subjected to WB, and probed with Syn-1 antibody. This procedure was carried out on media that underwent a spike in with or without 10 ugs of human aSyn UO.

3.4.7 ThT aggregation kinetics assay

Fluorescence-based ThT aggregation kinetics assay was set up in a black 96-well optimal clear bottom plate (Costar), and each well was added with six SiLibeads® ceramic beads (Sigmund Lindner) with a

diameter of 1.0–1.2 mm. 650 μ l of the master-mix solution containing 20 μ M of monomer and 20 μ M ThT was prepared in 1X PBS (GIBCO) for each test condition. To these wells, solutions containing aSyn species with or without seeds were added to set up the ThT kinetics assay. 110 μ l of each sample was added to the wells to have five repeats. To these wells, different percentages [2.5% (0.5 μ M), 5% (1 μ M), 10% (2 μ M)] of seeds (UO, DO, HO, fibrils) were added. Two of the conditions contained both oligomers and fibrils as seeds in equal proportion [5% (1 μ M) and 10% (2 μ M)]. After adding all the samples, the plate was sealed with Corning® microplate tape and transferred to a Fluostar Optima plate reader (BMG labtech) for the ThT fluorescence measurements. The plate reader was set with the following parameters: continuous orbital shaking at 600 rpm at 37 °C, ThT excitation at 450 ± 10 nm and emission at 480 ± 10 nm and the fluorescence was measured every 300 seconds. At the endpoint of the assays, the samples were analyzed by SDS-PAGE and TEM analysis. SDS-PAGE and TEM analysis was performed as described in⁶⁶¹. Lag time and rate of aggregation are calculated as described in⁵³⁵. Data were analyzed with non-parametric ANOVA analysis * $p < 0.05$, ** $p < 0.01$.

3.4.8 Intrastriatal injection of different types of aSyn oligomers

C57BL/6JRj male mice were ordered (Janvier Labs) at the age of 10 weeks and allowed to acclimate to the animal house for at least 2 weeks. About 4 mice were housed in a cage and kept at 23 °C (40% humidity) in a 12h/12h light/dark cycle with food ad libitum. 3 to 4-month-old C57BL/6JRj male mice were anesthetized by intraperitoneal injection of 100 mg/kg ketamine and 10 mg/kg xylazine. The animals were then mounted on a stereotaxic frame (model 963, Kopf, California, USA), and a lubricant eye ointment was applied. A hole was created in the right parietal bone (0.4 mm anterior and 2 mm lateral to the bregma) and 2.5 μ g of aSyn unmodified oligomers, dopamine-induced oligomers, HNE-induced oligomers, mouse PFFs, human PFFs were injected to 8 mice per test sample and control PBS samples (N=8) were injected with a 34G cannula at the flow rate of 0.1 μ l/min, 2.6 mm beneath the dura. In addition, 5 μ g of unmodified oligomers, 5 μ g of dopamine-induced oligomers and 5 μ g of HNE-induced oligomers were injected to assess the potential seeding of high doses aSyn oligomers (N=3 for each high dose conditions). The cannula remained in place for 5 min after injection, and it was retracted in steps slowly and smoothly. All animal experiments and procedures were approved by the Swiss Federal Veterinary Office (authorization number VD 3499).

3.4.9 pS129 level quantifications in different brain regions

The brains were isolated from injected mice after 2 months of intrastriatal injections and kept for fixation in PFA. The brains were cut 50 μ m and regions containing the striatum, amygdala and midbrain were collected and subjected to pS129 staining. DAB pS129 stainings were performed, and pS129 levels were quantified using QPATH.

3.5.0 XTT assay

Global cell viability was assessed with the Cell proliferation kit II [2,3-Bis-(2-methoxy-4-nitro-5-sulphophenyl)-2H-tetrazolium-5-carboxanilide (XTT)] (Roche Diagnostics) and the CytoTox 96® Non-Radioactive Cytotoxicity Assay (Promega AG). The assays were formatted in transparent, cell culture-treated, flat-bottom, 96-well microplates that were previously coated with 0.1mg/ml Cultrex poly-L-lysine (R&D Systems) for 1h at room temperature. Primary hippocampal neurons were plated at a density of 3×10^4 cells/ml and allowed to differentiate for 6 days. Cells were then challenged with different concentrations of aSyn oligomers and pre-formed fibrils for 14 days. Followingly, culture supernatants were collected and the cells were incubated with the XTT labelling buffer in fresh neuronal growth media at a 1:1 ratio supplemented with 0.3 mg/ml XTT electron coupling reagent for 4h in a humidified incubator with 5% CO₂ and 95% air. Microplates were shaken gently on a Microtitre plate shake for 5 min and absorbance was measured at 492 nm with a reference wavelength of 690 nm in the Infinite® 200 PRO microplate reader (Tecan). Absorbance values are proportional to the cleavage of the yellow tetrazolium salt XTT into the orange, water-soluble formazan product by the mitochondrial dehydrogenase, and thus reflect the number of viable, metabolically active cells in the respective microcultures. Values were corrected to the blanks (background absorbance coming from the incubation media without cells) and expressed as a percentage of control PBS-treated cells.

3.5.1 LDH release assay

Collected supernatants were assayed for their lactate dehydrogenase (LDH) content with CytoTox 96® Non-Radioactive Cytotoxicity kit; LDH is a stable cytoplasmic enzyme that is rapidly released in the supernatant upon plasma membrane perturbation. As per the manufacturer's protocol, 50 μ l of the collected supernatant was incubated with 50 μ l of the kit-provided reaction mixture for 30 min at room temperature with a gentle agitation under light-protecting conditions. The reaction was then stopped by the addition of the kit-provided stop solution and the absorbance was measured at 490 nm with a reference wavelength of 650 nm. Absorbance values were corrected to the blanks and processed for the calculation of the percentage of cytotoxicity according to the following formula:

% Cytotoxicity = (Experimental value)/(Maximum LDH release from lysed cells) x 100

3.5.2 Statistics

All the results were expressed as mean \pm standard deviation (SD) of three independent experiments (N =3). The Assumption of normality was examined with D'Agostino–Pearson's K-squared or Shapiro–Wilk tests. Differences among means were considered significant if $p \leq 0.05$. Data were analyzed with non-parametric ANOVA analysis Kruskal-Wallis Test with Dunn's multiple comparison test * $p < 0.05$, ** $p < 0.01$, *** $p < 0.001$. Statistical calculations were performed in GraphPad Prism 8 (GraphPad Software Inc., San Diego, CA, USA).

3.5 Contributions of the authors

Somanath Jagannath designed, performed and analyzed all experiments except toxicity studies, *in vivo* intrastriatal injections. Somanath Jagannath wrote the chapter. Pedro Magalhães contributed to experiments in Figure 3.2, 3.3. Salvatore Novello performed *in vivo* intrastriatal injections and contributed to pS129 stainings of brain sections from oligomer injected mice. Theodora Panagaki performed oligomer toxicity studies and wrote toxicity findings. Hilal A. Lashuel conceived and conceptualized the study and contributed to the design of the experiments, interpretation of data and writing of the chapter.

Chapter 4: Gene expression changes in the Amygdala of a PFF-based mouse model of Parkinson's disease reveal cell-type-specific dysregulation of PD risk genes and pathways

4.1 INTRODUCTION

Parkinson's disease (PD) is a chronic and progressive neurodegenerative disease affecting 2-3% of the population over 65 years of age – PD is mainly sporadic, with only about 5-10% familial cases¹⁹⁷. The major pathological hallmark of PD includes neurodegeneration in specific brain areas and Lewy bodies (LBs), intracellular proteinaceous inclusions containing several components, including misfolded and aggregated forms of α -synuclein (aSyn)^{5,200}. The motor symptoms in PD are attributed to either the presence of LBs in substantia nigra dopaminergic neurons or their neurodegeneration. In addition, PD patients suffer from several non-motor symptoms, including depression, apathy, anxiety, sleep disorders, restless legs, and olfactory deficits, much of which usually precede the motor symptoms¹⁹⁹. Many of these non-motor symptoms are linked with LBs or aSyn pathology formation in different brain regions such as the Amygdala, pedunculopontine nucleus (PPN), claustrum, locus coeruleus, the dorsal motor nucleus of the vagus, median raphe nucleus, lateral hypothalamus, ventral tegmental area and cortical regions^{203,205}. In PD, the cell loss is not just restricted to the SN, but it is also observed in other brain regions^{585,738} and several studies suggest a complex interplay between aSyn pathology formation and neurodegeneration, pointing to cell-type-dependent response to aSyn aggregation and pathology formation and underscore the importance of elucidating cell-autonomous factors that may render a specific population of neurons vulnerable to LB pathology and cell death than others.

In PD and DLB patients, it is known that several non-motor symptoms such as anxiety, depression and behavioral disorders are associated with the Amygdala and also several pathological studies point out that the amygdala brain region is also susceptible to developing LB inclusions and cell death^{590,739-741}. To recapitulate the disease process, PFF-based rodent models are developed. In these model systems, injection of aSyn PFFs into mice brains has been shown to induce aSyn pathology formation and spreading in different brain regions and behavioral deficits reflecting symptoms of PD patients⁷⁴²⁻⁷⁴⁴. Interestingly, in this model system, not all neurons develop pS129 positive aggregates, as seen in the post-mortem brains of PD patients. Instead, a selected population of neurons develops these pS129 positive inclusions

within different brain regions. In a previous study using a PFF-based seeding model of PD, Stoyka et al. showed pS129 positive aggregates in some populations of neurons in the amygdala brain region, suggesting cell-selective vulnerability to pathology formation⁵¹⁹. Previous studies have indicated that pS129 positive inclusions in specific brain regions depend on the amount of injected aSyn PFFs and the level of aSyn expression^{493,744}. In addition, it has been demonstrated that CamKII and SATB2 positive excitatory neurons are susceptible to developing pS129 positive aggregates but not inhibitory neurons⁵¹⁹. However, the molecular or gene expression changes that take place in neuronal types that develop pS129 positive aggregates versus those that do not develop pS129 aggregates and how neuronal and non-neuronal cell types in the Amygdala respond to pS129 aggregate burden in the amygdala brain region at an early disease stage is not well understood.

We hypothesize that the cellular environment of a particular cell type plays a crucial role in driving the disease process that includes susceptibility of cell types to develop pS129 positive aggregates and/or neurodegeneration and how different cell types respond to disease burden in terms of their gene expression changes. Towards testing this hypothesis, we investigated transcriptomics changes in different cell types in the amygdala brain region, which we and others have shown to be more susceptible to developing pS129 positive aggregates and where aSyn pathology is reproducibly observed following inoculation with aSyn preformed fibrils in the striatum^{372,518,519}. We performed snRNA sequencing on amygdala brain regions isolated and pooled from PBS (N=10) and PFF (N=10) injected mice brains and report findings from 6980 single-nuclei transcriptomics profiles of different cells types from the Amygdala and explored transcriptomics changes and associated pathways. We report that most of the top 100 differentially expressed genes (DEGs) are from inhibitory and excitatory neurons compared to non-neuronal cell types. Furthermore, we observed that inhibitory and excitatory neurons upregulate and non-neuronal cells downregulate several genes in these DEGs. Significantly upregulated genes in neurons are mainly involved in neuronal electrical activity, and various protein binding activities and downregulated genes in non-neuronal cell types are involved in multiple functions ranging from the receptor, ion and protein binding to GTPase regulatory activities. Specifically, several genes known to have a role in protein folding and degradation are downregulated in oligodendrocytes. Therefore, Functional gene enrichment analysis suggests that neuronal cells increase their neuronal activity, whereas non-neuronal cells display reduced regulatory activity (GTPase regulatory activity, kinase activity) upon LB-like inclusions in the Amygdala. In addition, we report here that the gene expression profile of a handful of PD risk genes such as Sncaip, Park7, Maob, Hspa8, Scl2a3 and Hsf3 and some pathways that have been associated with PD

are differentially altered in specific cell types. Our study highlights the importance of the involvement of unique gene expression changes and their associated pathways in different cell types that drive the disease process at an early stage in a PFF-based mouse model of PD.

4.2 RESULTS

4.2.1 Single-nucleus RNA sequencing of the Amygdala brain region from PBS and PFF injected mice

To perform single-nuclei RNA sequencing (snRNA-seq), we isolated ipsilateral and contralateral amygdala brain regions from PBS and PFF injected mouse brains and subjected them to nuclei separation protocol. Nuclei suspension was then used for library preparation and snRNA-seq with the 10X genomics platform. Sequencing raw data underwent pre-processing, filtering and analysis (Figure 4.1A).

The procedure to obtain homogenous clear nuclei suspension required optimization steps as the samples come from frozen adult mice brains. Optimization steps such as the introduction of an homogenization steps with douncer and OptiPrep purification as described in methods were performed and these steps resulted in obtaining higher percentages of good quality nuclei after sequencing. We targeted 4000 nuclei for sequencing in amygdala samples, and we obtained data from 3446 nuclei from PBS and 3758 from the PFF sample. After QC filtering, we obtained 3315 and 3665 from PBS and PFF samples, respectively, and we did not find any significant differences in QCs between our sample groups (Figure 4.1B).

To classify major cell types in our samples, we combined nuclei from PBS (n = 3315 nuclei) and PFF (n = 3665 nuclei) injected brains, followed by unsupervised clustering. For visualization purposes, we performed dimensionality reduction and embedding of the joined data (Figure 4.2A) using Uniform Manifold Approximation and Projection (UMAP). We identified a total of 18 distinct clusters that we annotated based on their gene expression profiles (Figure 4.2B and 4.2C). Specifically, we cross-referenced the literature for genes that were highly enriched in the different clusters, and we selected some gene markers to look at their expression in different clusters: Slc17a7 identified excitatory neurons, Gad1 inhibitory neurons, Cldn11 for oligodendrocytes, Clql1 for oligodendrocyte progenitor cells (OPC), Cx3cr1 for microglia, Aldh1l1 for astrocytes cells in different clusters of the combined dataset (Figure 4.2C). For analysis in this chapter, we focused on major types of neurons and non-neuronal cell types (Figure 4.2D). It has been reported previously that different types of neurons exhibit varied tendency to develop aggregates, with excitatory neurons more susceptible than inhibitory neurons. All major cell types

could be identified in our samples and the numbers of these cell types in both the groups remained similar. We could not classify the C8 cluster to a distinct cell type, which we think arises from RNA content from cytosolic fragments that were carried over in the nuclei preparation down to the 10X Genomics Chromium experiment. Since LB-like inclusions are found in cytosols, and these clusters represent contents that could mainly be located outside nuclei, we have included them in our dataset and analysis.

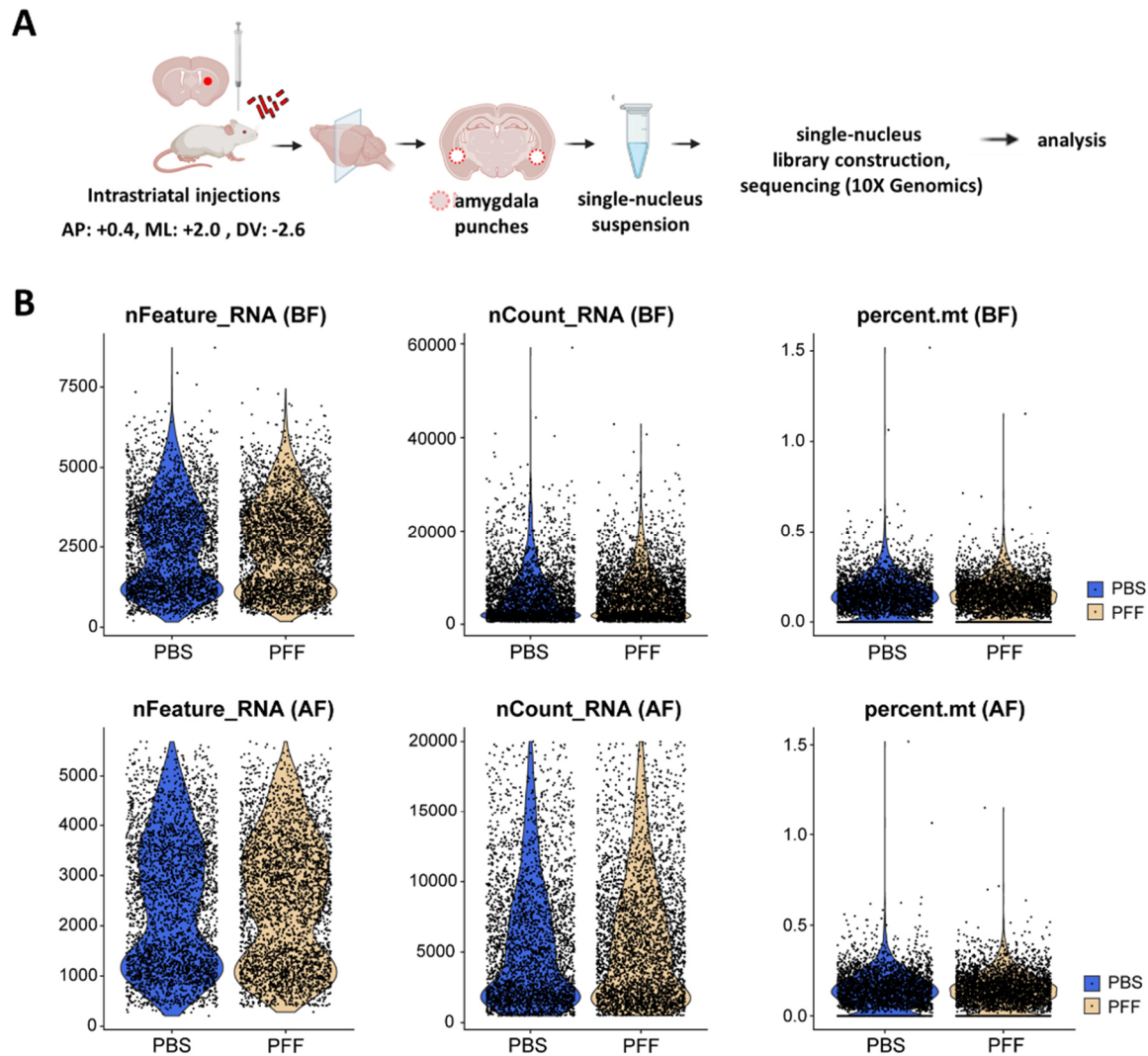


Figure 4.1: Workflow and QC of snRNA-seq from PBS and PFF amygdala brain regions. (A) Experimental workflow. (B) Quality control metrics: number of genes per cell (nFeature_RNA), number of UMI's per cell (nCount_RNA) and percentage of mitochondrial genes per cell (percent.mt) before and after filtering. Abbreviations: BF: before filtering; AF: After filtering

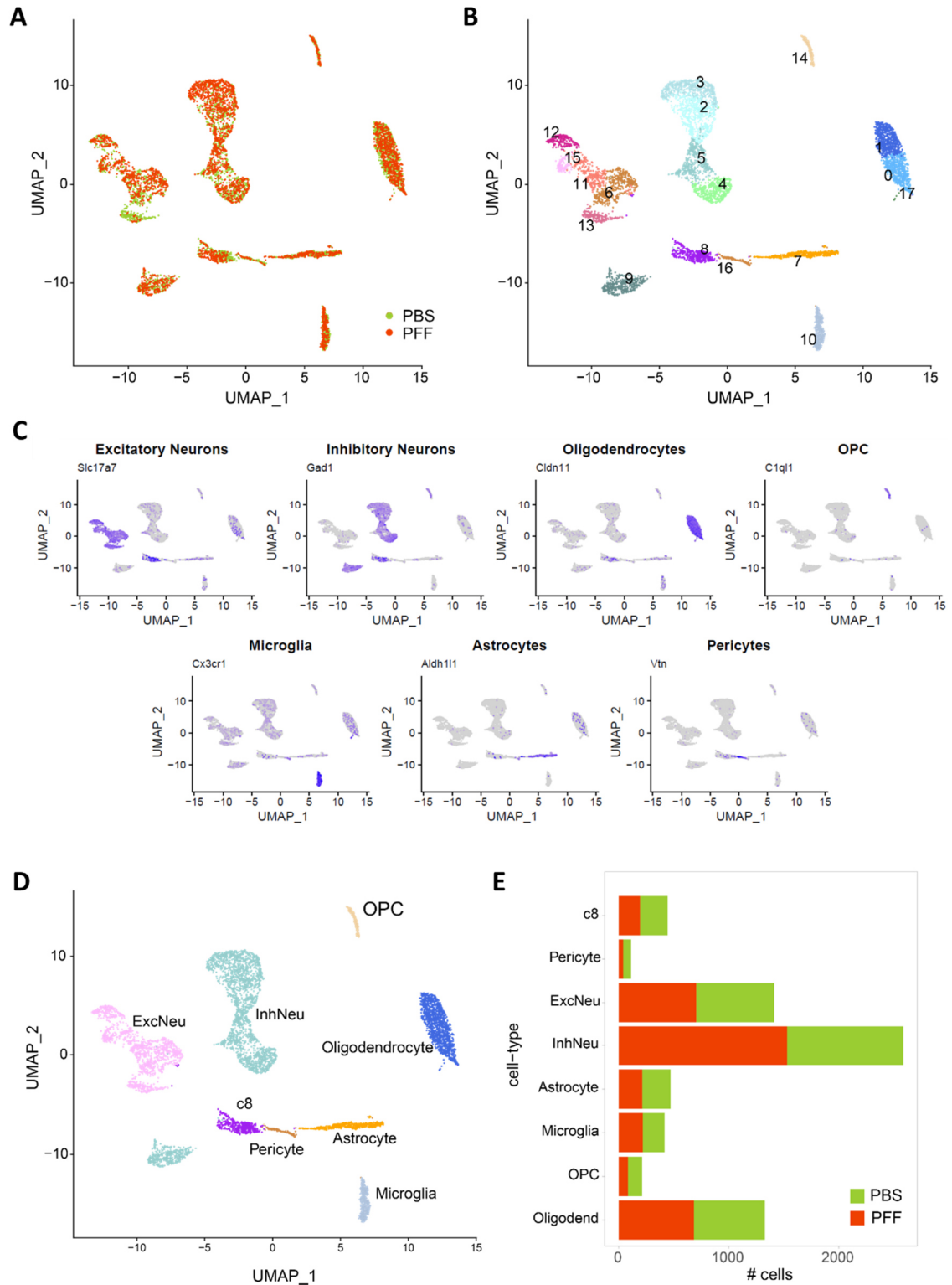


Figure 4.2: Dimensionality reduction, clustering and cell-type annotation. (A) UMAP plot overlay of PBS and PFF cells. (B) Unsupervised clustering of PBS and PFF by UMAP. (C) Violin plots showing specific markers expression in different clusters. (D) UMAP plots showing manually annotated cell types. (E) Cell-type populations in PBS and PFF datasets.

4.2.2 DEGs in different cell types indicate impaired neuronal signaling and regulatory pathways

To identify the effect of PFFs injections on each cell type of the Amygdala, we performed a pairwise comparison of gene expressions in PBS and PFF samples within the same cell types. A total of 1565 DEGs genes (757 upregulated and 808 downregulated) were identified across different cell types we classified (Figure 4.3A)– demonstrating that a large number of transcriptomic changes are seen in different cell types in the Amygdala, which is one of the regions affected at early PD stage. Interestingly, glial cells seem to have the highest number of DEGs expressed, especially in relation to the total number of genes. Analysis of the top 100 DEGs and their distribution in different cell types revealed that a substantial number of these changes are in inhibitory and excitatory neurons (Figure 4.3B). Gene expression levels of several genes are differentially affected in different cell types (Figure 4.3C). We observed these significant DEGs in inhibitory, excitatory and oligodendrocytes. Some of the DEGs in different cell types (Figure 4.3) and their involvement in the molecular or cellular functions will be discussed in the following sections.

4.2.2.1 Inhibitory neurons

The significantly upregulated genes in inhibitory neurons are mainly found to have several distinct functions. Among these, a handful of these genes are associated with PD. Ryr3 gene is involved in calcium release from the endoplasmic reticulum into the cytosol and thereby regulates calcium homeostasis, and calcium ion channels or controls several biological processes that require calcium for their activity^{745,746}. Association between the Ryr3 gene and Alzheimer's disease has been reported wherein it is known to play a dual role as a potential compensatory/protective role or pathological role of amplifying Abeta peptide production or synaptic deficits⁷⁴⁷. Moreover, Ryr3 is involved in beta2 adrenergic receptor signaling, associated with PD⁷⁴⁸. Therefore, Ryr3 gene upregulation in inhibitory neurons might be involved in calcium signaling and synaptic transmission, though not developing aggregates in inhibitory neurons. Another gene that regulates calcium levels is Cacnb2 (Calcium Voltage-Gated Channel Auxiliary Subunit Beta 2), a protein-coding gene that increases peak calcium current, shifting voltage dependencies of activation and inactivation, modulating G-protein inhibition and controlling alpha-1 subunit for membrane targeting. Increased expression of Cacnb2 suggests increased calcium concentration in the inhibitory neurons, which could be a response to LB-like inclusion burden in the Amygdala at the early disease stage. In addition, several genes have been described that play a regulatory role. i) Mme, a protein-coding gene believed to play a role in the ternary complex assembly of synaptic proteins at the postsynaptic membrane and coupling signal transduction to membrane/cytoskeleton remodeling. ii) Rgs9, a protein-coding gene involved in various signaling pathways by accelerating the deactivation of G proteins. iii) Pde10a, a protein

coding gene involved in regulating the intracellular concentration of cyclic nucleotides. iv) Strn, involved in dendritic Ca²⁺ signaling.

Specifically, downregulated genes in inhibitory neurons include i) Gnas, involved in regulating signaling pathways controlled by GPCRs, ras signaling pathway; ii) Shank1, required for development and function of neuronal synapses; iii) Cadm1, which plays a role in the formation of dendritic spines and in synapse assembly; iv) Slc8a1, contributes to the regulation of cytoplasmic calcium levels; Taken together, several of these specifically expressed genes in inhibitory neurons are involved in calcium signaling, GPCR based signal transduction, cytoskeleton remodeling, synaptic function, cyclic nucleotide-binding, which suggest the involvement of complex regulatory processes that might be taking place in interneurons to prevent aSyn aggregation or promoting degradation of aSyn aggregates.

4.2.2.2 Excitatory neurons

In excitatory neurons, several genes are specifically up and downregulated. Upregulated genes include:

i) Pde4d, involved in the hydrolysis and inactivation of cyclic adenosine monophosphate (cAMP). cAMP regulates signal transduction pathways such as cAMP/PKA/CREB and Epac/Akt signaling pathways⁷⁴⁹ – dysregulation of which is reported in several neurodegenerative diseases including PD. Interestingly, inhibition of Pde has been shown to reduce neuroinflammation, aSyn aggregate levels and neurodegeneration^{750,751}. To the best of our knowledge, this is the first time increased Pde4d levels are reported in excitatory neurons, which are susceptible to developing aSyn aggregates. Therefore, inhibiting Pde4d in excitatory neurons could be a therapeutic strategy for PD.

ii) Mef2c gene is particularly upregulated in excitatory neurons, which is thought to be involved in suppressing the number of excitatory synapses and thus regulating basal and evoked synaptic transmission; this function could be an indicator of reducing the spread of aggregates from cell to cell via synaptic terminals, as a measure by excitatory neurons to counteract aSyn aggregates.

iii) Rgs6, involved in the regulation of GPCR signaling cascades. GPCR signaling pathways are implicated in several neurodegenerative diseases, including PD and targeting them with therapeutic agents has shown to improve PD symptoms⁷⁵².

Significantly downregulated genes in Excitatory neurons include: i) Meis2, involved in transcription factor binding and activity; ii) Nr4a3, acts as a transcriptional activator; iii) Gpc5, encodes for heparan sulfate proteoglycans; iv) Sema3e, mediates reorganization of the actin cytoskeleton, specificity of synapse

formation. In sum, genes that are specifically expressed in excitatory neurons are involved in synaptic function, GPCR-based signaling cascades, expression of membrane proteins, reorganization of cytoskeletons and transcriptional control.

4.2.2.3 Oligodendrocytes

In oligodendrocytes, several genes are specifically up or downregulated. Upregulated genes include i) Plin4 gene is particularly upregulated in oligodendrocytes which is a protein-coding gene, and it is found to act as a coat protein involved in the biogenesis of lipid droplets; ii) Pex5l, a protein-coding gene which encodes an accessory subunit of hyperpolarization-activated cyclic nucleotide-gated (HCN) channels, regulating their cell-surface expression and cyclic nucleotide dependence; iii) Rhoj, involved in GTPs binding and GTPase activity; iv) Zbtb16, involved in DNA-binding transcription factor activity. Downregulated genes include i) Ttc3, encoding for E3 ubiquitin-protein ligase activity and ubiquitin-protein transferase activity; ii) Atp8b1, involved in nucleotide binding, cation-transporting ATPase activity; iii) Ahsa2, encodes for co-chaperone that stimulates HSP90 ATPase activity; iv) Nfat5, DNA-binding and transcription factor activity. Taken together, these genes are involved in diverse functions such as biogenesis of lipid droplets, GTPs binding, nucleotide binding and activation of ATPase activity.

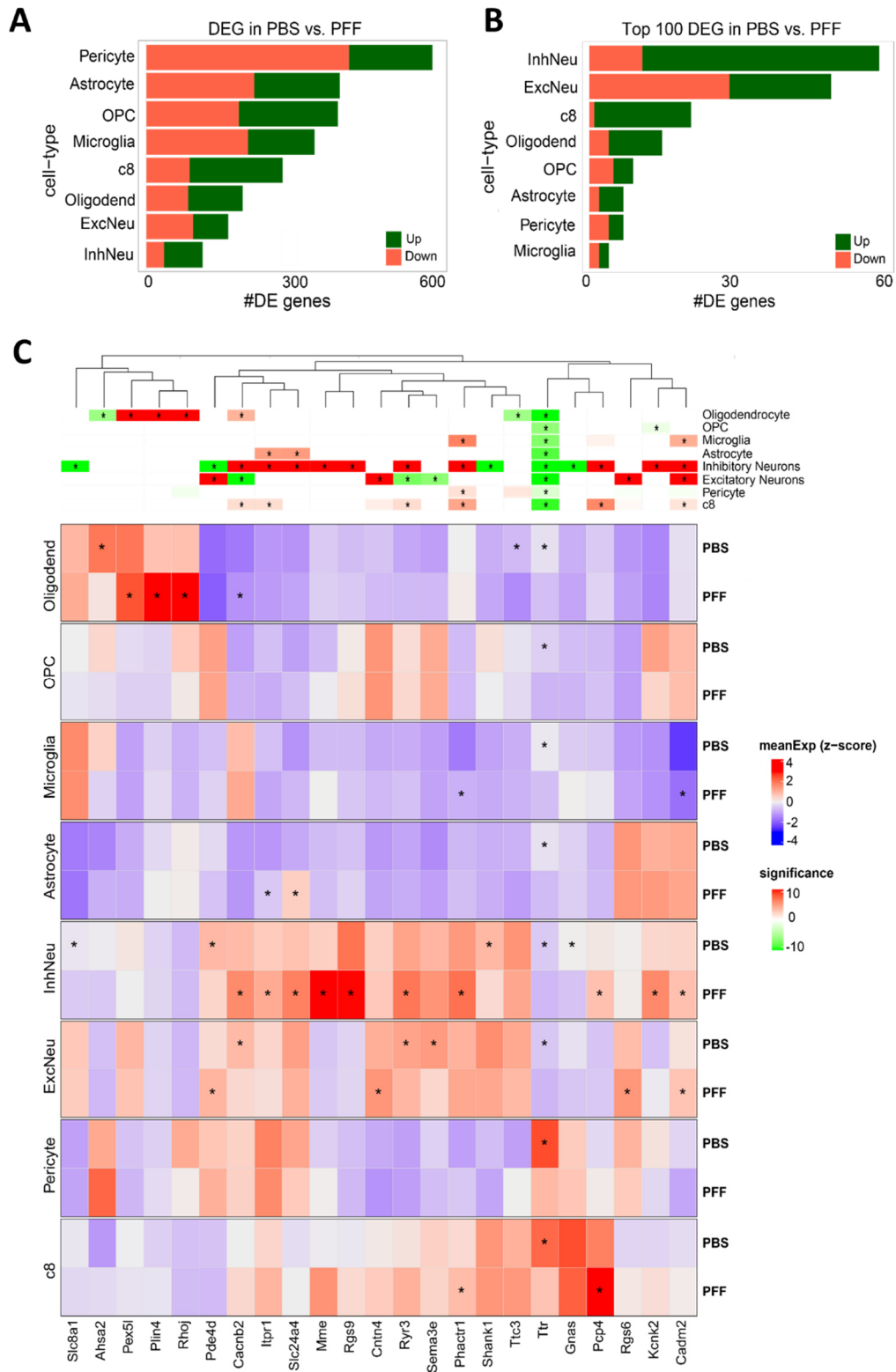


Figure 4.3: DEGs in different cell types in PBS and PFF amygdala samples. (A) total number of DEGs. (B) Top 100 DEGs genes in different cell types. (C) Heatmap showing mean expression of selected genes in different cell types in PBS and PFF samples. * indicates significance level

4.2.3 Gene Ontology functional annotation reveals several dysregulated molecular functions and specific cellular components in different cell types of the PFF amygdala brain

To gain an insight into the impact of gene expression changes on the function of in individual cell types, we functionally annotated upregulated or downregulated genes in particular cell types by performing gene ontology enrichment analysis using the molecular function, cellular component terms using gProfiler. For GO:MF terms for upregulated genes: we found that inhibitory neurons are associated with neuronal signaling in particular ion channel and ion transporter activities, cyclic-nucleotide phosphodiesterase activity, and protein binding (Figure 4.4A). The genes that are found to be associated with ion channel activity are *Cacnb2*, *Ryr3*, *Kcnk2*, *Kcnab1*, *Cacna2d3*, *Ano3*, *Slc24a4*, *Itpr1*, *Slc24a2*. *Itpr1* gene encodes for a receptor which, upon stimulation by inositol 1,4,5-triphosphate and cytosolic Ca^{2+} , causes calcium release from the endoplasmic reticulum⁷⁵³. Therefore, *Itpr1* could be involved in increased calcium levels and associated calcium signaling in inhibitory neurons. In excitatory neurons, we found molecular function terms associated with cell adhesion molecule binding, and cadherin binding. The genes that are found to be associated with cadherin binding are *Ctnna3*, *Ptprt*, *Cdh7*, *Cdh13*, and *Cdh8*. Among these, *Cdh8* encodes the Cadherin family of proteins involved in calcium-dependent cell-cell adhesion and GWAS studies have implicated *Cdh8* in being associated with PD⁷⁵⁴.

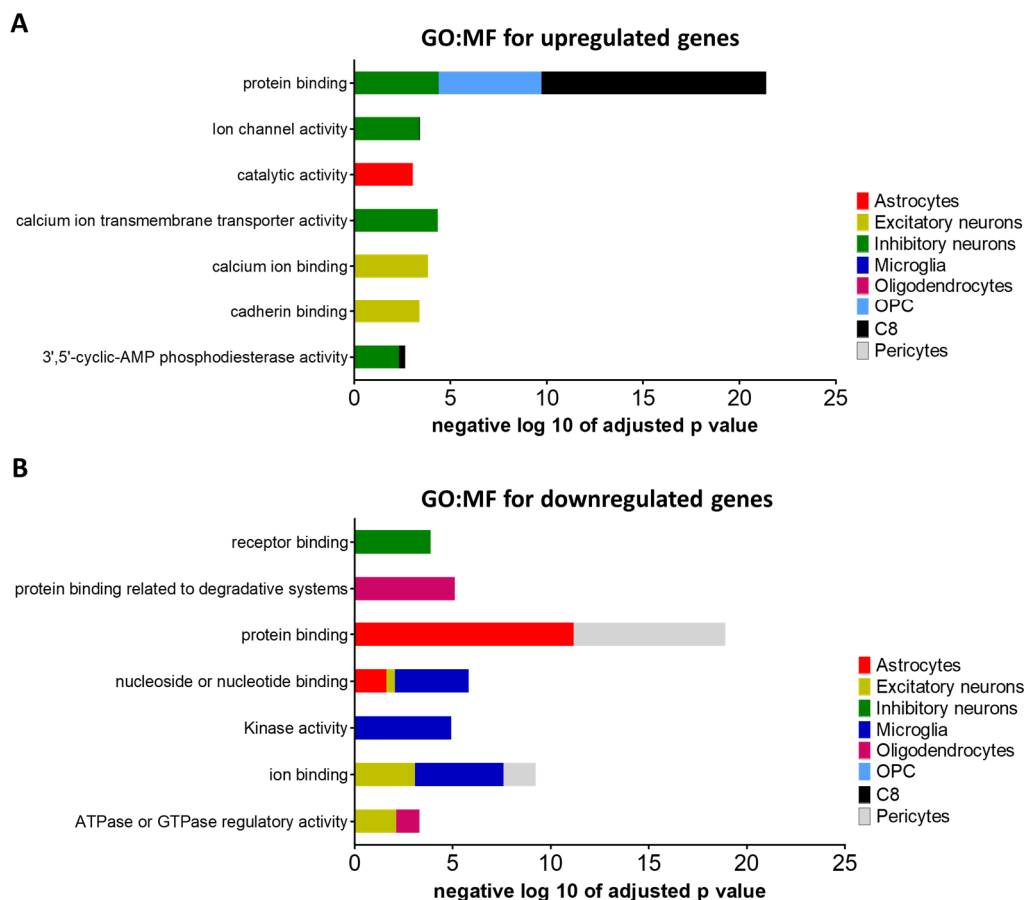


Figure 4.4: Gene Ontology enrichment analysis of molecular function terms. A) GO:MF of upregulated genes. B) GO:MF of downregulated genes in different cell types of PFF amygdala compared with PBS are plotted as a function of negative log 10 of the adjusted p-value.

We found molecular function terms for downregulated genes to be associated mainly in non-neuronal cell types. Nucleoside or nucleotide binding was significantly enriched across astrocytes, excitatory neurons, and microglia. In oligodendrocytes, these are associated with unfolded protein binding, heat shock protein binding, chaperone binding, and HSP70 protein binding – all of these terms are associated with processes involved in protein misfolding and degradation processes. Therefore, dysfunction of protein misfolding and degradative machinery in oligodendrocytes could be an early event in PD pathogenesis.

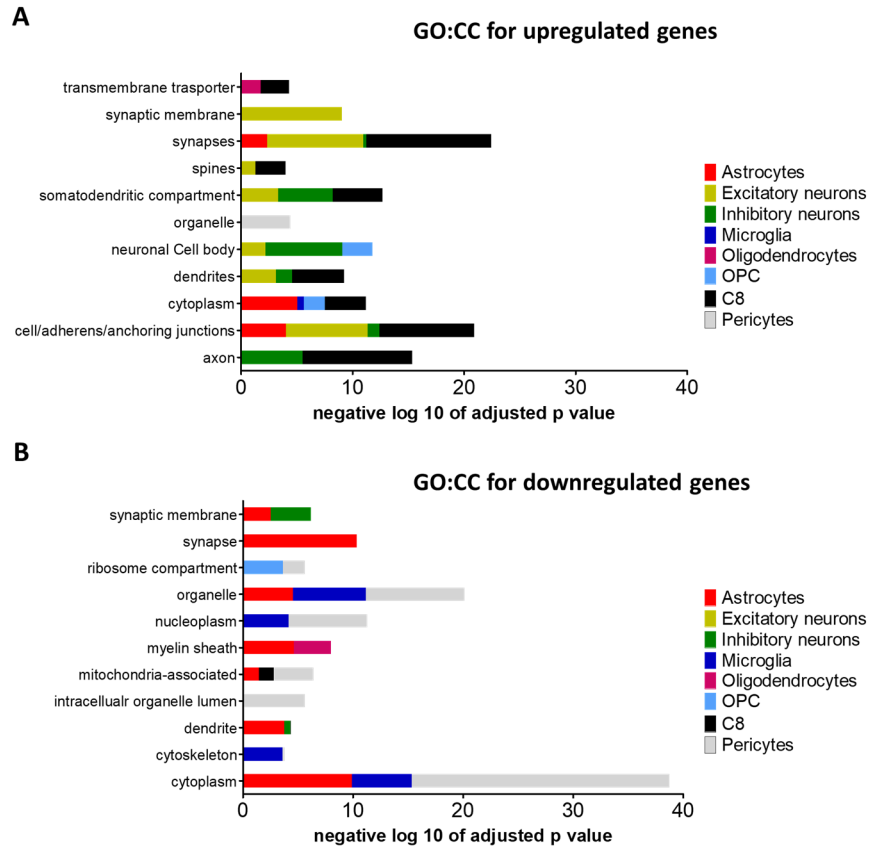


Figure 4.5: Gene Ontology enrichment analysis of cellular component terms. A) GO:CC of upregulated genes. B) GO:CC of downregulated genes in different cell types of Amygdala of PFF compared with PBS are plotted as a function of negative log 10 of the adjusted p value.

To identify the cellular components where these differentially expressed genes are acting on or present, we performed GO enrichment analysis using cellular component terms for upregulated genes (Figure 4.5A) in different cell types; we observed that upregulated genes are mainly associated with neuronal compartments such as synaptic membranes, synapses, neuronal cell body, spines, axons, ion transporter complexes in excitatory and inhibitory neurons. These results align with the finding that molecular functions of upregulated genes are mainly involved in neuronal signaling, and this signaling occurs mainly via plasma membrane and synapses. In contrast, GO enrichment analysis using cellular component terms for downregulated genes (Figure 4.5B) in different cell types revealed that distinct downregulated genes are localized in distinct locations such as organelle, nucleoplasm, myelin sheath, ribosome compartment and these were observed mainly for non-neuronal cell types. Furthermore, this analysis revealed that several of these differentially expressed genes in different cell types are localized to specific locations for their particular functions.

4.2.4 The expression of PD-risk genes is altered in specific cell types in the Amygdala of PFF injected mice brains

To identify specific cell types that significantly contribute to PD progression, we looked at gene expression levels of PD-risk genes in different cell types. We obtained the top 125 PD-risk genes based on gene-disease association scores from the DisGeNET database (UMLS CUI ID: C0030567) and quantified their gene expression levels in different cell types of PFF and PBS samples (Figure 4.6A). ~90% of these PD-risk genes have unchanged or no major change in gene expression levels in different cell types. Interestingly, we identified ~10% of these 125 top PD-risk genes (Sncaip, Park7, Maob, Hspa8, Aif1, Slc2a3, Hsf3, Hgf, Trpm2, Nr4a2, Bdnf) specifically up-or down-regulated in different cell types of Amygdala of PFF compared to PBS injected mice brain (Figure 4.7).

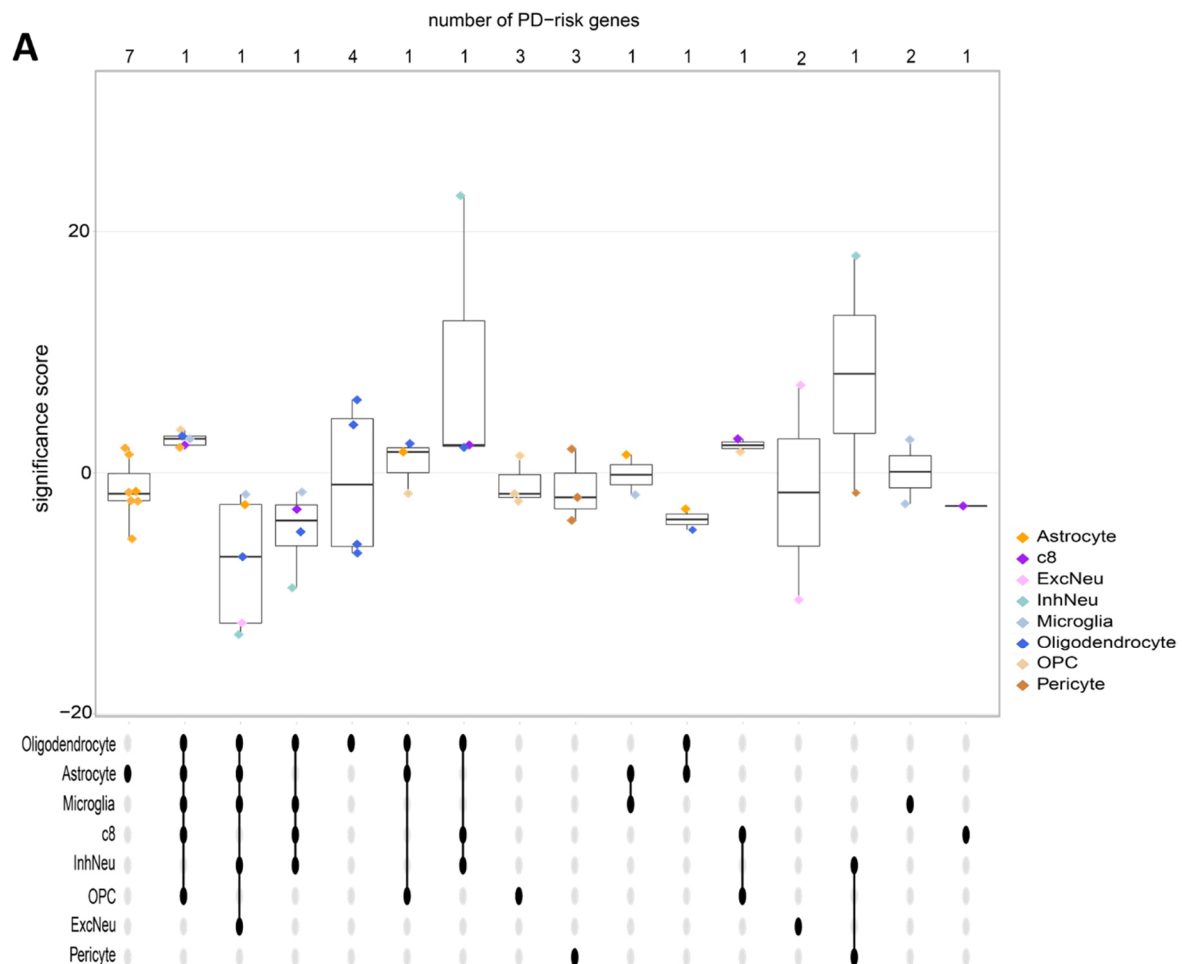


Figure 4.6: PD risk genes: UpSet plot representing the significance scores of PD-risk gene(s) differentially expressed in PFF compared with PBS. Dots represent the gene significances, colored by the associated cell type. The numbers above the boxplots represent the number of genes in the cell-type(s) group. PD risk genes are obtained from the DisGeNET database (UMLS CUI ID: C0030567)

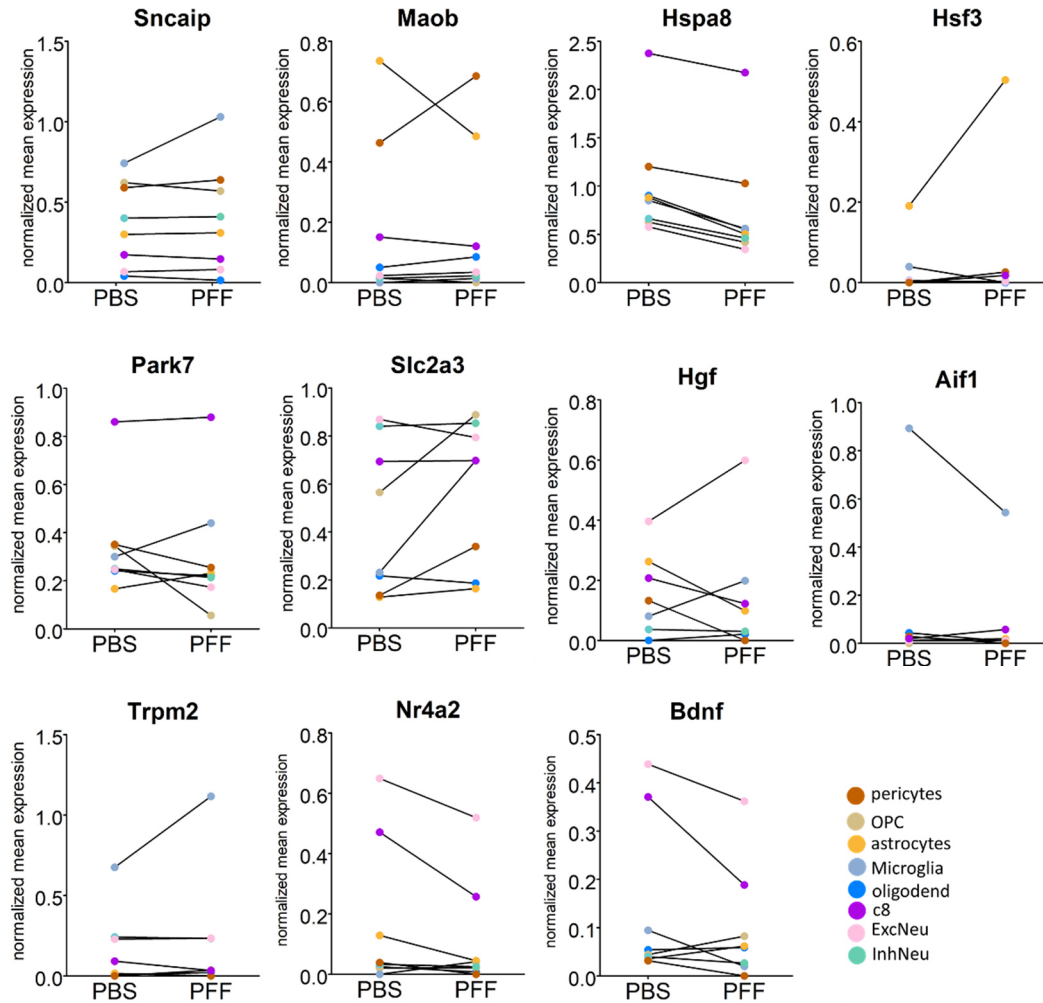


Figure 4.7: Normalized mean expression level of PD risk genes in different cell types of PFF compared with PBS. PD risk genes are obtained from the DisGeNET database (UMLS CUI ID: C0030567)

Sncaip is a protein coding gene that encodes aSyn interacting protein called Synphilin-1. Synphilin-1 has been shown to interact with aSyn³⁸⁵ and present in LBs²⁵³ and clearance of soluble and misfolded aSyn⁷⁵⁵. We detected an almost 1.5-fold increase in *Sncaip* gene expression in the microglia of the PFF sample. In PD, microglia are known to activate under pathological conditions^{756,757} and clear aSyn aggregates via autophagy⁷⁵⁸. Therefore, an increase in *Sncaip* gene expression might indicate the role of Synphilin-1 mediated clearance of aSyn in microglia.

Park7 is a protein-coding gene that encodes DJ-1. We detected an almost four-fold decrease in *Park7* gene expression in OPCs in the PFF sample. DJ-1 has been shown to act as a chaperone with protease activity, maintaining the mitochondrial function, anti-oxidant scavenger and regulating transcription activity, and mutations in *Park7* is linked with early-onset PD^{759,760}. In addition, DJ-1 has also been shown to inhibit aSyn

aggregation by acting as a molecular chaperone⁷⁶¹ and by regulating chaperone-mediated autophagy⁷⁶². A decreased expression of PARK7 in OPCs might be involved in aSyn aggregation and formation of glial cytoplasmic inclusion⁷⁶³, a pathological hallmark of Multiple System Atrophy (MSA).

Moab is a protein-coding gene that encodes monoamine oxidase-b. We detected an almost two-fold decrease in Moab in the PFF sample, specifically in astrocytes. Inhibition of Moab has been shown to facilitate aSyn secretion and delay its aggregation⁷⁶⁴. And also, astrocytes are shown to be involved in spreading aSyn aggregates⁷⁶⁵. These studies suggest that at early stages, decreased expression of Moab might be involved in transferring endocytosed aSyn aggregates by astrocytes to neighboring cell types and contribute to aSyn aggregate spreading in the brain. Interestingly, we found an almost 1.5-fold increase in Maob expression level in pericytes. Activation of pericytes, compromised blood-brain-barrier integrity⁷⁶⁶, and increased expression of monoamine oxidase-a has been reported in neighboring endothelial cells in vascular regions of brain⁷⁶⁷ in PD model systems – these alterations have been linked with PD. To the best of our knowledge, this is the first report where monoamine oxidase levels are increased in pericytes under disease conditions in PFF injected brain. Therefore, increased pericyte expression might lead to pericyte activation and a compromised blood-brain barrier.

Hspa8 is a protein-coding gene that encodes a heat shock protein 70. Hspa8 expression seems to be reduced in all cell types, suggesting compromised protein homeostasis and aggregates accumulation⁷⁶⁸.

Slc2a3 is a protein-coding gene that encodes a protein that is involved in glucose uptake across the cell membrane. Decreased glucose uptake and metabolism are associated with several neurodegenerative diseases, including AD, PD and HD⁷⁶⁹. In our study, expression of which is two-fold and threefold increased in OPC and microglia, respectively. These findings might suggest that compensatory mechanisms by OPCs and microglia to increase glucose uptake and glucose metabolism to provide energy required to facilitate various biological processes that are aimed toward the normal functioning of cells and degradation of aggregates, both are considered to be energy demanding.

Hsf3 is a protein-coding gene that encodes heat shock transcription factor 3, which binds to the heat shock promoter element and activates the transcription of non-classical heat shock genes (e.g., Pdzd2, Prom2) and protects cells against heat shock and proteotoxic stress⁷⁷⁰. Specifically, in astrocytes, we detected an almost three-fold increase in Hsf3 gene expression, which might indicate expression of non-classical heat shock genes, which might prevent astrocytes from proteotoxic stress upon increased aSyn aggregates level under pathological conditions.

Trpm2 encodes a tetrameric calcium-permeable cation channel which is sensitive to oxidative stress. We detected an almost two-fold increase in Trpm2 level in microglia. Under pathological conditions, Trpm-2 mediated calcium signaling has been shown in aberrant microglial activation and induction of neuroinflammation⁷⁷¹. Therefore, increased expression of Trpm2 might be playing a significant role in microglial dysfunction and exacerbating the disease process. In conclusion, differential gene expression levels of PD risk genes suggest that each cell type responds distinctively to the LB-like inclusion burden in the Amygdala.

4.2.5 Several pathways implicated in PD are affected in different cell types

To identify pathways that could be dysregulated in different cell types, we performed GO functional enrichment analysis and identified several KEGG pathways that are dysregulated in different cell types (Figure 4.8). Among these pathways, Parkinson's disease pathway (Figure 4.9) is a significant one, wherein we observed interesting changes in gene expression levels. Interestingly, the Ryr3 gene is upregulated in the inhibitory neuron (that do not develop aggregates), and Ryr3 is downregulated in excitatory neurons (that develop aggregates). Ryr3 plays a role in beta-2 adrenergic receptor signaling, and agonists of beta-adrenoreceptors are shown to reduce aSyn transcription⁷⁴⁸. Therefore, in inhibitory neurons, these receptors could be activated and, in turn, less or no aSyn transcription, suggesting no aggregates or fewer aggregates that degradative mechanisms could clear. In contrast, opposite in excitatory neurons, there could be higher aSyn transcription, thereby forming aSyn aggregate. We also report here several pathways, which are associated with PD and neurodegeneration, but it is not known how the genes we identified play a role in the pathogenesis of PD. Further studies are required to fill this knowledge gap.

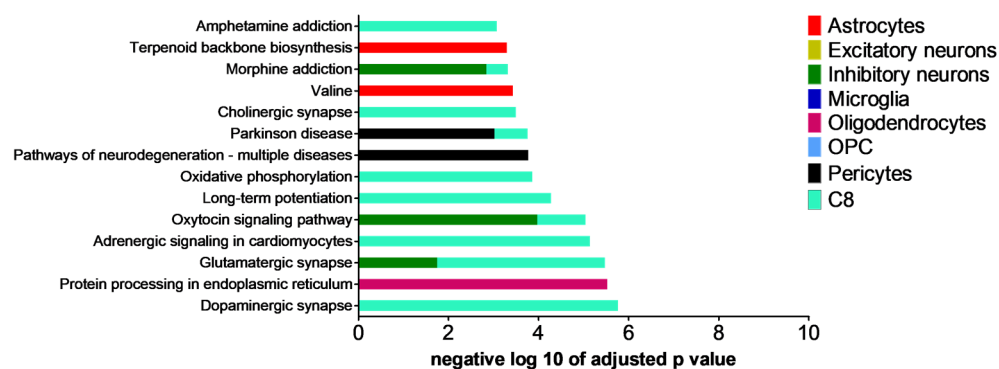


Figure 4.8: Gene Ontology enrichment analysis of KEGG pathway terms. Several pathways related to PD are dysregulated in PFF compared to PBS sample.

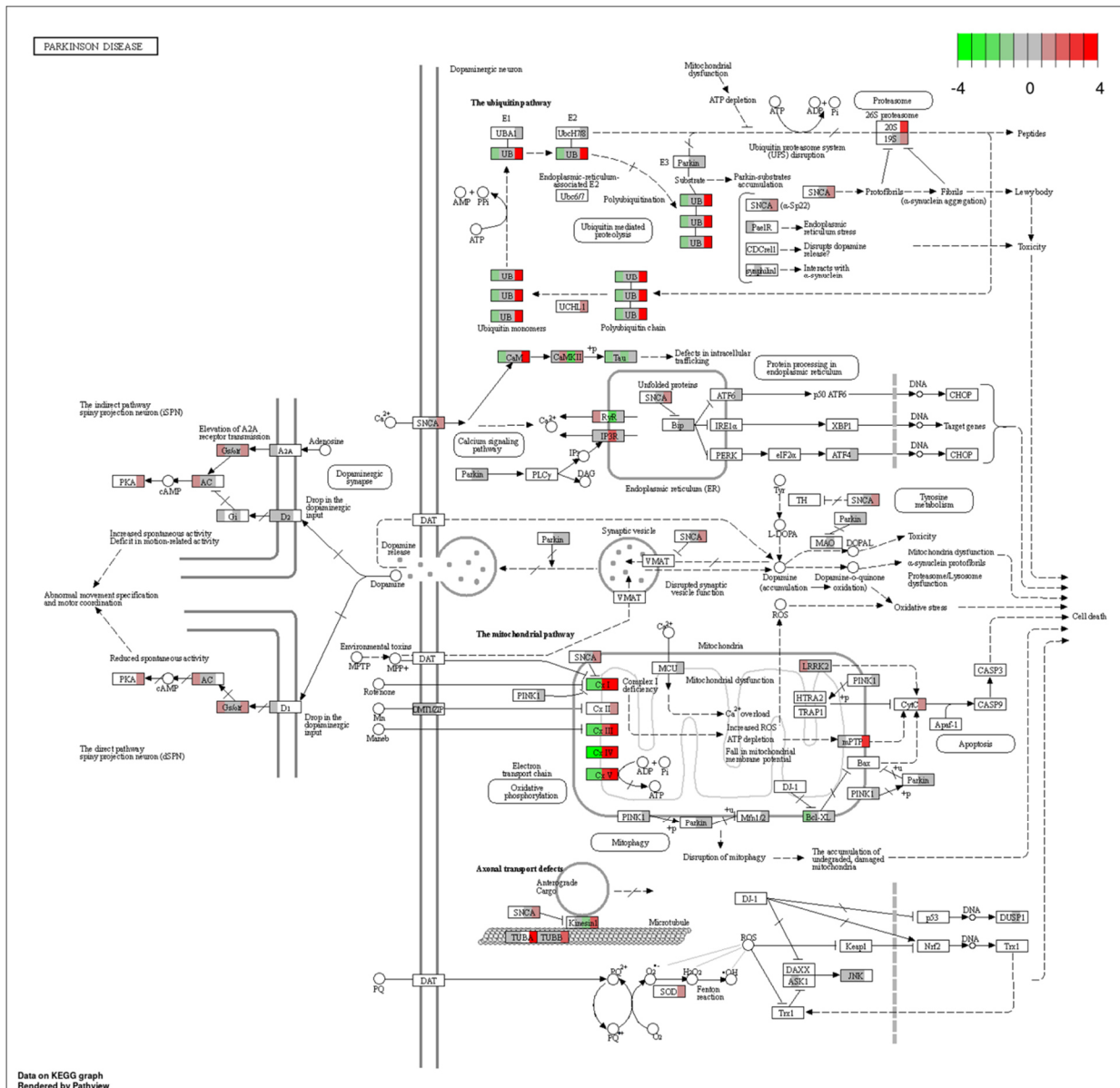


Figure 4.9: Parkinson disease related KEGG pathway marked by genes that were found to be significant for particular cell types. The colour code represents the avgLogFC in PBS vs. PFF for cell types (from left to right): InhNeu, ExcNeu, Pericytes and c8.

4.3 DISCUSSION

Although previous studies have carried out single-cell RNA sequencing studies in PD model systems, none of these studies used a model system wherein cells in the brain regions studied developed LB-like inclusions. To the best of our knowledge, this is the first study that investigates single-cell transcriptomics changes in different cell types such as neuronal (excitatory and inhibitory) and non-neuronal (astrocytes,

microglia, oligodendrocytes, OPC, pericytes) from a brain region (Amygdala) that abundantly develops pS129 positive aggregates in a PFF-based model of PD at an early time point during the disease process.

This study reports a total of 6980 single-cell transcriptomic profiles of ipsi and contralateral amygdala brain regions from age-matched PBS and PFFs injected mouse brains. We report several novel findings in this study. We found that different cell types respond differently to the aSyn aggregate burden in the amygdala brain region by differentially upregulating or downregulating genes. GO-based functional annotation revealed several unique molecular functions of upregulated genes. GO:MF terms for upregulated genes are enriched mainly in neurons but not in non-neuronal cell types – among these, significant changes in upregulation of genes are observed in inhibitory neurons compared to any other cell type, whereas downregulation of genes is observed mainly in non-neuronal cells. GO:MF terms for upregulated genes in inhibitory neurons are associated with neuronal signaling in particular ion channel and ion transporter activities, whereas downregulated genes in other cell types are associated with regulatory activity such as ATPase activator, protein or nucleotide binding, chaperone activity. These findings suggest that neuronal signaling-related functions are upregulated in neurons that do not develop aggregates, suggesting that increased neuronal signaling in inhibitory neurons could be a protective action in the early stage. We also report several pathways that are implicated in PD that are dysregulated in many or a few cell types.

It is previously believed that aSyn is one of the key drivers of the disease phenotype or formation of pS129 positive aggregates^{493,744}, but to our surprise, we did not observe any significant upregulation or downregulation of aSyn gene expression in any of the cell types we looked at. Our work also identified the contribution of specific cell types that might significantly contribute to PD progression. We identified several PD risk genes (Sncaip, Park7, Moab, Ddc, Hspa8, Aif1, Slc2a3, Hsf3, Trpm2) that are specifically up- or down-regulated in different cell types of the Amygdala of PFF compared to PBS injected mice brain— suggesting that targeting these genes in these specific cell types could be a novel strategy to manipulate the disease process and reduce pathological effects. In addition, we also report in this study several genes that are solely up or downregulated in particular cell types – which could be investigated further to delineate their specific contributions towards normal or disease state in a specific type of cell using genetic and/or pharmacological approach.

As major limitation of our study is the absence of biological repeats therefore results described here do not have statistical power to solidify our conclusions. In addition, proteomic analysis needs to be performed along with transcriptomics to correlate whether gene expression changes are also seen in

translated protein levels in different cell types in the follow-up studies. Although our study cannot distinguish between transcriptomic changes in excitatory neurons that develop pS129 positive aggregates versus those that do not, our findings, however, suggest that at early time points (2 months after PFF injections), different cell types such as those that develop pS129 positive aggregate (excitatory neurons) and those that do not develop aggregate (inhibitory neurons) show unique molecular, transcriptomic changes in response to aSyn aggregate burden in amygdala brain regions. These findings establish that different cell types either promote or prevent, or regulate aggregate formation in them, and they could be regulating transcriptomic changes and functioning synergistically to cope with the aSyn disease burden in the Amygdala. In the future, sophisticated genetic and functional studies are required to fill this knowledge gap.

4.4 METHODS

4.4.1 Preparation of recombinant mouse WT aSyn preformed fibrils

Recombinant mouse WT aSyn preformed fibrils (PFFs) were prepared as described previously⁸⁹. In brief, aSyn PFFs were generated from recombinant mouse (m) aSyn protein. The lyophilized protein was dissolved in PBS at 4mg per 600ul and set to pH 7.4. The solution was centrifuged for 5 min through a 0.2 µm filter at 5000 rpm, and purity was confirmed by mass spectrometry and HPLC. The supernatant was incubated under constant agitation of 900 rpm on an orbital shaker at 37°C for 5 days. The generated maSyn fibrils were sonicated briefly (40% amplitude, one pulse for 5 s) and then were aliquoted and stored at -80 °C. These sonicated fibrils (PFFs) were further characterized by ThT binding assay, Transmission electron microscopy, filtration protocol and SDS-PAGE analysis to quantify the presence of monomers and oligomers in the sample. Thioflavin T (ThT) binding was performed to assess amyloid formation with excitation at 450 nm, and emission at 485 nm (Bucher Analyst AD plate reader). Samples were treated with ThT (10 µM, in 50 mM glycine, pH8.5) in black 384-well plates (Nunc). The remaining soluble protein was subjected to filtration protocol⁷⁷² and analyzed by SDS-PAGE (15% polyacrylamide gel) and Coomassie (Life Technologies) staining. Samples were applied on glow-discharged Formvar/carbon-coated 200-mesh copper grids for analysis by transmission electron microscopy.

4.4.2 Animals and intrastriatal injection of recombinant mouse WT aSyn fibrils

C57BL/6JRj male mice were ordered (Janvier Labs) at an age of 10 weeks and allowed to acclimate to the animal house for at least 2 weeks. About 2-3 mice were housed in a cage and kept at 23 °C (40% humidity) in a 12h/12h light/dark cycle with food ad libitum.

4 to 5-month-old C57BL/6JRj male mice were anesthetized by intraperitoneal injection of 100 mg/kg ketamine and 10 mg/kg xylazine. The animals were then mounted on a stereotaxic frame (model 963, Kopf, California, USA), and a lubricant eye ointment was applied. A hole was created in the right parietal bone (0.4 mm anterior and 2 mm lateral to the bregma), and 10 µg of mouse WT aSyn PFFs in 2.5 µl of PBS or 2.5 µl of PBS as control were injected with a 34G cannula at the flow rate of 0.1 µl/min, 2.6 mm beneath the dura. The cannula remained in place for 5 min after injection, and it was retracted in steps slowly and smoothly. All animal experiments and procedures were approved by the Swiss Federal Veterinary Office (authorization number VD 3499).

4.4.3 Brain tissue dissection and nuclear extraction

After two months of PFFs injection time period, the animals were deeply anesthetized with intraperitoneal injection of 100 mg/kg ketamine and 10 mg/kg xylazine and sacrificed. The brains were collected and quickly frozen in liquid nitrogen and stored at -80 °C. Prior to amygdala brain region dissection, all the brains were kept on dry ice to prevent immediate thawing. Each of the brains was thawed for about 4-5 seconds and placed in acrylic brain matrix (brain matrix (Acrylic) for mouse Coronal, 1mm; TED PELLA) and cut using blades (PELCO® Blades for use with Brain Matrices, TED PELLA). Each of the brain sections were placed in PBS solution in a 6 well plate placed on ice until the Amygdala brain region dissection. The brain sections that contain the Amygdala brain region were separated, and ipsilateral and contralateral amygdala brain regions were punched and isolated using precision brain punches 2mm dia (TED PELLA). All the punched amygdala brain regions were kept in 2 ml solution D (250 mM sucrose, 25 mM KCl, 5 mM MgCl₂, 20 mM Tris-HCl pH 7.5, 1mg/ml actinomycin D, 0.02% sodium azide; 0.22µm filtered) and homogenized in a douncer with 40 strokes. The solution was transferred to a 15 ml falcon tube and centrifuged 1 min max at 4°C. Pellets were resuspended in 3 ml solution D, and 2ml Optiprep was added and centrifuged for 10 min at 3200g at 4°C. The resulting supernatant was discarded, and one more round of OptiPrep purification was performed. The resulting pellet was resuspended in a 500 µl Nuclear PBS buffer solution (1x PBS, 5% BSA, 20 U/µl RNAase inhibitors, 1mg/ml actinomycin D). This nucleus-containing solution was filtered using a 40 µm Flowmi Cell Strainer (Bel-Art). The filtered solution was integration and individuality of extracted nuclei, and nuclei were counted to have around 1000 nuclei/µl for library preparation and sequencing using 10x genomics technologies.

4.4.4 snRNA library construction and sequencing

15 to 20 ul of the nuclei suspension were used to perform 10x RNA library construction following the 10X 3' reagent kit v3.1 and user guide CG000204 Rev D in 10X Chromium single cell controller. The sequencing (with a target nuclei number 4000) was performed in the HiSeq4000 instrument by gene expression core facility, EPFL.

4.4.5 Data demultiplexing and quality control

A total of 273 Mio reads for the PBS sample (resp. 261 Mio reads for PFF sample) were processed using CellRanger workflow (v. 6.0.1), using the pre-built mouse reference genome mm10-2020-A. This resulted in 3446 estimated PBS nuclei and 3758 PFF nuclei, with 79K (resp. 69.5K) mean reads per cell and 2566 (resp. 2586) median genes per cell. PBS and PFF samples were then aggregated using the cellranger aggr function with the default settings. This resulted in 7204 nuclei, with 68.6K mean reads per cell and 2557 median genes per nuclei. Aggregated results were then imported and analyzed into R (v. 4.0.0) using the R package Seurat (v3.1.5). Nuclei with more than 20000 UMI counts, detecting less than 200 or more than 6000 genes, and detecting more than 10% of mitochondrial genes, were removed from the analysis. A total of 6980 nuclei (3315 PBS and 3665 PFF) and 19136 genes remained.

4.4.6 Clustering, cell-type annotation

The 18 clusters obtained at a resolution of 0.8 were characterized and associated with a given cell-type, based on some known cell-type markers expression levels.

4.4.7 Differential expression analysis and functional enrichment analysis

Marker gene identifications were performed using FindAllMarkers, requiring a minimum of 100 cells per group. Differential gene expression between PBS and PFF cells was done using FindMarkers, with a minimum group size of 5 cells. Upregulated genes were selected with the following criteria: $p < 0.05$ and positive negative log fold change, and down-regulated genes were selected with the following criteria: $p < 0.05$ and negative log fold change. Gene Ontology enrichment analysis (molecular function, cellular component, KEGG pathways) for upregulated and downregulated genes in different types of cells was performed using g:Profiler⁷⁷³ with the following parameters: significance threshold method: g_SCS; user threshold: 0.05, statistical domain scope: only annotated genes.

4.4.8 PD risk genes analysis and pathways analysis

To identify the expression level of PD risk genes in different cell types of the Amygdala, we obtained the top 125 PD-risk genes based on gene-disease association score from the DisGeNET database (UMLS CUI

ID: C0030567) and screened for gene expression changes by looking mean expression levels and significance level in different cell types of PBS and PFF samples.

4.5 Contributions of the authors

Somanath Jagannath and Hilal A. Lashuel conceived, conceptualized and designed the experiments. Somanath Jagannath performed raw data analysis and data extraction, interpretation and wrote the chapter with the feedback from all the authors. Marion Leleu performed bioinformatics analysis and generated figures 4.1B, 4.2, 4.3, 4.6, 4.9 based on the inputs from Somanath Jagannath, Gioele La Manno and Nicolas Guex.

CHAPTER 5: CONCLUSION

5.1 Achieved results, limitations and future perspectives

In Chapter 2 of this thesis, we used multiple techniques to assess the aSyn species specificity of several commonly used conformational-specific and aggregation state aSyn antibodies. This was achieved using well-characterized preparation of aSyn monomers, fibrils and different preparation of oligomers of distinct structural and biochemical properties. Our results demonstrated that: i) no antibodies could be identified that were solely monomer-specific, oligomer-specific or fibril specific; ii) all the antibodies that recognized aSyn oligomers also recognized aSyn fibrils and some recognized all three species (oligomers, fibrils and monomers); iii) the antibody clone 26F1 is the only antibody that was shown to be highly specific for β -sheet-enriched oligomers, it detects oligomers and HNE-induced oligomers and fibrils but not for unstructured DA-induced oligomers and structurally disordered monomers; All other antibodies recognized both structured (β -sheet enriched) and disordered oligomers, suggesting that their specificity could be driven by avidity rather than conformational specificity iv) the antibody clone 5G4 showed increased immunoreactivity toward β -sheet-enriched oligomers, HNE-induced oligomers and fibrils, and unstructured DA-induced oligomers and almost no immunoreactivity toward monomers; iv) antibodies clones A17183A, A17183E, SYNO4 preferentially detected all three types of oligomers and fibrils but reacted very weakly toward monomers; v) the majority of the other antibodies (such as 9029, 12C6, ASyO5, SYN-1, and SYN211) exhibited immunoreactivity towards all aSyn species under the conditions tested here. MJFR-14 shows more specificity to aggregated forms of aSyn by ELISA but showed higher immunoreactivity to monomers by slot blot and Western blot analyses.

Although we failed to identify antibodies that target a single specific form of aSyn i.e., monomers, oligomers or fibrils, our results show that it is possible to develop antibodies that target β -sheet rich aSyn oligomers and fibrils or oligomers and fibrils of diverse conformational properties. Such antibodies could represent more reliable tools for measuring the total levels of aggregated aSyn. Finally, our findings show that it is unlikely that any of the existing oligomer-specific immunoassays can provide an accurate assessment of the levels of aSyn oligomers or capture the diversity of aSyn by Western blots and possible in tissues. Therefore, we propose that these oligomer assays should be reassessed for their ability to distinguish between aSyn oligomers and fibrils. The interpretation of previous and future studies should take into account the specificity and limitation of the antibodies used. Future studies aimed at deciphering the role of different aSyn species in the pathogenesis of PD should be carried out using multiple antibodies characterized using aSyn multiple calibrants that capture, to the extent possible, the diversity possible of

aSyn species in the brain. A similar approach can be applied to facilitate the development of accurate assays to assess the target engagement of therapeutic antibodies.

One major limitation of our work is that while we used diverse and well-characterized aSyn preparations of monomers, oligomers (different types), and fibrils to screen the antibodies, it remains unclear how these species occur in the brain. That being said, we hypothesized that screening using a diverse set of species instead of using one specific type of aSyn oligomer is the best that we can do to approximate the complexity of aSyn species *in vivo*. In this direction, future work is required for the development of tools and techniques to isolate oligomers from the patient brains and use these patient-derived oligomers as immunogens to develop antibodies. This will ensure that antibodies will detect oligomers present in the brains and help identify the diversity of conformations of oligomers that might be present in the PD and related synucleinopathic brains. The second limitation is that our study focused on exploring the diversity of oligomers but not fibrils. Therefore, future studies that incorporate morphologically, structurally, and chemically different fibrils will enable us to identify the specificity of these antibodies. The third limitation is that aSyn is subjected to different modifications *in vivo*, while all our protein standards were generated from unmodified recombinant aSyn. However, it is important to note that while we know a great deal about the different types of PTMs that occur in LBs and LNs and aSyn aggregates, very little is known about the PTM patterns of aSyn oligomers *in vivo*. Therefore, further studies are required to generate PTM modified oligomers and assess whether any of these conformation-specific antibodies preferentially detect specific PTM modified oligomers and any cross-reactivity to different PTM modifications – this will help in detecting if oligomers in the patient brains are PTM modified and that information could be used to specifically target PTM modified oligomers to halt or slow the disease progression, similar to what has been reported with so-called oligomer-specific immunotherapy approach.

In chapter 3 of this thesis, we systematically addressed the current knowledge gaps on the role of aSyn oligomers in the initiation, seeding and pathology spreading of aSyn. Towards this goal, we used different biophysical approaches to investigate aSyn seeding *in vitro* and neurons and animal models of aSyn seeding and pathology spreading. Our results demonstrated that i) oligomeric forms of aSyn do not form in the PFF-based neuronal seeding model, where the process is dominated by fibril-mediated seeding and fibril growth; ii) different types of oligomers (UO, DO, and HO) do not have seeding activity *in vitro* and primary hippocampal neurons, and their presence slows rather than accelerates aSyn fibrillization; iii) fibrils and oligomer growth occur through monomer addition, and fibrils compete more efficiently for monomer addition. Also, depletion of monomers might favor oligomer dissociation or monomers that

could be cleared or re-enter the aggregation pathway through addition to fibrils. Finally, we demonstrate that only at higher concentrations we observe toxicity induced by oligomers, therefore, future studies are required to address oligomer toxicity wherein lower concentrations which are closer to physiological levels of aSyn and revisit the oligomer toxicity hypothesis put forth by several studies.

A major limitation of our work in chapter 3 is the use of the PFF-based neuronal seeding model to assess the presence of oligomers, it remains to be tested whether a similar phenomenon occurs in other model systems of PD, such as *de novo* cellular models of PD, lentiviral-based overexpression model systems. That being said, we hypothesized that PFF-based model system could be better in our study as this model develops LB-like inclusions that recapitulate several biochemical, and structural features of LBs observed in postmortem brains of PD patients. In this direction, future studies are required to address the presence of oligomers in different model systems of PD using a combination of tools that allow detection under non-denaturing conditions (dot blot, ELISA with oligomer-specific antibodies, gel-filtration chromatographic, clear native-PAGE) and those that allow detection under denaturing conditions (Western blotting, immunoprecipitations). The second limitation of our studies is that we used oligomers prepared from unmodified recombinant aSyn monomers to determine the seeding, spreading and toxicity studies. There could be PTM modified oligomers in the patient brains. Therefore, future studies are required to address whether PTM modified oligomers inhibit, promote or accelerate aSyn aggregation process. A third limitation of our work is the use of *in vitro* generated oligomers which might display different seeding/toxicity properties compared to oligomers derived from patient brain, future studies are required to address this limitation.

We investigated how different cell types in Amygdala might contribute to PD pathogenesis by single-cell transcriptomics in Chapter 4 of this thesis. We were able to identify several important findings that might explain why some neurons are susceptible or resistant to developing pS129 positive aggregates and how non-neuronal cell types such as astrocytes, microglia, oligodendrocytes, pericytes respond to aggregates load in the Amygdala brain region. Specifically, we demonstrated that different cell types respond differently to the aSyn aggregate burden in the amygdala brain region by differentially upregulating or downregulating genes. Inhibitory neurons that abundantly develop aggregate are shown to display several upregulated genes that are associated with neuronal activity. Conversely, non-neuronal cell types express several downregulated genes associated with regulatory activities such as ATPase activator, protein or nucleotide binding, and processes related to protein degradation. These findings indicate that neuronal signaling-related functions are upregulated in inhibitory neurons that do not develop aggregates,

suggesting that increased neuronal signaling in inhibitory neurons could be a protective action in the early disease stage. We also demonstrated that the expression level of several PD risk genes and pathways are differentially affected in different cell types. Further studies are required to validate these various gene expression changes in cellular and animal model systems by following approaches: 1) knockdown of upregulated genes using small interfering RNAs (siRNAs) and short haipin RNAs (shRNAs), or the suppression of translation of specific genes using microRNAs (miRNAs), 2) enhance gene expression of downregulated genes using lentiviral or adeno-associated virus-mediated strategies. We believe that this approach might help prevent or halt the seeding process and subsequent recruitment of endogenous aSyn for the maturation of LB-like inclusions and their clearance in different neurons.

In the future, it needs to be determined whether these changes are uniform across other brain regions and how transcriptomics changes are regulated at different stages of the disease process. A major limitation of our work is the absence of functional studies and morphological characterization of neurons that develop aggregates versus those that do not. Therefore, in the future, single-cell Patch-seq studies are required to correlate transcriptomics, electrophysiology and morphology of susceptible and resistant neurons at single-cell levels. These studies will pave the way for identifying cell-autonomous factors in different brain regions that might be driving the disease process and targeting these for therapeutic purposes or disease-modifying therapies.

REFERENCES

- 1 Maroteaux, L., Campanelli, J. T. & Scheller, R. H. Synuclein: a neuron-specific protein localized to the nucleus and presynaptic nerve terminal. *The Journal of neuroscience : the official journal of the Society for Neuroscience* **8**, 2804-2815, doi:10.1523/jneurosci.08-08-02804.1988 (1988).
- 2 Jakes, R., Spillantini, M. G. & Goedert, M. Identification of two distinct synucleins from human brain. *FEBS letters* **345**, 27-32, doi:10.1016/0014-5793(94)00395-5 (1994).
- 3 Clayton, D. F. & George, J. M. The synucleins: a family of proteins involved in synaptic function, plasticity, neurodegeneration and disease. *Trends Neurosci* **21**, 249-254, doi:10.1016/s0166-2236(97)01213-7 (1998).
- 4 Polymeropoulos, M. H. *et al.* Mutation in the alpha-synuclein gene identified in families with Parkinson's disease. *Science* **276**, 2045-2047 (1997).
- 5 Spillantini, M. G. *et al.* Alpha-synuclein in Lewy bodies. *Nature* **388**, 839-840, doi:10.1038/42166 (1997).
- 6 Crowther, R. A., Jakes, R., Spillantini, M. G. & Goedert, M. Synthetic filaments assembled from C-terminally truncated alpha-synuclein. *FEBS letters* **436**, 309-312 (1998).
- 7 Spillantini, M. G. *et al.* Filamentous alpha-synuclein inclusions link multiple system atrophy with Parkinson's disease and dementia with Lewy bodies. *Neuroscience letters* **251**, 205-208 (1998).
- 8 Conway, K. A., Harper, J. D. & Lansbury, P. T. Accelerated in vitro fibril formation by a mutant alpha-synuclein linked to early-onset Parkinson disease. *Nat Med* **4**, 1318-1320, doi:10.1038/3311 (1998).
- 9 Volles, M. J. *et al.* Vesicle permeabilization by protofibrillar alpha-synuclein: implications for the pathogenesis and treatment of Parkinson's disease. *Biochemistry* **40**, 7812-7819, doi:10.1021/bi0102398 (2001).
- 10 Alam, P., Bousset, L., Melki, R. & Otzen, D. E. α -synuclein oligomers and fibrils: a spectrum of species, a spectrum of toxicities. *Journal of Neurochemistry* **150**, 522-534, doi:https://doi.org/10.1111/jnc.14808 (2019).
- 11 Mehra, S., Sahay, S. & Maji, S. K. α -Synuclein misfolding and aggregation: Implications in Parkinson's disease pathogenesis. *Biochim Biophys Acta Proteins Proteom* **1867**, 890-908, doi:10.1016/j.bbapap.2019.03.001 (2019).
- 12 Ingelsson, M. Alpha-Synuclein Oligomers-Neurotoxic Molecules in Parkinson's Disease and Other Lewy Body Disorders. *Front Neurosci* **10**, 408, doi:10.3389/fnins.2016.00408 (2016).
- 13 Lee, H. J., Patel, S. & Lee, S. J. Intravesicular localization and exocytosis of alpha-synuclein and its aggregates. *The Journal of neuroscience : the official journal of the Society for Neuroscience* **25**, 6016-6024, doi:10.1523/JNEUROSCI.0692-05.2005 (2005).
- 14 Rodriguez, L., Marano, M. M. & Tandon, A. Import and Export of Misfolded α -Synuclein. *Frontiers in Neuroscience* **12**, doi:10.3389/fnins.2018.00344 (2018).
- 15 Volpicelli-Daley, L. A. *et al.* Exogenous alpha-synuclein fibrils induce Lewy body pathology leading to synaptic dysfunction and neuron death. *Neuron* **72**, 57-71, doi:10.1016/j.neuron.2011.08.033 (2011).
- 16 Mahul-Mellier, A.-L. *et al.* The process of Lewy body formation, rather than simply α -synuclein fibrillization, is one of the major drivers of neurodegeneration. *Proceedings of the National Academy of Sciences*, 201913904, doi:10.1073/pnas.1913904117 (2020).
- 17 Wu, Q. *et al.* α -Synuclein (α Syn) Preformed Fibrils Induce Endogenous α Syn Aggregation, Compromise Synaptic Activity and Enhance Synapse Loss in Cultured Excitatory Hippocampal Neurons. *The Journal of Neuroscience* **39**, 5080-5094, doi:10.1523/jneurosci.0060-19.2019 (2019).

- 18 Sulzer, D. & Edwards, R. H. The physiological role of α -synuclein and its relationship to Parkinson's Disease. *J Neurochem* **150**, 475-486, doi:10.1111/jnc.14810 (2019).
- 19 Burré, J., Sharma, M. & Südhof, T. C. Cell Biology and Pathophysiology of α -Synuclein. *Cold Spring Harb Perspect Med* **8**, a024091, doi:10.1101/cshperspect.a024091 (2018).
- 20 Burré, J. *et al.* Alpha-synuclein promotes SNARE-complex assembly in vivo and in vitro. *Science* **329**, 1663-1667, doi:10.1126/science.1195227 (2010).
- 21 Huang, M. *et al.* α -Synuclein: A Multifunctional Player in Exocytosis, Endocytosis, and Vesicle Recycling. *Frontiers in Neuroscience* **13**, doi:10.3389/fnins.2019.00028 (2019).
- 22 Snead, D. & Eliezer, D. Intrinsically disordered proteins in synaptic vesicle trafficking and release. *The Journal of biological chemistry* **294**, 3325-3342, doi:10.1074/jbc.REV118.006493 (2019).
- 23 Soll, L. G. *et al.* α -Synuclein-112 impairs synaptic vesicle recycling consistent with its enhanced membrane binding properties. *bioRxiv*, 2020.2004.2003.024125, doi:10.1101/2020.04.03.024125 (2020).
- 24 Somayaji, M. *et al.* A dual role for α -synuclein in facilitation and depression of dopamine release from substantia nigra neurons in vivo. *Proceedings of the National Academy of Sciences* **117**, 32701-32710, doi:10.1073/pnas.2013652117 (2020).
- 25 Kobayashi, J. *et al.* Extracellular α -synuclein enters dopaminergic cells by modulating flotillin-1-assisted dopamine transporter endocytosis. *FASEB journal : official publication of the Federation of American Societies for Experimental Biology* **33**, 10240-10256, doi:10.1096/fj.201802051R (2019).
- 26 Bendor, J. T., Logan, T. P. & Edwards, R. H. The function of α -synuclein. *Neuron* **79**, 1044-1066, doi:10.1016/j.neuron.2013.09.004 (2013).
- 27 Davies, P., Moualla, D. & Brown, D. R. Alpha-Synuclein Is a Cellular Ferrireductase. *PLOS ONE* **6**, e15814, doi:10.1371/journal.pone.0015814 (2011).
- 28 Sian-Hulsmann, J. & Riederer, P. The role of alpha-synuclein as ferrireductase in neurodegeneration associated with Parkinson's disease. *Journal of Neural Transmission* **127**, 749-754, doi:10.1007/s00702-020-02192-0 (2020).
- 29 Stolzenberg, E. *et al.* A Role for Neuronal Alpha-Synuclein in Gastrointestinal Immunity. *Journal of innate immunity* **9**, 456-463, doi:10.1159/000477990 (2017).
- 30 Harms, A. S. *et al.* MHCII is required for α -synuclein-induced activation of microglia, CD4 T cell proliferation, and dopaminergic neurodegeneration. *The Journal of neuroscience : the official journal of the Society for Neuroscience* **33**, 9592-9600, doi:10.1523/JNEUROSCI.5610-12.2013 (2013).
- 31 Sulzer, D. *et al.* T cells from patients with Parkinson's disease recognize α -synuclein peptides. *Nature* **546**, 656-661, doi:10.1038/nature22815 (2017).
- 32 Surguchev, A. A. & Surguchov, A. Synucleins and Gene Expression: Ramblers in a Crowd or Cops Regulating Traffic? *Front Mol Neurosci* **10**, 224-224, doi:10.3389/fnmol.2017.00224 (2017).
- 33 Koss, D. J. *et al.* Alpha-synuclein is present in the nucleus in human brain tissue and is pathologically modified in Dementia with Lewy Bodies. *bioRxiv*, 2021.2010.2020.465125, doi:10.1101/2021.10.20.465125 (2021).
- 34 Mori, F. *et al.* Alpha-synuclein immunoreactivity in normal and neoplastic Schwann cells. *Acta neuropathologica* **103**, 145-151, doi:10.1007/s004010100443 (2002).
- 35 Gosavi, N., Lee, H. J., Lee, J. S., Patel, S. & Lee, S. J. Golgi fragmentation occurs in the cells with prefibrillar alpha-synuclein aggregates and precedes the formation of fibrillar inclusion. *The Journal of biological chemistry* **277**, 48984-48992, doi:10.1074/jbc.M208194200 (2002).
- 36 Lee, H. J., Khoshaghideh, F., Patel, S. & Lee, S. J. Clearance of alpha-synuclein oligomeric intermediates via the lysosomal degradation pathway. *The Journal of neuroscience : the official*

- Journal of the Society for Neuroscience* **24**, 1888-1896, doi:10.1523/jneurosci.3809-03.2004 (2004).
- 37 Li, W. W. *et al.* Localization of alpha-synuclein to mitochondria within midbrain of mice. *Neuroreport* **18**, 1543-1546, doi:10.1097/WNR.0b013e3282f03db4 (2007).
- 38 Zhang, L. *et al.* Semi-quantitative analysis of alpha-synuclein in subcellular pools of rat brain neurons: an immunogold electron microscopic study using a C-terminal specific monoclonal antibody. *Brain research* **1244**, 40-52, doi:10.1016/j.brainres.2008.08.067 (2008).
- 39 Martínez, J. H. *et al.* Alpha-synuclein mitochondrial interaction leads to irreversible translocation and complex I impairment. *Archives of biochemistry and biophysics* **651**, 1-12, doi:10.1016/j.abb.2018.04.018 (2018).
- 40 Hoozemans, J. J. M. *et al.* Activation of the unfolded protein response in Parkinson's disease. *Biochemical and Biophysical Research Communications* **354**, 707-711, doi:https://doi.org/10.1016/j.bbrc.2007.01.043 (2007).
- 41 Paiva, I. *et al.* Alpha-synuclein deregulates the expression of COL4A2 and impairs ER-Golgi function. *Neurobiology of disease* **119**, 121-135, doi:10.1016/j.nbd.2018.08.001 (2018).
- 42 Weinreb, P. H., Zhen, W., Poon, A. W., Conway, K. A. & Lansbury, P. T., Jr. NACP, a protein implicated in Alzheimer's disease and learning, is natively unfolded. *Biochemistry* **35**, 13709-13715, doi:10.1021/bi961799n (1996).
- 43 Wang, C. *et al.* Versatile Structures of α -Synuclein. *Front Mol Neurosci* **9**, doi:10.3389/fnmol.2016.00048 (2016).
- 44 Bartels, T., Choi, J. G. & Selkoe, D. J. α -Synuclein occurs physiologically as a helically folded tetramer that resists aggregation. *Nature* **477**, 107-110, doi:10.1038/nature10324 (2011).
- 45 Wang, W. *et al.* A soluble α -synuclein construct forms a dynamic tetramer. *Proceedings of the National Academy of Sciences of the United States of America* **108**, 17797-17802, doi:10.1073/pnas.1113260108 (2011).
- 46 Dettmer, U., Newman, A. J., Luth, E. S., Bartels, T. & Selkoe, D. In vivo cross-linking reveals principally oligomeric forms of α -synuclein and β -synuclein in neurons and non-neural cells. *The Journal of biological chemistry* **288**, 6371-6385, doi:10.1074/jbc.M112.403311 (2013).
- 47 Selkoe, D. *et al.* Defining the native state of α -synuclein. *Neuro-degenerative diseases* **13**, 114-117, doi:10.1159/000355516 (2014).
- 48 Dettmer, U. *et al.* Parkinson-causing α -synuclein missense mutations shift native tetramers to monomers as a mechanism for disease initiation. *Nature Communications* **6**, 7314, doi:10.1038/ncomms8314 (2015).
- 49 Imberdis, T., Fanning, S., Newman, A., Ramalingam, N. & Dettmer, U. Studying α -Synuclein Conformation by Intact-Cell Cross-Linking. *Methods in molecular biology (Clifton, N.J.)* **1948**, 77-91, doi:10.1007/978-1-4939-9124-2_8 (2019).
- 50 Fernández, R. D. & Lucas, H. R. Mass spectrometry data confirming tetrameric α -synuclein N-terminal acetylation. *Data Brief* **20**, 1686-1691, doi:10.1016/j.dib.2018.09.026 (2018).
- 51 Paleologou, K. E. *et al.* Phosphorylation at Ser-129 but not the phosphomimics S129E/D inhibits the fibrillation of alpha-synuclein. *The Journal of biological chemistry* **283**, 16895-16905, doi:10.1074/jbc.M800747200 (2008).
- 52 Fauvet, B. *et al.* α -Synuclein in central nervous system and from erythrocytes, mammalian cells, and *Escherichia coli* exists predominantly as disordered monomer. *The Journal of biological chemistry* **287**, 15345-15364, doi:10.1074/jbc.M111.318949 (2012).
- 53 Binolfi, A., Theillet, F. X. & Selenko, P. Bacterial in-cell NMR of human α -synuclein: a disordered monomer by nature? *Biochemical Society transactions* **40**, 950-954, doi:10.1042/bst20120096 (2012).

- 54 Waudby, C. A. *et al.* In-Cell NMR Characterization of the Secondary Structure Populations of a Disordered Conformation of α -Synuclein within E. coli Cells. *PLOS ONE* **8**, e72286, doi:10.1371/journal.pone.0072286 (2013).
- 55 Burré, J. *et al.* Properties of native brain α -synuclein. *Nature* **498**, E4-6; discussion E6-7, doi:10.1038/nature12125 (2013).
- 56 Theillet, F.-X. *et al.* Structural disorder of monomeric α -synuclein persists in mammalian cells. *Nature* **530**, 45-50, doi:10.1038/nature16531 (2016).
- 57 Araki, K. *et al.* A small-angle X-ray scattering study of alpha-synuclein from human red blood cells. *Scientific Reports* **6**, 30473, doi:10.1038/srep30473 (2016).
- 58 Corbillé, A. G., Neunlist, M. & Derkinderen, P. Cross-linking for the analysis of α -synuclein in the enteric nervous system. *J Neurochem* **139**, 839-847, doi:10.1111/jnc.13845 (2016).
- 59 Luth, E. S., Bartels, T., Dettmer, U., Kim, N. C. & Selkoe, D. J. Purification of α -synuclein from human brain reveals an instability of endogenous multimers as the protein approaches purity. *Biochemistry* **54**, 279-292, doi:10.1021/bi501188a (2015).
- 60 George, J. M., Jin, H., Woods, W. S. & Clayton, D. F. Characterization of a novel protein regulated during the critical period for song learning in the zebra finch. *Neuron* **15**, 361-372, doi:10.1016/0896-6273(95)90040-3 (1995).
- 61 Davidson, W. S., Jonas, A., Clayton, D. F. & George, J. M. Stabilization of alpha-synuclein secondary structure upon binding to synthetic membranes. *The Journal of biological chemistry* **273**, 9443-9449, doi:10.1074/jbc.273.16.9443 (1998).
- 62 Perrin, R. J., Woods, W. S., Clayton, D. F. & George, J. M. Interaction of human alpha-Synuclein and Parkinson's disease variants with phospholipids. Structural analysis using site-directed mutagenesis. *The Journal of biological chemistry* **275**, 34393-34398, doi:10.1074/jbc.M004851200 (2000).
- 63 Eliezer, D., Kutluay, E., Bussell, R., Jr. & Browne, G. Conformational properties of alpha-synuclein in its free and lipid-associated states. *Journal of molecular biology* **307**, 1061-1073, doi:10.1006/jmbi.2001.4538 (2001).
- 64 Chandra, S., Chen, X., Rizo, J., Jahn, R. & Südhof, T. C. A broken alpha -helix in folded alpha -Synuclein. *The Journal of biological chemistry* **278**, 15313-15318, doi:10.1074/jbc.M213128200 (2003).
- 65 Bussell, R., Jr. & Eliezer, D. A structural and functional role for 11-mer repeats in alpha-synuclein and other exchangeable lipid binding proteins. *Journal of molecular biology* **329**, 763-778, doi:10.1016/s0022-2836(03)00520-5 (2003).
- 66 Bisaglia, M. *et al.* A topological model of the interaction between alpha-synuclein and sodium dodecyl sulfate micelles. *Biochemistry* **44**, 329-339, doi:10.1021/bi048448q (2005).
- 67 Ulmer, T. S., Bax, A., Cole, N. B. & Nussbaum, R. L. Structure and dynamics of micelle-bound human alpha-synuclein. *The Journal of biological chemistry* **280**, 9595-9603, doi:10.1074/jbc.M411805200 (2005).
- 68 Jao, C. C., Hegde, B. G., Chen, J., Haworth, I. S. & Langen, R. Structure of membrane-bound α -synuclein from site-directed spin labeling and computational refinement. *Proceedings of the National Academy of Sciences* **105**, 19666-19671, doi:10.1073/pnas.0807826105 (2008).
- 69 Georgieva, E. R., Ramlall, T. F., Borbat, P. P., Freed, J. H. & Eliezer, D. Membrane-bound alpha-synuclein forms an extended helix: long-distance pulsed ESR measurements using vesicles, bicelles, and rodlike micelles. *Journal of the American Chemical Society* **130**, 12856-12857, doi:10.1021/ja804517m (2008).
- 70 Doherty, C. P. A. *et al.* A short motif in the N-terminal region of α -synuclein is critical for both aggregation and function. *Nature structural & molecular biology* **27**, 249-259, doi:10.1038/s41594-020-0384-x (2020).

- 71 Stephens, A. D. *et al.* Extent of N-terminus exposure of monomeric alpha-synuclein determines its aggregation propensity. *Nature Communications* **11**, 2820, doi:10.1038/s41467-020-16564-3 (2020).
- 72 Das, T. & Eliezer, D. Membrane interactions of intrinsically disordered proteins: The example of alpha-synuclein. *Biochimica et Biophysica Acta (BBA) - Proteins and Proteomics* **1867**, 879-889, doi:https://doi.org/10.1016/j.bbapap.2019.05.001 (2019).
- 73 Uéda, K. *et al.* Molecular cloning of cDNA encoding an unrecognized component of amyloid in Alzheimer disease. *Proceedings of the National Academy of Sciences of the United States of America* **90**, 11282-11286, doi:10.1073/pnas.90.23.11282 (1993).
- 74 Han, H., Weinreb, P. H. & Lansbury, P. T., Jr. The core Alzheimer's peptide NAC forms amyloid fibrils which seed and are seeded by beta-amyloid: is NAC a common trigger or target in neurodegenerative disease? *Chemistry & biology* **2**, 163-169, doi:10.1016/1074-5521(95)90071-3 (1995).
- 75 Fusco, G. *et al.* Structural basis of synaptic vesicle assembly promoted by α -synuclein. *Nat Commun* **7**, 12563, doi:10.1038/ncomms12563 (2016).
- 76 Bertini, I. *et al.* Paramagnetism-based NMR restraints provide maximum allowed probabilities for the different conformations of partially independent protein domains. *Journal of the American Chemical Society* **129**, 12786-12794, doi:10.1021/ja0726613 (2007).
- 77 Wu, K. P., Kim, S., Fela, D. A. & Baum, J. Characterization of conformational and dynamic properties of natively unfolded human and mouse alpha-synuclein ensembles by NMR: implication for aggregation. *Journal of molecular biology* **378**, 1104-1115, doi:10.1016/j.jmb.2008.03.017 (2008).
- 78 Lorenzen, N. *et al.* The role of stable α -synuclein oligomers in the molecular events underlying amyloid formation. *Journal of the American Chemical Society* **136**, 3859-3868, doi:10.1021/ja411577t (2014).
- 79 Li, B. *et al.* Cryo-EM of full-length α -synuclein reveals fibril polymorphs with a common structural kernel. *Nat Commun* **9**, 3609, doi:10.1038/s41467-018-05971-2 (2018).
- 80 Guerrero-Ferreira, R. *et al.* Cryo-EM structure of alpha-synuclein fibrils. *eLife* **7**, doi:10.7554/eLife.36402 (2018).
- 81 Yan, X., Uronen, R.-L. & Huttunen, H. J. The interaction of α -synuclein and Tau: A molecular conspiracy in neurodegeneration? *Seminars in Cell & Developmental Biology* **99**, 55-64, doi:https://doi.org/10.1016/j.semcdb.2018.05.005 (2020).
- 82 Goers, J. *et al.* Nuclear localization of alpha-synuclein and its interaction with histones. *Biochemistry* **42**, 8465-8471, doi:10.1021/bi0341152 (2003).
- 83 Cherny, D., Hoyer, W., Subramaniam, V. & Jovin, T. M. Double-stranded DNA stimulates the fibrillation of alpha-synuclein in vitro and is associated with the mature fibrils: an electron microscopy study. *Journal of molecular biology* **344**, 929-938, doi:10.1016/j.jmb.2004.09.096 (2004).
- 84 Kontopoulos, E., Parvin, J. D. & Feany, M. B. α -synuclein acts in the nucleus to inhibit histone acetylation and promote neurotoxicity. *Human Molecular Genetics* **15**, 3012-3023, doi:10.1093/hmg/ddl243 (2006).
- 85 Sugeno, N. *et al.* α -Synuclein enhances histone H3 lysine-9 dimethylation and H3K9me2-dependent transcriptional responses. *Scientific reports* **6**, 36328-36328, doi:10.1038/srep36328 (2016).
- 86 Jiang, P., Gan, M., Yen, S. H., McLean, P. J. & Dickson, D. W. Histones facilitate α -synuclein aggregation during neuronal apoptosis. *Acta neuropathologica* **133**, 547-558, doi:10.1007/s00401-016-1660-z (2017).

- 87 Plotegher, N. *et al.* The chaperone-like protein 14-3-3 η interacts with human α -synuclein aggregation intermediates rerouting the amyloidogenic pathway and reducing α -synuclein cellular toxicity. *Human Molecular Genetics* **23**, 5615-5629, doi:10.1093/hmg/ddu275 (2014).
- 88 Burmann, B. M. *et al.* Regulation of α -synuclein by chaperones in mammalian cells. *Nature* **577**, 127-132, doi:10.1038/s41586-019-1808-9 (2020).
- 89 Mahul-Mellier, A.-L. *et al.* The making of a Lewy body: the role of α -synuclein post-fibrillization modifications in regulating the formation and the maturation of pathological inclusions. *bioRxiv*, 500058, doi:10.1101/500058 (2018).
- 90 Jensen, P. H. *et al.* alpha-synuclein binds to Tau and stimulates the protein kinase A-catalyzed tau phosphorylation of serine residues 262 and 356. *The Journal of biological chemistry* **274**, 25481-25489, doi:10.1074/jbc.274.36.25481 (1999).
- 91 Giasson, B. I. *et al.* Initiation and synergistic fibrillization of tau and alpha-synuclein. *Science* **300**, 636-640, doi:10.1126/science.1082324 (2003).
- 92 Dasari, A. K. R., Kaye, R., Wi, S. & Lim, K. H. Tau Interacts with the C-Terminal Region of α -Synuclein, Promoting Formation of Toxic Aggregates with Distinct Molecular Conformations. *Biochemistry* **58**, 2814-2821, doi:10.1021/acs.biochem.9b00215 (2019).
- 93 Feng, S. T. *et al.* Update on the association between alpha-synuclein and tau with mitochondrial dysfunction: Implications for Parkinson's disease. *The European journal of neuroscience*, doi:10.1111/ejn.14699 (2020).
- 94 Jo, E., McLaurin, J., Yip, C. M., St George-Hyslop, P. & Fraser, P. E. alpha-Synuclein membrane interactions and lipid specificity. *The Journal of biological chemistry* **275**, 34328-34334, doi:10.1074/jbc.M004345200 (2000).
- 95 Cole, N. B. *et al.* Lipid droplet binding and oligomerization properties of the Parkinson's disease protein alpha-synuclein. *The Journal of biological chemistry* **277**, 6344-6352, doi:10.1074/jbc.M108414200 (2002).
- 96 Masaracchia, C. *et al.* Membrane binding, internalization, and sorting of alpha-synuclein in the cell. *Acta neuropathologica communications* **6**, 79, doi:10.1186/s40478-018-0578-1 (2018).
- 97 Chung, P. J. *et al.* The C-Terminal Domain of α -Synuclein Confers Steric Stabilization on Synaptic Vesicle-Like Surfaces. *Advanced Materials Interfaces* **7**, 1902151, doi:10.1002/admi.201902151 (2020).
- 98 Park, S. M. *et al.* Stress-induced aggregation profiles of GST-alpha-synuclein fusion proteins: role of the C-terminal acidic tail of alpha-synuclein in protein thermosolubility and stability. *Biochemistry* **41**, 4137-4146, doi:10.1021/bi015961k (2002).
- 99 Lautenschläger, J. *et al.* C-terminal calcium binding of α -synuclein modulates synaptic vesicle interaction. *Nature Communications* **9**, 712, doi:10.1038/s41467-018-03111-4 (2018).
- 100 Fernández, C. O. *et al.* NMR of alpha-synuclein-polyamine complexes elucidates the mechanism and kinetics of induced aggregation. *EMBO J* **23**, 2039-2046, doi:10.1038/sj.emboj.7600211 (2004).
- 101 Lewandowski, N. M. *et al.* Polyamine pathway contributes to the pathogenesis of Parkinson disease. *Proceedings of the National Academy of Sciences of the United States of America* **107**, 16970-16975, doi:10.1073/pnas.1011751107 (2010).
- 102 Herrera, F. E. *et al.* Inhibition of α -Synuclein Fibrillization by Dopamine Is Mediated by Interactions with Five C-Terminal Residues and with E83 in the NAC Region. *PLOS ONE* **3**, e3394, doi:10.1371/journal.pone.0003394 (2008).
- 103 Tavassoly, O., Nokhrin, S., Dmitriev, O. Y. & Lee, J. S. Cu(II) and dopamine bind to α -synuclein and cause large conformational changes. *The FEBS journal* **281**, 2738-2753, doi:10.1111/febs.12817 (2014).

- 104 Nielsen, M. S., Vorum, H., Lindersson, E. & Jensen, P. H. Ca²⁺ binding to alpha-synuclein regulates ligand binding and oligomerization. *The Journal of biological chemistry* **276**, 22680-22684, doi:10.1074/jbc.M101181200 (2001).
- 105 Rcom-H'cheo-Gauthier, A., Goodwin, J. & Pountney, D. L. Interactions between calcium and alpha-synuclein in neurodegeneration. *Biomolecules* **4**, 795-811, doi:10.3390/biom4030795 (2014).
- 106 Paik, S. R., Shin, H. J., Lee, J. H., Chang, C. S. & Kim, J. Copper(II)-induced self-oligomerization of alpha-synuclein. *The Biochemical journal* **340 (Pt 3)**, 821-828 (1999).
- 107 Rasia, R. M. *et al.* Structural characterization of copper(II) binding to alpha-synuclein: Insights into the bioinorganic chemistry of Parkinson's disease. *Proceedings of the National Academy of Sciences of the United States of America* **102**, 4294-4299, doi:10.1073/pnas.0407881102 (2005).
- 108 Binolfi, A. *et al.* Interaction of alpha-synuclein with divalent metal ions reveals key differences: a link between structure, binding specificity and fibrillation enhancement. *Journal of the American Chemical Society* **128**, 9893-9901, doi:10.1021/ja0618649 (2006).
- 109 Wang, C., Liu, L., Zhang, L., Peng, Y. & Zhou, F. Redox reactions of the α -synuclein-Cu(2+) complex and their effects on neuronal cell viability. *Biochemistry* **49**, 8134-8142, doi:10.1021/bi1010909 (2010).
- 110 Ahmad, A., Burns, C. S., Fink, A. L. & Uversky, V. N. Peculiarities of copper binding to alpha-synuclein. *Journal of biomolecular structure & dynamics* **29**, 825-842, doi:10.1080/073911012010525023 (2012).
- 111 Ranjan, P. *et al.* Differential copper binding to alpha-synuclein and its disease-associated mutants affect the aggregation and amyloid formation. *Biochimica et biophysica acta. General subjects* **1861**, 365-374, doi:10.1016/j.bbagen.2016.11.043 (2017).
- 112 Valiente-Gabioud, A. A. *et al.* Structural basis behind the interaction of Zn²⁺ with the protein α -synuclein and the A β peptide: a comparative analysis. *Journal of inorganic biochemistry* **117**, 334-341, doi:10.1016/j.jinorgbio.2012.06.011 (2012).
- 113 Bharathi & Rao, K. S. J. Thermodynamics imprinting reveals differential binding of metals to α -synuclein: Relevance to parkinson's disease. *Biochemical and Biophysical Research Communications* **359**, 115-120, doi:https://doi.org/10.1016/j.bbrc.2007.05.060 (2007).
- 114 Peng, Y., Wang, C., Xu, H. H., Liu, Y. N. & Zhou, F. Binding of alpha-synuclein with Fe(III) and with Fe(II) and biological implications of the resultant complexes. *Journal of inorganic biochemistry* **104**, 365-370, doi:10.1016/j.jinorgbio.2009.11.005 (2010).
- 115 Chen, B. *et al.* Interactions between iron and α -synuclein pathology in Parkinson's disease. *Free radical biology & medicine* **141**, 253-260, doi:10.1016/j.freeradbiomed.2019.06.024 (2019).
- 116 Dedmon, M. M., Lindorff-Larsen, K., Christodoulou, J., Vendruscolo, M. & Dobson, C. M. Mapping long-range interactions in alpha-synuclein using spin-label NMR and ensemble molecular dynamics simulations. *Journal of the American Chemical Society* **127**, 476-477, doi:10.1021/ja044834j (2005).
- 117 Sung, Y.-H. & Eliezer, D. Residual structure, backbone dynamics, and interactions within the synuclein family. *Journal of molecular biology* **372**, 689-707, doi:10.1016/j.jmb.2007.07.008 (2007).
- 118 McClendon, S., Rospigliosi, C. C. & Eliezer, D. Charge neutralization and collapse of the C-terminal tail of alpha-synuclein at low pH. *Protein Science* **18**, 1531-1540, doi:10.1002/pro.149 (2009).
- 119 Wu, K. P. & Baum, J. Detection of transient interchain interactions in the intrinsically disordered protein alpha-synuclein by NMR paramagnetic relaxation enhancement. *Journal of the American Chemical Society* **132**, 5546-5547, doi:10.1021/ja9105495 (2010).
- 120 Esteban-Martín, S., Silvestre-Ryan, J., Bertoncini, C. W. & Salvatella, X. Identification of fibril-like tertiary contacts in soluble monomeric α -synuclein. *Biophysical journal* **105**, 1192-1198, doi:10.1016/j.bpj.2013.07.044 (2013).

- 121 Bertoncini, C. W. *et al.* Release of long-range tertiary interactions potentiates aggregation of natively unstructured α -synuclein. *Proceedings of the National Academy of Sciences of the United States of America* **102**, 1430-1435, doi:10.1073/pnas.0407146102 (2005).
- 122 Zhou, W. *et al.* Methionine oxidation stabilizes non-toxic oligomers of α -synuclein through strengthening the auto-inhibitory intra-molecular long-range interactions. *Biochimica et Biophysica Acta (BBA) - Molecular Basis of Disease* **1802**, 322-330, doi:https://doi.org/10.1016/j.bbadis.2009.12.004 (2010).
- 123 Ranjan, P. & Kumar, A. Perturbation in Long-Range Contacts Modulates the Kinetics of Amyloid Formation in α -Synuclein Familial Mutants. *ACS Chemical Neuroscience* **8**, 2235-2246, doi:10.1021/acscchemneuro.7b00149 (2017).
- 124 Sorrentino, Z. A. & Giasson, B. I. The emerging role of α -synuclein truncation in aggregation and disease. *The Journal of biological chemistry*, doi:10.1074/jbc.REV120.011743 (2020).
- 125 McGlinchey, R. P., Ni, X., Shadish, J. A., Jiang, J. & Lee, J. C. The N terminus of α -synuclein dictates fibril formation. *Proceedings of the National Academy of Sciences* **118**, e2023487118, doi:doi:10.1073/pnas.2023487118 (2021).
- 126 Kang, L. *et al.* N-terminal acetylation of α -synuclein induces increased transient helical propensity and decreased aggregation rates in the intrinsically disordered monomer. *Protein science : a publication of the Protein Society* **21**, 911-917, doi:10.1002/pro.2088 (2012).
- 127 Dikiy, I. & Eliezer, D. N-terminal acetylation stabilizes N-terminal helicity in lipid- and micelle-bound α -synuclein and increases its affinity for physiological membranes. *The Journal of biological chemistry* **289**, 3652-3665, doi:10.1074/jbc.M113.512459 (2014).
- 128 Runfola, M., De Simone, A., Vendruscolo, M., Dobson, C. M. & Fusco, G. The N-terminal Acetylation of α -Synuclein Changes the Affinity for Lipid Membranes but not the Structural Properties of the Bound State. *Scientific Reports* **10**, 204, doi:10.1038/s41598-019-57023-4 (2020).
- 129 Maltsev, A. S., Ying, J. & Bax, A. Impact of N-terminal acetylation of α -synuclein on its random coil and lipid binding properties. *Biochemistry* **51**, 5004-5013, doi:10.1021/bi300642h (2012).
- 130 Burai, R., Ait-Bouziad, N., Chiki, A. & Lashuel, H. A. Elucidating the Role of Site-Specific Nitration of α -Synuclein in the Pathogenesis of Parkinson's Disease via Protein Semisynthesis and Mutagenesis. *Journal of the American Chemical Society* **137**, 5041-5052, doi:10.1021/ja5131726 (2015).
- 131 Dikiy, I. *et al.* Semisynthetic and in Vitro Phosphorylation of Alpha-Synuclein at Y39 Promotes Functional Partly Helical Membrane-Bound States Resembling Those Induced by PD Mutations. *ACS chemical biology* **11**, 2428-2437, doi:10.1021/acscchembio.6b00539 (2016).
- 132 Dikiy, I. *et al.* Semisynthetic and in Vitro Phosphorylation of Alpha-Synuclein at Y39 Promotes Functional Partly Helical Membrane-Bound States Resembling Those Induced by PD Mutations. *ACS chemical biology* **11**, 2428-2437, doi:10.1021/acscchembio.6b00539 (2016).
- 133 Mahul-Mellier, A. L. *et al.* c-Abl phosphorylates α -synuclein and regulates its degradation: implication for α -synuclein clearance and contribution to the pathogenesis of Parkinson's disease. *Hum Mol Genet* **23**, 2858-2879, doi:10.1093/hmg/ddt674 (2014).
- 134 Na, C. H. *et al.* Development of a novel method for the quantification of tyrosine 39 phosphorylated α - and β -synuclein in human cerebrospinal fluid. *Clinical Proteomics* **17**, 13, doi:10.1186/s12014-020-09277-8 (2020).
- 135 Paleologou, K. E. *et al.* Phosphorylation at S87 is enhanced in synucleinopathies, inhibits alpha-synuclein oligomerization, and influences synuclein-membrane interactions. *The Journal of neuroscience : the official journal of the Society for Neuroscience* **30**, 3184-3198, doi:10.1523/JNEUROSCI.5922-09.2010 (2010).

- 136 Creekmore, B. C., Chang, Y. W. & Lee, E. B. The Cryo-EM Effect: Structural Biology of Neurodegenerative Disease Aggregates. *J Neuropathol Exp Neurol* **80**, 514-529, doi:10.1093/jnen/nlab039 (2021).
- 137 Kumar, P., Schilderink, N., Subramaniam, V. & Huber, M. Membrane Binding of Parkinson's Protein α -Synuclein: Effect of Phosphorylation at Positions 87 and 129 by the S to D Mutation Approach. *Israel journal of chemistry* **57**, 762-770, doi:10.1002/ijch.201600083 (2017).
- 138 Pronin, A. N., Morris, A. J., Surguchov, A. & Benovic, J. L. Synucleins are a novel class of substrates for G protein-coupled receptor kinases. *The Journal of biological chemistry* **275**, 26515-26522, doi:10.1074/jbc.M003542200 (2000).
- 139 Nübling, G. S. *et al.* Modelling Ser129 phosphorylation inhibits membrane binding of pore-forming alpha-synuclein oligomers. *PLoS One* **9**, e98906, doi:10.1371/journal.pone.0098906 (2014).
- 140 Fiske, M. *et al.* Familial Parkinson's Disease Mutant E46K α -Synuclein Localizes to Membranous Structures, Forms Aggregates, and Induces Toxicity in Yeast Models. *ISRN Neurol* **2011**, 521847-521847, doi:10.5402/2011/521847 (2011).
- 141 Kuwahara, T. *et al.* Familial Parkinson mutant alpha-synuclein causes dopamine neuron dysfunction in transgenic *Caenorhabditis elegans*. *The Journal of biological chemistry* **281**, 334-340, doi:10.1074/jbc.M504860200 (2006).
- 142 Lou, X., Kim, J., Hawk, B. J. & Shin, Y. K. α -Synuclein may cross-bridge v-SNARE and acidic phospholipids to facilitate SNARE-dependent vesicle docking. *The Biochemical journal* **474**, 2039-2049, doi:10.1042/bcj20170200 (2017).
- 143 Hawk, B. J. D., Khounlo, R. & Shin, Y.-K. Alpha-Synuclein Continues to Enhance SNARE-Dependent Vesicle Docking at Exorbitant Concentrations. *Frontiers in Neuroscience* **13**, doi:10.3389/fnins.2019.00216 (2019).
- 144 Burré, J., Sharma, M. & Südhof, T. C. α -Synuclein assembles into higher-order multimers upon membrane binding to promote SNARE complex formation. *Proceedings of the National Academy of Sciences* **111**, E4274-E4283, doi:10.1073/pnas.1416598111 (2014).
- 145 Li, W. *et al.* Aggregation promoting C-terminal truncation of alpha-synuclein is a normal cellular process and is enhanced by the familial Parkinson's disease-linked mutations. *Proceedings of the National Academy of Sciences of the United States of America* **102**, 2162-2167, doi:10.1073/pnas.0406976102 (2005).
- 146 Ohrfelt, A. *et al.* Identification of novel α -synuclein isoforms in human brain tissue by using an online nanoLC-ESI-FTICR-MS method. *Neurochemical research* **36**, 2029-2042, doi:10.1007/s11064-011-0527-x (2011).
- 147 Kellie, J. F. *et al.* Quantitative Measurement of Intact Alpha-Synuclein Proteoforms from Post-Mortem Control and Parkinson's Disease Brain Tissue by Intact Protein Mass Spectrometry. *Scientific Reports* **4**, 5797, doi:10.1038/srep05797 (2014).
- 148 Bhattacharjee, P. *et al.* Mass Spectrometric Analysis of Lewy Body-Enriched α -Synuclein in Parkinson's Disease. *Journal of proteome research* **18**, 2109-2120, doi:10.1021/acs.jproteome.8b00982 (2019).
- 149 Baba, M. *et al.* Aggregation of alpha-synuclein in Lewy bodies of sporadic Parkinson's disease and dementia with Lewy bodies. *The American Journal of Pathology* **152**, 879-884 (1998).
- 150 Sorrentino, Z. A. *et al.* Physiological C-terminal truncation of α -synuclein potentiates the prion-like formation of pathological inclusions. *The Journal of biological chemistry* **293**, 18914-18932, doi:10.1074/jbc.RA118.005603 (2018).
- 151 Yin, G. *et al.* α -Synuclein interacts with the switch region of Rab8a in a Ser129 phosphorylation-dependent manner. *Neurobiology of disease* **70**, 149-161, doi:10.1016/j.nbd.2014.06.018 (2014).

- 152 Schaser, A. J. *et al.* Alpha-synuclein is a DNA binding protein that modulates DNA repair with implications for Lewy body disorders. *Scientific Reports* **9**, 10919, doi:10.1038/s41598-019-47227-z (2019).
- 153 McLean, P. J., Ribich, S. & Hyman, B. T. Subcellular localization of alpha-synuclein in primary neuronal cultures: effect of missense mutations. *Journal of neural transmission. Supplementum*, 53-63, doi:10.1007/978-3-7091-6284-2_5 (2000).
- 154 Seo, J. H. *et al.* Alpha-synuclein regulates neuronal survival via Bcl-2 family expression and PI3/Akt kinase pathway. *FASEB journal : official publication of the Federation of American Societies for Experimental Biology* **16**, 1826-1828, doi:10.1096/fj.02-0041fje (2002).
- 155 Mbefo, M. K. *et al.* Phosphorylation of synucleins by members of the Polo-like kinase family. *The Journal of biological chemistry* **285**, 2807-2822, doi:10.1074/jbc.M109.081950 (2010).
- 156 Lee, B. R., Matsuo, Y., Cashikar, A. G. & Kamitani, T. Role of Ser129 phosphorylation of α -synuclein in melanoma cells. *Journal of Cell Science* **126**, 696-704, doi:10.1242/jcs.122093 (2013).
- 157 Masliah, E. *et al.* Dopaminergic loss and inclusion body formation in alpha-synuclein mice: implications for neurodegenerative disorders. *Science* **287**, 1265-1269 (2000).
- 158 Wakamatsu, M. *et al.* Accumulation of phosphorylated alpha-synuclein in dopaminergic neurons of transgenic mice that express human alpha-synuclein. *Journal of neuroscience research* **85**, 1819-1825, doi:10.1002/jnr.21310 (2007).
- 159 Schell, H., Hasegawa, T., Neumann, M. & Kahle, P. J. Nuclear and neuritic distribution of serine-129 phosphorylated alpha-synuclein in transgenic mice. *Neuroscience* **160**, 796-804, doi:10.1016/j.neuroscience.2009.03.002 (2009).
- 160 Amschl, D. *et al.* Time course and progression of wild type α -synuclein accumulation in a transgenic mouse model. *BMC Neurosci* **14**, 6-6, doi:10.1186/1471-2202-14-6 (2013).
- 161 Gonçalves, S. & Outeiro, T. F. Assessing the subcellular dynamics of alpha-synuclein using photoactivation microscopy. *Molecular neurobiology* **47**, 1081-1092, doi:10.1007/s12035-013-8406-x (2013).
- 162 Fares, M. B. *et al.* The novel Parkinson's disease linked mutation G51D attenuates in vitro aggregation and membrane binding of α -synuclein, and enhances its secretion and nuclear localization in cells. *Hum Mol Genet* **23**, 4491-4509, doi:10.1093/hmg/ddu165 (2014).
- 163 Mbefo, M. K. *et al.* Parkinson disease mutant E46K enhances α -synuclein phosphorylation in mammalian cell lines, in yeast, and in vivo. *The Journal of biological chemistry* **290**, 9412-9427, doi:10.1074/jbc.M114.610774 (2015).
- 164 Lashuel, H. A. *et al.* Neighbouring modifications interfere with the detection of phosphorylated alpha-synuclein at Serine 129: Revisiting the specificity of pS129 antibodies. *bioRxiv*, 2022.2003.2030.486322, doi:10.1101/2022.03.30.486322 (2022).
- 165 Pinho, R. *et al.* Nuclear localization and phosphorylation modulate pathological effects of alpha-synuclein. *Hum Mol Genet* **28**, 31-50, doi:10.1093/hmg/ddy326 (2019).
- 166 Devi, L., Raghavendran, V., Prabhu, B. M., Avadhani, N. G. & Anandatheerthavarada, H. K. Mitochondrial import and accumulation of alpha-synuclein impair complex I in human dopaminergic neuronal cultures and Parkinson disease brain. *The Journal of biological chemistry* **283**, 9089-9100, doi:10.1074/jbc.M710012200 (2008).
- 167 Ma, K. L. *et al.* The nuclear accumulation of alpha-synuclein is mediated by importin alpha and promotes neurotoxicity by accelerating the cell cycle. *Neuropharmacology* **82**, 132-142, doi:10.1016/j.neuropharm.2013.07.035 (2014).
- 168 Bernal-Conde, L. D. *et al.* Alpha-Synuclein Physiology and Pathology: A Perspective on Cellular Structures and Organelles. *Front Neurosci* **13**, 1399, doi:10.3389/fnins.2019.01399 (2019).

- 169 Webb, J. L., Ravikumar, B., Atkins, J., Skepper, J. N. & Rubinsztein, D. C. Alpha-Synuclein is degraded by both autophagy and the proteasome. *The Journal of biological chemistry* **278**, 25009-25013, doi:10.1074/jbc.M300227200 (2003).
- 170 Chau, K. Y., Ching, H. L., Schapira, A. H. & Cooper, J. M. Relationship between alpha synuclein phosphorylation, proteasomal inhibition and cell death: relevance to Parkinson's disease pathogenesis. *J Neurochem* **110**, 1005-1013, doi:10.1111/j.1471-4159.2009.06191.x (2009).
- 171 Machiya, Y. *et al.* Phosphorylated alpha-synuclein at Ser-129 is targeted to the proteasome pathway in a ubiquitin-independent manner. *The Journal of biological chemistry* **285**, 40732-40744, doi:10.1074/jbc.M110.141952 (2010).
- 172 Inglis, K. J. *et al.* Polo-like kinase 2 (PLK2) phosphorylates alpha-synuclein at serine 129 in central nervous system. *The Journal of biological chemistry* **284**, 2598-2602, doi:10.1074/jbc.C800206200 (2009).
- 173 Oueslati, A., Schneider, B. L., Aebischer, P. & Lashuel, H. A. Polo-like kinase 2 regulates selective autophagic α -synuclein clearance and suppresses its toxicity in vivo. *Proceedings of the National Academy of Sciences of the United States of America* **110**, E3945-3954, doi:10.1073/pnas.1309991110 (2013).
- 174 Lee, G. *et al.* Casein kinase II-mediated phosphorylation regulates alpha-synuclein/synphilin-1 interaction and inclusion body formation. *The Journal of biological chemistry* **279**, 6834-6839, doi:10.1074/jbc.M312760200 (2004).
- 175 Waxman, E. A. & Giasson, B. I. Specificity and regulation of casein kinase-mediated phosphorylation of alpha-synuclein. *J Neuropathol Exp Neurol* **67**, 402-416, doi:10.1097/NEN.0b013e31816fc995 (2008).
- 176 Sancenon, V. *et al.* Suppression of α -synuclein toxicity and vesicle trafficking defects by phosphorylation at S129 in yeast depends on genetic context. *Hum Mol Genet* **21**, 2432-2449, doi:10.1093/hmg/dd5058 (2012).
- 177 Hara, S. *et al.* Serine 129 phosphorylation of membrane-associated α -synuclein modulates dopamine transporter function in a G protein-coupled receptor kinase-dependent manner. *Molecular biology of the cell* **24**, 1649-1660, S1641-1643, doi:10.1091/mbc.E12-12-0903 (2013).
- 178 Arawaka, S. *et al.* The role of G-protein-coupled receptor kinase 5 in pathogenesis of sporadic Parkinson's disease. *The Journal of neuroscience : the official journal of the Society for Neuroscience* **26**, 9227-9238, doi:10.1523/jneurosci.0341-06.2006 (2006).
- 179 Qing, H., Wong, W., McGeer, E. G. & McGeer, P. L. Lrrk2 phosphorylates alpha synuclein at serine 129: Parkinson disease implications. *Biochem Biophys Res Commun* **387**, 149-152, doi:10.1016/j.bbrc.2009.06.142 (2009).
- 180 Tenreiro, S. *et al.* Phosphorylation modulates clearance of alpha-synuclein inclusions in a yeast model of Parkinson's disease. *PLoS genetics* **10**, e1004302, doi:10.1371/journal.pgen.1004302 (2014).
- 181 Kofoed, R. H. *et al.* Polo-like kinase 2 modulates α -synuclein protein levels by regulating its mRNA production. *Neurobiology of disease* **106**, 49-62, doi:https://doi.org/10.1016/j.nbd.2017.06.014 (2017).
- 182 Obergasteiger, J. *et al.* Kinase inhibition of G2019S-LRRK2 enhances autolysosome formation and function to reduce endogenous alpha-synuclein intracellular inclusions. *Cell Death Discovery* **6**, 45, doi:10.1038/s41420-020-0279-y (2020).
- 183 Karim, M. R. *et al.* α -Synucleinopathy associated c-Abl activation causes p53-dependent autophagy impairment. *Mol Neurodegener* **15**, 27, doi:10.1186/s13024-020-00364-w (2020).
- 184 Bennett, M. C. *et al.* Degradation of alpha-synuclein by proteasome. *The Journal of biological chemistry* **274**, 33855-33858, doi:10.1074/jbc.274.48.33855 (1999).

- 185 Rideout, H. J., Larsen, K. E., Sulzer, D. & Stefanis, L. Proteasomal inhibition leads to formation of ubiquitin/alpha-synuclein-immunoreactive inclusions in PC12 cells. *J Neurochem* **78**, 899-908 (2001).
- 186 Tofaris, G. K. *et al.* Ubiquitin ligase Nedd4 promotes α -synuclein degradation by the endosomal-lysosomal pathway. *Proceedings of the National Academy of Sciences* **108**, 17004-17009, doi:10.1073/pnas.1109356108 (2011).
- 187 Mund, T., Masuda-Suzukake, M., Goedert, M. & Pelham, H. R. Ubiquitination of alpha-synuclein filaments by Nedd4 ligases. *PLOS ONE* **13**, e0200763, doi:10.1371/journal.pone.0200763 (2018).
- 188 Nonaka, T., Iwatsubo, T. & Hasegawa, M. Ubiquitination of alpha-synuclein. *Biochemistry* **44**, 361-368, doi:10.1021/bi0485528 (2005).
- 189 Gerez, J. A. *et al.* A cullin-RING ubiquitin ligase targets exogenous alpha-synuclein and inhibits Lewy body-like pathology. *Science translational medicine* **11**, doi:10.1126/scitranslmed.aau6722 (2019).
- 190 Hejjaoui, M., Haj-Yahya, M., Kumar, K. S., Brik, A. & Lashuel, H. A. Towards elucidation of the role of ubiquitination in the pathogenesis of Parkinson's disease with semisynthetic ubiquitinated α -synuclein. *Angewandte Chemie (International ed. in English)* **50**, 405-409, doi:10.1002/anie.201005546 (2011).
- 191 Meier, F. *et al.* Semisynthetic, site-specific ubiquitin modification of α -synuclein reveals differential effects on aggregation. *Journal of the American Chemical Society* **134**, 5468-5471, doi:10.1021/ja300094r (2012).
- 192 Haj-Yahya, M. *et al.* Synthetic polyubiquitinated α -Synuclein reveals important insights into the roles of the ubiquitin chain in regulating its pathophysiology. *Proceedings of the National Academy of Sciences of the United States of America* **110**, 17726-17731, doi:10.1073/pnas.1315654110 (2013).
- 193 Jin, J. *et al.* Identification of novel proteins associated with both alpha-synuclein and DJ-1. *Molecular & cellular proteomics : MCP* **6**, 845-859, doi:10.1074/mcp.M600182-MCP200 (2007).
- 194 Betzer, C. *et al.* Identification of synaptosomal proteins binding to monomeric and oligomeric α -synuclein. *PLoS One* **10**, e0116473, doi:10.1371/journal.pone.0116473 (2015).
- 195 Chung, C. Y. *et al.* In Situ Peroxidase Labeling and Mass-Spectrometry Connects Alpha-Synuclein Directly to Endocytic Trafficking and mRNA Metabolism in Neurons. *Cell systems* **4**, 242-250 e244, doi:10.1016/j.cels.2017.01.002 (2017).
- 196 McFarland, M. A., Ellis, C. E., Markey, S. P. & Nussbaum, R. L. Proteomics analysis identifies phosphorylation-dependent alpha-synuclein protein interactions. *Molecular & cellular proteomics : MCP* **7**, 2123-2137, doi:10.1074/mcp.M800116-MCP200 (2008).
- 197 Poewe, W. *et al.* Parkinson disease. *Nature reviews. Disease primers* **3**, 17013, doi:10.1038/nrdp.2017.13 (2017).
- 198 Moustafa, A. A. *et al.* Motor symptoms in Parkinson's disease: A unified framework. *Neuroscience and biobehavioral reviews* **68**, 727-740, doi:10.1016/j.neubiorev.2016.07.010 (2016).
- 199 Chaudhuri, K. R. & Schapira, A. H. Non-motor symptoms of Parkinson's disease: dopaminergic pathophysiology and treatment. *The Lancet. Neurology* **8**, 464-474, doi:10.1016/s1474-4422(09)70068-7 (2009).
- 200 Tretiakoff, K. Contribution à l'étude de l'anatomie pathologique du locus niger de Soemmering avec quelques déductions relatives à la pathogénie des troubles du tonus musculaire et de la maladie de Parkinson. (1919).
- 201 Song, Y. J. *et al.* Degeneration in different parkinsonian syndromes relates to astrocyte type and astrocyte protein expression. *J Neuropathol Exp Neurol* **68**, 1073-1083, doi:10.1097/NEN.0b013e3181b66f1b (2009).

- 202 Cabezas R, A. M., Torrente D, El-Bachá RS, Morales L, Gonzalez J, Barreto GE. Astrocytes Role in
Parkinson: A Double-Edged Sword. In: Uday Kishore (ed) *Neurodegenerative disease.*,
doi:{10.5772/54305} (2013).
- 203 Braak, H. et al. Staging of brain pathology related to sporadic Parkinson's disease. *Neurobiology
of aging* **24**, 197-211 (2003).
- 204 Seidel, K. et al. The brainstem pathologies of Parkinson's disease and dementia with Lewy bodies.
Brain pathology (Zurich, Switzerland) **25**, 121-135, doi:10.1111/bpa.12168 (2015).
- 205 Wakabayashi, K., Hayashi, S., Yoshimoto, M., Kudo, H. & Takahashi, H. NACP/ α -synuclein-positive
filamentous inclusions in astrocytes and oligodendrocytes of Parkinson's disease brains. *Acta
neuropathologica* **99**, 14-20, doi:10.1007/pl00007400 (2000).
- 206 Olanow, C. W., Stocchi, F., and Lang, A. *Parkinson's Disease: Non-motor and Non-dopaminergic
Features.* (John Wiley & Sons, 2011).
- 207 Fujiwara, H. et al. α -Synuclein is phosphorylated in synucleinopathy lesions. *Nature cell
biology* **4**, 160-164, doi:10.1038/ncb748 (2002).
- 208 Anderson, J. P. et al. Phosphorylation of Ser-129 is the dominant pathological modification of
 α -synuclein in familial and sporadic Lewy body disease. *The Journal of biological chemistry*
281, 29739-29752, doi:10.1074/jbc.M600933200 (2006).
- 209 Oueslati, A., Paleologou, K. E., Schneider, B. L., Aebischer, P. & Lashuel, H. A. Mimicking
Phosphorylation at Serine 87 Inhibits the Aggregation of Human α -Synuclein and Protects against
Its Toxicity in a Rat Model of Parkinson's Disease. *The Journal of Neuroscience* **32**, 1536-1544,
doi:10.1523/jneurosci.3784-11.2012 (2012).
- 210 Kiely, A. P. et al. α -Synucleinopathy associated with G51D SNCA mutation: a link between
Parkinson's disease and multiple system atrophy? *Acta neuropathologica* **125**, 753-769,
doi:10.1007/s00401-013-1096-7 (2013).
- 211 Hasegawa, M. et al. Phosphorylated α -synuclein is ubiquitinated in α -synucleinopathy
lesions. *The Journal of biological chemistry* **277**, 49071-49076, doi:10.1074/jbc.M208046200
(2002).
- 212 Kuusisto, E., Suuronen, T. & Salminen, A. Ubiquitin-binding protein p62 expression is induced
during apoptosis and proteasomal inhibition in neuronal cells. *Biochem Biophys Res Commun* **280**,
223-228, doi:10.1006/bbrc.2000.4107 (2001).
- 213 Mamais, A. et al. Divergent α -synuclein solubility and aggregation properties in G2019S LRRK2
Parkinson's disease brains with Lewy Body pathology compared to idiopathic cases. *Neurobiology
of disease* **58**, 183-190, doi:10.1016/j.nbd.2013.05.017 (2013).
- 214 Ishii, T., Haga, S. & Tokutake, S. Presence of neurofilament protein in Alzheimer's neurofibrillary
tangles (ANT). An immunofluorescent study. *Acta neuropathologica* **48**, 105-112 (1979).
- 215 Dahl, D., Selkoe, D. J., Pero, R. T. & Bignami, A. Immunostaining of neurofibrillary tangles in
Alzheimer's senile dementia with a neurofilament antiserum. *The Journal of neuroscience : the
official journal of the Society for Neuroscience* **2**, 113-119 (1982).
- 216 Rutherford, N. J., Moore, B. D., Golde, T. E. & Giasson, B. I. Divergent effects of the H50Q and
G51D SNCA mutations on the aggregation of α -synuclein. *J Neurochem*,
doi:10.1111/jnc.12806 (2014).
- 217 Kumar, S. et al. Role of Sporadic Parkinson Disease Associated Mutations A18T and A29S in
Enhanced α -Synuclein Fibrillation and Cytotoxicity. *ACS Chem Neurosci* **9**, 230-240,
doi:10.1021/acschemneuro.6b00430 (2018).
- 218 Goldman, J. E., Yen, S. H., Chiu, F. C. & Peress, N. S. Lewy bodies of Parkinson's disease contain
neurofilament antigens. *Science* **221**, 1082-1084 (1983).
- 219 Huang, Y. & Halliday, G. Can we clinically diagnose dementia with Lewy bodies yet? *Translational
neurodegeneration* **2**, 4, doi:10.1186/2047-9158-2-4 (2013).

- 220 Fares, M. B. *et al.* The novel Parkinson's disease linked mutation G51D attenuates in vitro aggregation and membrane binding of alpha-synuclein, and enhances its secretion and nuclear localization in cells. *Hum Mol Genet*, doi:10.1093/hmg/ddu165 (2014).
- 221 Irwin, D. J., Lee, V. M. & Trojanowski, J. Q. Parkinson's disease dementia: convergence of alpha-synuclein, tau and amyloid-beta pathologies. *Nature reviews. Neuroscience* **14**, 626-636, doi:10.1038/nrn3549 (2013).
- 222 Gai, W. P. *et al.* In situ and in vitro study of colocalization and segregation of alpha-synuclein, ubiquitin, and lipids in Lewy bodies. *Experimental neurology* **166**, 324-333, doi:10.1006/exnr.2000.7527 (2000).
- 223 Shahmoradian, S. H. *et al.* Lewy pathology in Parkinson's disease consists of crowded organelles and lipid membranes. *Nature Neuroscience* **22**, 1099-1109, doi:10.1038/s41593-019-0423-2 (2019).
- 224 Fares, M. B., Jagannath, S. & Lashuel, H. A. Reverse engineering Lewy bodies: how far have we come and how far can we go? *Nature Reviews Neuroscience* **22**, 111-131, doi:10.1038/s41583-020-00416-6 (2021).
- 225 Duffy, P. E. & Tennyson, V. M. Phase and Electron Microscopic Observations of Lewy Bodies and Melanin Granules in the Substantia Nigra and Locus Caeruleus in Parkinson's Disease*†. *Journal of Neuropathology & Experimental Neurology* **24**, 398-414, doi:10.1097/00005072-196507000-00003 (1965).
- 226 Kuusisto, E., Parkkinen, L. & Alafuzoff, I. Morphogenesis of Lewy bodies: dissimilar incorporation of alpha-synuclein, ubiquitin, and p62. *J Neuropathol Exp Neurol* **62**, 1241-1253 (2003).
- 227 Wakabayashi, K., Tanji, K., Mori, F. & Takahashi, H. The Lewy body in Parkinson's disease: molecules implicated in the formation and degradation of alpha-synuclein aggregates. *Neuropathology : official journal of the Japanese Society of Neuropathology* **27**, 494-506 (2007).
- 228 Katsuse, O., Iseki, E., Marui, W. & Kosaka, K. Developmental stages of cortical Lewy bodies and their relation to axonal transport blockage in brains of patients with dementia with Lewy bodies. *Journal of the neurological sciences* **211**, 29-35 (2003).
- 229 Braak, H., Rub, U., Gai, W. P. & Del Tredici, K. Idiopathic Parkinson's disease: possible routes by which vulnerable neuronal types may be subject to neuroinvasion by an unknown pathogen. *J Neural Transm (Vienna)* **110**, 517-536, doi:10.1007/s00702-002-0808-2 (2003).
- 230 Hawkes, C. H., Del Tredici, K. & Braak, H. Parkinson's disease: a dual-hit hypothesis. *Neuropathology and applied neurobiology* **33**, 599-614, doi:10.1111/j.1365-2990.2007.00874.x (2007).
- 231 Braak, H., de Vos, R. A., Bohl, J. & Del Tredici, K. Gastric alpha-synuclein immunoreactive inclusions in Meissner's and Auerbach's plexuses in cases staged for Parkinson's disease-related brain pathology. *Neuroscience letters* **396**, 67-72, doi:10.1016/j.neulet.2005.11.012 (2006).
- 232 Forno, L. S. Concentric hyalin intraneuronal inclusions of Lewy type in the brains of elderly persons (50 incidental cases): relationship to parkinsonism. *Journal of the American Geriatrics Society* **17**, 557-575, doi:10.1111/j.1532-5415.1969.tb01316.x (1969).
- 233 Forno, L. S. & Norville, R. L. Ultrastructure of Lewy bodies in the stellate ganglion. *Acta neuropathologica* **34**, 183-197, doi:10.1007/bf00688674 (1976).
- 234 Langston, J. W. & Forno, L. S. The hypothalamus in Parkinson disease. *Annals of neurology* **3**, 129-133, doi:10.1002/ana.410030207 (1978).
- 235 Forno, L. S. Neuropathology of Parkinson's disease. *J Neuropathol Exp Neurol* **55**, 259-272, doi:10.1097/00005072-199603000-00001 (1996).
- 236 Ikeda, K., Hori, A. & Bode, G. Progressive dementia with "diffuse Lewy-type inclusions" in cerebral cortex. A case report. *Archiv fur Psychiatrie und Nervenkrankheiten* **228**, 243-248 (1980).

- 237 Yagishita, S., Itoh, Y., Amano, N. & Nakano, T. Atypical senile dementia with widespread Lewy type
inclusion in the cerebral cortex. *Acta neuropathologica* **49**, 187-191, doi:10.1007/bf00707105
(1980).
- 238 Tomonaga, M. Neurofibrillary tangles and Lewy bodies in the locus ceruleus neurons of the aged
brain. *Acta neuropathologica* **53**, 165-168, doi:10.1007/bf00689998 (1981).
- 239 Dustin, P. & Brion, J. P. [Pathology of the cytoskeleton]. *Annales de pathologie* **8**, 3-19 (1988).
- 240 Wakabayashi, K. *et al.* The Lewy body in Parkinson's disease and related neurodegenerative
disorders. *Molecular neurobiology* **47**, 495-508, doi:10.1007/s12035-012-8280-y (2013).
- 241 Castellani, R., Smith, M. A., Richey, P. L. & Perry, G. Glycooxidation and oxidative stress in Parkinson
disease and diffuse Lewy body disease. *Brain research* **737**, 195-200 (1996).
- 242 Schipper, H. M., Liberman, A. & Stopa, E. G. Neural heme oxygenase-1 expression in idiopathic
Parkinson's disease. *Experimental neurology* **150**, 60-68, doi:10.1006/exnr.1997.6752 (1998).
- 243 Schmidt, M. L. *et al.* Epitope map of neurofilament protein domains in cortical and peripheral
nervous system Lewy bodies. *The American Journal of Pathology* **139**, 53-65 (1991).
- 244 Lowe, J. *et al.* Dementia with beta-amyloid deposition: involvement of alpha B-crystallin supports
two main diseases. *Lancet (London, England)* **336**, 515-516 (1990).
- 245 Lowe, J. *et al.* alpha B crystallin expression in non-lenticular tissues and selective presence in
ubiquitinated inclusion bodies in human disease. *The Journal of pathology* **166**, 61-68,
doi:10.1002/path.1711660110 (1992).
- 246 Liu, I. H. *et al.* Agrin binds alpha-synuclein and modulates alpha-synuclein fibrillation. *Glycobiology*
15, 1320-1331, doi:10.1093/glycob/cwj014 (2005).
- 247 Nishiyama, K. *et al.* Cu/Zn superoxide dismutase-like immunoreactivity is present in Lewy bodies
from Parkinson disease: a light and electron microscopic immunocytochemical study. *Acta
neuropathologica* **89**, 471-474, doi:10.1007/bf00571500 (1995).
- 248 Kawamoto, Y. *et al.* 14-3-3 proteins in Lewy bodies in Parkinson disease and diffuse Lewy body
disease brains. *J Neuropathol Exp Neurol* **61**, 245-253 (2002).
- 249 Ubl, A. *et al.* 14-3-3 protein is a component of Lewy bodies in Parkinson's disease-mutation
analysis and association studies of 14-3-3 eta. *Brain research. Molecular brain research* **108**, 33-
39 (2002).
- 250 Gai, W. P., Blumbergs, P. C. & Blessing, W. W. Microtubule-associated protein 5 is a component
of Lewy bodies and Lewy neurites in the brainstem and forebrain regions affected in Parkinson's
disease. *Acta neuropathologica* **91**, 78-81, doi:10.1007/s004010050395 (1995).
- 251 Jensen, P. H. *et al.* Microtubule-associated protein 1B is a component of cortical Lewy bodies and
binds alpha-synuclein filaments. *The Journal of biological chemistry* **275**, 21500-21507,
doi:10.1074/jbc.M000099200 (2000).
- 252 Iwatsubo, T., Nakano, I., Fukunaga, K. & Miyamoto, E. Ca²⁺/calmodulin-dependent protein kinase
II immunoreactivity in Lewy bodies. *Acta neuropathologica* **82**, 159-163 (1991).
- 253 Wakabayashi, K. *et al.* Synphilin-1 is present in Lewy bodies in Parkinson's disease. *Annals of
neurology* **47**, 521-523 (2000).
- 254 Wakabayashi, K. *et al.* Immunocytochemical localization of synphilin-1, an alpha-synuclein-
associated protein, in neurodegenerative disorders. *Acta neuropathologica* **103**, 209-214,
doi:10.1007/s004010100451 (2002).
- 255 Bandopadhyay, R. *et al.* Synphilin-1 and parkin show overlapping expression patterns in human
brain and form aggresomes in response to proteasomal inhibition. *Neurobiology of disease* **20**,
401-411, doi:10.1016/j.nbd.2005.03.021 (2005).
- 256 Ryu, M. Y. *et al.* Localization of CKII beta subunits in Lewy bodies of Parkinson's disease. *Journal
of the neurological sciences* **266**, 9-12, doi:10.1016/j.jns.2007.08.027 (2008).

- 257 Galloway, P. G., Bergeron, C. & Perry, G. The presence of tau distinguishes Lewy bodies of diffuse
Lewy body disease from those of idiopathic Parkinson disease. *Neuroscience letters* **100**, 6-10
(1989).
- 258 Ishizawa, T., Mattila, P., Davies, P., Wang, D. & Dickson, D. W. Colocalization of tau and alpha-
synuclein epitopes in Lewy bodies. *J Neuropathol Exp Neurol* **62**, 389-397 (2003).
- 259 Brion, J. P. & Couck, A. M. Cortical and brainstem-type Lewy bodies are immunoreactive for the
cyclin-dependent kinase 5. *Am J Pathol* **147**, 1465-1476 (1995).
- 260 Takahashi, M., Iseki, E. & Kosaka, K. Cyclin-dependent kinase 5 (Cdk5) associated with Lewy bodies
in diffuse Lewy body disease. *Brain research* **862**, 253-256 (2000).
- 261 Honjo, Y. *et al.* FKBP12-immunopositive inclusions in patients with alpha-synucleinopathies. *Brain
research* **1680**, 39-45, doi:10.1016/j.brainres.2017.12.012 (2018).
- 262 Ferrer, I. *et al.* Active, phosphorylation-dependent mitogen-activated protein kinase (MAPK/ERK),
stress-activated protein kinase/c-Jun N-terminal kinase (SAPK/JNK), and p38 kinase expression in
Parkinson's disease and Dementia with Lewy bodies. *Journal of Neural Transmission* **108**, 1383-
1396, doi:10.1007/s007020100015 (2001).
- 263 Ito, T. *et al.* Dofin localizes to Lewy bodies and ubiquitylates synphilin-1. *The Journal of biological
chemistry* **278**, 29106-29114, doi:10.1074/jbc.M302763200 (2003).
- 264 Nagao, M. & Hayashi, H. Glycogen synthase kinase-3beta is associated with Parkinson's disease.
Neuroscience letters **449**, 103-107, doi:10.1016/j.neulet.2008.10.104 (2009).
- 265 Tanji, K. *et al.* NUB1 suppresses the formation of Lewy body-like inclusions by proteasomal
degradation of synphilin-1. *Am J Pathol* **169**, 553-565, doi:10.2353/ajpath.2006.051067 (2006).
- 266 Tanji, K. *et al.* Immunohistochemical localization of NUB1, a synphilin-1-binding protein, in
neurodegenerative disorders. *Acta neuropathologica* **114**, 365-371, doi:10.1007/s00401-007-
0238-1 (2007).
- 267 Greggio, E. *et al.* Kinase activity is required for the toxic effects of mutant LRRK2/dardarin.
Neurobiology of disease **23**, 329-341, doi:10.1016/j.nbd.2006.04.001 (2006).
- 268 Miklossy, J. *et al.* LRRK2 expression in normal and pathologic human brain and in human cell lines.
J Neuropathol Exp Neurol **65**, 953-963, doi:10.1097/01.jnen.0000235121.98052.54 (2006).
- 269 Zhu, X., Siedlak, S. L., Smith, M. A., Perry, G. & Chen, S. G. LRRK2 protein is a component of Lewy
bodies. *Annals of neurology* **60**, 617-618; author reply 618-619, doi:10.1002/ana.20928 (2006).
- 270 Ryo, A. *et al.* Prolyl-isomerase Pin1 accumulates in lewy bodies of parkinson disease and facilitates
formation of alpha-synuclein inclusions. *The Journal of biological chemistry* **281**, 4117-4125,
doi:10.1074/jbc.M507026200 (2006).
- 271 Gandhi, S. *et al.* PINK1 protein in normal human brain and Parkinson's disease. *Brain : a journal of
neurology* **129**, 1720-1731, doi:10.1093/brain/awl114 (2006).
- 272 Schlossmacher, M. G. *et al.* Parkin Localizes to the Lewy Bodies of Parkinson Disease and Dementia
with Lewy Bodies. *The American Journal of Pathology* **160**, 1655-1667, doi:10.1016/s0002-
9440(10)61113-3 (2002).
- 273 Murakami, T. *et al.* Pael-R is accumulated in Lewy bodies of Parkinson's disease. *Annals of
neurology* **55**, 439-442, doi:10.1002/ana.20064 (2004).
- 274 Mahul-Mellier, A. L. *et al.* c-Abl phosphorylates alpha-synuclein and regulates its degradation:
implication for alpha-synuclein clearance and contribution to the pathogenesis of Parkinson's
disease. *Hum Mol Genet* **23**, 2858-2879, doi:10.1093/hmg/ddt674 (2014).
- 275 Liani, E. *et al.* Ubiquitylation of synphilin-1 and alpha-synuclein by SIAH and its presence in cellular
inclusions and Lewy bodies imply a role in Parkinson's disease. *Proceedings of the National
Academy of Sciences of the United States of America* **101**, 5500-5505,
doi:10.1073/pnas.0401081101 (2004).

- 276 Kwak, S., Masaki, T., Ishiura, S. & Sugita, H. Multicatalytic proteinase is present in Lewy bodies and
neurofibrillary tangles in diffuse Lewy body disease brains. *Neuroscience letters* **128**, 21-24 (1991).
- 277 Lowe, J. *et al.* Ubiquitin is a common factor in intermediate filament inclusion bodies of diverse
type in man, including those of Parkinson's disease, Pick's disease, and Alzheimer's disease, as
well as Rosenthal fibres in cerebellar astrocytomas, cytoplasmic bodies in muscle, and mallory
bodies in alcoholic liver disease. *The Journal of pathology* **155**, 9-15,
doi:10.1002/path.1711550105 (1988).
- 278 Kuzuhara, S., Mori, H., Izumiyama, N., Yoshimura, M. & Ihara, Y. Lewy bodies are ubiquitinated. A
light and electron microscopic immunocytochemical study. *Acta neuropathologica* **75**, 345-353
(1988).
- 279 Togo, T. *et al.* Glial involvement in the degeneration process of Lewy body-bearing neurons and
the degradation process of Lewy bodies in brains of dementia with Lewy bodies. *Journal of the
neurological sciences* **184**, 71-75 (2001).
- 280 Noda, K. *et al.* Phosphorylated I κ B α is a component of Lewy body of Parkinson's disease.
Biochem Biophys Res Commun **331**, 309-317, doi:10.1016/j.bbrc.2005.03.167 (2005).
- 281 McNaught, K. S. *et al.* Impairment of the ubiquitin-proteasome system causes dopaminergic cell
death and inclusion body formation in ventral mesencephalic cultures. *J Neurochem* **81**, 301-306
(2002).
- 282 Nakamura, S., Kawamoto, Y., Nakano, S., Akiguchi, I. & Kimura, J. p35nck5a and cyclin-dependent
kinase 5 colocalize in Lewy bodies of brains with Parkinson's disease. *Acta neuropathologica* **94**,
153-157 (1997).
- 283 Shimohama, S. *et al.* Abnormal accumulation of phospholipase C-delta in filamentous inclusions
of human neurodegenerative diseases. *Neuroscience letters* **162**, 183-186 (1993).
- 284 Miki, Y. *et al.* Alteration of mitochondrial protein PDHA1 in Lewy body disease and PARK14.
Biochem Biophys Res Commun **489**, 439-444, doi:10.1016/j.bbrc.2017.05.162 (2017).
- 285 Junn, E., Ronchetti, R. D., Quezado, M. M., Kim, S. Y. & Mouradian, M. M. Tissue transglutaminase-
induced aggregation of alpha-synuclein: Implications for Lewy body formation in Parkinson's
disease and dementia with Lewy bodies. *Proceedings of the National Academy of Sciences of the
United States of America* **100**, 2047-2052, doi:10.1073/pnas.0438021100 (2003).
- 286 Galloway, P. G., Grundke-Iqbal, I., Iqbal, K. & Perry, G. Lewy Bodies Contain Epitopes Both Shared
and Distinct from Alzheimer Neurofibrillary Tangles. *Journal of Neuropathology & Experimental
Neurology* **47**, 654-663, doi:10.1097/00005072-198811000-00008 (1988).
- 287 Fukuda, T., Tanaka, J., Watabe, K., Numoto, R. T. & Minamitani, M. Immunohistochemistry of
neuronal inclusions in the cerebral cortex and brain-stem in Lewy body disease. *Acta pathologica
japonica* **43**, 545-551 (1993).
- 288 Zucchelli, S. *et al.* TRAF6 promotes atypical ubiquitination of mutant DJ-1 and alpha-synuclein and
is localized to Lewy bodies in sporadic Parkinson's disease brains. *Hum Mol Genet* **19**, 3759-3770,
doi:10.1093/hmg/ddq290 (2010).
- 289 Tanji, K. *et al.* TRIM9, a novel brain-specific E3 ubiquitin ligase, is repressed in the brain of
Parkinson's disease and dementia with Lewy bodies. *Neurobiology of disease* **38**, 210-218,
doi:10.1016/j.nbd.2010.01.007 (2010).
- 290 Wakabayashi, K., Takahashi, H., Obata, K. & Ikuta, F. Immunocytochemical localization of synaptic
vesicle-specific protein in Lewy body-containing neurons in Parkinson's disease. *Neuroscience
letters* **138**, 237-240 (1992).
- 291 D'Andrea, M. R., Ilyin, S. & Plata-Salaman, C. R. Abnormal patterns of microtubule-associated
protein-2 (MAP-2) immunolabeling in neuronal nuclei and Lewy bodies in Parkinson's disease
substantia nigra brain tissues. *Neuroscience letters* **306**, 137-140 (2001).

- 292 Fergusson, J. *et al.* Pathological lesions of Alzheimer's disease and dementia with Lewy bodies
brains exhibit immunoreactivity to an ATPase that is a regulatory subunit of the 26S proteasome.
Neuroscience letters **219**, 167-170 (1996).
- 293 Ii, K., Ito, H., Tanaka, K. & Hirano, A. Immunocytochemical co-localization of the proteasome in
ubiquitinated structures in neurodegenerative diseases and the elderly. *J Neuropathol Exp Neurol*
56, 125-131 (1997).
- 294 Lindersson, E. *et al.* Proteasomal inhibition by alpha-synuclein filaments and oligomers. *The*
Journal of biological chemistry **279**, 12924-12934, doi:10.1074/jbc.M306390200 (2004).
- 295 Ihara, M. *et al.* Association of the cytoskeletal GTP-binding protein Sept4/H5 with cytoplasmic
inclusions found in Parkinson's disease and other synucleinopathies. *The Journal of biological*
chemistry **278**, 24095-24102, doi:10.1074/jbc.M301352200 (2003).
- 296 Kovacs, G. G. *et al.* Natively unfolded tubulin polymerization promoting protein TPPP/p25 is a
common marker of alpha-synucleinopathies. *Neurobiology of disease* **17**, 155-162,
doi:10.1016/j.nbd.2004.06.006 (2004).
- 297 Lindersson, E. *et al.* p25alpha Stimulates alpha-synuclein aggregation and is co-localized with
aggregated alpha-synuclein in alpha-synucleinopathies. *The Journal of biological chemistry* **280**,
5703-5715, doi:10.1074/jbc.M410409200 (2005).
- 298 Takahashi-Fujigasaki, J. & Fujigasaki, H. Histone deacetylase (HDAC) 4 involvement in both Lewy
and Marinesco bodies. *Neuropathology and applied neurobiology* **32**, 562-566,
doi:10.1111/j.1365-2990.2006.00733.x (2006).
- 299 Masaki, T., Ishiura, S., Sugita, H. & Kwak, S. Multicatalytic proteinase is associated with
characteristic oval structures in cortical Lewy bodies: an immunocytochemical study with light
and electron microscopy. *Journal of the neurological sciences* **122**, 127-134 (1994).
- 300 Bedford, L. *et al.* Depletion of 26S proteasomes in mouse brain neurons causes
neurodegeneration and Lewy-like inclusions resembling human pale bodies. *The Journal of*
neuroscience : the official journal of the Society for Neuroscience **28**, 8189-8198,
doi:10.1523/JNEUROSCI.2218-08.2008 (2008).
- 301 Dil Kuazi, A. *et al.* NEDD8 protein is involved in ubiquitinated inclusion bodies. *The Journal of*
pathology **199**, 259-266, doi:10.1002/path.1283 (2003).
- 302 Mori, F. *et al.* Accumulation of NEDD8 in neuronal and glial inclusions of neurodegenerative
disorders. *Neuropathology and applied neurobiology* **31**, 53-61, doi:10.1111/j.1365-
2990.2004.00603.x (2005).
- 303 Hashimoto, M., Takeda, A., Hsu, L. J., Takenouchi, T. & Masliah, E. Role of cytochrome c as a
stimulator of alpha-synuclein aggregation in Lewy body disease. *The Journal of biological*
chemistry **274**, 28849-28852 (1999).
- 304 Strauss, K. M. *et al.* Loss of function mutations in the gene encoding Omi/HtrA2 in Parkinson's
disease. *Hum Mol Genet* **14**, 2099-2111, doi:10.1093/hmg/ddi215 (2005).
- 305 Kawamoto, Y. *et al.* Accumulation of HtrA2/Omi in neuronal and glial inclusions in brains with
alpha-synucleinopathies. *J Neuropathol Exp Neurol* **67**, 984-993,
doi:10.1097/NEN.0b013e31818809f4 (2008).
- 306 Corti, O. The p38 subunit of the aminoacyl-tRNA synthetase complex is a Parkin substrate: linking
protein biosynthesis and neurodegeneration. *Human Molecular Genetics* **12**, 1427-1437,
doi:10.1093/hmg/ddg159 (2003).
- 307 Lee, S. S. *et al.* Cell cycle aberrations by α -synuclein over-expression and cyclin B immunoreactivity
in Lewy bodies. *Neurobiology of aging* **24**, 687-696, doi:10.1016/s0197-4580(02)00196-3 (2003).
- 308 Jordan-Sciutto, K. L., Dorsey, R., Chalovich, E. M., Hammond, R. R. & Achim, C. L. Expression
patterns of retinoblastoma protein in Parkinson disease. *J Neuropathol Exp Neurol* **62**, 68-74
(2003).

- 309 Crews, L. *et al.* Selective molecular alterations in the autophagy pathway in patients with Lewy
body disease and in models of alpha-synucleinopathy. *PLoS One* **5**, e9313,
doi:10.1371/journal.pone.0009313 (2010).
- 310 Higashi, S. *et al.* Localization of MAP1-LC3 in vulnerable neurons and Lewy bodies in brains of
patients with dementia with Lewy bodies. *J Neuropathol Exp Neurol* **70**, 264-280,
doi:10.1097/NEN.0b013e318211c86a (2011).
- 311 Tanji, K., Mori, F., Kakita, A., Takahashi, H. & Wakabayashi, K. Alteration of autophagosomal
proteins (LC3, GABARAP and GATE-16) in Lewy body disease. *Neurobiology of disease* **43**, 690-
697, doi:10.1016/j.nbd.2011.05.022 (2011).
- 312 Arai, H., Lee, V. M., Hill, W. D., Greenberg, B. D. & Trojanowski, J. Q. Lewy bodies contain beta-
amyloid precursor proteins of Alzheimer's disease. *Brain research* **585**, 386-390 (1992).
- 313 Yamada, T., McGeer, P. L., Baimbridge, K. G. & McGeer, E. G. Relative sparing in Parkinson's
disease of substantia nigra dopamine neurons containing calbindin-D28K. *Brain research* **526**,
303-307 (1990).
- 314 Dugger, B. N. & Dickson, D. W. Cell type specific sequestration of choline acetyltransferase and
tyrosine hydroxylase within Lewy bodies. *Acta neuropathologica* **120**, 633-639,
doi:10.1007/s00401-010-0739-1 (2010).
- 315 Goker-Alpan, O., Stubblefield, B. K., Giasson, B. I. & Sidransky, E. Glucocerebrosidase is present in
alpha-synuclein inclusions in Lewy body disorders. *Acta neuropathologica* **120**, 641-649,
doi:10.1007/s00401-010-0741-7 (2010).
- 316 Nishimura, M. *et al.* Synaptophysin and chromogranin A immunoreactivities of Lewy bodies in
Parkinson's disease brains. *Brain research* **634**, 339-344 (1994).
- 317 Odagiri, S. *et al.* Autophagic adapter protein NBR1 is localized in Lewy bodies and glial cytoplasmic
inclusions and is involved in aggregate formation in alpha-synucleinopathy. *Acta
neuropathologica* **124**, 173-186, doi:10.1007/s00401-012-0975-7 (2012).
- 318 Huynh, D. P., Scoles, D. R., Nguyen, D. & Pulst, S. M. The autosomal recessive juvenile Parkinson
disease gene product, parkin, interacts with and ubiquitinates synaptotagmin XI. *Hum Mol Genet*
12, 2587-2597, doi:10.1093/hmg/ddg269 (2003).
- 319 Kawaguchi, Y. *et al.* The deacetylase HDAC6 regulates aggresome formation and cell viability in
response to misfolded protein stress. *Cell* **115**, 727-738 (2003).
- 320 Miki, Y. *et al.* Accumulation of histone deacetylase 6, an aggresome-related protein, is specific to
Lewy bodies and glial cytoplasmic inclusions. *Neuropathology : official journal of the Japanese
Society of Neuropathology* **31**, 561-568, doi:10.1111/j.1440-1789.2011.01200.x (2011).
- 321 Mori, F. *et al.* Relationship among alpha-synuclein accumulation, dopamine synthesis, and
neurodegeneration in Parkinson disease substantia nigra. *J Neuropathol Exp Neurol* **65**, 808-815,
doi:10.1097/01.jnen.0000230520.47768.1a (2006).
- 322 Nakashima, S. & Ikuta, F. Tyrosine hydroxylase protein in Lewy bodies of parkinsonian and senile
brains. *Journal of the neurological sciences* **66**, 91-96 (1984).
- 323 Yamamoto, S., Fukae, J., Mori, H., Mizuno, Y. & Hattori, N. Positive immunoreactivity for vesicular
monoamine transporter 2 in Lewy bodies and Lewy neurites in substantia nigra. *Neuroscience
letters* **396**, 187-191, doi:10.1016/j.neulet.2005.11.068 (2006).
- 324 Shin, Y., Klucken, J., Patterson, C., Hyman, B. T. & McLean, P. J. The co-chaperone carboxyl
terminus of Hsp70-interacting protein (CHIP) mediates alpha-synuclein degradation decisions
between proteasomal and lysosomal pathways. *The Journal of biological chemistry* **280**, 23727-
23734, doi:10.1074/jbc.M503326200 (2005).
- 325 Loeffler, D. A., Camp, D. M. & Conant, S. B. Complement activation in the Parkinson's disease
substantia nigra: an immunocytochemical study. *Journal of neuroinflammation* **3**, 29,
doi:10.1186/1742-2094-3-29 (2006).

- 326 Yamada, T., McGeer, P. L. & McGeer, E. G. Lewy bodies in Parkinson's disease are recognized by
antibodies to complement proteins. *Acta neuropathologica* **84**, 100-104, doi:10.1007/bf00427222
(1992).
- 327 Sasaki, K., Doh-ura, K., Wakisaka, Y. & Iwaki, T. Clusterin/apolipoprotein J is associated with
cortical Lewy bodies: immunohistochemical study in cases with alpha-synucleinopathies. *Acta*
neuropathologica **104**, 225-230, doi:10.1007/s00401-002-0546-4 (2002).
- 328 Orr, C. F., Rowe, D. B., Mizuno, Y., Mori, H. & Halliday, G. M. A possible role for humoral immunity
in the pathogenesis of Parkinson's disease. *Brain : a journal of neurology* **128**, 2665-2674,
doi:10.1093/brain/awh625 (2005).
- 329 Durrenberger, P. F. *et al.* DnaJB6 is present in the core of Lewy bodies and is highly up-regulated
in parkinsonian astrocytes. *Journal of neuroscience research* **87**, 238-245, doi:10.1002/jnr.21819
(2009).
- 330 den Jager, W. A. Sphingomyelin in Lewy inclusion bodies in Parkinson's disease. *Archives of*
neurology **21**, 615-619 (1969).
- 331 Issidorides, M. R., Panayotacopoulou, M. T. & Tiniacos, G. Similarities Between Neuronal Lewy
Bodies in Parkinsonism and Hepatic Mallory Bodies in Alcoholism. *Pathology - Research and*
Practice **186**, 473-478, doi:10.1016/s0344-0338(11)80466-8 (1990).
- 332 Auluck, P. K., Chan, H. Y., Trojanowski, J. Q., Lee, V. M. & Bonini, N. M. Chaperone suppression of
alpha-synuclein toxicity in a Drosophila model for Parkinson's disease. *Science* **295**, 865-868,
doi:10.1126/science.1067389 (2002).
- 333 McLean, P. J. *et al.* TorsinA and heat shock proteins act as molecular chaperones: suppression of
alpha-synuclein aggregation. *J Neurochem* **83**, 846-854 (2002).
- 334 Llorens, F. *et al.* YKL-40 in the brain and cerebrospinal fluid of neurodegenerative dementias. *Mol*
Neurodegener **12**, 83, doi:10.1186/s13024-017-0226-4 (2017).
- 335 Shashidharan, P. *et al.* TorsinA accumulation in Lewy bodies in sporadic Parkinson's disease. *Brain*
research **877**, 379-381 (2000).
- 336 Sharma, N. *et al.* A Close Association of TorsinA and α -Synuclein in Lewy Bodies. *The American*
Journal of Pathology **159**, 339-344, doi:10.1016/s0002-9440(10)61700-2 (2001).
- 337 Tanikawa, S. *et al.* Endosomal sorting related protein CHMP2B is localized in Lewy bodies and glial
cytoplasmic inclusions in alpha-synucleinopathy. *Neuroscience letters* **527**, 16-21,
doi:10.1016/j.neulet.2012.08.035 (2012).
- 338 Kurashige, T. *et al.* Localization of CHMP2B-immunoreactivity in the brainstem of Lewy body
disease. *Neuropathology : official journal of the Japanese Society of Neuropathology* **33**, 237-245,
doi:10.1111/j.1440-1789.2012.01346.x (2013).
- 339 Yamada, T., Horisberger, M. A., Kawaguchi, N., Moroo, I. & Toyoda, T. Immunohistochemistry
using antibodies to alpha-interferon and its induced protein, MxA, in Alzheimer's and Parkinson's
disease brain tissues. *Neuroscience letters* **181**, 61-64 (1994).
- 340 Hasegawa, T. *et al.* The AAA-ATPase VPS4 regulates extracellular secretion and lysosomal
targeting of alpha-synuclein. *PLoS One* **6**, e29460, doi:10.1371/journal.pone.0029460 (2011).
- 341 Munch, G. *et al.* Crosslinking of alpha-synuclein by advanced glycation endproducts--an early
pathophysiological step in Lewy body formation? *Journal of chemical neuroanatomy* **20**, 253-257
(2000).
- 342 Longhena, F. *et al.* Synapsin III is a key component of α -synuclein fibrils in Lewy bodies of PD
brains. *Brain Pathology*, doi:10.1111/bpa.12587 (2018).
- 343 Kokoulina, P. & Rohn, T. T. Caspase-cleaved transactivation response DNA-binding protein 43 in
Parkinson's disease and dementia with Lewy bodies. *Neuro-degenerative diseases* **7**, 243-250,
doi:10.1159/000287952 (2010).

- 344 Deng, H. X. *et al.* Identification of TMEM230 mutations in familial Parkinson's disease. *Nature genetics* **48**, 733-739, doi:10.1038/ng.3589 (2016).
- 345 Bandopadhyay, R. *et al.* The expression of DJ-1 (PARK7) in normal human CNS and idiopathic Parkinson's disease. *Brain : a journal of neurology* **127**, 420-430, doi:10.1093/brain/awh054 (2004).
- 346 Jin, J. *et al.* Quantitative proteomic analysis of mitochondrial proteins: relevance to Lewy body formation and Parkinson's disease. *Brain research. Molecular brain research* **134**, 119-138, doi:10.1016/j.molbrainres.2004.10.003 (2005).
- 347 Power, J. H. T., Shannon, J. M., Blumbergs, P. C. & Gai, W.-P. Nonselenium Glutathione Peroxidase in Human Brain. *The American Journal of Pathology* **161**, 885-894, doi:10.1016/s0002-9440(10)64249-6 (2002).
- 348 Su, B. *et al.* Ectopic localization of FOXO3a protein in Lewy bodies in Lewy body dementia and Parkinson's disease. *Molecular Neurodegeneration* **4**, 32, doi:10.1186/1750-1326-4-32 (2009).
- 349 Leverenz, J. B. *et al.* Proteomic identification of novel proteins in cortical lewy bodies. *Brain pathology (Zurich, Switzerland)* **17**, 139-145, doi:10.1111/j.1750-3639.2007.00048.x (2007).
- 350 Basso, M. *et al.* Proteome analysis of human substantia nigra in Parkinson's disease. *Proteomics* **4**, 3943-3952, doi:10.1002/pmic.200400848 (2004).
- 351 Werner, C. J., Heyny-von Haussen, R., Mall, G. & Wolf, S. Proteome analysis of human substantia nigra in Parkinson's disease. *Proteome Science* **6**, 8, doi:10.1186/1477-5956-6-8 (2008).
- 352 Kitsou, E. *et al.* Identification of proteins in human substantia nigra. *Proteomics. Clinical applications* **2**, 776-782, doi:10.1002/prca.200800028 (2008).
- 353 Licker, V. *et al.* Proteomic analysis of human substantia nigra identifies novel candidates involved in Parkinson's disease pathogenesis. *Proteomics* **14**, 784-794, doi:10.1002/pmic.201300342 (2014).
- 354 van Dijk, K. D. *et al.* The proteome of the locus ceruleus in Parkinson's disease: relevance to pathogenesis. *Brain pathology (Zurich, Switzerland)* **22**, 485-498, doi:10.1111/j.1750-3639.2011.00540.x (2012).
- 355 Bereczki, E. *et al.* Synaptic markers of cognitive decline in neurodegenerative diseases: a proteomic approach. *Brain : a journal of neurology* **141**, 582-595, doi:10.1093/brain/awx352 (2018).
- 356 Kasap, M., Akpinar, G. & Kanli, A. Proteomic studies associated with Parkinson's disease. *Expert review of proteomics* **14**, 193-209, doi:10.1080/14789450.2017.1291344 (2017).
- 357 Dixit, A., Mehta, R. & Singh, A. K. Proteomics in Human Parkinson's Disease: Present Scenario and Future Directions. *Cellular and molecular neurobiology* **39**, 901-915, doi:10.1007/s10571-019-00700-9 (2019).
- 358 Rideout, H. J., Dietrich, P., Wang, Q., Dauer, W. T. & Stefanis, L. alpha-synuclein is required for the fibrillar nature of ubiquitinated inclusions induced by proteasomal inhibition in primary neurons. *The Journal of biological chemistry* **279**, 46915-46920, doi:10.1074/jbc.M405146200 (2004).
- 359 Sherer, T. B. *et al.* An in vitro model of Parkinson's disease: linking mitochondrial impairment to altered alpha-synuclein metabolism and oxidative damage. *The Journal of neuroscience : the official journal of the Society for Neuroscience* **22**, 7006-7015, doi:20026721 (2002).
- 360 Ostrerova-Golts, N. *et al.* The A53T alpha-synuclein mutation increases iron-dependent aggregation and toxicity. *The Journal of neuroscience : the official journal of the Society for Neuroscience* **20**, 6048-6054 (2000).
- 361 Kakimura, J. *et al.* Release and aggregation of cytochrome c and alpha-synuclein are inhibited by the antiparkinsonian drugs, talipexole and pramipexole. *European journal of pharmacology* **417**, 59-67 (2001).

- 362 Lee, H. J., Shin, S. Y., Choi, C., Lee, Y. H. & Lee, S. J. Formation and removal of alpha-synuclein
aggregates in cells exposed to mitochondrial inhibitors. *The Journal of biological chemistry* **277**,
5411-5417, doi:10.1074/jbc.M105326200 (2002).
- 363 Paxinou, E. *et al.* Induction of alpha-synuclein aggregation by intracellular nitrative insult. *The*
Journal of neuroscience : the official journal of the Society for Neuroscience **21**, 8053-8061 (2001).
- 364 Giraldez-Perez, R., Antolin-Vallespin, M., Munoz, M. & Sanchez-Capelo, A. Models of alpha-
synuclein aggregation in Parkinson's disease. *Acta neuropathologica communications* **2**, 176,
doi:10.1186/s40478-014-0176-9 (2014).
- 365 Fornai, F. *et al.* Parkinson-like syndrome induced by continuous MPTP infusion: convergent roles
of the ubiquitin-proteasome system and alpha-synuclein. *Proceedings of the National Academy*
of Sciences of the United States of America **102**, 3413-3418, doi:10.1073/pnas.0409713102
(2005).
- 366 Gibrat, C. *et al.* Differences between subacute and chronic MPTP mice models: investigation of
dopaminergic neuronal degeneration and alpha-synuclein inclusions. *J Neurochem* **109**, 1469-
1482, doi:10.1111/j.1471-4159.2009.06072.x (2009).
- 367 Shimoji, M., Zhang, L., Mandir, A. S., Dawson, V. L. & Dawson, T. M. Absence of inclusion body
formation in the MPTP mouse model of Parkinson's disease. *Brain research. Molecular brain*
research **134**, 103-108, doi:10.1016/j.molbrainres.2005.01.012 (2005).
- 368 Alvarez-Fischer, D. *et al.* Modelling Parkinson-like neurodegeneration via osmotic minipump
delivery of MPTP and probenecid. *J Neurochem* **107**, 701-711, doi:10.1111/j.1471-
4159.2008.05651.x (2008).
- 369 Meredith, G. E. *et al.* Lysosomal malfunction accompanies alpha-synuclein aggregation in a
progressive mouse model of Parkinson's disease. *Brain research* **956**, 156-165 (2002).
- 370 Meredith, G. E., Totterdell, S., Potashkin, J. A. & Surmeier, D. J. Modeling PD pathogenesis in mice:
advantages of a chronic MPTP protocol. *Parkinsonism & related disorders* **14 Suppl 2**, S112-115,
doi:10.1016/j.parkreldis.2008.04.012 (2008).
- 371 Luk, K. C. *et al.* Exogenous alpha-synuclein fibrils seed the formation of Lewy body-like intracellular
inclusions in cultured cells. *Proceedings of the National Academy of Sciences of the United States*
of America **106**, 20051-20056, doi:10.1073/pnas.0908005106 (2009).
- 372 Luk, K. C. *et al.* Intracerebral inoculation of pathological alpha-synuclein initiates a rapidly
progressive neurodegenerative alpha-synucleinopathy in mice. *The Journal of experimental*
medicine **209**, 975-986, doi:10.1084/jem.20112457 (2012).
- 373 Tabrizi, S. J. *et al.* Expression of mutant alpha-synuclein causes increased susceptibility to
dopamine toxicity. *Hum Mol Genet* **9**, 2683-2689 (2000).
- 374 Stefanis, L., Larsen, K. E., Rideout, H. J., Sulzer, D. & Greene, L. A. Expression of A53T Mutant But
Not Wild-Type α -Synuclein in PC12 Cells Induces Alterations of the Ubiquitin-Dependent
Degradation System, Loss of Dopamine Release, and Autophagic Cell Death. *The Journal of*
Neuroscience **21**, 9549-9560, doi:10.1523/jneurosci.21-24-09549.2001 (2001).
- 375 McLean, P. J., Kawamata, H. & Hyman, B. T. Alpha-synuclein-enhanced green fluorescent protein
fusion proteins form proteasome sensitive inclusions in primary neurons. *Neuroscience* **104**, 901-
912 (2001).
- 376 Tofaris, G. K., Layfield, R. & Spillantini, M. G. alpha-synuclein metabolism and aggregation is linked
to ubiquitin-independent degradation by the proteasome. *FEBS letters* **509**, 22-26 (2001).
- 377 Matsuzaki, M. *et al.* Histochemical features of stress-induced aggregates in alpha-synuclein
overexpressing cells. *Brain research* **1004**, 83-90, doi:10.1016/j.brainres.2004.01.017 (2004).
- 378 Pandey, N., Schmidt, R. E. & Galvin, J. E. The alpha-synuclein mutation E46K promotes aggregation
in cultured cells. *Experimental neurology* **197**, 515-520, doi:10.1016/j.expneurol.2005.10.019
(2006).

- 379 Vekrellis, K., Xilouri, M., Emmanouilidou, E. & Stefanis, L. Inducible over-expression of wild type
alpha-synuclein in human neuronal cells leads to caspase-dependent non-apoptotic death. *J*
Neurochem **109**, 1348-1362, doi:10.1111/j.1471-4159.2009.06054.x (2009).
- 380 Welander, H. *et al.* Gelsolin co-occurs with Lewy bodies in vivo and accelerates alpha-synuclein
aggregation in vitro. *Biochem Biophys Res Commun* **412**, 32-38, doi:10.1016/j.bbrc.2011.07.027
(2011).
- 381 Burré, J., Sharma, M. & Südhof, T. C. Definition of a molecular pathway mediating α -synuclein
neurotoxicity. *The Journal of neuroscience : the official journal of the Society for Neuroscience* **35**,
5221-5232, doi:10.1523/JNEUROSCI.4650-14.2015 (2015).
- 382 Fares, M. B. *et al.* Induction of de novo alpha-synuclein fibrillization in a neuronal model for
Parkinson's disease. *Proceedings of the National Academy of Sciences of the United States of*
America **113**, E912-921, doi:10.1073/pnas.1512876113 (2016).
- 383 Trimmer, P. A., Borland, M. K., Keeney, P. M., Bennett, J. P., Jr. & Parker, W. D., Jr. Parkinson's
disease transgenic mitochondrial cybrids generate Lewy inclusion bodies. *J Neurochem* **88**, 800-
812 (2004).
- 384 Melnikova, A., Pozdyshev, D., Barinova, K., Kudryavtseva, S. & Muronetz, V. I. α -Synuclein
Overexpression in SH-SY5Y Human Neuroblastoma Cells Leads to the Accumulation of Thioflavin
S-positive Aggregates and Impairment of Glycolysis. *Biochemistry. Biokhimiia* **85**, 604-613,
doi:10.1134/s0006297920050090 (2020).
- 385 Engelender, S. *et al.* Synphilin-1 associates with alpha-synuclein and promotes the formation of
cytosolic inclusions. *Nature genetics* **22**, 110-114, doi:10.1038/8820 (1999).
- 386 Danzer, K. M. *et al.* Different species of alpha-synuclein oligomers induce calcium influx and
seeding. *The Journal of neuroscience : the official journal of the Society for Neuroscience* **27**, 9220-
9232, doi:10.1523/jneurosci.2617-07.2007 (2007).
- 387 O'Farrell, C. *et al.* Transfected synphilin-1 forms cytoplasmic inclusions in HEK293 cells. *Brain*
research. Molecular brain research **97**, 94-102, doi:10.1016/s0169-328x(01)00292-3 (2001).
- 388 Desplats, P. *et al.* Inclusion formation and neuronal cell death through neuron-to-neuron
transmission of alpha-synuclein. *Proceedings of the National Academy of Sciences of the United*
States of America **106**, 13010-13015, doi:10.1073/pnas.0903691106 (2009).
- 389 Tanaka, M. *et al.* Aggresomes formed by alpha-synuclein and synphilin-1 are cytoprotective. *The*
Journal of biological chemistry **279**, 4625-4631, doi:10.1074/jbc.M310994200 (2004).
- 390 Nonaka, T., Watanabe, S. T., Iwatsubo, T. & Hasegawa, M. Seeded aggregation and toxicity of
{alpha}-synuclein and tau: cellular models of neurodegenerative diseases. *The Journal of*
biological chemistry **285**, 34885-34898, doi:10.1074/jbc.M110.148460 (2010).
- 391 Smith, W. W. *et al.* Alpha-synuclein phosphorylation enhances eosinophilic cytoplasmic inclusion
formation in SH-SY5Y cells. *The Journal of neuroscience : the official journal of the Society for*
Neuroscience **25**, 5544-5552, doi:10.1523/JNEUROSCI.0482-05.2005 (2005).
- 392 Waxman, E. A. & Giasson, B. I. Induction of Intracellular Tau Aggregation Is Promoted by α -
Synuclein Seeds and Provides Novel Insights into the Hyperphosphorylation of Tau. *The Journal of*
Neuroscience **31**, 7604-7618, doi:10.1523/jneurosci.0297-11.2011 (2011).
- 393 Buttner, S. *et al.* Synphilin-1 enhances alpha-synuclein aggregation in yeast and contributes to
cellular stress and cell death in a Sir2-dependent manner. *PLoS One* **5**, e13700,
doi:10.1371/journal.pone.0013700 (2010).
- 394 Xie, Y. Y. *et al.* Interaction with synphilin-1 promotes inclusion formation of alpha-synuclein:
mechanistic insights and pathological implication. *FASEB journal : official publication of the*
Federation of American Societies for Experimental Biology **24**, 196-205, doi:10.1096/fj.09-133082
(2010).

395 Dryanovski, D. I. *et al.* Calcium entry and alpha-synuclein inclusions elevate dendritic
mitochondrial oxidant stress in dopaminergic neurons. *The Journal of neuroscience : the official
journal of the Society for Neuroscience* **33**, 10154-10164, doi:10.1523/JNEUROSCI.5311-12.2013
(2013).

396 Klucken, J. *et al.* Alpha-synuclein aggregation involves a bafilomycin A 1-sensitive autophagy
pathway. *Autophagy* **8**, 754-766, doi:10.4161/auto.19371 (2012).

397 Volpicelli-Daley, L. A. *et al.* Formation of alpha-synuclein Lewy neurite-like aggregates in axons
impedes the transport of distinct endosomes. *Molecular biology of the cell* **25**, 4010-4023,
doi:10.1091/mbc.E14-02-0741 (2014).

398 Tran, H. T. *et al.* A-synuclein immunotherapy blocks uptake and templated propagation of
misfolded α -synuclein and neurodegeneration. *Cell Rep* **7**, 2054-2065,
doi:10.1016/j.celrep.2014.05.033 (2014).

399 Outeiro, T. F. & Lindquist, S. Yeast cells provide insight into alpha-synuclein biology and
pathobiology. *Science* **302**, 1772-1775, doi:10.1126/science.1090439 (2003).

400 Domert, J. *et al.* Aggregated Alpha-Synuclein Transfer Efficiently between Cultured Human
Neuron-Like Cells and Localize to Lysosomes. *PloS one* **11**, e0168700-e0168700,
doi:10.1371/journal.pone.0168700 (2016).

401 Gitler, A. D. *et al.* The Parkinson's disease protein alpha-synuclein disrupts cellular Rab
homeostasis. *Proceedings of the National Academy of Sciences of the United States of America*
105, 145-150, doi:10.1073/pnas.0710685105 (2008).

402 Mao, X. *et al.* Pathological α -synuclein transmission initiated by binding lymphocyte-activation
gene 3. *Science* **353**, doi:10.1126/science.aah3374 (2016).

403 Opazo, F., Krenz, A., Heermann, S., Schulz, J. B. & Falkenburger, B. H. Accumulation and clearance
of alpha-synuclein aggregates demonstrated by time-lapse imaging. *J Neurochem* **106**, 529-540,
doi:10.1111/j.1471-4159.2008.05407.x (2008).

404 Tapias, V. *et al.* Synthetic alpha-synuclein fibrils cause mitochondrial impairment and selective
dopamine neurodegeneration in part via iNOS-mediated nitric oxide production. *Cellular and
molecular life sciences : CMLS* **74**, 2851-2874, doi:10.1007/s00018-017-2541-x (2017).

405 Soper, J. H., Kehm, V., Burd, C. G., Bankaitis, V. A. & Lee, V. M. Aggregation of alpha-synuclein in
S. cerevisiae is associated with defects in endosomal trafficking and phospholipid biosynthesis.
Journal of molecular neuroscience : MN **43**, 391-405, doi:10.1007/s12031-010-9455-5 (2011).

406 Henderson, M. X. *et al.* Unbiased Proteomics of Early Lewy Body Formation Model Implicates
Active Microtubule Affinity-Regulating Kinases (MARKs) in Synucleinopathies. *The Journal of
neuroscience : the official journal of the Society for Neuroscience* **37**, 5870-5884,
doi:10.1523/JNEUROSCI.2705-16.2017 (2017).

407 Pranke, I. M. *et al.* alpha-Synuclein and ALPS motifs are membrane curvature sensors whose
contrasting chemistry mediates selective vesicle binding. *The Journal of cell biology* **194**, 89-103,
doi:10.1083/jcb.201011118 (2011).

408 Froula, J. M. *et al.* α -Synuclein fibril-induced paradoxical structural and functional defects in
hippocampal neurons. *Acta neuropathologica communications* **6**, 35, doi:10.1186/s40478-018-
0537-x (2018).

409 Hansen, C. *et al.* alpha-Synuclein propagates from mouse brain to grafted dopaminergic neurons
and seeds aggregation in cultured human cells. *The Journal of clinical investigation* **121**, 715-725,
doi:10.1172/JCI43366 (2011).

410 Lázaro, D. F. *et al.* The effects of the novel A53E alpha-synuclein mutation on its oligomerization
and aggregation. *Acta neuropathologica communications* **4**, 128, doi:10.1186/s40478-016-0402-
8 (2016).

411 Grassi, D. *et al.* Identification of a highly neurotoxic α -synuclein species inducing mitochondrial
 damage and mitophagy in Parkinson's disease. *Proceedings of the National Academy of Sciences*
115, E2634-E2643, doi:10.1073/pnas.1713849115 (2018).

412 Raiss, C. C. *et al.* Functionally different α -synuclein inclusions yield insight into Parkinson's disease
 pathology. *Scientific Reports* **6**, 23116, doi:10.1038/srep23116 (2016).

413 Wang, X. *et al.* Pathogenic alpha-synuclein aggregates preferentially bind to mitochondria and
 affect cellular respiration. *Acta neuropathologica communications* **7**, 41, doi:10.1186/s40478-
 019-0696-4 (2019).

414 Dettmer, U. *et al.* Loss of native α -synuclein multimerization by strategically mutating its
 amphipathic helix causes abnormal vesicle interactions in neuronal cells. *Hum Mol Genet* **26**,
 3466-3481, doi:10.1093/hmg/ddx227 (2017).

415 Xiao, Y. *et al.* Iron promotes α -synuclein aggregation and transmission by inhibiting TFEB-
 mediated autophagosome-lysosome fusion. *Journal of Neurochemistry* **145**, 34-50,
 doi:10.1111/jnc.14312 (2018).

416 Wu, Z.-C. *et al.* Alpha-synuclein is highly prone to distribution in the hippocampus and midbrain
 in tree shrews, and its fibrils seed Lewy body-like pathology in primary neurons. *Experimental*
Gerontology **116**, 37-45, doi:https://doi.org/10.1016/j.exger.2018.12.008 (2019).

417 Imberdis, T. *et al.* Cell models of lipid-rich α -synuclein aggregation validate known modifiers of α -
 synuclein biology and identify stearyl-CoA desaturase. *Proceedings of the National Academy of*
Sciences **116**, 20760-20769, doi:10.1073/pnas.1903216116 (2019).

418 Grassi, D., Diaz-Perez, N., Volpicelli-Daley, L. A. & Lasmézas, C. I. P α -syn* mitotoxicity is linked to
 MAPK activation and involves tau phosphorylation and aggregation at the mitochondria.
Neurobiology of disease **124**, 248-262, doi:10.1016/j.nbd.2018.11.015 (2019).

419 Frey, B. *et al.* Monitoring alpha-synuclein oligomerization and aggregation using bimolecular
 fluorescence complementation assays: what you see is not always what you get. *Journal of*
Neurochemistry **n/a**, doi:10.1111/jnc.15147 (2020).

420 Shrivastava, A. N. *et al.* Differential Membrane Binding and Seeding of Distinct α -Synuclein Fibrillar
 Polymorphs. *Biophysical journal*, doi:https://doi.org/10.1016/j.bpj.2020.01.022 (2020).

421 Lopes da Fonseca, T., Pinho, R. & Outeiro, T. F. A familial ATP13A2 mutation enhances alpha-
 synuclein aggregation and promotes cell death. *Hum Mol Genet* **25**, 2959-2971,
 doi:10.1093/hmg/ddw147 (2016).

422 Lautenschläger, J. *et al.* Intramitochondrial proteostasis is directly coupled to α -synuclein and
 amyloid β 1-42 pathologies. *The Journal of biological chemistry* **295**, 10138-10152,
 doi:10.1074/jbc.RA119.011650 (2020).

423 Wang, R. *et al.* Iron-induced oxidative stress contributes to α -synuclein phosphorylation and up-
 regulation via polo-like kinase 2 and casein kinase 2. *Neurochemistry International* **125**, 127-135,
 doi:https://doi.org/10.1016/j.neuint.2019.02.016 (2019).

424 Morgan, S. A. *et al.* α -Synuclein filaments from transgenic mouse and human synucleinopathy-
 containing brains are major seed-competent species. *The Journal of biological chemistry* **295**,
 6652-6664, doi:10.1074/jbc.RA119.012179 (2020).

425 Roberti, M. J., Bertocini, C. W., Klement, R., Jares-Erijman, E. A. & Jovin, T. M. Fluorescence
 imaging of amyloid formation in living cells by a functional, tetracysteine-tagged alpha-synuclein.
Nature methods **4**, 345-351, doi:10.1038/nmeth1026 (2007).

426 Courte, J. *et al.* The expression level of alpha-synuclein in different neuronal populations is the
 primary determinant of its prion-like seeding. *Sci Rep* **10**, 4895, doi:10.1038/s41598-020-61757-x
 (2020).

- 427 Roberts, R. F., Wade-Martins, R. & Alegre-Abarategui, J. Direct visualization of alpha-synuclein
oligomers reveals previously undetected pathology in Parkinson's disease brain. *Brain : a journal
of neurology* **138**, 1642-1657, doi:10.1093/brain/awv040 (2015).
- 428 Devine, M. J. *et al.* Parkinson's disease induced pluripotent stem cells with triplication of the
alpha-synuclein locus. *Nat Commun* **2**, 440, doi:10.1038/ncomms1453 (2011).
- 429 Byers, B. *et al.* SNCA triplication Parkinson's patient's iPSC-derived DA neurons accumulate alpha-
synuclein and are susceptible to oxidative stress. *PLoS One* **6**, e26159,
doi:10.1371/journal.pone.0026159 (2011).
- 430 Soldner, F. *et al.* Generation of isogenic pluripotent stem cells differing exclusively at two early
onset Parkinson point mutations. *Cell* **146**, 318-331, doi:10.1016/j.cell.2011.06.019 (2011).
- 431 Chung, C. Y. *et al.* Identification and rescue of alpha-synuclein toxicity in Parkinson patient-derived
neurons. *Science* **342**, 983-987, doi:10.1126/science.1245296 (2013).
- 432 Ryan, Scott D. *et al.* Isogenic Human iPSC Parkinson's Model Shows Nitrosative Stress-Induced
Dysfunction in MEF2-PGC1 α Transcription. *Cell* **155**, 1351-1364,
doi:https://doi.org/10.1016/j.cell.2013.11.009 (2013).
- 433 Flierl, A. *et al.* Higher vulnerability and stress sensitivity of neuronal precursor cells carrying an
alpha-synuclein gene triplication. *PLoS One* **9**, e112413, doi:10.1371/journal.pone.0112413
(2014).
- 434 Oliveira, L. M. *et al.* Elevated alpha-synuclein caused by SNCA gene triplication impairs neuronal
differentiation and maturation in Parkinson's patient-derived induced pluripotent stem cells. *Cell
death & disease* **6**, e1994, doi:10.1038/cddis.2015.318 (2015).
- 435 Dettmer, U. *et al.* Parkinson-causing alpha-synuclein missense mutations shift native tetramers to
monomers as a mechanism for disease initiation. *Nat Commun* **6**, 7314,
doi:10.1038/ncomms8314 (2015).
- 436 Lin, L. *et al.* Molecular Features Underlying Neurodegeneration Identified through In Vitro
Modeling of Genetically Diverse Parkinson's Disease Patients. *Cell Rep* **15**, 2411-2426,
doi:10.1016/j.celrep.2016.05.022 (2016).
- 437 Kouroupi, G. *et al.* Defective synaptic connectivity and axonal neuropathology in a human iPSC-
based model of familial Parkinson's disease. *Proceedings of the National Academy of Sciences of
the United States of America* **114**, E3679-E3688, doi:10.1073/pnas.1617259114 (2017).
- 438 Zambon, F. *et al.* Cellular α -synuclein pathology is associated with bioenergetic dysfunction in
Parkinson's iPSC-derived dopamine neurons. *Human Molecular Genetics* **28**, 2001-2013,
doi:10.1093/hmg/ddz038 (2019).
- 439 Feany, M. B. & Bender, W. W. A Drosophila model of Parkinson's disease. *Nature* **404**, 394-398,
doi:10.1038/35006074
35006074 [pii] (2000).
- 440 Bethlem, J. & Den Hartog Jager, W. A. The incidence and characteristics of Lewy bodies in
idiopathic paralysis agitans (Parkinson's disease). *Journal of neurology, neurosurgery, and
psychiatry* **23**, 74-80, doi:10.1136/jnnp.23.1.74 (1960).
- 441 Takahashi, M. *et al.* Phosphorylation of alpha-synuclein characteristic of synucleinopathy lesions
is recapitulated in alpha-synuclein transgenic Drosophila. *Neuroscience letters* **336**, 155-158,
doi:10.1016/s0304-3940(02)01258-2 (2003).
- 442 Mougenot, A. L. *et al.* Prion-like acceleration of a synucleinopathy in a transgenic mouse model.
Neurobiology of aging **33**, 2225-2228, doi:10.1016/j.neurobiolaging.2011.06.022 (2012).
- 443 Chen, L. & Feany, M. B. Alpha-synuclein phosphorylation controls neurotoxicity and inclusion
formation in a Drosophila model of Parkinson disease. *Nat Neurosci* **8**, 657-663,
doi:10.1038/nn1443 (2005).

- 444 Ordonez, D. G., Lee, M. K. & Feany, M. B. alpha-synuclein Induces Mitochondrial Dysfunction
through Spectrin and the Actin Cytoskeleton. *Neuron* **97**, 108-124 e106,
doi:10.1016/j.neuron.2017.11.036 (2018).
- 445 Lakso, M. *et al.* Dopaminergic neuronal loss and motor deficits in Caenorhabditis elegans
overexpressing human alpha-synuclein. *J Neurochem* **86**, 165-172 (2003).
- 446 Guo, J. L. *et al.* Distinct alpha-synuclein strains differentially promote tau inclusions in neurons.
Cell **154**, 103-117, doi:10.1016/j.cell.2013.05.057 (2013).
- 447 Watts, J. C. *et al.* Transmission of multiple system atrophy prions to transgenic mice. *Proceedings
of the National Academy of Sciences of the United States of America* **110**, 19555-19560,
doi:10.1073/pnas.1318268110 (2013).
- 448 van Ham, T. J. *et al.* C. elegans model identifies genetic modifiers of alpha-synuclein inclusion
formation during aging. *PLoS genetics* **4**, e1000027, doi:10.1371/journal.pgen.1000027 (2008).
- 449 Sacino, A. N. *et al.* Induction of CNS alpha-synuclein pathology by fibrillar and non-amyloidogenic
recombinant alpha-synuclein. *Acta neuropathologica communications* **1**, 38, doi:10.1186/2051-
5960-1-38 (2013).
- 450 Masuda-Suzukake, M. *et al.* Prion-like spreading of pathological alpha-synuclein in brain. *Brain : a
journal of neurology* **136**, 1128-1138, doi:10.1093/brain/awt037 (2013).
- 451 van der Putten, H. *et al.* Neuropathology in mice expressing human alpha-synuclein. *The Journal
of neuroscience : the official journal of the Society for Neuroscience* **20**, 6021-6029 (2000).
- 452 Sacino, A. N. *et al.* Brain injection of alpha-synuclein induces multiple proteinopathies, gliosis, and
a neuronal injury marker. *The Journal of neuroscience : the official journal of the Society for
Neuroscience* **34**, 12368-12378, doi:10.1523/JNEUROSCI.2102-14.2014 (2014).
- 453 Matsuoka, Y. *et al.* Lack of nigral pathology in transgenic mice expressing human alpha-synuclein
driven by the tyrosine hydroxylase promoter. *Neurobiology of disease* **8**, 535-539 (2001).
- 454 Masuda-Suzukake, M. *et al.* Pathological alpha-synuclein propagates through neural networks.
Acta neuropathologica communications **2**, 88, doi:10.1186/PREACCEPT-1296467154135944
(2014).
- 455 Kahle, P. J. *et al.* Selective insolubility of alpha-synuclein in human Lewy body diseases is
recapitulated in a transgenic mouse model. *Am J Pathol* **159**, 2215-2225, doi:10.1016/s0002-
9440(10)63072-6 (2001).
- 456 Recasens, A. *et al.* Lewy body extracts from Parkinson disease brains trigger alpha-synuclein
pathology and neurodegeneration in mice and monkeys. *Annals of neurology* **75**, 351-362,
doi:10.1002/ana.24066 (2014).
- 457 Rieker, C. *et al.* Neuropathology in Mice Expressing Mouse Alpha-Synuclein. *PLOS ONE* **6**, e24834,
doi:10.1371/journal.pone.0024834 (2011).
- 458 Sacino, A. N. *et al.* Intramuscular injection of alpha-synuclein induces CNS alpha-synuclein
pathology and a rapid-onset motor phenotype in transgenic mice. *Proceedings of the National
Academy of Sciences of the United States of America* **111**, 10732-10737,
doi:10.1073/pnas.1321785111 (2014).
- 459 Giasson, B. I. *et al.* Neuronal alpha-synucleinopathy with severe movement disorder in mice
expressing A53T human alpha-synuclein. *Neuron* **34**, 521-533, doi:S0896627302006827 [pii]
(2002).
- 460 Paumier, K. L. *et al.* Intrastriatal injection of pre-formed mouse alpha-synuclein fibrils into rats
triggers alpha-synuclein pathology and bilateral nigrostriatal degeneration. *Neurobiology of
disease* **82**, 185-199, doi:10.1016/j.nbd.2015.06.003 (2015).
- 461 Klein, R. L., King, M. A., Hamby, M. E. & Meyer, E. M. Dopaminergic cell loss induced by human
A30P alpha-synuclein gene transfer to the rat substantia nigra. *Human gene therapy* **13**, 605-612,
doi:10.1089/10430340252837206 (2002).

- 462 Osterberg, V. R. *et al.* Progressive aggregation of alpha-synuclein and selective degeneration of
lewy inclusion-bearing neurons in a mouse model of parkinsonism. *Cell Rep* **10**, 1252-1260,
doi:10.1016/j.celrep.2015.01.060 (2015).
- 463 Kirik, D. *et al.* Parkinson-like neurodegeneration induced by targeted overexpression of alpha-
synuclein in the nigrostriatal system. *The Journal of neuroscience : the official journal of the Society
for Neuroscience* **22**, 2780-2791, doi:20026246 (2002).
- 464 Peelaerts, W. *et al.* alpha-Synuclein strains cause distinct synucleinopathies after local and
systemic administration. *Nature* **522**, 340-344, doi:10.1038/nature14547 (2015).
- 465 Lee, M. K. *et al.* Human alpha-synuclein-harboring familial Parkinson's disease-linked Ala-53 -->
Thr mutation causes neurodegenerative disease with alpha-synuclein aggregation in transgenic
mice. *Proceedings of the National Academy of Sciences of the United States of America* **99**, 8968-
8973, doi:10.1073/pnas.132197599 (2002).
- 466 Schweighauser, M. *et al.* Formaldehyde-fixed brain tissue from spontaneously ill alpha-synuclein
transgenic mice induces fatal alpha-synucleinopathy in transgenic hosts. *Acta neuropathologica*
129, 157-159, doi:10.1007/s00401-014-1360-5 (2015).
- 467 Lo Bianco, C., Ridet, J. L., Schneider, B. L., Deglon, N. & Aebischer, P. alpha -Synucleinopathy and
selective dopaminergic neuron loss in a rat lentiviral-based model of Parkinson's disease.
Proceedings of the National Academy of Sciences of the United States of America **99**, 10813-10818,
doi:10.1073/pnas.152339799 (2002).
- 468 Luk, K. C. *et al.* Molecular and Biological Compatibility with Host Alpha-Synuclein Influences Fibril
Pathogenicity. *Cell Rep* **16**, 3373-3387, doi:10.1016/j.celrep.2016.08.053 (2016).
- 469 Richfield, E. K. *et al.* Behavioral and neurochemical effects of wild-type and mutated human alpha-
synuclein in transgenic mice. *Experimental neurology* **175**, 35-48 (2002).
- 470 Rey, N. L. *et al.* Widespread transneuronal propagation of α -synucleinopathy triggered in olfactory
bulb mimics prodromal Parkinson's disease. *The Journal of experimental medicine* **213**, 1759-
1778, doi:10.1084/jem.20160368 (2016).
- 471 Rockenstein, E. *et al.* Differential neuropathological alterations in transgenic mice expressing
alpha-synuclein from the platelet-derived growth factor and Thy-1 promoters. *Journal of
neuroscience research* **68**, 568-578, doi:10.1002/jnr.10231 (2002).
- 472 Breid, S. *et al.* Neuroinvasion of alpha-Synuclein Prionoids after Intraperitoneal and Intraglossal
Inoculation. *Journal of virology* **90**, 9182-9193, doi:10.1128/jvi.01399-16 (2016).
- 473 Neumann, M. *et al.* Misfolded proteinase K-resistant hyperphosphorylated alpha-synuclein in
aged transgenic mice with locomotor deterioration and in human alpha-synucleinopathies. *The
Journal of clinical investigation* **110**, 1429-1439, doi:10.1172/JCI15777 (2002).
- 474 Kim, C. *et al.* Exposure to bacterial endotoxin generates a distinct strain of alpha-synuclein fibril.
Sci Rep **6**, 30891, doi:10.1038/srep30891 (2016).
- 475 Gomez-Isla, T. *et al.* Motor dysfunction and gliosis with preserved dopaminergic markers in human
alpha-synuclein A30P transgenic mice. *Neurobiology of aging* **24**, 245-258 (2003).
- 476 Tarutani, A. *et al.* The Effect of Fragmented Pathogenic α -Synuclein Seeds on Prion-like
Propagation. *The Journal of biological chemistry* **291**, 18675-18688,
doi:10.1074/jbc.M116.734707 (2016).
- 477 Kirik, D. *et al.* Nigrostriatal alpha-synucleinopathy induced by viral vector-mediated
overexpression of human alpha-synuclein: a new primate model of Parkinson's disease.
Proceedings of the National Academy of Sciences of the United States of America **100**, 2884-2889,
doi:10.1073/pnas.0536383100 (2003).
- 478 Karampetsou, M. *et al.* Phosphorylated exogenous alpha-synuclein fibrils exacerbate pathology
and induce neuronal dysfunction in mice. *Sci Rep* **7**, 16533, doi:10.1038/s41598-017-15813-8
(2017).

- 479 Lauwers, E. *et al.* Neuropathology and neurodegeneration in rodent brain induced by lentiviral
vector-mediated overexpression of alpha-synuclein. *Brain pathology (Zurich, Switzerland)* **13**,
364-372 (2003).
- 480 Abdelmotilib, H. *et al.* α -Synuclein fibril-induced inclusion spread in rats and mice correlates with
dopaminergic Neurodegeneration. *Neurobiology of disease* **105**, 84-98,
doi:10.1016/j.nbd.2017.05.014 (2017).
- 481 Thiruchelvam, M. J., Powers, J. M., Cory-Slechta, D. A. & Richfield, E. K. Risk factors for
dopaminergic neuron loss in human alpha-synuclein transgenic mice. *The European journal of
neuroscience* **19**, 845-854 (2004).
- 482 Blumenstock, S. *et al.* Seeding and transgenic overexpression of alpha-synuclein triggers dendritic
spine pathology in the neocortex. *EMBO molecular medicine* **9**, 716-731,
doi:10.15252/emmm.201607305 (2017).
- 483 Yamada, M., Iwatsubo, T., Mizuno, Y. & Mochizuki, H. Overexpression of alpha-synuclein in rat
substantia nigra results in loss of dopaminergic neurons, phosphorylation of alpha-synuclein and
activation of caspase-9: resemblance to pathogenetic changes in Parkinson's disease. *J
Neurochem* **91**, 451-461, doi:10.1111/j.1471-4159.2004.02728.x (2004).
- 484 Rutherford, N. J. *et al.* Comparison of the in vivo induction and transmission of alpha-synuclein
pathology by mutant alpha-synuclein fibril seeds in transgenic mice. *Hum Mol Genet* **26**, 4906-
4915, doi:10.1093/hmg/ddx371 (2017).
- 485 Chandra, S., Gallardo, G., Fernandez-Chacon, R., Schluter, O. M. & Sudhof, T. C. Alpha-synuclein
cooperates with CSPalpha in preventing neurodegeneration. *Cell* **123**, 383-396,
doi:10.1016/j.cell.2005.09.028 (2005).
- 486 Sorrentino, Z. A. *et al.* Intrastriatal injection of alpha-synuclein can lead to widespread
synucleinopathy independent of neuroanatomic connectivity. *Mol Neurodegener* **12**, 40,
doi:10.1186/s13024-017-0182-z (2017).
- 487 Eslamboli, A. *et al.* Long-term consequences of human alpha-synuclein overexpression in the
primate ventral midbrain. *Brain : a journal of neurology* **130**, 799-815, doi:10.1093/brain/awl382
(2007).
- 488 Harms, A. S. *et al.* α -Synuclein fibrils recruit peripheral immune cells in the rat brain prior to
neurodegeneration. *Acta neuropathologica communications* **5**, 85-85, doi:10.1186/s40478-017-
0494-9 (2017).
- 489 Shimozaawa, A. *et al.* Propagation of pathological alpha-synuclein in marmoset brain. *Acta
neuropathologica communications* **5**, 12, doi:10.1186/s40478-017-0413-0 (2017).
- 490 St Martin, J. L. *et al.* Dopaminergic neuron loss and up-regulation of chaperone protein mRNA
induced by targeted over-expression of alpha-synuclein in mouse substantia nigra. *J Neurochem*
100, 1449-1457, doi:10.1111/j.1471-4159.2006.04310.x (2007).
- 491 Nouraei, N. *et al.* Critical appraisal of pathology transmission in the α -synuclein fibril model of
Lewy body disorders. *Experimental neurology* **299**, 172-196,
doi:https://doi.org/10.1016/j.expneurol.2017.10.017 (2018).
- 492 Nuber, S. *et al.* Neurodegeneration and motor dysfunction in a conditional model of Parkinson's
disease. *The Journal of neuroscience : the official journal of the Society for Neuroscience* **28**, 2471-
2484, doi:10.1523/JNEUROSCI.3040-07.2008 (2008).
- 493 Luna, E. *et al.* Differential α -synuclein expression contributes to selective vulnerability of
hippocampal neuron subpopulations to fibril-induced toxicity. *Acta neuropathologica* **135**, 855-
875, doi:10.1007/s00401-018-1829-8 (2018).
- 494 Wakamatsu, M. *et al.* Selective loss of nigral dopamine neurons induced by overexpression of
truncated human alpha-synuclein in mice. *Neurobiology of aging* **29**, 574-585,
doi:10.1016/j.neurobiolaging.2006.11.017 (2008).

- 495 Okuzumi, A. *et al.* Rapid dissemination of alpha-synuclein seeds through neural circuits in an in-
vivo prion-like seeding experiment. *Acta neuropathologica communications* **6**, 96,
doi:10.1186/s40478-018-0587-0 (2018).
- 496 Azeredo da Silveira, S. *et al.* Phosphorylation does not prompt, nor prevent, the formation of
alpha-synuclein toxic species in a rat model of Parkinson's disease. *Hum Mol Genet* **18**, 872-887,
doi:10.1093/hmg/ddn417 (2009).
- 497 Rey, N. L. *et al.* Spread of aggregates after olfactory bulb injection of alpha-synuclein fibrils is
associated with early neuronal loss and is reduced long term. *Acta neuropathologica* **135**, 65-83,
doi:10.1007/s00401-017-1792-9 (2018).
- 498 Daher, J. P. *et al.* Conditional transgenic mice expressing C-terminally truncated human alpha-
synuclein (alphaSyn119) exhibit reduced striatal dopamine without loss of nigrostriatal pathway
dopaminergic neurons. *Mol Neurodegener* **4**, 34, doi:10.1186/1750-1326-4-34 (2009).
- 499 Duffy, M. F. *et al.* Lewy body-like alpha-synuclein inclusions trigger reactive microgliosis prior to
nigral degeneration. *Journal of neuroinflammation* **15**, 129, doi:10.1186/s12974-018-1171-z
(2018).
- 500 Cao, S., Theodore, S. & Standaert, D. G. Fcγ receptors are required for NF-κB signaling,
microglial activation and dopaminergic neurodegeneration in an AAV-synuclein mouse model of
Parkinson's disease. *Mol Neurodegener* **5**, 42, doi:10.1186/1750-1326-5-42 (2010).
- 501 Ayers, J. I. *et al.* Localized Induction of Wild-Type and Mutant Alpha-Synuclein Aggregation
Reveals Propagation along Neuroanatomical Tracts. *Journal of virology* **92**, doi:10.1128/jvi.00586-
18 (2018).
- 502 Emmer, K. L., Waxman, E. A., Covy, J. P. & Giasson, B. I. E46K human alpha-synuclein transgenic
mice develop Lewy-like and tau pathology associated with age-dependent, detrimental motor
impairment. *The Journal of biological chemistry* **286**, 35104-35118, doi:10.1074/jbc.M111.247965
(2011).
- 503 Milanese, C. *et al.* Activation of the DNA damage response in vivo in synucleinopathy models of
Parkinson's disease. *Cell death & disease* **9**, 818, doi:10.1038/s41419-018-0848-7 (2018).
- 504 Decressac, M., Mattsson, B., Lundblad, M., Weikop, P. & Bjorklund, A. Progressive
neurodegenerative and behavioural changes induced by AAV-mediated overexpression of alpha-
synuclein in midbrain dopamine neurons. *Neurobiology of disease* **45**, 939-953,
doi:10.1016/j.nbd.2011.12.013 (2012).
- 505 Terada, M. *et al.* The effect of truncation on prion-like properties of alpha-synuclein. *The Journal
of biological chemistry* **293**, 13910-13920, doi:10.1074/jbc.RA118.001862 (2018).
- 506 Cannon, J. R. *et al.* Expression of human E46K-mutated alpha-synuclein in BAC-transgenic rats
replicates early-stage Parkinson's disease features and enhances vulnerability to mitochondrial
impairment. *Experimental neurology* **240**, 44-56, doi:10.1016/j.expneurol.2012.11.007 (2013).
- 507 Durante, V. *et al.* Alpha-synuclein targets GluN2A NMDA receptor subunit causing striatal synaptic
dysfunction and visuospatial memory alteration. *Brain : a journal of neurology* **142**, 1365-1385,
doi:10.1093/brain/awz065 (2019).
- 508 Nuber, S. *et al.* A progressive dopaminergic phenotype associated with neurotoxic conversion of
alpha-synuclein in BAC-transgenic rats. *Brain : a journal of neurology* **136**, 412-432,
doi:10.1093/brain/awz358 (2013).
- 509 Earls, R. H. *et al.* Intrastriatal injection of preformed alpha-synuclein fibrils alters central and
peripheral immune cell profiles in non-transgenic mice. *Journal of neuroinflammation* **16**, 250,
doi:10.1186/s12974-019-1636-8 (2019).
- 510 Oliveras-Salva, M. *et al.* rAAV2/7 vector-mediated overexpression of alpha-synuclein in mouse
substantia nigra induces protein aggregation and progressive dose-dependent
neurodegeneration. *Mol Neurodegener* **8**, 44, doi:10.1186/1750-1326-8-44 (2013).

- 511 Espa, E. *et al.* Seeding of protein aggregation causes cognitive impairment in rat model of cortical synucleinopathy. *Movement Disorders* **34**, 1699-1710, doi:10.1002/mds.27810 (2019).
- 512 Rothman, S. M. *et al.* Neuronal expression of familial Parkinson's disease A53T alpha-synuclein causes early motor impairment, reduced anxiety and potential sleep disturbances in mice. *Journal of Parkinson's disease* **3**, 215-229, doi:10.3233/JPD-120130 (2013).
- 513 Sastry, N. *et al.* No apparent transmission of transgenic α -synuclein into nigrostriatal dopaminergic neurons in multiple mouse models. *Translational neurodegeneration* **4**, 23, doi:10.1186/s40035-015-0046-9 (2015).
- 514 Hayakawa, H. *et al.* Structurally distinct α -synuclein fibrils induce robust parkinsonian pathology. *Movement Disorders* **35**, 256-267, doi:10.1002/mds.27887 (2020).
- 515 Thakur, P. *et al.* Modeling Parkinson's disease pathology by combination of fibril seeds and alpha-synuclein overexpression in the rat brain. *Proceedings of the National Academy of Sciences of the United States of America* **114**, E8284-E8293, doi:10.1073/pnas.1710442114 (2017).
- 516 Zhang, J. *et al.* Apoptosis signal regulating kinase 1 deletion mitigates α -synuclein pre-formed fibril propagation in mice. *Neurobiology of aging* **85**, 49-57, doi:https://doi.org/10.1016/j.neurobiolaging.2019.09.012 (2020).
- 517 Wegrzynowicz, M. *et al.* Depopulation of dense α -synuclein aggregates is associated with rescue of dopamine neuron dysfunction and death in a new Parkinson's disease model. *Acta neuropathologica* **138**, 575-595, doi:10.1007/s00401-019-02023-x (2019).
- 518 Burtscher, J. *et al.* Chronic corticosterone aggravates behavioural and neuronal symptomatology in a mouse model of alpha-synuclein pathology. *Neurobiology of aging*, doi:https://doi.org/10.1016/j.neurobiolaging.2019.08.007 (2019).
- 519 Stoyka, L. E. *et al.* Behavioral defects associated with amygdala and cortical dysfunction in mice with seeded α -synuclein inclusions. *Neurobiology of disease* **134**, 104708, doi:https://doi.org/10.1016/j.nbd.2019.104708 (2020).
- 520 Kuo, Y. M. *et al.* Extensive enteric nervous system abnormalities in mice transgenic for artificial chromosomes containing Parkinson disease-associated alpha-synuclein gene mutations precede central nervous system changes. *Hum Mol Genet* **19**, 1633-1650, doi:10.1093/hmg/ddq038 (2010).
- 521 Pan-Montojo, F. *et al.* Progression of Parkinson's disease pathology is reproduced by intragastric administration of rotenone in mice. *PLoS One* **5**, e8762, doi:10.1371/journal.pone.0008762 (2010).
- 522 Holmqvist, S. *et al.* Direct evidence of Parkinson pathology spread from the gastrointestinal tract to the brain in rats. *Acta neuropathologica* **128**, 805-820, doi:10.1007/s00401-014-1343-6 (2014).
- 523 McCormack, A. L. *et al.* Pathologic modifications of alpha-synuclein in 1-methyl-4-phenyl-1,2,3,6-tetrahydropyridine (MPTP)-treated squirrel monkeys. *J Neuropathol Exp Neurol* **67**, 793-802, doi:10.1097/NEN.0b013e318180f0bd (2008).
- 524 Uemura, N. *et al.* Inoculation of α -synuclein preformed fibrils into the mouse gastrointestinal tract induces Lewy body-like aggregates in the brainstem via the vagus nerve. *Molecular Neurodegeneration* **13**, doi:10.1186/s13024-018-0257-5 (2018).
- 525 Manfredsson, F. P. *et al.* Induction of alpha-synuclein pathology in the enteric nervous system of the rat and non-human primate results in gastrointestinal dysmotility and transient CNS pathology. *Neurobiology of disease* **112**, 106-118, doi:10.1016/j.nbd.2018.01.008 (2018).
- 526 Kim, S. *et al.* Transneuronal Propagation of Pathologic α -Synuclein from the Gut to the Brain Models Parkinson's Disease. *Neuron* **103**, 627-641.e627, doi:https://doi.org/10.1016/j.neuron.2019.05.035 (2019).

- 527 Halliday, G. *et al.* No Lewy pathology in monkeys with over 10 years of severe MPTP Parkinsonism. *Movement disorders : official journal of the Movement Disorder Society* **24**, 1519-1523, doi:10.1002/mds.22481 (2009).
- 528 Van Den Berge, N. *et al.* Evidence for bidirectional and trans-synaptic parasympathetic and sympathetic propagation of alpha-synuclein in rats. *Acta neuropathologica* **138**, 535-550, doi:10.1007/s00401-019-02040-w (2019).
- 529 Betarbet, R. *et al.* Chronic systemic pesticide exposure reproduces features of Parkinson's disease. *Nat Neurosci* **3**, 1301-1306, doi:10.1038/81834 (2000).
- 530 Ahn, E. H. *et al.* Initiation of Parkinson's disease from gut to brain by δ -secretase. *Cell Research* **30**, 70-87, doi:10.1038/s41422-019-0241-9 (2020).
- 531 Sherer, T. B., Kim, J. H., Betarbet, R. & Greenamyre, J. T. Subcutaneous rotenone exposure causes highly selective dopaminergic degeneration and alpha-synuclein aggregation. *Experimental neurology* **179**, 9-16 (2003).
- 532 Challis, C. *et al.* Gut-seeded α -synuclein fibrils promote gut dysfunction and brain pathology specifically in aged mice. *Nature Neuroscience*, doi:10.1038/s41593-020-0589-7 (2020).
- 533 McNaught, K. S., Perl, D. P., Brownell, A. L. & Olanow, C. W. Systemic exposure to proteasome inhibitors causes a progressive model of Parkinson's disease. *Annals of neurology* **56**, 149-162, doi:10.1002/ana.20186 (2004).
- 534 Musgrove, R. E. *et al.* Oxidative stress in vagal neurons promotes parkinsonian pathology and intercellular α -synuclein transfer. *The Journal of clinical investigation* **129**, 3738-3753, doi:10.1172/jci127330 (2019).
- 535 Arosio, P., Knowles, T. P. & Linse, S. On the lag phase in amyloid fibril formation. *Phys Chem Chem Phys* **17**, 7606-7618, doi:10.1039/c4cp05563b (2015).
- 536 Lashuel, H. A. *et al.* Alpha-synuclein, especially the Parkinson's disease-associated mutants, forms pore-like annular and tubular protofibrils. *Journal of molecular biology* **322**, 1089-1102 (2002).
- 537 Bertoncini, C. W. *et al.* Release of long-range tertiary interactions potentiates aggregation of natively unstructured alpha-synuclein. *Proceedings of the National Academy of Sciences of the United States of America* **102**, 1430-1435, doi:10.1073/pnas.0407146102 (2005).
- 538 Sharon, R. *et al.* The formation of highly soluble oligomers of alpha-synuclein is regulated by fatty acids and enhanced in Parkinson's disease. *Neuron* **37**, 583-595, doi:10.1016/s0896-6273(03)00024-2 (2003).
- 539 Sengupta, U. *et al.* Pathological interface between oligomeric alpha-synuclein and tau in synucleinopathies. *Biol Psychiatry* **78**, 672-683, doi:10.1016/j.biopsych.2014.12.019 (2015).
- 540 El-Agnaf, O. M. *et al.* Detection of oligomeric forms of alpha-synuclein protein in human plasma as a potential biomarker for Parkinson's disease. *FASEB journal : official publication of the Federation of American Societies for Experimental Biology* **20**, 419-425, doi:10.1096/fj.03-1449com (2006).
- 541 Tokuda, T. *et al.* Detection of elevated levels of α -synuclein oligomers in CSF from patients with Parkinson disease. *Neurology* **75**, 1766-1772, doi:10.1212/WNL.0b013e3181fd613b (2010).
- 542 Park, M. J., Cheon, S. M., Bae, H. R., Kim, S. H. & Kim, J. W. Elevated levels of α -synuclein oligomer in the cerebrospinal fluid of drug-naïve patients with Parkinson's disease. *J Clin Neurol* **7**, 215-222, doi:10.3988/jcn.2011.7.4.215 (2011).
- 543 Majbour, N. K. *et al.* Cerebrospinal α -Synuclein Oligomers Reflect Disease Motor Severity in DeNoPa Longitudinal Cohort. *Movement Disorders* **36**, 2048-2056, doi:https://doi.org/10.1002/mds.28611 (2021).
- 544 Majbour, N. K. *et al.* Oligomeric and phosphorylated alpha-synuclein as potential CSF biomarkers for Parkinson's disease. *Mol Neurodegener* **11**, 7, doi:10.1186/s13024-016-0072-9 (2016).

- 545 Foulds, P. G. *et al.* Post mortem cerebrospinal fluid α -synuclein levels are raised in multiple system atrophy and distinguish this from the other α -synucleinopathies, Parkinson's disease and Dementia with Lewy bodies. *Neurobiology of disease* **45**, 188-195, doi:10.1016/j.nbd.2011.08.003 (2012).
- 546 Kayed, R. *et al.* Common structure of soluble amyloid oligomers implies common mechanism of pathogenesis. *Science* **300**, 486-489, doi:10.1126/science.1079469 (2003).
- 547 Zhang, X. *et al.* Conformation-dependent scFv antibodies specifically recognize the oligomers assembled from various amyloids and show colocalization of amyloid fibrils with oligomers in patients with amyloidoses. *Biochim Biophys Acta* **1814**, 1703-1712, doi:10.1016/j.bbapap.2011.09.005 (2011).
- 548 Tanji, K. *et al.* Proteinase K-resistant α -synuclein is deposited in presynapses in human Lewy body disease and A53T α -synuclein transgenic mice. *Acta neuropathologica* **120**, 145-154, doi:10.1007/s00401-010-0676-z (2010).
- 549 Kramer, M. L. & Schulz-Schaeffer, W. J. Presynaptic α -Synuclein Aggregates, Not Lewy Bodies, Cause Neurodegeneration in Dementia with Lewy Bodies. *The Journal of Neuroscience* **27**, 1405, doi:10.1523/JNEUROSCI.4564-06.2007 (2007).
- 550 Schulz-Schaeffer, W. J. The synaptic pathology of alpha-synuclein aggregation in dementia with Lewy bodies, Parkinson's disease and Parkinson's disease dementia. *Acta neuropathologica* **120**, 131-143, doi:10.1007/s00401-010-0711-0 (2010).
- 551 Sekiya, H. *et al.* Wide distribution of alpha-synuclein oligomers in multiple system atrophy brain detected by proximity ligation. *Acta neuropathologica* **137**, 455-466, doi:10.1007/s00401-019-01961-w (2019).
- 552 Volles, M. J. & Lansbury, P. T., Jr. Vesicle permeabilization by protofibrillar alpha-synuclein is sensitive to Parkinson's disease-linked mutations and occurs by a pore-like mechanism. *Biochemistry* **41**, 4595-4602 (2002).
- 553 Butterfield, S. M. & Lashuel, H. A. Amyloidogenic Protein–Membrane Interactions: Mechanistic Insight from Model Systems. *Angewandte Chemie International Edition* **49**, 5628-5654, doi:https://doi.org/10.1002/anie.200906670 (2010).
- 554 Schmidt, F. *et al.* Single-Channel Electrophysiology Reveals a Distinct and Uniform Pore Complex Formed by α -Synuclein Oligomers in Lipid Membranes. *PLOS ONE* **7**, e42545, doi:10.1371/journal.pone.0042545 (2012).
- 555 Zhang, H., Griggs, A., Rochet, J. C. & Stanciu, L. A. In vitro study of α -synuclein protofibrils by cryo-EM suggests a Cu(2+)-dependent aggregation pathway. *Biophysical journal* **104**, 2706-2713, doi:10.1016/j.bpj.2013.04.050 (2013).
- 556 Fusco, G. *et al.* Structural basis of membrane disruption and cellular toxicity by α -synuclein oligomers. *Science* **358**, 1440-1443, doi:doi:10.1126/science.aan6160 (2017).
- 557 Yoshiike, Y., Kaye, R., Milton, S. C., Takashima, A. & Glabe, C. G. Pore-Forming Proteins Share Structural and Functional Homology with Amyloid Oligomers. *NeuroMolecular Medicine* **9**, 270-275, doi:10.1007/s12017-007-0003-6 (2007).
- 558 Choi, B. K. *et al.* Large α -synuclein oligomers inhibit neuronal SNARE-mediated vesicle docking. *Proceedings of the National Academy of Sciences of the United States of America* **110**, 4087-4092, doi:10.1073/pnas.1218424110 (2013).
- 559 Prots, I. *et al.* α -Synuclein oligomers impair neuronal microtubule-kinesin interplay. *The Journal of biological chemistry* **288**, 21742-21754, doi:10.1074/jbc.M113.451815 (2013).
- 560 Diógenes, M. J. *et al.* Extracellular alpha-synuclein oligomers modulate synaptic transmission and impair LTP via NMDA-receptor activation. *The Journal of neuroscience : the official journal of the Society for Neuroscience* **32**, 11750-11762, doi:10.1523/jneurosci.0234-12.2012 (2012).

- 561 van Diggelen, F. *et al.* Two conformationally distinct α -synuclein oligomers share common epitopes and the ability to impair long-term potentiation. *PLoS One* **14**, e0213663, doi:10.1371/journal.pone.0213663 (2019).
- 562 Trudler, D. *et al.* α -Synuclein Oligomers Induce Glutamate Release from Astrocytes and Excessive Extrasynaptic NMDAR Activity in Neurons, Thus Contributing to Synapse Loss. *The Journal of neuroscience : the official journal of the Society for Neuroscience* **41**, 2264-2273, doi:10.1523/jneurosci.1871-20.2020 (2021).
- 563 Colla, E. *et al.* Accumulation of toxic α -synuclein oligomer within endoplasmic reticulum occurs in α -synucleinopathy in vivo. *The Journal of neuroscience : the official journal of the Society for Neuroscience* **32**, 3301-3305, doi:10.1523/jneurosci.5368-11.2012 (2012).
- 564 Colla, E. *et al.* Endoplasmic reticulum stress is important for the manifestations of α -synucleinopathy in vivo. *The Journal of neuroscience : the official journal of the Society for Neuroscience* **32**, 3306-3320, doi:10.1523/jneurosci.5367-11.2012 (2012).
- 565 Castillo-Carranza, D. L. *et al.* Differential activation of the ER stress factor XBP1 by oligomeric assemblies. *Neurochemical research* **37**, 1707-1717, doi:10.1007/s11064-012-0780-7 (2012).
- 566 Ludtmann, M. H. R. *et al.* α -synuclein oligomers interact with ATP synthase and open the permeability transition pore in Parkinson's disease. *Nature Communications* **9**, 2293, doi:10.1038/s41467-018-04422-2 (2018).
- 567 Luth, E. S., Stavrovskaya, I. G., Bartels, T., Kristal, B. S. & Selkoe, D. J. Soluble, prefibrillar α -synuclein oligomers promote complex I-dependent, Ca^{2+} -induced mitochondrial dysfunction. *The Journal of biological chemistry* **289**, 21490-21507, doi:10.1074/jbc.M113.545749 (2014).
- 568 Di Maio, R. *et al.* α -Synuclein binds to TOM20 and inhibits mitochondrial protein import in Parkinson's disease. *Science translational medicine* **8**, 342ra378, doi:10.1126/scitranslmed.aaf3634 (2016).
- 569 Plotegher, N., Gratton, E. & Bubacco, L. Number and Brightness analysis of alpha-synuclein oligomerization and the associated mitochondrial morphology alterations in live cells. *Biochimica et Biophysica Acta (BBA) - General Subjects* **1840**, 2014-2024, doi:https://doi.org/10.1016/j.bbagen.2014.02.013 (2014).
- 570 Chavarría, C., Rodríguez-Bottero, S., Quijano, C., Cassina, P. & Souza, J. M. Impact of monomeric, oligomeric and fibrillar alpha-synuclein on astrocyte reactivity and toxicity to neurons. *The Biochemical journal* **475**, 3153-3169, doi:10.1042/bcj20180297 (2018).
- 571 Kumar, V. *et al.* Alpha-synuclein aggregation, Ubiquitin proteasome system impairment, and l-Dopa response in zinc-induced Parkinsonism: resemblance to sporadic Parkinson's disease. *Molecular and Cellular Biochemistry* **444**, 149-160, doi:10.1007/s11010-017-3239-y (2018).
- 572 Emmanouilidou, E., Stefanis, L. & Vekrellis, K. Cell-produced α -synuclein oligomers are targeted to, and impair, the 26S proteasome. *Neurobiology of aging* **31**, 953-968, doi:https://doi.org/10.1016/j.neurobiolaging.2008.07.008 (2010).
- 573 Wilkaniec, A. *et al.* Extracellular Alpha-Synuclein Oligomers Induce Parkin S-Nitrosylation: Relevance to Sporadic Parkinson's Disease Etiopathology. *Molecular neurobiology* **56**, 125-140, doi:10.1007/s12035-018-1082-0 (2019).
- 574 Roberts, H. L. & Brown, D. R. Seeking a mechanism for the toxicity of oligomeric α -synuclein. *Biomolecules* **5**, 282-305, doi:10.3390/biom5020282 (2015).
- 575 Yang, X., Wang, B., Hoop, C. L., Williams, J. K. & Baum, J. NMR unveils an N-terminal interaction interface on acetylated- α -synuclein monomers for recruitment to fibrils. *Proceedings of the National Academy of Sciences* **118**, e2017452118, doi:doi:10.1073/pnas.2017452118 (2021).
- 576 Lau, D. *et al.* Single Molecule Fingerprinting Reveals Different Amplification Properties of α -Synuclein Oligomers and Preformed Fibrils in Seeding Assay. *ACS Chem Neurosci* **13**, 883-896, doi:10.1021/acscchemneuro.1c00553 (2022).

- 577 Bae, E. J. *et al.* Lipid peroxidation product 4-hydroxy-2-nonenal promotes seeding-capable
oligomer formation and cell-to-cell transfer of α -synuclein. *Antioxid Redox Signal* **18**, 770-783,
doi:10.1089/ars.2011.4429 (2013).
- 578 Danzer, K. M. *et al.* Heat-shock protein 70 modulates toxic extracellular α -synuclein oligomers and
rescues trans-synaptic toxicity. *FASEB journal : official publication of the Federation of American
Societies for Experimental Biology* **25**, 326-336, doi:10.1096/fj.10-164624 (2011).
- 579 Shearer, L. J., Petersen, N. O. & Woodside, M. T. Internalization of α -synuclein oligomers into SH-
SY5Y cells. *Biophysical journal* **120**, 877-885, doi:10.1016/j.bpj.2020.12.031 (2021).
- 580 Danzer, K. M., Krebs, S. K., Wolff, M., Birk, G. & Hengerer, B. Seeding induced by α -synuclein
oligomers provides evidence for spreading of α -synuclein pathology. *Journal of Neurochemistry*
111, 192-203, doi:https://doi.org/10.1111/j.1471-4159.2009.06324.x (2009).
- 581 Danzer, K. M. *et al.* Exosomal cell-to-cell transmission of alpha synuclein oligomers. *Mol
Neurodegener* **7**, 42, doi:10.1186/1750-1326-7-42 (2012).
- 582 van Diggelen, F., Tepper, A. W. J. W., Apetri, M. M. & Otzen, D. E. α -Synuclein Oligomers: A Study
in Diversity. *Israel journal of chemistry* **57**, 699-723, doi:https://doi.org/10.1002/ijch.201600116
(2017).
- 583 Rey, N. L., Petit, G. H., Bousset, L., Melki, R. & Brundin, P. Transfer of human α -synuclein from the
olfactory bulb to interconnected brain regions in mice. *Acta neuropathologica* **126**, 555-573,
doi:10.1007/s00401-013-1160-3 (2013).
- 584 Fagerqvist, T. *et al.* Off-pathway α -synuclein oligomers seem to alter α -synuclein turnover in a cell
model but lack seeding capability in vivo. *Amyloid* **20**, 233-244,
doi:10.3109/13506129.2013.835726 (2013).
- 585 Surmeier, D. J., Obeso, J. A. & Halliday, G. M. Selective neuronal vulnerability in Parkinson disease.
Nature reviews. Neuroscience **18**, 101-113, doi:10.1038/nrn.2016.178 (2017).
- 586 Milber, J. M. *et al.* Lewy pathology is not the first sign of degeneration in vulnerable neurons in
Parkinson disease. *Neurology* **79**, 2307-2314, doi:10.1212/WNL.0b013e318278fe32 (2012).
- 587 Damier, P., Hirsch, E. C., Agid, Y. & Graybiel, A. M. The substantia nigra of the human brain. II.
Patterns of loss of dopamine-containing neurons in Parkinson's disease. *Brain : a journal of
neurology* **122 (Pt 8)**, 1437-1448 (1999).
- 588 Halliday, G. M. *et al.* Midbrain neuropathology in idiopathic Parkinson's disease and diffuse Lewy
body disease. *Journal of clinical neuroscience : official journal of the Neurosurgical Society of
Australasia* **3**, 52-60 (1996).
- 589 Halliday, G. M. *et al.* Neuropathology of immunohistochemically identified brainstem neurons in
Parkinson's disease. *Annals of neurology* **27**, 373-385, doi:10.1002/ana.410270405 (1990).
- 590 Harding, A. J., Stimson, E., Henderson, J. M. & Halliday, G. M. Clinical correlates of selective
pathology in the amygdala of patients with Parkinson's disease. *Brain : a journal of neurology* **125**,
2431-2445 (2002).
- 591 Ansorge, O., Daniel, S. E. & Pearce, R. K. Neuronal loss and plasticity in the supraoptic nucleus in
Parkinson's disease. *Neurology* **49**, 610-613 (1997).
- 592 MacDonald, V. & Halliday, G. M. Selective loss of pyramidal neurons in the pre-supplementary
motor cortex in Parkinson's disease. *Movement disorders : official journal of the Movement
Disorder Society* **17**, 1166-1173, doi:10.1002/mds.10258 (2002).
- 593 Sulzer, D. Multiple hit hypotheses for dopamine neuron loss in Parkinson's disease. *Trends
Neurosci* **30**, 244-250, doi:10.1016/j.tins.2007.03.009 (2007).
- 594 Roberts, R. C. in *The Basal Ganglia VI* (eds Ann M. Graybiel, Mahlon R. DeLong, & Stephen T. Kitai)
369-378 (Springer US, 2003).

595 Matsuda, W. *et al.* Single Nigrostriatal Dopaminergic Neurons Form Widely Spread and Highly
Dense Axonal Arborizations in the Neostriatum. *The Journal of Neuroscience* **29**, 444,
doi:10.1523/JNEUROSCI.4029-08.2009 (2009).

596 Pacelli, C. *et al.* Elevated Mitochondrial Bioenergetics and Axonal Arborization Size Are Key
Contributors to the Vulnerability of Dopamine Neurons. *Curr Biol* **25**, 2349-2360,
doi:10.1016/j.cub.2015.07.050 (2015).

597 Bean, B. P. The action potential in mammalian central neurons. *Nature reviews. Neuroscience* **8**,
451-465, doi:10.1038/nrn2148 (2007).

598 Goldberg, J. A. *et al.* Calcium entry induces mitochondrial oxidant stress in vagal neurons at risk
in Parkinson's disease. *Nature Neuroscience* **15**, 1414-1421, doi:10.1038/nn.3209 (2012).

599 Sanchez-Padilla, J. *et al.* Mitochondrial oxidant stress in locus coeruleus is regulated by activity
and nitric oxide synthase. *Nat Neurosci* **17**, 832-840, doi:10.1038/nn.3717 (2014).

600 Matschke, L. A. *et al.* A concerted action of L- and T-type Ca(2+) channels regulates locus coeruleus
pacemaking. *Mol Cell Neurosci* **68**, 293-302, doi:10.1016/j.mcn.2015.08.012 (2015).

601 Catoni, C., Cali, T. & Brini, M. Calcium, Dopamine and Neuronal Calcium Sensor 1: Their
Contribution to Parkinson's Disease. *Front Mol Neurosci* **12**, doi:10.3389/fnmol.2019.00055
(2019).

602 Xu, J., Minobe, E. & Kameyama, M. Ca²⁺ Dyshomeostasis Links Risk Factors to Neurodegeneration
in Parkinson's Disease. *Frontiers in Cellular Neuroscience* **16**, doi:10.3389/fncel.2022.867385
(2022).

603 Nedergaard, S., Flatman, J. A. & Engberg, I. Nifedipine- and omega-conotoxin-sensitive Ca²⁺
conductances in guinea-pig substantia nigra pars compacta neurones. *J Physiol* **466**, 727-747
(1993).

604 Putzier, I., Kullmann, P. H. M., Horn, J. P. & Levitan, E. S. Cav1.3 channel voltage dependence, not
Ca²⁺ selectivity, drives pacemaker activity and amplifies bursts in nigral dopamine neurons. *The
Journal of neuroscience : the official journal of the Society for Neuroscience* **29**, 15414-15419,
doi:10.1523/JNEUROSCI.4742-09.2009 (2009).

605 Guzman, J. N. *et al.* Oxidant stress evoked by pacemaking in dopaminergic neurons is attenuated
by DJ-1. *Nature* **468**, 696-700, doi:10.1038/nature09536 (2010).

606 Gupta, A., Dawson, V. L. & Dawson, T. M. What causes cell death in Parkinson's disease? *Annals
of neurology* **64 Suppl 2**, S3-15, doi:10.1002/ana.21573 (2008).

607 Wong, E. & Cuervo, A. M. Autophagy gone awry in neurodegenerative diseases. *Nat Neurosci* **13**,
805-811, doi:10.1038/nn.2575 (2010).

608 Gómez-Sintes, R., Ledesma, M. D. & Boya, P. Lysosomal cell death mechanisms in aging. *Ageing
Res Rev* **32**, 150-168, doi:10.1016/j.arr.2016.02.009 (2016).

609 Dufty, B. M. *et al.* Calpain-cleavage of alpha-synuclein: connecting proteolytic processing to
disease-linked aggregation. *Am J Pathol* **170**, 1725-1738, doi:10.2353/ajpath.2007.061232 (2007).

610 Diepenbroek, M. *et al.* Overexpression of the calpain-specific inhibitor calpastatin reduces human
alpha-Synuclein processing, aggregation and synaptic impairment in [A30P]αSyn transgenic mice.
Hum Mol Genet **23**, 3975-3989, doi:10.1093/hmg/ddu112 (2014).

611 Mosharov, E. V. *et al.* Interplay between cytosolic dopamine, calcium, and alpha-synuclein causes
selective death of substantia nigra neurons. *Neuron* **62**, 218-229,
doi:10.1016/j.neuron.2009.01.033 (2009).

612 Volpicelli-Daley, L. A., Luk, K. C. & Lee, V. M. Addition of exogenous alpha-synuclein preformed
fibrils to primary neuronal cultures to seed recruitment of endogenous alpha-synuclein to Lewy
body and Lewy neurite-like aggregates. *Nature protocols* **9**, 2135-2146,
doi:10.1038/nprot.2014.143 (2014).

- 613 Luna, E. *et al.* Differential alpha-synuclein expression contributes to selective vulnerability of
hippocampal neuron subpopulations to fibril-induced toxicity. *Acta neuropathologica* **135**, 855-
875, doi:10.1007/s00401-018-1829-8 (2018).
- 614 Henderson, M. X. *et al.* The roles of connectivity and neuronal phenotype in determining the
pattern of α -synuclein pathology in Parkinson's disease. *Neurobiology of disease* **168**, 105687,
doi:10.1016/j.nbd.2022.105687 (2022).
- 615 Vitak, S. A. *et al.* Sequencing thousands of single-cell genomes with combinatorial indexing.
Nature methods **14**, 302-308, doi:10.1038/nmeth.4154 (2017).
- 616 Bryois, J. *et al.* Genetic identification of cell types underlying brain complex traits yields insights
into the etiology of Parkinson's disease. *Nature genetics* **52**, 482-493, doi:10.1038/s41588-020-
0610-9 (2020).
- 617 Fernandes, H. J. R. *et al.* Single-Cell Transcriptomics of Parkinson's Disease Human In Vitro Models
Reveals Dopamine Neuron-Specific Stress Responses. *Cell Rep* **33**, 108263,
doi:https://doi.org/10.1016/j.celrep.2020.108263 (2020).
- 618 Tiklová, K. *et al.* Single-cell RNA sequencing reveals midbrain dopamine neuron diversity emerging
during mouse brain development. *Nature Communications* **10**, 581, doi:10.1038/s41467-019-
08453-1 (2019).
- 619 Tiklová, K. *et al.* Single cell transcriptomics identifies stem cell-derived graft composition in a
model of Parkinson's disease. *Nature Communications* **11**, 2434, doi:10.1038/s41467-020-16225-
5 (2020).
- 620 Lang, C. *et al.* Single-Cell Sequencing of iPSC-Dopamine Neurons Reconstructs Disease Progression
and Identifies HDAC4 as a Regulator of Parkinson Cell Phenotypes. *Cell Stem Cell* **24**, 93-106.e106,
doi:10.1016/j.stem.2018.10.023 (2019).
- 621 Zhong, J. *et al.* Single-cell brain atlas of Parkinson's disease mouse model. *Journal of Genetics and
Genomics* **48**, 277-288, doi:https://doi.org/10.1016/j.jgg.2021.01.003 (2021).
- 622 Goedert, M., Jakes, R. & Spillantini, M. G. The Synucleinopathies: Twenty Years On. *Journal of
Parkinson's disease* **7**, S51-S69, doi:10.3233/jpd-179005 (2017).
- 623 Lashuel, H. A. Do Lewy bodies contain alpha-synuclein fibrils? and Does it matter? A brief history
and critical analysis of recent reports. *Neurobiology of disease*, 104876,
doi:10.1016/j.nbd.2020.104876 (2020).
- 624 Spillantini, M. G., Crowther, R. A., Jakes, R., Hasegawa, M. & Goedert, M. alpha-Synuclein in
filamentous inclusions of Lewy bodies from Parkinson's disease and dementia with lewy bodies.
Proceedings of the National Academy of Sciences of the United States of America **95**, 6469-6473,
doi:10.1073/pnas.95.11.6469 (1998).
- 625 Colosimo, C., Hughes, A. J., Kilford, L. & Lees, A. J. Lewy body cortical involvement may not always
predict dementia in Parkinson's disease. *Journal of neurology, neurosurgery, and psychiatry* **74**,
852-856, doi:10.1136/jnnp.74.7.852 (2003).
- 626 Parkkinen, L., Pirttilä, T. & Alafuzoff, I. Applicability of current staging/categorization of alpha-
synuclein pathology and their clinical relevance. *Acta neuropathologica* **115**, 399-407,
doi:10.1007/s00401-008-0346-6 (2008).
- 627 Parkkinen, L., Kauppinen, T., Pirttilä, T., Autere, J. M. & Alafuzoff, I. Alpha-synuclein pathology
does not predict extrapyramidal symptoms or dementia. *Annals of neurology* **57**, 82-91,
doi:10.1002/ana.20321 (2005).
- 628 Frigerio, R. *et al.* Incidental Lewy body disease: do some cases represent a preclinical stage of
dementia with Lewy bodies? *Neurobiology of aging* **32**, 857-863,
doi:10.1016/j.neurobiolaging.2009.05.019 (2011).

- 629 Kay, D. M., Kramer, P., Higgins, D., Zabetian, C. P. & Payami, H. Escaping Parkinson's disease: a neurologically healthy octogenarian with the LRRK2 G2019S mutation. *Movement disorders : official journal of the Movement Disorder Society* **20**, 1077-1078, doi:10.1002/mds.20618 (2005).
- 630 Gaig, C. *et al.* LRRK2 Mutations in Spanish Patients With Parkinson Disease: Frequency, Clinical Features, and Incomplete Penetrance. *Archives of neurology* **63**, 377-382, doi:10.1001/archneur.63.3.377 (2006).
- 631 Cookson, M. R., Hardy, J. & Lewis, P. A. Genetic neuropathology of Parkinson's disease. *International journal of clinical and experimental pathology* **1**, 217-231 (2008).
- 632 Johansen, K. K., Torp, S. H., Farrer, M. J., Gustavsson, E. K. & Aasly, J. O. A Case of Parkinson's Disease with No Lewy Body Pathology due to a Homozygous Exon Deletion in Parkin. *Case reports in neurological medicine* **2018**, 6838965, doi:10.1155/2018/6838965 (2018).
- 633 Nelson, P. T. *et al.* Correlation of Alzheimer disease neuropathologic changes with cognitive status: a review of the literature. *J Neuropathol Exp Neurol* **71**, 362-381, doi:10.1097/NEN.0b013e31825018f7 (2012).
- 634 Jung, Y. *et al.* Regional beta-amyloid burden does not correlate with cognitive or language deficits in Alzheimer's disease presenting as aphasia. *European journal of neurology* **23**, 313-319, doi:10.1111/ene.12761 (2016).
- 635 Arboleda-Velasquez, J. F. *et al.* Resistance to autosomal dominant Alzheimer's disease in an APOE3 Christchurch homozygote: a case report. *Nat Med* **25**, 1680-1683, doi:10.1038/s41591-019-0611-3 (2019).
- 636 Conway, K. A. *et al.* Acceleration of oligomerization, not fibrillization, is a shared property of both alpha-synuclein mutations linked to early-onset Parkinson's disease: implications for pathogenesis and therapy. *Proceedings of the National Academy of Sciences of the United States of America* **97**, 571-576, doi:10.1073/pnas.97.2.571 (2000).
- 637 Cappai, R. *et al.* Dopamine promotes alpha-synuclein aggregation into SDS-resistant soluble oligomers via a distinct folding pathway. *FASEB journal : official publication of the Federation of American Societies for Experimental Biology* **19**, 1377-1379, doi:10.1096/fj.04-3437fje (2005).
- 638 Tokuda, T. *et al.* Detection of elevated levels of alpha-synuclein oligomers in CSF from patients with Parkinson disease. *Neurology* **75**, 1766-1772, doi:10.1212/WNL.0b013e3181fd613b (2010).
- 639 Hirohata, M., Ono, K., Morinaga, A., Ikeda, T. & Yamada, M. Cerebrospinal fluid from patients with multiple system atrophy promotes in vitro alpha-synuclein fibril formation. *Neuroscience letters* **491**, 48-52, doi:10.1016/j.neulet.2011.01.005 (2011).
- 640 Wang, W. *et al.* A soluble α -synuclein construct forms a dynamic tetramer. *Proceedings of the National Academy of Sciences* **108**, 17797-17802, doi:10.1073/pnas.1113260108 (2011).
- 641 Vivacqua, G. *et al.* Abnormal Salivary Total and Oligomeric Alpha-Synuclein in Parkinson's Disease. *PLoS One* **11**, e0151156, doi:10.1371/journal.pone.0151156 (2016).
- 642 Hamm-Alvarez, S. F. *et al.* Oligomeric α -synuclein is increased in basal tears of Parkinson's patients. *Biomarkers in Medicine* **13**, 941-952, doi:10.2217/bmm-2019-0167 (2019).
- 643 Paleologou, K. E. *et al.* Detection of elevated levels of soluble α -synuclein oligomers in post-mortem brain extracts from patients with dementia with Lewy bodies. *Brain : a journal of neurology* **132**, 1093-1101, doi:10.1093/brain/awn349 (2009).
- 644 Tofaris, G. K., Razaq, A., Ghatti, B., Lilley, K. S. & Spillantini, M. G. Ubiquitination of alpha-synuclein in Lewy bodies is a pathological event not associated with impairment of proteasome function. *The Journal of biological chemistry* **278**, 44405-44411, doi:10.1074/jbc.M308041200 (2003).
- 645 Jang, A. *et al.* Non-classical exocytosis of alpha-synuclein is sensitive to folding states and promoted under stress conditions. *J Neurochem* **113**, 1263-1274, doi:10.1111/j.1471-4159.2010.06695.x (2010).

- 646 Lee, H. J. *et al.* Assembly-dependent endocytosis and clearance of extracellular alpha-synuclein. *The international journal of biochemistry & cell biology* **40**, 1835-1849, doi:10.1016/j.biocel.2008.01.017 (2008).
- 647 Diógenes, M. J. *et al.* Extracellular Alpha-Synuclein Oligomers Modulate Synaptic Transmission and Impair LTP Via NMDA-Receptor Activation. *The Journal of Neuroscience* **32**, 11750-11762, doi:10.1523/jneurosci.0234-12.2012 (2012).
- 648 Rockenstein, E. *et al.* Accumulation of oligomer-prone alpha-synuclein exacerbates synaptic and neuronal degeneration in vivo. *Brain : a journal of neurology* **137**, 1496-1513, doi:10.1093/brain/awu057 (2014).
- 649 Kaufmann, T. J., Harrison, P. M., Richardson, M. J., Pinheiro, T. J. & Wall, M. J. Intracellular soluble alpha-synuclein oligomers reduce pyramidal cell excitability. *J Physiol* **594**, 2751-2772, doi:10.1113/jp271968 (2016).
- 650 Cuervo, A. M., Stefanis, L., Fredenburg, R., Lansbury, P. T. & Sulzer, D. Impaired degradation of mutant alpha-synuclein by chaperone-mediated autophagy. *Science* **305**, 1292-1295, doi:10.1126/science.1101738 (2004).
- 651 Klucken, J. *et al.* Alpha-synuclein aggregation involves a bafilomycin A 1-sensitive autophagy pathway. *Autophagy* **8**, 754-766, doi:10.4161/auto.19371 (2012).
- 652 Tekirdag, K. & Cuervo, A. M. Chaperone-mediated autophagy and endosomal microautophagy: Joint by a chaperone. *The Journal of biological chemistry* **293**, 5414-5424, doi:10.1074/jbc.R117.818237 (2018).
- 653 Colla, E. *et al.* Endoplasmic Reticulum Stress Is Important for the Manifestations of α -Synucleinopathy *in Vivo*. *The Journal of Neuroscience* **32**, 3306-3320, doi:10.1523/jneurosci.5367-11.2012 (2012).
- 654 Parihar, M. S., Parihar, A., Fujita, M., Hashimoto, M. & Ghafourifar, P. Alpha-synuclein overexpression and aggregation exacerbates impairment of mitochondrial functions by augmenting oxidative stress in human neuroblastoma cells. *The international journal of biochemistry & cell biology* **41**, 2015-2024, doi:10.1016/j.biocel.2009.05.008 (2009).
- 655 Di Maio, R. *et al.* alpha-Synuclein binds to TOM20 and inhibits mitochondrial protein import in Parkinson's disease. *Science translational medicine* **8**, 342ra378, doi:10.1126/scitranslmed.aaf3634 (2016).
- 656 Wilms, H. *et al.* Suppression of MAP kinases inhibits microglial activation and attenuates neuronal cell death induced by alpha-synuclein protofibrils. *International journal of immunopathology and pharmacology* **22**, 897-909, doi:10.1177/039463200902200405 (2009).
- 657 Lashuel, H. A. & Lansbury, P. T. Are amyloid diseases caused by protein aggregates that mimic bacterial pore-forming toxins? *Quarterly Reviews of Biophysics* **39**, 167-201, doi:10.1017/S0033583506004422 (2006).
- 658 Stöckl, M. T., Zijlstra, N. & Subramaniam, V. α -Synuclein Oligomers: an Amyloid Pore? *Molecular neurobiology* **47**, 613-621, doi:10.1007/s12035-012-8331-4 (2013).
- 659 Cremades, N., Chen, S. W. & Dobson, C. M. Structural Characteristics of alpha-Synuclein Oligomers. *International review of cell and molecular biology* **329**, 79-143, doi:10.1016/bs.ircmb.2016.08.010 (2017).
- 660 Ruggeri, F. S. *et al.* Identification and nanomechanical characterization of the fundamental single-strand protofilaments of amyloid α -synuclein fibrils. *Proceedings of the National Academy of Sciences* **115**, 7230-7235, doi:10.1073/pnas.1721220115 (2018).
- 661 Kumar, S. T., Donzelli, S., Chiki, A., Syed, M. M. K. & Lashuel, H. A. A simple, versatile and robust centrifugation-based filtration protocol for the isolation and quantification of alpha-synuclein monomers, oligomers and fibrils: Towards improving experimental reproducibility in alpha-synuclein research. *J Neurochem* **153**, 103-119, doi:10.1111/jnc.14955 (2020).

- 662 Paslawski, W. *et al.* High stability and cooperative unfolding of alpha-synuclein oligomers. *Biochemistry* **53**, 6252-6263, doi:10.1021/bi5007833 (2014).
- 663 Paslawski, W., Mysling, S., Thomsen, K., Jørgensen, T. J. D. & Otzen, D. E. Co-existence of Two Different α -Synuclein Oligomers with Different Core Structures Determined by Hydrogen/Deuterium Exchange Mass Spectrometry. *Angewandte Chemie International Edition* **53**, 7560-7563, doi:10.1002/anie.201400491 (2014).
- 664 Qin, Z. *et al.* Effect of 4-hydroxy-2-nonenal modification on alpha-synuclein aggregation. *The Journal of biological chemistry* **282**, 5862-5870, doi:10.1074/jbc.M608126200 (2007).
- 665 Ehrnhoefer, D. E. *et al.* EGCG redirects amyloidogenic polypeptides into unstructured, off-pathway oligomers. *Nature structural & molecular biology* **15**, 558-566, doi:10.1038/nsmb.1437 (2008).
- 666 Näsström, T. *et al.* Antibodies against Alpha-Synuclein Reduce Oligomerization in Living Cells. *PLOS ONE* **6**, e27230, doi:10.1371/journal.pone.0027230 (2011).
- 667 Tsigelny, I. F., Sharikov, Y., Miller, M. A. & Masliah, E. Mechanism of alpha-synuclein oligomerization and membrane interaction: theoretical approach to unstructured proteins studies. *Nanomedicine* **4**, 350-357, doi:10.1016/j.nano.2008.05.005 (2008).
- 668 Kumar, S. T. *et al.* Characterization and validation of 15 α -synuclein conformation-specific antibodies using well-characterized preparations of α -synuclein monomers, fibrils and oligomers with distinct structures and morphology: How specific are the conformation-specific α -synuclein antibodies? *bioRxiv*, 2020.2006.2015.151514, doi:10.1101/2020.06.15.151514 (2020).
- 669 Covell, D. J. *et al.* Novel conformation-selective alpha-synuclein antibodies raised against different in vitro fibril forms show distinct patterns of Lewy pathology in Parkinson's disease. *Neuropathology and applied neurobiology* **43**, 604-620, doi:10.1111/nan.12402 (2017).
- 670 Guo, J. L. *et al.* Distinct α -synuclein strains differentially promote tau inclusions in neurons. *Cell* **154**, 103-117, doi:10.1016/j.cell.2013.05.057 (2013).
- 671 Vaikath, N. N. *et al.* Generation and characterization of novel conformation-specific monoclonal antibodies for alpha-synuclein pathology. *Neurobiology of disease* **79**, 81-99, doi:10.1016/j.nbd.2015.04.009 (2015).
- 672 Kovacs, G. G. *et al.* An antibody with high reactivity for disease-associated alpha-synuclein reveals extensive brain pathology. *Acta neuropathologica* **124**, 37-50, doi:10.1007/s00401-012-0964-x (2012).
- 673 Giasson, B. I. *et al.* A panel of epitope-specific antibodies detects protein domains distributed throughout human alpha-synuclein in Lewy bodies of Parkinson's disease. *Journal of neuroscience research* **59**, 528-533, doi:10.1002/(sici)1097-4547(20000215)59:4<528::aid-jnr8>3.0.co;2-0 (2000).
- 674 Perrin, R. J. *et al.* Epitope mapping and specificity of the anti-alpha-synuclein monoclonal antibody Syn-1 in mouse brain and cultured cell lines. *Neuroscience letters* **349**, 133-135, doi:10.1016/s0304-3940(03)00781-x (2003).
- 675 Conway, K. A., Rochet, J. C., Bieganski, R. M. & Lansbury, P. T., Jr. Kinetic stabilization of the alpha-synuclein protofibril by a dopamine-alpha-synuclein adduct. *Science* **294**, 1346-1349, doi:10.1126/science.1063522 (2001).
- 676 Norris, E. H. *et al.* Reversible inhibition of alpha-synuclein fibrillization by dopaminochrome-mediated conformational alterations. *The Journal of biological chemistry* **280**, 21212-21219, doi:10.1074/jbc.M412621200 (2005).
- 677 Leong, S. L., Cappai, R., Barnham, K. J. & Pham, C. L. Modulation of alpha-synuclein aggregation by dopamine: a review. *Neurochemical research* **34**, 1838-1846, doi:10.1007/s11064-009-9986-8 (2009).

- 678 Rekas, A. *et al.* The structure of dopamine induced alpha-synuclein oligomers. *European biophysics journal : EBJ* **39**, 1407-1419, doi:10.1007/s00249-010-0595-x (2010).
- 679 Choi, B.-K. *et al.* Large α -synuclein oligomers inhibit neuronal SNARE-mediated vesicle docking. *Proceedings of the National Academy of Sciences* **110**, 4087-4092, doi:10.1073/pnas.1218424110 (2013).
- 680 Planchard, M. S., Exley, S. E., Morgan, S. E. & Rangachari, V. Dopamine-induced alpha-synuclein oligomers show self- and cross-propagation properties. *Protein science : a publication of the Protein Society* **23**, 1369-1379, doi:10.1002/pro.2521 (2014).
- 681 Broersen, K., van den Brink, D., Fraser, G., Goedert, M. & Davletov, B. Alpha-synuclein adopts an alpha-helical conformation in the presence of polyunsaturated fatty acids to hinder micelle formation. *Biochemistry* **45**, 15610-15616, doi:10.1021/bi061743l (2006).
- 682 Trostchansky, A. *et al.* Interaction with phospholipids modulates alpha-synuclein nitration and lipid-protein adduct formation. *The Biochemical journal* **393**, 343-349, doi:10.1042/BJ20051277 (2006).
- 683 Nasstrom, T. *et al.* The lipid peroxidation metabolite 4-oxo-2-nonenal cross-links alpha-synuclein causing rapid formation of stable oligomers. *Biochem Biophys Res Commun* **378**, 872-876, doi:10.1016/j.bbrc.2008.12.005 (2009).
- 684 Näsström, T. *et al.* The lipid peroxidation products 4-oxo-2-nonenal and 4-hydroxy-2-nonenal promote the formation of α -synuclein oligomers with distinct biochemical, morphological, and functional properties. *Free radical biology & medicine* **50**, 428-437, doi:10.1016/j.freeradbiomed.2010.11.027 (2011).
- 685 De Franceschi, G. *et al.* Structural and morphological characterization of aggregated species of alpha-synuclein induced by docosahexaenoic acid. *The Journal of biological chemistry* **286**, 22262-22274, doi:10.1074/jbc.M110.202937 (2011).
- 686 Xiang, W. *et al.* Oxidative stress-induced posttranslational modifications of alpha-synuclein: specific modification of alpha-synuclein by 4-hydroxy-2-nonenal increases dopaminergic toxicity. *Mol Cell Neurosci* **54**, 71-83, doi:10.1016/j.mcn.2013.01.004 (2013).
- 687 Lowe, R., Pountney, D. L., Jensen, P. H., Gai, W. P. & Voelcker, N. H. Calcium(II) selectively induces alpha-synuclein annular oligomers via interaction with the C-terminal domain. *Protein science : a publication of the Protein Society* **13**, 3245-3252, doi:10.1110/ps.04879704 (2004).
- 688 Cole, N. B. *et al.* Metal-catalyzed oxidation of alpha-synuclein: helping to define the relationship between oligomers, protofibrils, and filaments. *The Journal of biological chemistry* **280**, 9678-9690, doi:10.1074/jbc.M409946200 (2005).
- 689 Wright, J. A., Wang, X. & Brown, D. R. Unique copper-induced oligomers mediate alpha-synuclein toxicity. *The FASEB Journal* **23**, 2384-2393, doi:10.1096/fj.09-130039 (2009).
- 690 Schmidt, F. *et al.* Single-channel electrophysiology reveals a distinct and uniform pore complex formed by alpha-synuclein oligomers in lipid membranes. *PLoS One* **7**, e42545, doi:10.1371/journal.pone.0042545 (2012).
- 691 Illes-Toth, E., Ramos, M. R., Cappai, R., Dalton, C. & Smith, D. P. Distinct higher-order alpha-synuclein oligomers induce intracellular aggregation. *The Biochemical journal* **468**, 485-493, doi:10.1042/bj20150159 (2015).
- 692 Ruesink, H. *et al.* Stabilization of α -synuclein oligomers using formaldehyde. *PLOS ONE* **14**, e0216764, doi:10.1371/journal.pone.0216764 (2019).
- 693 Bae, E.-J. *et al.* Lipid peroxidation product 4-hydroxy-2-nonenal promotes seeding-capable oligomer formation and cell-to-cell transfer of α -synuclein. *Antioxidants & redox signaling* **18**, 770-783, doi:10.1089/ars.2011.4429 (2013).
- 694 Fecchio, C. *et al.* α -Synuclein Oligomers Induced by Docosahexaenoic Acid Affect Membrane Integrity. *PLOS ONE* **8**, e82732, doi:10.1371/journal.pone.0082732 (2013).

- 695 Paslawski, W., Lorenzen, N. & Otzen, D. E. Formation and Characterization of alpha-Synuclein
Oligomers. *Methods in molecular biology (Clifton, N.J.)* **1345**, 133-150, doi:10.1007/978-1-4939-
2978-8_9 (2016).
- 696 Mor, D. E. *et al.* Dopamine induces soluble alpha-synuclein oligomers and nigrostriatal
degeneration. *Nat Neurosci* **20**, 1560-1568, doi:10.1038/nn.4641 (2017).
- 697 Mahul-Mellier, A. L. *et al.* Fibril growth and seeding capacity play key roles in alpha-synuclein-
mediated apoptotic cell death. *Cell death and differentiation* **22**, 2107-2122,
doi:10.1038/cdd.2015.79 (2015).
- 698 Shahmoradian, S. H. *et al.* Lewy pathology in Parkinson's disease consists of crowded organelles
and lipid membranes. *Nat Neurosci* **22**, 1099-1109, doi:10.1038/s41593-019-0423-2 (2019).
- 699 Guerrero-Ferreira, R. *et al.* Two new polymorphic structures of human full-length alpha-synuclein
fibrils solved by cryo-electron microscopy. *eLife* **8**, e48907, doi:10.7554/eLife.48907 (2019).
- 700 Weihofen, A. *et al.* Development of an aggregate-selective, human-derived α -synuclein antibody
BIB054 that ameliorates disease phenotypes in Parkinson's disease models. *Neurobiology of
disease* **124**, 276-288, doi:10.1016/j.nbd.2018.10.016 (2019).
- 701 Sampson, T. R. *et al.* Gut Microbiota Regulate Motor Deficits and Neuroinflammation in a Model
of Parkinson's Disease. *Cell* **167**, 1469-1480 e1412, doi:10.1016/j.cell.2016.11.018 (2016).
- 702 Elfarrash, S. *et al.* Organotypic slice culture model demonstrates inter-neuronal spreading of
alpha-synuclein aggregates. *Acta neuropathologica communications* **7**, 213, doi:10.1186/s40478-
019-0865-5 (2019).
- 703 Kawahata, I., Bousset, L., Melki, R. & Fukunaga, K. Fatty Acid-Binding Protein 3 is Critical for α -
Synuclein Uptake and MPP(+)-Induced Mitochondrial Dysfunction in Cultured Dopaminergic
Neurons. *Int J Mol Sci* **20**, 5358, doi:10.3390/ijms20215358 (2019).
- 704 Martinez T. N., J. P. H., Luk K. C., Gottler L., Chou S., Mille-Baker B., Verkaar F., Jensen A., Haber
C., Steinbrueck S., Lashuel H. A., Fauvet B., Tong X., Morris A. L., Polinski N. K., Dave K. D. . *The
Michael J. Fox Foundation's Strategy to Generate, Characterize, and Distribute Preclinical Alpha-
Synuclein Research Tools for Molecular Biology*,
<https://files.michaeljfox.org/TNM_asyn_molecular_tools_poster_2016.pdf> (2016).
- 705 abcamCat.No.ab209538. Recombinant Anti-Alpha-synuclein aggregate antibody [MJFR-14-6-4-2]
- Conformation-Specific (ab209538), <[https://www.abcam.com/alpha-synuclein-aggregate-
antibody-mjfr-14-6-4-2-conformation-specific-ab209538.html](https://www.abcam.com/alpha-synuclein-aggregate-antibody-mjfr-14-6-4-2-conformation-specific-ab209538.html)> (
- 706 Lassen, L. B. *et al.* ELISA method to detect α -synuclein oligomers in cell and animal models. *PLoS
One* **13**, e0196056, doi:10.1371/journal.pone.0196056 (2018).
- 707 AgriseraCat.No.AS132718. ASyO5 | Mouse anti-human alpha-synuclein | oligomer-specific (clone
number 2.4), <<https://www.agrisera.com/en/artiklar/asyo5-2.html>> (
- 708 Fauvet, B. *et al.* alpha-Synuclein in central nervous system and from erythrocytes, mammalian
cells, and Escherichia coli exists predominantly as disordered monomer. *The Journal of biological
chemistry* **287**, 15345-15364, doi:10.1074/jbc.M111.318949 (2012).
- 709 Wiedemann, C., Bellstedt, P. & Görlach, M. CAPITO--a web server-based analysis and plotting tool
for circular dichroism data. *Bioinformatics (Oxford, England)* **29**, 1750-1757,
doi:10.1093/bioinformatics/btt278 (2013).
- 710 Rissin, D. M. *et al.* Single-molecule enzyme-linked immunosorbent assay detects serum proteins
at subfemtomolar concentrations. *Nature Biotechnology* **28**, 595-599, doi:10.1038/nbt.1641
(2010).
- 711 Kuhle, J. *et al.* Comparison of three analytical platforms for quantification of the neurofilament
light chain in blood samples: ELISA, electrochemiluminescence immunoassay and Simoa. *Clinical
chemistry and laboratory medicine* **54**, 1655-1661, doi:10.1515/cclm-2015-1195 (2016).

712 Hartmann, A. Postmortem studies in Parkinson's disease. *Dialogues Clin Neurosci* **6**, 281-293, doi:10.31887/DCNS.2004.6.3/ahartmann (2004).

713 Erskine, D. *et al.* Lewy body pathology is more prevalent in older individuals with mitochondrial disease than controls. *Acta neuropathologica* **139**, 219-221, doi:10.1007/s00401-019-02105-w (2020).

714 Zhao, X. *et al.* Lewy Body-Associated Proteins A-Synuclein (a-syn) as a Plasma-Based Biomarker for Parkinson's Disease. *Frontiers in Aging Neuroscience* **14**, doi:10.3389/fnagi.2022.869797 (2022).

715 Winner, B. *et al.* In vivo demonstration that alpha-synuclein oligomers are toxic. *Proceedings of the National Academy of Sciences of the United States of America* **108**, 4194-4199, doi:10.1073/pnas.1100976108 (2011).

716 Cascella, R. *et al.* The release of toxic oligomers from α -synuclein fibrils induces dysfunction in neuronal cells. *Nature Communications* **12**, 1814, doi:10.1038/s41467-021-21937-3 (2021).

717 Wang, X., Yu, S., Li, F. & Feng, T. Detection of α -synuclein oligomers in red blood cells as a potential biomarker of Parkinson's disease. *Neuroscience letters* **599**, 115-119, doi:https://doi.org/10.1016/j.neulet.2015.05.030 (2015).

718 Hansson, O. *et al.* Levels of cerebrospinal fluid α -synuclein oligomers are increased in Parkinson's disease with dementia and dementia with Lewy bodies compared to Alzheimer's disease. *Alzheimers Res Ther* **6**, 25, doi:10.1186/alzrt255 (2014).

719 Duran, R. *et al.* Plasma alpha-synuclein in patients with Parkinson's disease with and without treatment. *Movement disorders : official journal of the Movement Disorder Society* **25**, 489-493, doi:10.1002/mds.22928 (2010).

720 Kang, W. *et al.* Salivary total α -synuclein, oligomeric α -synuclein and SNCA variants in Parkinson's disease patients. *Scientific Reports* **6**, 28143, doi:10.1038/srep28143 (2016).

721 Tian, C. *et al.* Erythrocytic α -Synuclein as a potential biomarker for Parkinson's disease. *Translational neurodegeneration* **8**, 15, doi:10.1186/s40035-019-0155-y (2019).

722 Vivacqua, G. *et al.* Salivary alpha-synuclein in the diagnosis of Parkinson's disease and Progressive Supranuclear Palsy. *Parkinsonism & related disorders* **63**, 143-148, doi:10.1016/j.parkreldis.2019.02.014 (2019).

723 Sandal, M. *et al.* Conformational equilibria in monomeric alpha-synuclein at the single-molecule level. *PLoS Biol* **6**, e6, doi:10.1371/journal.pbio.0060006 (2008).

724 Kumari, M., Kumar, B., Bisht, K. S. & Maiti, T. K. Glycation renders α -synuclein oligomeric strain and modulates microglia activation. *bioRxiv*, 2022.2001.2015.476311, doi:10.1101/2022.01.15.476311 (2022).

725 Prots, I. *et al.* α -Synuclein oligomers induce early axonal dysfunction in human iPSC-based models of synucleinopathies. *Proceedings of the National Academy of Sciences of the United States of America* **115**, 7813-7818, doi:10.1073/pnas.1713129115 (2018).

726 Helwig, M. *et al.* Brain propagation of transduced α -synuclein involves non-fibrillar protein species and is enhanced in α -synuclein null mice. *Brain : a journal of neurology* **139**, 856-870, doi:10.1093/brain/awv376 (2016).

727 Froula, J. M. *et al.* Defining α -synuclein species responsible for Parkinson's disease phenotypes in mice. *The Journal of biological chemistry* **294**, 10392-10406, doi:10.1074/jbc.RA119.007743 (2019).

728 Pieri, L., Madiona, K. & Melki, R. Structural and functional properties of prefibrillar α -synuclein oligomers. *Scientific Reports* **6**, 24526, doi:10.1038/srep24526 (2016).

729 Outeiro, T. F. *et al.* Formation of Toxic Oligomeric α -Synuclein Species in Living Cells. *PLOS ONE* **3**, e1867, doi:10.1371/journal.pone.0001867 (2008).

730 Chai, Y. J. *et al.* The secreted oligomeric form of α -synuclein affects multiple steps of membrane
trafficking. *FEBS letters* **587**, 452-459, doi:10.1016/j.febslet.2013.01.008 (2013).

731 Chen, L. *et al.* Oligomeric α -synuclein inhibits tubulin polymerization. *Biochemical and Biophysical
Research Communications* **356**, 548-553, doi:https://doi.org/10.1016/j.bbrc.2007.02.163 (2007).

732 Ávila, C. L. *et al.* Structural characterization of heparin-induced glyceraldehyde-3-phosphate
dehydrogenase protofibrils preventing α -synuclein oligomeric species toxicity. *The Journal of
biological chemistry* **289**, 13838-13850, doi:10.1074/jbc.M113.544288 (2014).

733 Angelova, P. R. *et al.* Ca^{2+} is a key factor in α -synuclein-induced neurotoxicity. *J Cell Sci* **129**, 1792-
1801, doi:10.1242/jcs.180737 (2016).

734 Ferreira, D. G. *et al.* Adenosine A2A Receptors Modulate α -Synuclein Aggregation and Toxicity.
Cereb Cortex **27**, 718-730, doi:10.1093/cercor/bhv268 (2017).

735 Vasili, E. *et al.* Endogenous Levels of Alpha-Synuclein Modulate Seeding and Aggregation in
Cultured Cells. *Molecular neurobiology* **59**, 1273-1284, doi:10.1007/s12035-021-02713-2 (2022).

736 Celej, M. S. *et al.* Toxic prefibrillar α -synuclein amyloid oligomers adopt a distinctive antiparallel
 β -sheet structure. *The Biochemical journal* **443**, 719-726, doi:10.1042/bj20111924 (2012).

737 Yang, D. *et al.* Impairment of mitochondrial respiration in mouse fibroblasts by oncogenic H-
RAS(Q61L). *Cancer Biol Ther* **9**, 122-133, doi:10.4161/cbt.9.2.10379 (2010).

738 Gonzalez-Rodriguez, P., Zampese, E. & Surmeier, D. J. Selective neuronal vulnerability in
Parkinson's disease. *Prog Brain Res* **252**, 61-89, doi:10.1016/bs.pbr.2020.02.005 (2020).

739 Yamazaki, M. *et al.* Alpha-synuclein inclusions in amygdala in the brains of patients with the
parkinsonism-dementia complex of Guam. *J Neuropathol Exp Neurol* **59**, 585-591,
doi:10.1093/jnen/59.7.585 (2000).

740 Popescu, A., Lippa, C. F., Lee, V. M. & Trojanowski, J. Q. Lewy bodies in the amygdala: increase of
alpha-synuclein aggregates in neurodegenerative diseases with tau-based inclusions. *Archives of
neurology* **61**, 1915-1919, doi:10.1001/archneur.61.12.1915 (2004).

741 Sorrentino, Z. A. *et al.* Unique α -synuclein pathology within the amygdala in Lewy body dementia:
implications for disease initiation and progression. *Acta neuropathologica communications* **7**, 142,
doi:10.1186/s40478-019-0787-2 (2019).

742 Luk, K. C. *et al.* Pathological α -synuclein transmission initiates Parkinson-like neurodegeneration
in nontransgenic mice. *Science (New York, N.Y.)* **338**, 949-953, doi:10.1126/science.1227157
(2012).

743 Bartscher, J. *et al.* Chronic corticosterone aggravates behavioral and neuronal symptomatology in
a mouse model of alpha-synuclein pathology. *Neurobiology of aging* **83**, 11-20,
doi:https://doi.org/10.1016/j.neurobiolaging.2019.08.007 (2019).

744 Henderson, M. X. *et al.* Spread of α -synuclein pathology through the brain connectome is
modulated by selective vulnerability and predicted by network analysis. *Nat Neurosci* **22**, 1248-
1257, doi:10.1038/s41593-019-0457-5 (2019).

745 Rosenberg, S. S. & Spitzer, N. C. Calcium signaling in neuronal development. *Cold Spring Harb
Perspect Biol* **3**, a004259, doi:10.1101/cshperspect.a004259 (2011).

746 Bading, H. Nuclear calcium signalling in the regulation of brain function. *Nature reviews.
Neuroscience* **14**, 593-608, doi:10.1038/nrn3531 (2013).

747 Del Prete, D., Checler, F. & Chami, M. Ryanodine receptors: physiological function and
deregulation in Alzheimer disease. *Mol Neurodegener* **9**, 21, doi:10.1186/1750-1326-9-21 (2014).

748 Mittal, S. *et al.* β 2-Adrenoreceptor is a regulator of the α -synuclein gene driving risk of Parkinson's
disease. *Science* **357**, 891-898, doi:10.1126/science.aaf3934 (2017).

749 Erro, R., Mencacci, N. E. & Bhatia, K. P. The Emerging Role of Phosphodiesterases in Movement
Disorders. *Movement Disorders* **36**, 2225-2243, doi:https://doi.org/10.1002/mds.28686 (2021).

750 Zhong, J. *et al.* Inhibition of phosphodiesterase 4 by FCPR16 protects SH-SY5Y cells against MPP(+)-
induced decline of mitochondrial membrane potential and oxidative stress. *Redox Biol* **16**, 47-58,
doi:10.1016/j.redox.2018.02.008 (2018).

751 Schwenkgrub, J. *et al.* The phosphodiesterase inhibitor, ibudilast, attenuates neuroinflammation
in the MPTP model of Parkinson's disease. *PLoS One* **12**, e0182019,
doi:10.1371/journal.pone.0182019 (2017).

752 Ahlers, K. E., Chakravarti, B. & Fisher, R. A. RGS6 as a Novel Therapeutic Target in CNS Diseases
and Cancer. *Aaps j* **18**, 560-572, doi:10.1208/s12248-016-9899-9 (2016).

753 Apicco, D. J. *et al.* The Parkinson's disease-associated gene ITPKB protects against
α-synuclein aggregation by regulating ER-to-mitochondria calcium release. *Proceedings of
the National Academy of Sciences* **118**, e2006476118, doi:doi:10.1073/pnas.2006476118 (2021).

754 Kibbe, W. A. *et al.* Disease Ontology 2015 update: an expanded and updated database of human
diseases for linking biomedical knowledge through disease data. *Nucleic Acids Res* **43**, D1071-
1078, doi:10.1093/nar/gku1011 (2015).

755 Casadei, N. *et al.* Overexpression of synphilin-1 promotes clearance of soluble and misfolded
α-synuclein without restoring the motor phenotype in aged A30P transgenic mice. *Hum Mol
Genet* **23**, 767-781, doi:10.1093/hmg/ddt467 (2014).

756 Ouchi, Y. *et al.* Microglial activation and dopamine terminal loss in early Parkinson's disease.
Annals of neurology **57**, 168-175, doi:10.1002/ana.20338 (2005).

757 Lavis, S. *et al.* Increased microglial activation in patients with Parkinson disease using [(18)F]-
DPA714 TSPO PET imaging. *Parkinsonism & related disorders* **82**, 29-36,
doi:10.1016/j.parkreldis.2020.11.011 (2021).

758 Choi, I. *et al.* Microglia clear neuron-released α-synuclein via selective autophagy and prevent
neurodegeneration. *Nature Communications* **11**, 1386, doi:10.1038/s41467-020-15119-w (2020).

759 Bonifati, V. *et al.* Mutations in the DJ-1 gene associated with autosomal recessive early-onset
parkinsonism. *Science* **299**, 256-259, doi:10.1126/science.1077209 (2003).

760 Choi, J. *et al.* Oxidative damage of DJ-1 is linked to sporadic Parkinson and Alzheimer diseases.
The Journal of biological chemistry **281**, 10816-10824, doi:10.1074/jbc.M509079200 (2006).

761 Shendelman, S., Jonason, A., Martinat, C., Leete, T. & Abeliovich, A. DJ-1 is a redox-dependent
molecular chaperone that inhibits α-synuclein aggregate formation. *PLoS Biol* **2**, e362,
doi:10.1371/journal.pbio.0020362 (2004).

762 Xu, C. Y. *et al.* DJ-1 Inhibits α-Synuclein Aggregation by Regulating Chaperone-Mediated
Autophagy. *Front Aging Neurosci* **9**, 308, doi:10.3389/fnagi.2017.00308 (2017).

763 Kaji, S. *et al.* Pathological Endogenous α-Synuclein Accumulation in Oligodendrocyte Precursor
Cells Potentially Induces Inclusions in Multiple System Atrophy. *Stem Cell Reports* **10**, 356-365,
doi:10.1016/j.stemcr.2017.12.001 (2018).

764 Nakamura, Y. *et al.* Monoamine Oxidase-B Inhibition Facilitates α-Synuclein Secretion In Vitro and
Delays Its Aggregation in rAAV-Based Rat Models of Parkinson's Disease. *The Journal of
neuroscience : the official journal of the Society for Neuroscience* **41**, 7479-7491,
doi:10.1523/jneurosci.0476-21.2021 (2021).

765 Rostami, J. *et al.* Human Astrocytes Transfer Aggregated Alpha-Synuclein via Tunneling
Nanotubes. *The Journal of neuroscience : the official journal of the Society for Neuroscience* **37**,
11835-11853, doi:10.1523/jneurosci.0983-17.2017 (2017).

766 Elabi, O. *et al.* Human α-synuclein overexpression in a mouse model of Parkinson's disease leads
to vascular pathology, blood brain barrier leakage and pericyte activation. *Sci Rep* **11**, 1120,
doi:10.1038/s41598-020-80889-8 (2021).

- 767 Pediaditakis, I. *et al.* Modeling alpha-synuclein pathology in a human brain-chip to assess blood-brain barrier disruption. *Nature Communications* **12**, 5907, doi:10.1038/s41467-021-26066-5 (2021).
- 768 Sirtori, R., Riva, C., Ferrarese, C. & Sala, G. HSPA8 knock-down induces the accumulation of neurodegenerative disorder-associated proteins. *Neuroscience letters* **736**, 135272, doi:10.1016/j.neulet.2020.135272 (2020).
- 769 Han, R., Liang, J. & Zhou, B. Glucose Metabolic Dysfunction in Neurodegenerative Diseases-New Mechanistic Insights and the Potential of Hypoxia as a Prospective Therapy Targeting Metabolic Reprogramming. *Int J Mol Sci* **22**, doi:10.3390/ijms22115887 (2021).
- 770 Fujimoto, M. *et al.* A novel mouse HSF3 has the potential to activate nonclassical heat-shock genes during heat shock. *Molecular biology of the cell* **21**, 106-116, doi:10.1091/mbc.e09-07-0639 (2010).
- 771 Malko, P., Syed Mortadza, S. A., McWilliam, J. & Jiang, L.-H. TRPM2 Channel in Microglia as a New Player in Neuroinflammation Associated With a Spectrum of Central Nervous System Pathologies. *Frontiers in Pharmacology* **10**, doi:10.3389/fphar.2019.00239 (2019).
- 772 Kumar, S. T., Donzelli, S., Chiki, A., Syed, M. M. K. & Lashuel, H. A. A simple, versatile and robust centrifugation-based filtration protocol for the isolation and quantification of α -synuclein monomers, oligomers and fibrils: Towards improving experimental reproducibility in α -synuclein research. *J Neurochem* **153**, 103-119, doi:10.1111/jnc.14955 (2020).
- 773 Raudvere, U. *et al.* g:Profiler: a web server for functional enrichment analysis and conversions of gene lists (2019 update). *Nucleic Acids Research* **47**, W191-W198, doi:10.1093/nar/gkz369 (2019).

Somanath Jagannath

EPFL SV BMI LMNN
AI 2148 (AI building), Station 19
Lausanne 1015, Switzerland
somanath.jagannath@epfl.ch

EDUCATION

- Ph.D. (Neuroscience)** Dec. 2017 – present
École Polytechnique Fédérale de Lausanne (EPFL), Switzerland
- Master of Science (Interdisciplinary Neuroscience)** Oct. 2014 – Mar. 2017
Goethe-Universität Frankfurt am Main, Germany
- Bachelor of Engineering (Biotechnology)** Sep. 2010 – Aug. 2014
B.M.S. College of Engineering, Bangalore, India

RESEARCH EXPERIENCE

- PhD thesis** Dec 2017 – Present
Supervisor: Professor Hilal A. Lashuel
Laboratory of Molecular and Chemical Biology of Neurodegeneration, EPFL
Title: Molecular and cellular determinants of alpha-synuclein seeding and toxicity
- Scientific Assistant**, Institute for Human Genetics, Apr 2017 – Nov 2017
J.G. University of Mainz, and Institute of Neurophysiology, Goethe-Universität Frankfurt, Germany.
 - Studying the electrophysiological properties of Locus Coeruleus Neurons in maternal KCNK9 Knockout and complete knockouts to investigate their role in the sleep-wake cycle.
- Master's Thesis** Sep 2016 – Apr 2017
Supervisor: Professor Jochen Roeper, Institute of Neurophysiology
Goethe-Universität Frankfurt am Main, Germany
Title: The functional and pharmacological diversity of voltage-gated calcium channels among dopamine neurons across the substantia nigra.
- Research Assistant (Hiwi)**, Department of Connectomics, Feb 2015 – Apr 2016
Max Planck Institute for Brain Research, Frankfurt am Main, Germany
 - Reconstructed neuronal networks from large-scale electron microscopy data.
- Bachelor's thesis** Sep 2013 – June 2014
Supervisor: Dr. Savithri Bhat, B.M.S. college of Engineering, Bangalore, India.
Title: Studies on the effect of Withaferin-A (a compound from *Withania somnifera*) on mammalian cell lines (HeLa, HEK-293, C.H.O.)

INSTRUMENTATION AND LABORATORY SKILLS

Ex Vivo, In Vivo

- Mouse handling, intracardial perfusions and injections; basics of stereotaxic injections, microtome and vibratome brain sectioning, immunohistochemistry.
- *In vitro* whole-cell patch clamp (current-clamp and voltage-clamp) technique; cell-attached and nucleated outside-out recordings in acute brain slices and primary neurons, calcium imaging, single-cell Patch-seq technique.

Staining and Imaging

- Immunocytochemistry, immunohistochemistry (IF, DAB staining), light microscopy, confocal laser scanning microscopy, transmission electron microscopy.

In vitro

- Transfection, transformation, expression and purification of recombinant proteins, FPLC, UPLC, ESI-MS, CD, preparation and characterization of morphologically and structurally different types of α -synuclein oligomers and fibrils, Aggregation kinetics of Amyloid proteins.

Cell culture

- Primary neuronal (cortical, hippocampal, midbrain) and astrocytes cultures from rodent brains. Mammalian cell lines. toxicity assays.

Molecular and Biochemical Analysis

- DNA and RNA isolation, PCR, SDS-PAGE, Slot Blot, Western Blot.

Computer

- Electrophysiological data analysis using Patchmaster and Fitmaster (HEKA), IgorPro (Wavemetrics).
- Single-cell RNA sequencing/transcriptomics analysis using R, Python.
- Statistical analysis using GraphPad Prism (GraphPad)
- Image analysis using Fiji (ImageJ) and Adobe illustrator (basics).

SCIENTIFIC PUBLICATIONS

Fares M.B.*; **Jagannath S.***; Lashuel H.A.*. "Reverse engineering Lewy bodies: How far have we come and how far can we go?" **Nature Reviews Neuroscience**, 2021 (* equal contributions)

Kumar N.; Shetti N.P.; **Jagannath S.**; Aminabhavi T.M.; "Electrochemical sensors for the detection of the SARS-CoV-2 Virus" **Chemical Engineering Journal**, 2021

Kumar S.T.*; **Jagannath S.***; Francois C; Vanderstichele H.; Stoops E.; Lashuel H.A. "How specific are the conformation-specific α -synuclein antibodies?" **Neurobiology of Disease**, 2020 (* equal contributions)

Cooper A.; Butto T.; Hammer N.; **Jagannath S.**, Akhtar J, Radyushkin K, Lesage F, Roeper J, Schweiger S, Zechner U. "Inhibition of histone deacetylation rescues Birk-Barel - Intellectual Disability syndrome in mice" **Nature Communications**, 2020

REFERENCES AVAILABLE UPON REQUEST